# Enhancing Pavement Surface Macrotexture Characterization

Daniel E. Mogrovejo Carrasco

Thesis submitted to the faculty of the Virginia Polytechnic Institute and State University in partial fulfillment of the requirements for the degree of

Doctor of Philosophy

in

Civil Engineering

Gerardo W. Flintsch, Chair

Edgar de Leon Izeppi

Antonio Trani

John Ferris

March 22, 2015

Blacksburg, Virginia

# Enhancing Pavement Surface Macrotexture Characterization

Daniel E. Mogrovejo Carrasco

## ABSTRACT

One of the most important objectives for transportation engineers is to understand pavement surface properties and their positive and negative effects on the user. This can improve the design of the infrastructure, adequacy of tools, and consistency of methodologies that are essential for transportation practitioners regarding macrotexture characterization. Important pavement surface characteristics, or tire-pavement interactions, such as friction, tire-pavement noise, splash and spray, and rolling resistance, are significantly influenced by pavement macrotexture.

This dissertation compares static and dynamic macrotexture measurements and proposes and enhanced method to quantify the macrotexture. Dynamic measurements performed with vehicle-mounted lasers have the advantage of measuring macrotexture at traffic speed. One drawback of these laser devices is the presence of "spikes" in the collected data, which impact the texture measurements. The dissertation proposes two robust and innovative methods to overcome this limitation.

The first method is a data-driven adaptive method that detects and removes the spikes from high-speed laser texture measurements. The method first calculates the discrete wavelet transform of the texture measurements. It then detects (at all levels) and removes the spikes from the obtained wavelet coefficients (or differences). Finally, it calculates the inverse discrete wavelet transform with the processed wavelet coefficients (without outliers) to obtain the Mean Profile Depth (MPD) from the measurements with the spikes removed. The method was validated by comparing the results with MPD measurements obtained with a Circular Texture Meter (CTMeter) that was chosen as the control device.

Although this first method was able to successfully remove the spikes, it has the drawback that it depends on manual modeling of the distribution of the wavelet coefficients to correctly define an appropriate threshold. The next step of this dissertation proposes an enhanced to the spike removal methodology for macrotexture measurements taken with high-speed laser devices. This denoising methodology uses an algorithm that defines the distribution of texture measurements by using the family of Generalized Gaussian Distributions (GGD), along with the False Discovery Rate (FDR) method that controls the proportion of wrongly identified spikes among all identified spikes. The FDR control allows for an adaptive threshold selection that differentiates between valid measurements and spikes. The validation of the method showed that the MPD results obtained with denoised dynamic measurements are comparable to MPD results from the control devices. This second method is included as a crucial step in the last stage of this dissertation as explained following.

The last part of the dissertation presents an enhanced macrotexture characterization index based on the Effective Area for Water Evacuation (EAWE), which: (1) Estimates the potential of the pavement to drain water and (2) Correlates better with two pavement surface properties affected by macrotexture (friction and noise) that the current MPD method. The proposed index is defined by a three-step process that: (1) removes the spikes, assuring the reliability of the texture profile data, (2) finds the enveloping profile that is necessary to delimit the area between the tire and the pavement when contact occurs, and (3) computes the EAWE. Comparisons of current (MPD) and proposed (EAWE) macrotexture characterization indices showed that the MPD overestimates the ability of the pavement for draining the surface water under a tire.

# ACKNOWLEDGEMENTS

# TABLE OF CONTENTS

# LIST OF FIGURES

# LIST OF TABLES

# Chapter 1 - INTRODUCTION

The physical surface properties of pavement impact the interaction between the vehicle and the road and are determined by the pavement texture. The term 'texture' is often used to cover the whole range of surface irregularities, from tiny grains of the fine aggregate to large unevenness in the road, is divided in categories according to the wavelength of these irregularities. The miniscule grains of fine aggregate and features that make up the actual surface of coarse aggregate provide what is known as the pavement microtexture. Bigger features of the pavement surface that are formed by the spaces between the aggregate particles are classified as macrotexture. Larger features are classified as megatexture and unevenness.

The study of texture is important because it impacts tire-pavement interactions, one of the most important being safety. For example, microtexture is one of the most significant contributor to low-speed friction or skid resistance, whereas macrotexture has been shown to be one of the primary component of high-speed, wet friction (*1*). Pavement macrotexture is an important property that affects friction, tire-pavement noise, splash and spray, and rolling resistance. An adequate pavement surface macrotexture is essential to prevent accidents by providing good skid resistance through efficiently draining water out of the contact area, reduce splash and spray, and mitigate tire-pavement noise.

Macrotexture measurement devices are generally divided into two classes: static and dynamic. The static methods are labor intensive, time consuming and require traffic control. Dynamic devices use vehicle-mounted lasers to measure macrotexture at traffic speed. They allow the characterization of pavement surfaces at a high degree of detail without interrupting traffic. However, two fundamental questions must be addressed:

1. How effectively are these high-speed methodologies and equipment for characterizing pavement macrotexture taking into account the presence of noise in the data or spikes?

2. How can we best implement these new methods (specifically for network-level measurements) after overcoming the potential problems of spikes?

The laser technology used in current high-speed measuring vehicles allows the collection of data at high frequency, making high-speed measurements possible. However, an accurate data analysis for the dynamic measures is needed to correctly characterize the pavement and overcome potentially bad results caused by noise in the raw data.

## BACKGROUND

### Texture Basics

The following general terminology is revised for a better understanding of the spectrum of pavement surface properties as classified by the World Road Association.

According to International Organization for Standardization ISO 13473-5:2009, pavement texture is the "deviation of a pavement surface from a true planar surface, with a texture wavelength (quantity describing the horizontal dimension of the irregularities of a texture profile, or basically the distance between peaks) less than 0,5 m" (*2*). For texture wavelengths over 0.5 m, these deviations are known as unevenness or roughness, usually up to 50 m wavelength, but even wavelengths longer than 50 m would be considered unevenness in some specific road profile analysis, such as airfield applications (*3*).

The World Road Association (PIARC) has adopted the ISO classification and established standard categories of texture (and roughness) as explained below. Figure 1-1 depicts a spatial representation of the effects that these categories (microtexture, macrotexture, megatexture, and unevenness) have on pavement surface properties in terms of how "good" or "bad" their influence is, as well as their corresponding wavelength ($\lambda$) range. Physical images of the ISO/PIARC classification are shown in Figure 1-2.
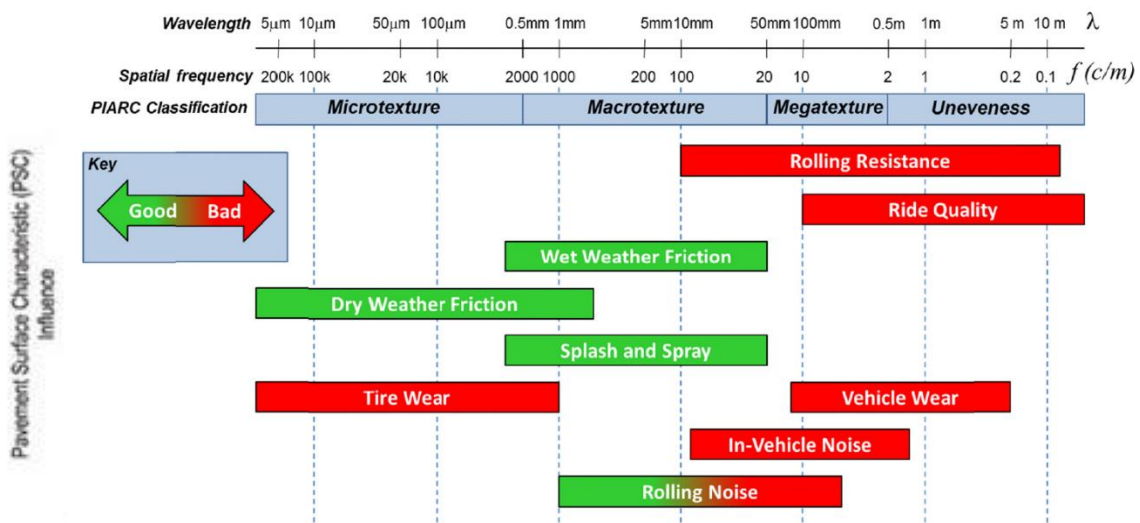


Figure 1-1 PIARC classification for pavement surface characteristics according to texture wavelength (*3; 4*)

|Texture categorization|Texture Wavelength ($\lambda$)|
|---|---|
|Microtexture|$\lambda < 0.5$ mm|
|Macrotexture|$0.5$ mm $< \lambda < 50$ mm|
|Megatexture|$50$ mm $< \lambda < 500$ mm|
|Roughness/Smoothness|$0.5$ m $< \lambda < 50$ m|

Microtexture: $\lambda$, up to 0.5 mm    Macrotexture: $\lambda$ from 0.5 to 50 mm    Megatexture: $\lambda$ from 50 to 500 mm

Figure 1-2 Physical representation of pavement texture (*4; 5*)

The term microtexture, $\lambda < 0.5$ mm, refers basically to the irregularities or deviations related with the actual asperities of the aggregate particles; a good analogy for a surface with marked microtexture may be a fine sand paper. Therefore, the main "positive" impact of microtexture is its effect on dry friction. Microtexture also influence wet friction but to a lesser degree than that on dry weather conditions. Microtexture also influences tire-pavement (rumbling) noise since it helps "deforming" the actual tire contact surface, decreasing the rumbling effect and the stick-related noise.

The next PIARC category, macrotexture ($0.5$ mm $< \lambda < 50$ mm) addresses characteristics such as aggregate particle size, voids and spacing between aggregates, grinding and grooving, and high porosity. *Macrotexture may be the most influential category over the range of surface properties*. For instance, macrotexture is closely related to wet-weather friction since it affects the water-carrying capacity potential of the pavement surface. It is also influential in splash and spray. Tire-pavement noise can also be reduced for most cases if high macrotexture is present (high and low frequencies are the most effected). Studies suggest that the optical properties of the surface pavement are also affected by macrotexture (*3*). Pavement surfaces should be designed with sufficient macrotexture to obtain appropriate friction and water drainage within the tire-road interface.

Examples of megatexture ($50$ mm $< \lambda < 0.5$ m) include rumble strips on the shoulder, concrete or rock blocks, and pavement functional deterioration such as potholes, corrugation, rutting, and step faulting. Due to the relatively bigger wavelengths, megatexture's adversely impacts tire-pavement noise generation. In-vehicle noise is also increased for the impact and vibration effects. Friction is affected minimally by megatexture (almost negligible due to the lack of contact time, for instance), and rolling resistance is negatively affected. Moreover, the increased vibration, impact, and loss of stability will adversely affect vehicle mechanics and ride quality. A good use of megatexture, though, is in rumble strips alongside the road for safety (*6*).

The final category is unevenness ($\lambda > 0.5$ m), which is commonly referred to as smoothness or roughness. It includes irregularities connected with geometric design, construction process, uneven compaction, geological problems, and pavement deterioration such as levelling and subgrade deformation. Unevenness negatively affects rolling resistance (due to loss of tire-pavement contact), ride quality (due to vibrations and resonance), and vehicle wear, at least in short wavelengths ($\lambda < 10$ m). For long wavelengths ($\lambda > 10$ m), vehicle stability can be affected along with the previously mentioned surface properties.

**Pavement Surface Characteristics Impact on The user**

According to the texture wavelength, the main pavement surface characteristics or properties have significant effects on the interaction of the vehicle with the road (safety, fuel consumption, comfort,

maneuverability, etc.), as summarized in Figure 1-1. Table 1-1 summarizes the vehicle-road interactions that are impacted by the pavement macrotexture, along with the optimal macrotexture values for each.

Table 1-1 Effect of macrotexture by property

| Property/ Interaction | Macrotexture Positive or Negative Effect | | Optimal (MPD) Values | Reference |
|---|---|---|---|---|
| Dry Friction | Sufficient macrotexture (high MPD) in its lower wavelength (λ) range improves dry friction. | Positive effect on safety. | Higher are better, especially for wet friction (e.g., MPD > 1.2 mm) | (*3; 7*) |
| | | Positive effect on comfort and maneuverability. | | |
| Wet Friction | Sufficient macrotexture in its entire wavelength range improves wet friction especially at high speeds. | Positive effect on safety. | | (*3; 8*) |
| | | Positive effect on maneuverability and hydroplaning potential. | | (*9*) |
| Tire-Pavement Noise | Positive effect at lower λ values (1 mm – 10 mm) and negative at λ > 10 mm. | Negative effect on comfort. | Lower values are better (e.g., MPD < 0.8 mm). Negative texture is better than positive | (*3; 10-12*) |
| Rolling Resistance | As λ exceeds 10 mm, it has a negative effect on rolling resistance. | High rolling resistance will lead to a negative effect on fuel consumption. | The lower the better to decrease fuel consumption. MPD < 0.8 mm, | (*13*) |
| | | Negative effect on safety and maneuverability. | | (*3; 14-16*) |
| Splash and Spray | Macrotexture impacts splash and spray. Draining surfaces significantly reduce splash and spray | Positive effect on comfort and safety. | Higher values of MPD will be beneficial as long as the conditions are below saturation; for saturated conditions, on the other hand, higher MPD becomes adverse. | (*3; 17; 18*) |
| Tire Wear | Macrotexture influence is more adverse around its lower wavelengths (microtexture is much more significant). | Negative effect on safety and maneuverability. | N/A | (*3; 7*) |
| In-Vehicle Noise | High macrotexture wavelengths have a negative effect on in-vehicle noise because vibrations and impact become more significant. | Negative effect on comfort. | The lower the better: MPD < 0.8 mm. | (*3*) |

**Macrotexture Measurements**

*CTMeter*

This method is defined and explained under the ASTM E2157-09 standard and basically consists of a charge-coupled device with a laser-displacement sensor mounted on a rotating arm 80 mm above the surface. The sensor follows a circular track of 142 mm radius. The equipment reports the mean profile depth (MPD) and the root mean square (RMS) in SI units (*19*). A picture of the equipment is presented in Figure 1-3. The CTMeter segments the data into eight 111.5-mm arcs of 128 samples each (Figure 1-4). The precision of the results produce a standard deviation of the eight measurements on the same surface of less than 0.03 mm (*19*).
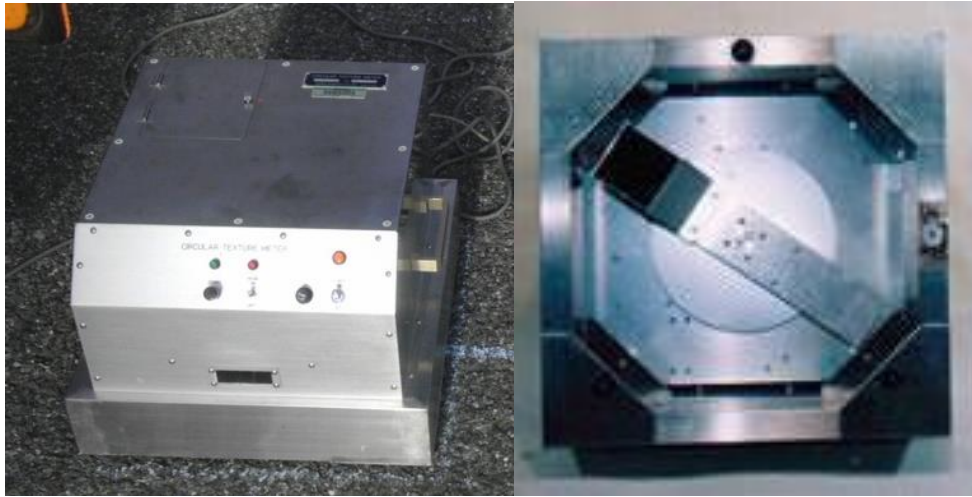


Figure 1-3 CTMeter being used on the Virginia Smart Road



Figure 1-4 Segments of the circular track profile (*19*)

The standard also defines the nature of the texture as negative or positive. This is determined by comparing the MPD and the RMS for a surface. Negative texture is the "macrotexture produced by depressions in the surface," and positive texture is the "macrotexture produced by asperities projecting above the surface" (*19*).

The average MPD value found with the CTMeter method is highly correlated with MTD measured by the sand patch method. Therefore this method can replace the volumetric measurements for determination of the MTP using the following equation as stated in the standard (*19*):

$$MTD = 0.947*MPD + 0.069 \qquad\qquad Eq.\ 1.1.$$

Where: MTD and MPD are expressed in millimeters.

*High-Speed, High-Frequency Single-Point Laser Devices*

High-Speed Laser Devices (HSLD) are currently being used to collect macrotexture data at highway speeds. The ASTM Standard E 1845 describes the method to compute the MPD from data that is collected by a single point laser along a longitudinal path (*20*). For this dissertation, dynamic measurements were taken with an AMES profiler that uses a high-speed laser device (HSLD) developed by LMI technologies. Detailed information about this dynamic device can be found in (*21*). The HSLD (Figure 1-5) is capable of collecting measurements at speeds between 25 and 65 mph (40 and 105 km/h) and was used to gather the dynamic measurements. It has a laser spot with a diameter of 0.2 mm and a sampling frequency of 64 kHz.



Figure 1-5 High-speed, high-frequency laser device

*Other Devices*

Table 1-2 presents a brief summary of the other devices that are currently available for macrotexture measurement.

Table 1-2 Summary of the most relevant macrotexture measurement devices

| Device | Description | Indices, Type | Standard | Picture |
|--------|-------------|---------------|----------|---------|
| Sand Patch | It relies on a given volume of sand that is spread out on a road surface. The sand is distributed to form a circular patch, the diameter of which is measured. By dividing the volume of sand with the area covered, a value is obtained that represents the average depth of the sand layer (e.g. an average texture depth). | Mean Texture Depth (MTD), Static, Volumetric | ASTM E 965 |  http://www.pavestech.com/our-equipment.php |
| Hydrotimer | The base sealing ring simulates a tire footprint. A measured volume of water is released in the center of the sealing ring while an electronic timer indicates how long it takes the water to pass through texture voids in the pavement under the seal. This test also provides a visual display of escaping water.

Macrotexture is effective for drainage only when surface voids are connected by water flow channels below the tire contact points. The Hydrotimer shows the effectiveness of the surface voids in channeling water from under the tire footprint. | Mean Texture Depth (MTD), Static, Volumetric | ATM E 2380-05 |  http://www.afcec.af.mil/shared/media/photodb/web/2014/02/140121-F-XX475-003.JPG |

| Device | Description | Indices, Type | Standard | Picture |
|---|---|---|---|---|
| Laser Texture Scanner | It measures a series of short profiles (e.g., 10 runs over 100 mm each) over the area under the equipment, calculates the standardized MPD for each profile, and then averages the 10 MPD values to present a single result. It requires measurement time similar to the CTMeter. | Mean Profile Depth (MPD), Root Mean Square (RMS), Static, Profile | ASTM E2157-09 |  |

**Drop-outs and Spikes in the Measurements**

High-speed laser data are subjected to a variety of potential problems during the measurement process besides calibration and assembly (systematic errors that are supposed to be taken care of before the fieldwork). Many variables produce noise in the measurements. For example, shiny, mirror-like surfaces change the amount and direction of light reflected to the receiving lens, and black materials scatter only a small part of the incident light. Black and shiny materials (like fresh asphalt) have both of these problems. Transparent or semitransparent materials (e.g., pavements with certain minerals in the aggregate, reflective paint on the road, etc.) will cause offsets in the reflection and will also absorb or deviate a portion of the light (21). Other variables, such as temperature, geometry, secondary reflections, bandwidth, and sample rate, are also potential sources of noise in the measurements.

Current measuring devices have built-in software that accounts for this noise, but only what is defined as drop-outs, not the noise defined as spikes. The most common definition for drop-out in the context of continuous longitudinal signals (as is the case for texture profiles) is the following: a drop-out refers to an invalid reading or intermittent missing value along the measured signal.

Most laser sensors on devices for macrotexture measurements (e.g., CTMeter) are equipped with software that detects invalid readings or drop-outs by measuring the amount of light reflected (intensity) of the laser spot, and flagging the data when this intensity is below a certain threshold. In other words, if there is any disturbance in the amount of returning light into the optical receptor, the software determines if the returning light is insufficient and, if so, marks the corresponding data point as a drop-out. The software then corrects the data by taking out this drop-out in order to report reliable measurements in the results.

However, despite the fact that the software compares the intensity of the reflection all the time, some of the invalid readings are not detected. This is the case, for example, when the laser hits very smooth surfaces and so-called specular reflection takes place. *These undetected invalid readings are the ones we define as spikes* (or drop-outs that were not detected). Notice that specular reflection is only one type of many potential disturbances that occur during data collection.

The ISO standard 13473 states that "up to 10 per cent drop outs is acceptable if they are linearly interpolated between the closest valid readings and 5 per cent if they are not" (2). However, this statement

may not be valid in reality since some studies suggests that "extremely large deviations from the true values of MPD and texture spectra where found in some cases, even at drop out percentages far below the 5 % limit" (*2*). It was confirmed also in this work by the Virginia Tech Transportation Institute, were deviations where significant, even when using drop-out-filtered data, and, with relatively low percentages of spikes (around 0.13%, which are significantly less than 5%).

## PROBLEM STATEMENT

Static pavement macrotexture measurements (with a CTMeter, for example) are not practical for network-level data collection. The long-term goal of this effort is to support the implementation of new high-speed measuring technologies for network-level texture characterization, which allow the measurement of pavement macrotexture without traffic control. The short-term goal is to make these measurements reliable.

In order to do this, the first task is to correct the problems of spike noise in the laser measurements. The high-speed macrotexture laser signal has noise (besides drop-outs) that results in spikes in the collected data, which biases the texture measurements. There is, therefore, a need to remove these spikes in order to get accurate macrotexture measurements at highway speeds.

In addition, the literature reviewed suggests that MPD is not the best approach for texture characterization. By definition, MPD is calculated using the peaks of the profile over a defined base length, but this value may not represent the true ability of the pavement to drain water. Therefore, a better methodology for macrotexture characterization is needed.

## OBJECTIVES

The following are the main objectives of this thesis:

- Develop a methodology that can objectively identify and remove the spikes from the data collected using high speed laser devices.

- Develop an enhanced method to characterize pavement macrotexture based on the surface water-carrying capacity potential.

The following are the secondary objectives of this thesis:

- Test the denoising methodologies with real data collected over different pavement surfaces.

- Calculate and compare the MPD values obtained before and after removing the spikes and their associated statistical parameters for both proposed methods.

- Validate the denoising methods with MPD measurements obtained with a CTMeter, chosen as the standardized control method, taken at the same locations.
- Perform a comprehensive comparison between MPD and the new macrotexture index, using measurements from a significant amount of different sections.
- Analyze the correlation of the proposed index with friction and noise.

## RESEARCH APPROACH

The dissertation is composed of three manuscripts that propose enhanced pavement surface macrotexture characterization procedures. The first two manuscripts, "Latest Development in the Processing of Pavement Macrotexture Measurements of High Speed Laser Devices" and "Adaptive Spike Removal

9

Method for High Speed Pavement Macrotexture Measurements by Controlling the False Discovery Rate," describe spike removal methodologies developed as the first step of this research. The third manuscript, "Enhancing Pavement Surface Macrotexture Characterization by Using the Effective Area for Water Evacuation," describes the proposed new macrotexture characterization index.

The first part of this research addresses the first main objective about spike removal. It included a significant amount of field tests on the Virginia Smart Road and on demonstration projects constructed as part of the Virginia Quiet Pavement Implementation Program (VQPIP). Two different methods are proposed for the spike removal process: the wavelet transform method and the false discovery rate method. The spike removal methodologies were validated by comparing the dynamic measurements with two static (CTMeter) devices.

The second part addresses the second main objective of this dissertation, the development of a new method of characterizing texture based on water-carrying capacity. The proposed index computes the effective area for water evacuation assuming different tire stiffness. The index was compared to the MPD calculations and correlated with other pavement surface properties, such as friction and noise.

## SIGNIFICANCE

Although macrotexture measurements using static methodologies are already standardized, a reliable methodology to measure pavement macrotexture at highway speeds for network-level investigation is still needed. One of the main problems is the presence of spikes in the raw data; therefore, for high-speed measurements, before any methodology definition or standardization can be performed, spikes must be removed. This dissertation proposed a robust methodology for accomplishing this.

Moreover, the current measurements approach (MPD) is not enough to sufficiently characterize macrotexture. For example, two completely different surfaces can have the same MPD value and not have the same safety performance. As a result, there is a need for a better texture characterization approach. An alternative index that better correlates surface texture with safety potential is obtained by computing the water-carrying capacity of the pavement under a tire.

## ATTRIBUTIOS

This study includes three independent papers developed at the Center for Sustainable Transportation Infrastructure at the Virginia Tech Transportation Institute. This attribution section clarifies all co-authors contributions in these manuscripts.

**Chapter 2** Latest Development in the Processing of Pavement Macrotexture Measurements of High Speed Laser Devices: Daniel Mogrovejo conducted the literature review, collected and processed the data, analyzed the model, developed part of the codification, and prepared the paper. Samer Katicha developed most of the Matlab code, reviewed the paper, and provided suggestions for revisions. Gerardo Flintsch and Edgar de León Izeppi reviewed the paper and provided suggestions for revisions.

**Chapter 3** Adaptive Spike Removal Method for High Speed Pavement Macrotexture Measurements by Controlling the False Discovery Rate: Daniel Mogrovejo conducted the literature review, collected and processed the data, evaluated the models, worked on part of the codification, and prepared the paper. Samer Katicha worked on the structure of the code, contributed with the methodology, reviewed the paper, and provided suggestions for revisions. Edgar de León Izeppi contributed to the formulation of the method, helped with the analysis, and provided ideas and suggestions for revisions. Gerardo Flintsch contributed reviewed the paper and provided suggestions for revisions.

**Chapter 4** Enhancing Pavement Surface Macrotexture Characterization by Using the Effective Area for Water Evacuation: Daniel Mogrovejo conducted the literature review, collected and processed the data, developed the computer code, evaluated all the models, and prepared the paper. Samer Katicha contributed with suggestions for the codification, and methodology implementation, provided suggestions for revisions. Edgar de León Izeppi contributed with ideas on the method, supported literature review, and provided suggestions for revisions. Gerardo Flintsch contributed with the method and interpretation, reviewed the paper, and provided significant suggestions for revisions.

## REFERENCES

[1] McGhee, K. K., and G. W. Flintsch. High-Speed Texture Measurement of Pavements.In, United States, 2003. p. 30p.

[2] International Organization for Standardization. *Characterization of pavement texture by use of surface profiles* https://www.iso.org/obp/ui/#iso:std:iso:13473:-5:ed-1:v1:en. Accessed 1/21/2015.

[3] Loprencipe, G., Cantisani, G. Unified Analysis of Road Pavement Profiles for Evaluation of Surface Characteristics. *Canadian Center of Science and Education,* Vol. 7, 2013.

[4] Rasmussen, R. O. Pavement texture fundamentals. *CE News,* Vol. 25, No. 7, 2013, pp. pp 48-50.

[5] Flintsch, G. W., E. De Leon, K. K. McGhee, and I. L. Al-Qadi. Pavement Surface Macrotexture Measurement and Applications.In, National Research Council, 2003. pp. 168-177.

[6] Harwood, D. W., H. American Association of State, O. Transportation, B. National Research Council . Transportation Research, and A. United States. Federal Highway. *Use of rumble strips to enhance safety*. National Academy Press, Washington, D.C, 1993.

[7] Ulrich, P., J. Medzorian, M. Chawla, M. Gunaratne, and N. Bandara. Correlation of Tire Wear and Friction to Texture of Concrete Pavements. *Journal of Materials in Civil Engineering,* Vol. 12, No. 1, 2000, pp. 46-54.

[8] Sprinkel, M. M., Roosevelt, Daniel S., Flintsch, Gerardo W., de León, and E. Izeppi, Mokarem, David W. . Evaluation of the Cargill SafeLane TM Surface Overlay.In, Charlottesville, 2009. p. 55.

[9] Kasbergen, C., K. Anupam, A. Scarpas, and S. K. Srirangam. Hydroplaning of Rolling Tires under Different Operating Conditions.In. pp. 561-572.

[10] Rasmussen, R., S. Karamihas, E. Mun, and G. Chang. Relating pavement texture to tire-pavement noise.In *35th International Congress and Exposition on Noise Control Engineering, INTER-NOISE 2006, December 3, 2006 - December 6, 2006, No. 1*, Institute of Noise Control Engineering of the USA, Honolulu, HI, United states, 2006. pp. 422-431.

[11] Rasmussen, R., Bernhard, R., Sandberg, U., Mun, e. *The Little Book of Quieter Pavements* FHWA-IF-08-004, Washington,, 2007.

[12] Mogrovejo, D. E., G. W. Flintsch, E. De León, and K. K. McGhee. Tire-Pavement Noise Evaluation and Equipment Comparison Using On Board Sound Intensity Methodology over Several Pavement Surfaces in Virginia. *Transportation Research Board*, 2013.

[13] Amos, D. Pavement Smoothness and Fuel Efficiency: An Analysis of the Economic Dimensions of the Missouri Smooth Road Initiative In, Missouri Department of Transportation 2006.

[14] Yero, S., Hainin, M., Yacoob, H. Determination of Surface Roughness Index of Various Bituminous Pavements *International Journal of Research and Reviews in Applied Sciences,* Vol. 13, 2012.

[15] NCHRP. Evauation of Pavement Friction Characteristics. *Transportation Research Board*, 2000.

[16] Sprinkel, M., McGhee, K., de León Izeppi, e. Virginia High Friction Surface Treatments, Friction and HFST Workshop.In, 2014.

[17] Snyder, M. Current Perspectives on Pavement Surface Characteristics.In, 2014.

[18] Flintsch, G. W. T., Lijie; Katicha, Samer; de Leon, Edgar; Viner, Helen; Dunford, Alan; Nesnas, Kamal; Coyle, Fiona; Sanders, Peter; Gibbons, Ronald; Williams, Brian; Hargreaves, David; Parry, Tony; McGhee, Kevin; Larson, Roger M.; Smith, Kelly. Splash and Spray Assessment Tool Development Program: Final Report.In, FHWA - VTTI, 2014.

[19] ASTM. ASTM E2157-09 Standard Test Method for Measuring Pavement Macrotexture Properties Using the Circular Track Meter In, ASTM International, PA 19428-2959. United States, 2009.

[20] Perera, R. Development of Procedures to Characterize and Validate Macrotexture Measurements.In, 2014.

[21] LMI-Technologies. Selcom Optocator User's manual.In, LMI Technologies INC., Sweden, 2013.

[22] VTTI. *Virginia Smart Road*. https://www.vtti.vt.edu/smart-road/virginia-smart-road.html Accessed July 7th, 2014, 2014.

# Chapter 2 - LATEST DEVELOPMENT IN THE PROCESSING OF PAVEMENT MACROTEXTURE MEASUREMENTS OF HIGH SPEED LASER DEVICES [1]

## ABSTRACT

Pavement macrotexture is an important property that affects tire-pavement interactions like friction, tire-pavement noise, splash and spray, and rolling resistance. Macrotexture measurement is generally divided into two classes: static measurements and dynamic measurements. Dynamic measurements are performed with vehicle mounted lasers that measure macrotexture at traffic speed. One drawback of these laser devices is the presence of "spikes" in the collected data which causes erroneous texture measurements. In this paper, we develop a data driven adaptive method that detects and removes the spikes from high speed laser texture measurements. The method is based on the discrete wavelet transform and can be summarized in the following three steps: (1) calculate the discrete wavelet transform of texture measurements, (2) detect and remove the "spikes" from the obtained wavelet coefficients, and (3) calculate the inverse discrete wavelet transform with the processed wavelet coefficients to obtain Mean Profile Depth (MPD) measurements with the "spikes" removed. The crucial step in the proposed method is step 2 which we detail in this paper. We compare the results of calculated MPD obtained by removing the "spikes" with the proposed method with the results obtained without removing the "spikes", and validate the proposed method with MPD measurements obtained with a Circular Texture Meter (CTMeter).

_____

13

## INTRODUCTION

Pavement surface texture, specifically pavement macrotexture is an important property that affects friction, tire-pavement noise, splash and spray, and rolling resistance. Adequate surface macrotexture of a pavement is essential to: prevent accidents, provide good skid resistance, prevent accidents by efficiently drain water out of the contact area, reduce splash and spray, mitigate tire-pavement noise, among other benefits. Macrotexture measurements are generally divided into two classes: static measurements and dynamic measurements. Dynamic measurements are obtained with vehicle mounted lasers that measure macrotexture at traffic speed. The type of lasers used by the available commercial systems vary and therefore the measuring capabilities of the device. A sub-classification can also be made according to the following two laser configuration: (1) laser beams, that acquire data continuously with more than one laser point (normally distributed transversally), and (2) single point lasers.

### Problem statement

A drawback of laser devices is the presence of "spikes" in the collected data. These spikes make measurements inaccurate and cause erroneous calculated texture (mean profile depth) values. Therefore, identifying and removing these spikes is essential to obtaining accurate MPD measurements.

## OBJECTIVE

The main objectives of this study are to: (a) Develop a method that can objectively identify and remove the spikes from the collected data, (b) Compare the results of the calculated mean profile depth (MPD) obtained by removing the "spikes" with the proposed method with the results obtained without removing the "spikes" and (c) Validate the method with MPD measurements obtained with a Circular Texture Meter (CTMeter) taken at the same locations.

## BACKGROUND

### The Presence of Spikes in Laser Measurements

Although there has been a considerable advancement in high speed laser texture measurement devices, the presence of spikes in laser measurements has hindered the adoption of these devices. Goubert & Bergiers point out this issue highlighting the fact that it appears that the quality of measurements has not improved in recent years for laser profilometers *(1)*. They clearly state that, besides the traditional low-pass filtering, slope suppression, and drop out correction, the calculation of MPD values must be free of erroneous data such as spikes.

Perera and Kohn *(2)* and Sayers and Karamihas *(3)* have observed the presence of spikes in pavement profile measurements, with Perera and Kohn suggestions that the change in surface reflectivity caused by pavement markings, silica, polished aggregates, water, etc., could potentially be the source of these spikes. Our work at the Virginia Tech Transportation Institute (VTTI) has also highlighted this issue and this paper presents a detailed method to identify and remove spikes from high speed laser texture measurements using the wavelet transform

### Basic theory about Wavelet Transform analysis

The wavelet transform (WT) is a particularly useful for signal processing *(4),* which makes this type of transform ideal to analyze pavement texture data gathered with lasers. Wavelet transform analysis uses wavelike functions known as wavelets to transform the signal into another representation which presents the signal information in a more useful form, this transformation of the signal is known as the wavelet transform *(4,5)* and the resulting signal representation is given in both time and scale. The main feature of the wavelet transform that allows us to use it to identify and remove the spikes is that the wavelet

coefficients that result from the presence of the spikes will be significantly larger than the rest of the coefficients therefore singling out the location of the spikes in the collected data.

*Analyzing texture with a wavelet transform*

Different families or selection of wavelet can be used for signal analysis, with some of the most common wavelets shown in Figure 2-1. The choice of best wavelet for a particular application depends on both, the nature of the signal and what we require for the analysis *(4)*. In our case we are interested on discovering (and later on removing) the spikes (or outliers) from the profile texture signal, therefore a Discrete Wavelet Transform type Haar, that allows to look for 'differences' between adjacent data points at different levels may be the best option (more detailed explanation will be provided below).
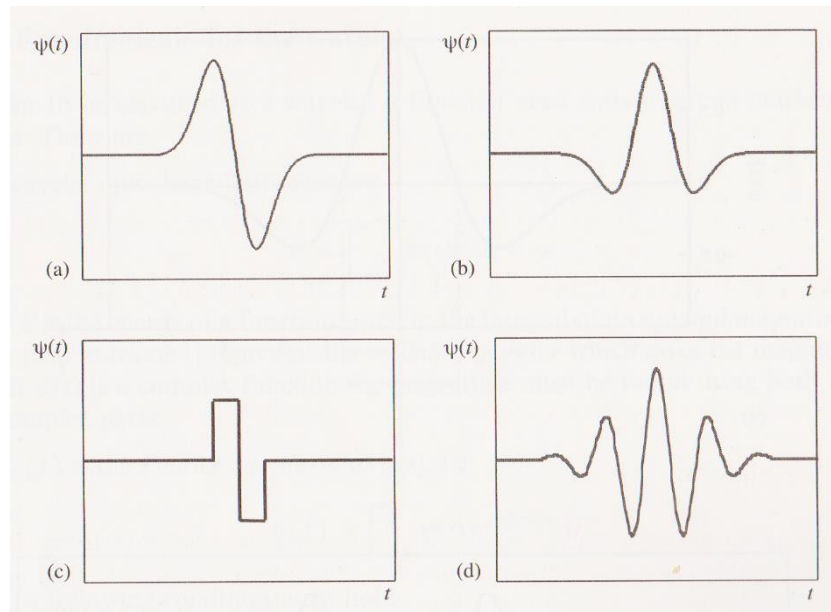


Figure 2-1 Commonly used wavelets. (a) Gaussian wave.
(b) Mexican Hat. (c) Haar. (d) Morlet.

## METHODOLOGY

### Test Site

An asphalt section that consists of a 38 mm SM 9.5D surface mix (where: "SM" means Surface Mix, "9.5" represents the maximum aggregate size in millimeters, and "D" represents type of binder in this case D=70-22), located at the Virginia Smart Road was selected for testing the proposed methodology. Pictures of the section are presented in Figure 2-2

Figure 2-2 test locations

## Equipment and Field Data Collection

Both, static and dynamic measurements were taken for this study. Static reference measurements were taken with the CTMeter device following the ASTM E2157 *(6)*. Dynamic Measurements were taken with a High Speed Laser Device (HSLD) at 50 mph with a laser sampling frequency of 64 kHz. Detailed information about this dynamic device can be found in *(7)*.

Seventy two CTmeter Measurements were taken within a 20 meter section of the pavement, varying the equipment locations longitudinally along the wheel path, and transversally offsetting the measurements along the same path. Individual CTmeter sector measurements (corresponding to the 8 CTmeter sectors) were used for the analysis giving a total of 576 mean profile depth (MPD) measurements from the Control device. An analysis of variance (ANOVA) was performed for this CTmeter set of data points to assess the influence of offsetting the equipment and moving it longitudinally along the control section, detailed information about this analysis is presented in the results Section.

Within the same 20 meters, 5 runs at 50 mph with the high speed laser device were performed resulting in a total of 200 MPD measurements for each run. Figure 2-3 below depicts the static and dynamic equipment used for the analysis.
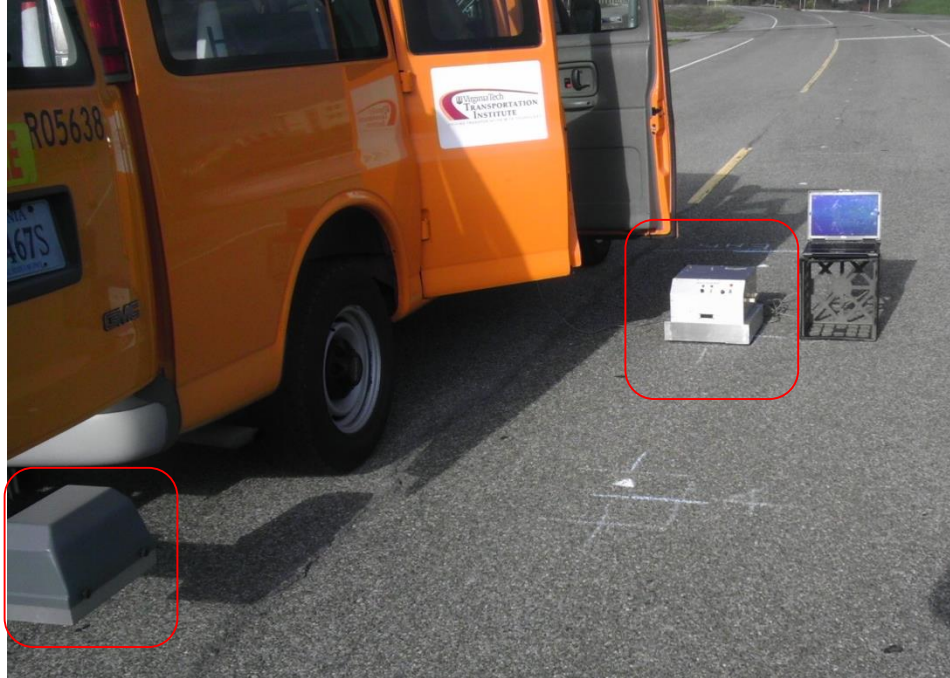
Figure 2-3 High Speed Laser Device (left), and Circular texture Meter (right)

**Proposed Methodology for Spikes Removal for the High Speed Laser Measurements**

The proposed method is based on the discrete wavelet transform and can be summarized in the following three steps:
1. Calculate the discrete wavelet transform of texture measurements,
2. Detect and remove the "spikes" from the obtained wavelet coefficients, and
3. Calculate the inverse discrete wavelet transform with the processed wavelet coefficients to obtain MPD measurements with the "spikes" removed.

*1. Discrete wavelet transform decomposition level*

First, we need to choose the adequate decomposition level to perform the wavelet transform. Because MPD is calculated over a 100 mm length and texture measurements were obtained at 0.5 mm intervals, the maximum decomposition level, j, used is 8, which ensures that the whole 100 mm length is investigated for the spikes (at each decomposition level, j, the number of data points being considered is $2^j$; therefore, $2^8 = 256$ data points every 0.5 mm means 256*0.5 = 128 mm)

*2. Spikes detection and removal*

**Defining the Distribution of Wavelet Coefficients**: The method is based on the wavelet transform and the characteristics of the wavelet coefficients of the texture measurements. As a background, wavelet coefficients of many signals have been shown to follow certain probabilistic distributions (this has been mostly studied for the case of images). Azzalini, A. et al. *(8)* showed that the correct choice of the threshold for de-noising depends on the distribution and, thus, the first step will be the accurate definition of the distribution of the wavelet coefficients. Some distributions that have been used by the authors during this analysis for this purpose include the Gaussian (normal) distribution, the Laplace distribution, and mixtures of distributions (e.g. mixture of Laplace and Gaussian distributions).

Figure 2-4 shows one of the measured texture profile (about 40,000 measurements every 0.5 mm along 20 m over the control section).
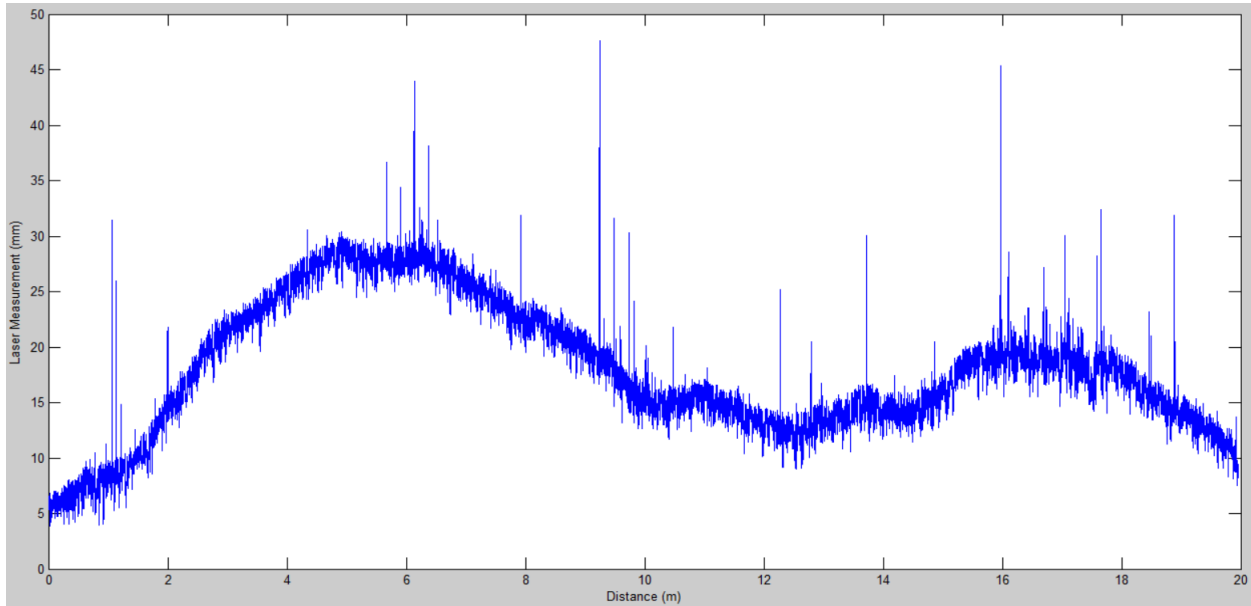


Figure 2-4 Texture Measurements

Figure 2-5 shows the distribution (histogram) of the wavelet coefficients at the finest scale of the measured texture. The histogram spans a long range because of the spikes (outliers) in the data. Figure 2-6 shows the histogram zoomed in with a Gaussian distribution fit (red dashed line) and a Laplace distribution fit (black dotted line). The distributions do not exactly match the histogram but the data seems to be somewhere in between. Figure 2-7 shows a mixture (50%/50%) of the Gaussian and the Laplace distribution which fits the data quite well. This distribution definition helps defining the adequate threshold and standard deviation to be used in the definition of what will be considered as outliers (as explained following).
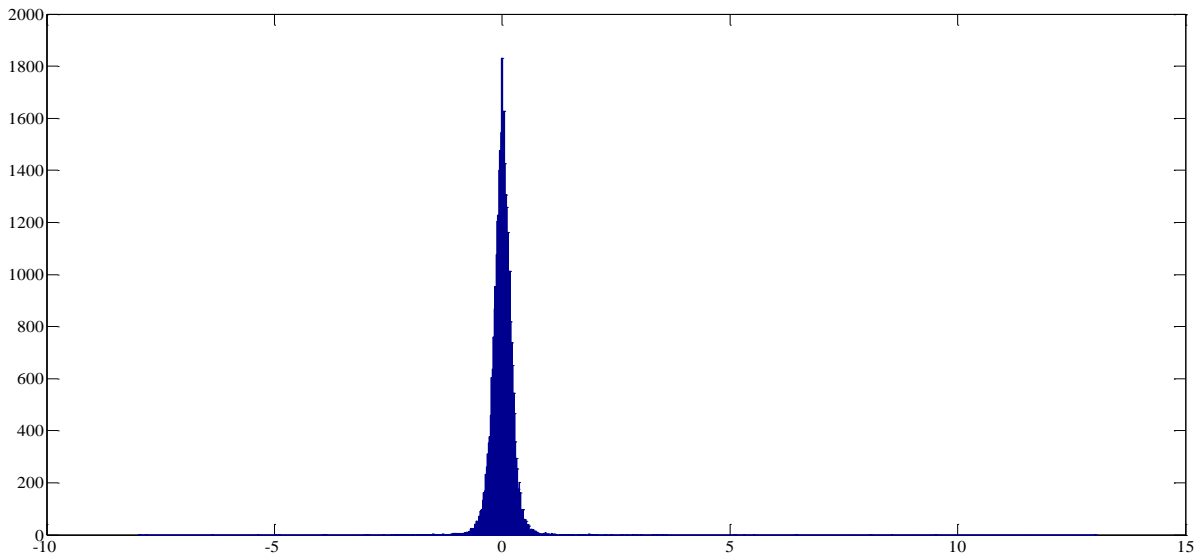


Figure 2-5  Histogram of Finest Scale Wavelet Coefficients

18
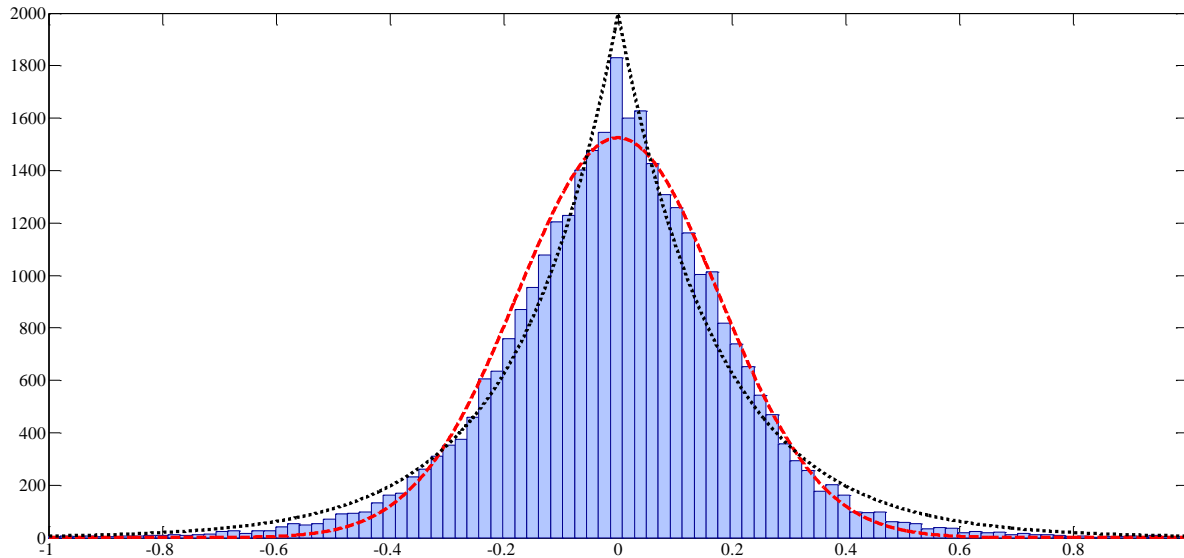
Figure 2-6  Zooming on the Histogram with Gaussian and Laplace Distribution Fits
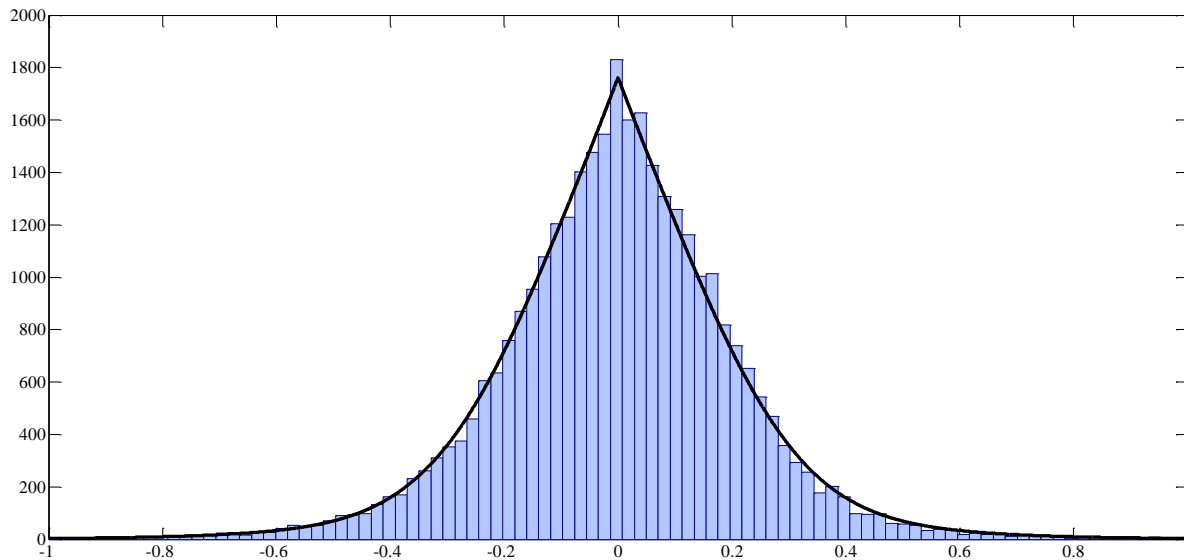


Figure 2-7  Mixture (50%) of Gaussian and Laplace Distribution Fits

**Identifying Outliers (Spikes)**:  Spikes (outliers) are identified as the wavelet coefficients that are significantly larger than the coefficients that are expected from the distribution that is fitted to the histogram.  Figure 2-7 shows that the mixture of the two distributions provides a good representation of the empirical distribution (histogram) of the calculated wavelet coefficients.

The spikes are identified by applying a threshold that determines whether a wavelet coefficient results from a spike. A simple and effective threshold is the so called universal threshold that was first proposed by Donoho and Johnstone *(9)* in the content of wavelet transform denoising.  For a given distribution, if we randomly sample $n$ observations from that distribution, the universal threshold is a threshold that is with high probability larger than all the $n$ observations. What this means is that any measurement larger than the universal threshold has a high probability of being a spike (outlier).

The universal threshold depends on the number of measurements, $n$. Mathematically, if we label the universal threshold as a function of $n$, $\lambda_u(n)$, and we have $n$ measurements $X_i$ (with $i = 1 \ldots n$) from the distribution, as $n \to \infty$:

$$P\left\{ \max_{1 \le i \le n} |X_i| > \lambda_u(n) \right\} \to 0 \qquad \text{Eq. 2.1.}$$

Where $P$ stands for probability. This indicates the probability of having a measurements from the distribution larger than the universal threshold tends to zero.

For the standard Gaussian distribution, the universal threshold ($T_G$) is:

$$T_G = \lambda_u(n) = \sqrt{2 \log n} \qquad \text{Eq. 2.2.}$$

Which gives 3.0349, 3.7169, 4.219, and 4.6518, for $n$ equal to 100, 1000, 10000, and 50000. Clearly, the thresholds are high (and larger than the threshold of the well-known 6 sigma method, which is 3).

For the standard Laplace distribution, the universal threshold ($T_L$) is:

$$T_L = \lambda_u(n) = \sqrt{\frac{1}{2} \log n} \qquad \text{Eq. 2.3.}$$

Which gives 3.2563, 4.8845, 6.5127, and 7.6507 for $n$ equal to 100, 1000, 10000, and 50000. These are much higher than the case of the Gaussian distribution because the Laplace distribution has a heavier tail.

Since a Gaussian and Laplace distribution mixture (50% each) fits the empirical distribution (histogram) of the wavelet coefficients very well, an adequate threshold can be calculated as the average of the two thresholds as shown below (the good fit of the distribution confirms the robustness of the following equation):

$$T_{ave} = \frac{(T_G + T_L)}{2} \qquad \text{Eq. 2.4.}$$

With the same concept in mind about the wavelet coefficients histogram, the following definition of the adequate standard deviation values is defined below:

$$\sigma_{ave} = \sqrt{\left(\frac{\sigma_G^2 + \sigma_L^2}{2}\right)} \qquad \text{Eq. 2.5.}$$

Where $\sigma_G = 1.4826 * MAD$, and $\sigma_L = 2.0404 * MAD$; $\sigma_G$ and $\sigma_L$ represent the standard deviation for data points following a Gaussian and a Laplace distribution respectively; and $MAD$ represents the median absolute deviation. The MAD is used (instead of the mean) basically because it is robust to outliers *(10,11).*

Finally, after defining the universal threshold, and the standard deviation equations for the Gaussian and Laplace distribution and its averages, the boundaries (B) are defined as follows:

$$B(\sigma, T) = T_{ave} * \sigma_{ave} \qquad \text{Eq. 2.6.}$$

**Spikes Removal**: Wavelet coefficients that have an absolute value larger than the boundary $B(\sigma,T)$ are identified as outliers and removed; the inverse wavelet transform is then used to obtain the texture measurements without the spikes.

Figure 2-8 compares the results before and after the spike removal process.

*3. Mean Profile Depth Calculation*

The MPD calculations were performed according to the ASTM E1845-09 *(12)*. MPD measurements were obtained every 100 mm along the 20 m section.
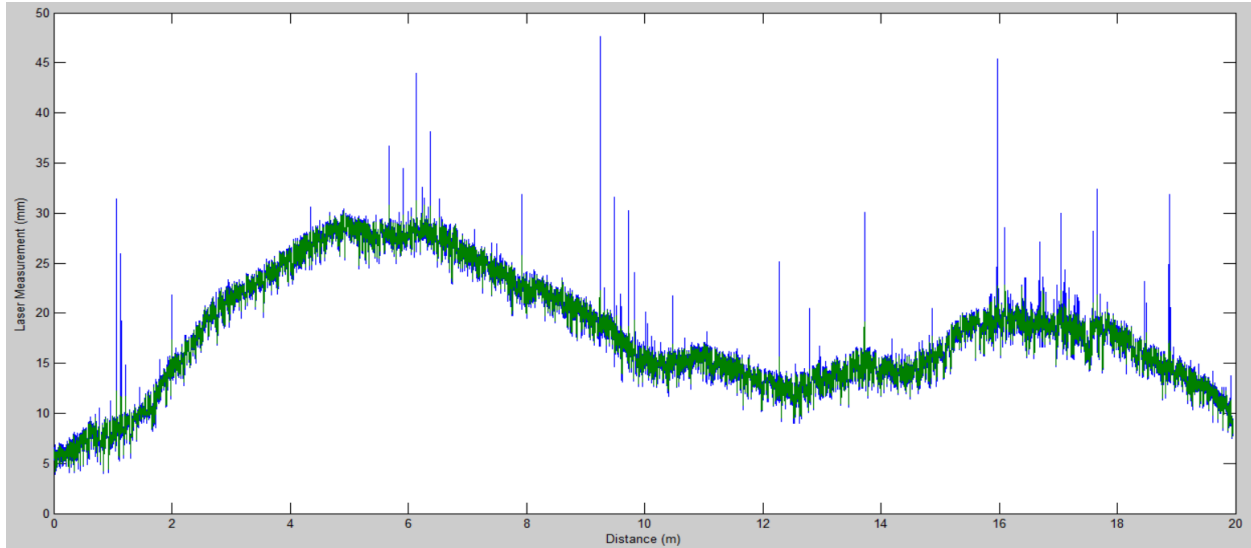


Figure 2-8 Texture Measurements: Original Data (in blue), and Spikes Removed (in green)

**RESULTS**

**Validation**

To validate the results of the proposed method, we compared the computed texture values with the MPD measurements obtained using the CTmeter as the reference device. We first evaluate the variability of the CTmeter as a function of test location and measurement sector. For the test location, we performed CTmeter measurements at 6 different locations along the longitudinal path in the outer wheelpath, and 6 more in-between (off) the wheelpaths, considering the individual result for each one of the 8 CTmeter sectors along this 12 different locations, a total number of 96 data points were used for the analysis. A 3-way analysis of variance (ANOVA) test was performed to evaluate effect of transversal shifting (in and off wheelpath) (X1), longitudinal shifting (X2), and CTmeter sector (X3). The results of the ANOVA are presented in Table 2-1

Table 2-1 N-Way ANOVA for 3 variables

| Source | Sum Sq. | d.f. | Mean Sq. | F | Prob>F |
|--------|---------|------|----------|------|--------|
| X1 | 0.03974 | 1 | 0.03974 | 0.46 | 0.5016 |
| X2 | 0.4261 | 5 | 0.08522 | 0.98 | 0.437 |
| X3 | 0.74054 | 7 | 0.10579 | 1.21 | 0.3053 |
| Error | 7.15424 | 82 | 0.08725 | | |
| Total | 8.36063 | 95 | | | |

21

By looking at the last column on Table 2-1, all the p-values for the three analyzed variables are high (p-values → 0 are significant). This indicates that CTmeter sector, longitudinal spatial location of the test, and whether the test is performed in the wheelpath or off the wheelpath have no effect on the measured MPD. This is an important result as it allows us to compare the CTmeter with the high speed device without having to worry about an exact match for the test location.

The MPD results are summarized in Figure 9. The results include MPD calculated directly from the measurements, MPD calculated using the measurements processed with the software provided by the manufacturer (using a 2.5 mm low-pass filter), MPD calculated using the proposed method, and the MPD calculated from the CTmeter. The plot in Figure 9 shows the mean (red dot), median (line), 50 percent range (box), and the maximum and minimum (whiskers). Because of the spikes, the mean MPD calculated by the commercial software is about 50% larger than the mean MPD calculated by the CTmeter (2.1 mm compared to 1.4). Processing the measurements with the proposed method, the mean MPD calculated by the high speed laser device resulted to be to be essentially the same as the mean MPD calculated by the CTmeter (1.4 to 1.45 compared to 1.4).
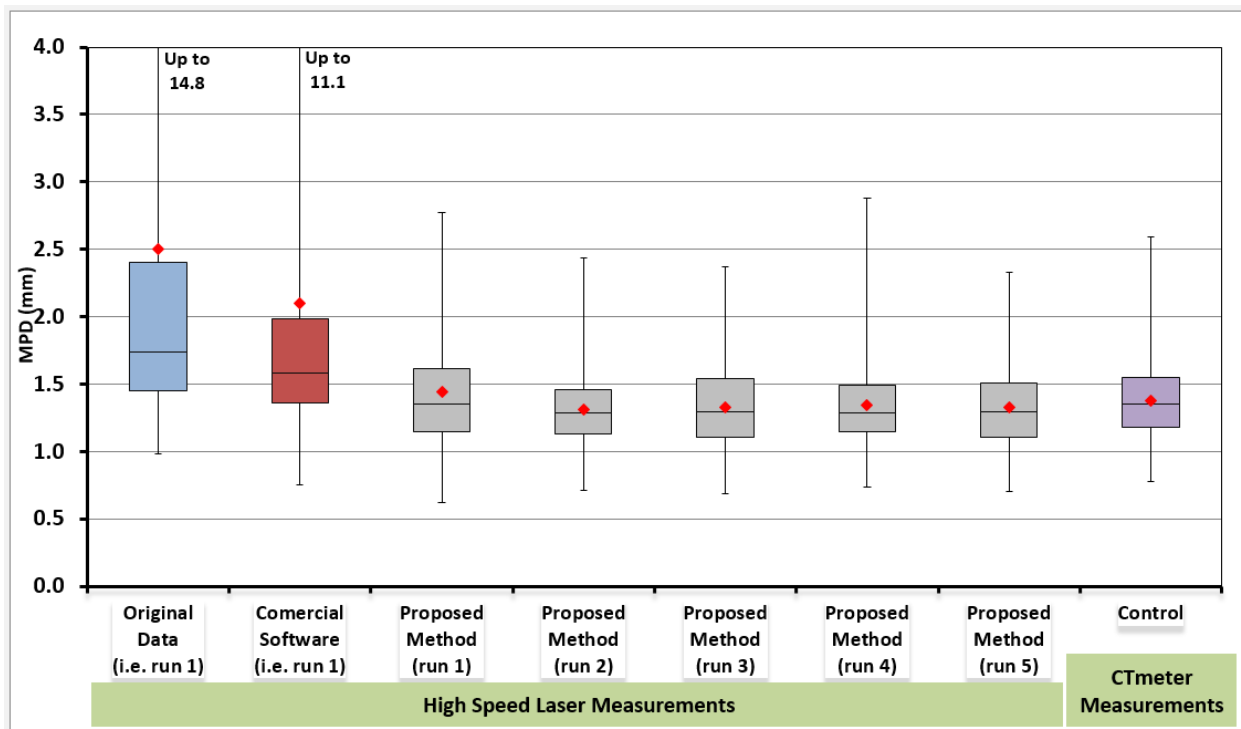


Figure 2-9 Box and Whiskers comparison for MPD measurements

In general, the range of MPD values calculated by the high speed device is slightly wider than that calculated by the CTmeter. This is expected as much more measurements are obtained from the high speed device which increases the probability of observing larger extreme values. Another interesting result is that the median MPD is a much better estimate of the pavement MPD when the spikes are not removed since it is more robust than the mean to the presence of spikes in the measurements.

## CONCLUSIONS

In this paper, we propose a method to detect and remove spikes in high speed laser texture measurements based on the discrete wavelet transform. The method was validated by comparing MPD measurements calculated from the high speed device after spikes were removed with MPD measurements with a CTmeter. The variability of MPD measurements obtained by the CTmeter was also investigated.

The main findings of the paper can be summarized as follows:

1. The CTmeter sector, spatial location longitudinally, and whether the measurements were collected in the wheelpath or off the wheelpath did not have an effect on the MPD. This allowed us to confidently compare measurement from the high speed device and the CTmeter without having to worry about exactly matching the location of measurements. It must be noted that the road section is from a test track that has very little traffic that may create changes of texture in the wheel path.

2. Spikes in the measurements collected with the high-speed laser devices resulted in calculated MPD values that were about 50% higher than those provided by the CTmeter. Removing the spikes with the proposed method resulted in mean MPD calculated from the high-speed device that were essentially the same as the one calculated from the CTmeter.

3. In all cases, the median seems to be a better choice than the mean in characterizing the MPD of a pavement section as it is much more robust to the presence of spikes (or any outliers).

The method of spike removal proposed in this paper depends on modeling the distribution of the wavelet coefficients of texture measurements. This was done by trial and error, which is a limitation for practical adoption in commercial devices. An automated method would be more practical and is currently being investigated.

**REFERENCES**

[1]    Goubert, L.B.A., About the reproducibility of texture profiles and the problem of spikes. Surf 0079, 2012.

[2]    Perera, R.K., S. , Issues in Pavement Smoothness, A Summary Report. Transportation Research Board, 2002.

[3]    Sayers, M.K., S., Interpretation of Road Roughness Profile Data. 1996, Federal Highway Administration.

[4]    Addison, P., The Illustrated Wavelet Transform Handbook. 2002, London: Institute of Physics Publishing.

[5]    Nason, G.P. and B.W. Silverman, The Stationary Wavelet Transform and some Statistical Applications, in Wavelets and Statistics, A. Antoniadis and G. Oppenheim, Editors. 1995, Springer New York. p. 281-299.

[6]    ASTM, ASTM E2157-09 Standard Test Method for Measuring Pavement Macrotexture Properties Using the Circular Track Meter 2009, ASTM International: PA 19428-2959. United States.

[7]    LMI-Technologies, Selcom Optocator User's manual. 2013, LMI Technologies INC.: Sweden.

[8]    Azzalini, A., M. Farge, and K. Schneider, Nonlinear wavelet thresholding: A recursive method to determine the optimal denoising threshold. Applied and Computational Harmonic Analysis, 2005. 18(2): p. 177-185.

[9]    Donoho, D.J., I, Ideal spatial adaptation by wavelet shrinkage. 1994.

[10]  Ruppert, D. and SpringerLink, Statistics and Data Analysis for Financial Engineering. 2011, New York, NY: Springer New York.

[11]  Hogg, R.V., J. Ledolter. , Engineering Statistics. 1987, New York: MacMillan.

[12]  ASTM, ASTM E1845-09 Standard Practice for Calculating Pavement Macrotexture Mean Profile Depth. 2009, ASTM International: PA 19428-2959. United States.

# Chapter 3 ADAPTIVE SPIKE REMOVAL METHOD FOR HIGH SPEED PAVEMENT MACROTEXTURE MEASUREMENTS BY CONTROLLING THE FALSE DISCOVERY RATE[2]

## ABSTRACT

Tire-pavement interactions, like: friction, tire-pavement noise, splash and spray, and rolling resistance, are significantly influenced by pavement macrotexture. Accurate texture data collection and analysis at a network level is key to achieve the desired level of safety, comfort, and sustainability of pavements. This study focuses on addressing the problem of noise in the form of spikes revealed in dynamic measurements that are performed with vehicle mounted lasers used to measure macrotexture at traffic speed. The presence of "spikes" in the collected data leads to erroneous texture measurements that do not reflect the actual pavement texture profile.

As a solution to this problem, in this paper, the development of an innovative denoising methodology is presented, it consists of an algorithm that: first, determines the distribution of texture measurements by using the family of Generalized Gaussian Distributions (GGD) which allows for the tail of the distribution to be heavier or thinner than the normal distribution; and second, by using the False Discovery Rate (FDR) method that controls the proportion of wrongly identified spikes among all identified spikes. The FRD control allows for an adaptive threshold selection that differentiates between valid measurements and spikes.

Finally, the validation of the method showed that the MPD results obtained with denoised dynamic measurements are comparable to MPD results from the control devices on all the pavement sections investigated, making this method proposal a significant step towards the development of standardized procedures that allow the use of these devices for texture investigation at network level.

_____

## INTRODUCTION

Most of the tire-pavement interactions, such as: friction, tire-pavement noise, splash and spray, and rolling resistance; are significantly influenced by pavement macrotexture *(1)*. Therefore, adequate surface macrotexture is essential to provide good skid resistance and prevent accidents, efficiently drain water out of the contact area to reduce splash and spray, and mitigate tire-pavement noise *(2)*.

The collection of macrotexture at the network level requires measurements at highway speeds. Although laser technology allows the collection of data at high frequency, an accurate data analysis for the dynamic measures is needed to correctly characterize the pavement and help in the design process to balance desired levels of safety, ride quality, and sustainability of pavements.

## Background

Today's technology allows collection and analysis of pavement macrotexture, not only with static, but also with dynamic methods, that can collect the pavement profile with significant precision even at traffic speed. High-speed measurement devices have been evolving and their application to texture investigation at network level is the next step. A standardized procedure for texture measurements at network level is not yet available, and development in this field is needed *(3)*.

Along with this evolution, some problems have emerged. For example, the data collection phase often presents noise in the form of spikes in the measurements. Goubert and Bergiers point out this issue highlighting the fact that it appears that the quality of the laser profilometers has not improved significantly in recent years *(2,4)*. Their study concluded that besides the traditional low-pass filtering, slope suppression, and drop out correction; the calculus of MPD values must be free of spikes *(2)*.

Flintsch et al *(5)* studied harmonization of macrotexture measuring devices and found high correlations between macrotexture measurements taken with laser devices and the CTMeter. However, the laser measurements were generally higher than the ones taken with the CTMeter; for example: for a certain laser device, macrotexture values were 96 % larger than the CTMeter. This large difference between the laser device measurements and the other measurements was thought to be due to the specific method used by to calculate the MPD. Current work at the Virginia Tech Transportation Institute (VTTI) has suggested that even with newer software the problem persists, and new data suggest that the problem could be linked to the presence of spikes.

Perera and Kohn in a National Cooperative Highway Research Program (NCHRP) report indicate that the "analysis of profile data collected by Long Term Pavement Performance (LTPP) profilers revealed problems due to spikes in the data" *(2,6)*. As explained in the problem statement section, a number of different mechanisms may be at play to produce these spikes in the data. A study published by the Federal Highway Administration (FHWA) and conducted by Sayers and Karamihas *(2,7)* also showed the problems of spikes in the data taken for International Roughness Index (IRI) measurements.

## Problem statement

High-speed laser data are subjected to a variety of potential problems during the measurement process. Besides calibration and assembly (systematic errors that are supposed to be taken care of before the fieldwork), many variables produce noise in the measurements.

For example, shiny mirror-like surfaces change the amount and direction of light reflected to the receiving lens, and black materials scatter only a small part of the incident light. Black and shiny materials (like fresh asphalt) have both of these problems overlapped. Transparent/semitransparent materials (e.g., pavements with these types of minerals in the aggregate, reflective paint on the road, etc.) will cause offsets in the reflection, and will also absorb/deviate a portion of the light *(8)*.

Other variables, such as temperature, geometry, secondary reflections, bandwidth, sample rate, etc., are also potential sources of noise in the measurements. This generated noise is often presented in

the form of spikes in the collected data, which can create biases on the texture measurements. There is, therefore, a need for removing these spikes in order to get accurate macrotexture measurements.


**OBJECTIVE**
The main objectives of this study are to: (a) develop an innovative methodology that can objectively identify and remove the spikes from the collected data, (b) test this methodology with real data collected over different pavement surfaces, (c) calculate and compare the mean profile depth (MPD) values obtained before and after removing the spikes and their associated statistical parameters, and (d) validate the proposed method by comparing the results with the ones obtained by the Circular Texture Meter (CTMeter), chosen as the standardized control method.


**METHODOLOGY**
In the developed methodology, spikes are identified as outliers not belonging to the distribution of the texture measurements. The methodology consists of an algorithm that first determines the distribution of texture measurements and second determines which measurements are outliers and therefore spikes. The details of each step are presented below


**Texture Measurements Distribution**

One important aspect of outlier identification is to first determine what is a valid measurement, specifically what is the distribution of valid measurements. Once this distribution is determined, measurements that are (very) unlikely to belong to the determined distribution are flagged as outliers. As an example, pavement researchers are generally familiar with the normal distribution and the 3 sigma threshold of outlier detection. While the method we propose is similar to the 3 sigma with the normal distribution, we do not specify a priori that the texture measurements are normally distributed and that the 3 sigma threshold is the appropriate threshold to detect the outliers. This is because in practice, texture measurements are not normally distributed and a fixed choice of threshold is not appropriate when a large number of measurements are analyzed. For the measurements distribution, we use the family of Generalized Gaussian Distributions (GGD) which allows for the tail of the distribution to be heavier or thinner than the normal distribution. The GGD is a parameterized family of distributions with a shape parameter $\beta$. A value of $\beta = 2$ gives the Gaussian (normal) distribution while a value of $\beta = 1$ gives the Laplace (double exponential) distribution. Figure 3-1 shows the GGD with different values of $\beta$. The probability density function of the GDD is as follows:

$$p(x) = \frac{\beta}{2\alpha\Gamma(1/\beta)} \exp\left(-\left(\frac{|x-\mu|}{\alpha}\right)^{\beta}\right)$$

Eq. 3.1.

Where: $\beta$ is a shape parameter (positive), $\alpha$ is a scale parameter related to the variance (positive), and $\mu$ is a location parameter (average).

Figure 3-2 shows the distribution of texture measurements obtained on a 20 m pavement section. The empirical distribution is not symmetric and two different GGDs were fitted to the positive and negative texture measurements. For the positive texture, a GGD with a parameter $\beta = 2.4$ fitted the data while for the negative texture, a GGD with a parameter $\beta = 1.41$ fitted the data. To obtain the parameter $\beta$, the distribution is fitted to the 90th to 97th percentiles of the data. The reason this range was chosen is because the tail of the distribution determines whether a data point is an outlier or not and therefore the fit should be done to the higher percentiles of the data. The reason for not including percentiles higher than 97 % is because higher percentages could actually be outliers in the data. A 97 % limit ensures that the GGD fit will be robust to the presence of as much as 3 % of outlier data. If it is suspected that more than 3

27

% of the measurements are contaminated with spikes, the upper percentile limit can be lowered. In practice, barring the presence of factors such as a wet pavement, the percentage of data contaminated with outliers is significantly lower than 3 % (in the data we present later, the percentage of outliers is about 0.13 %).
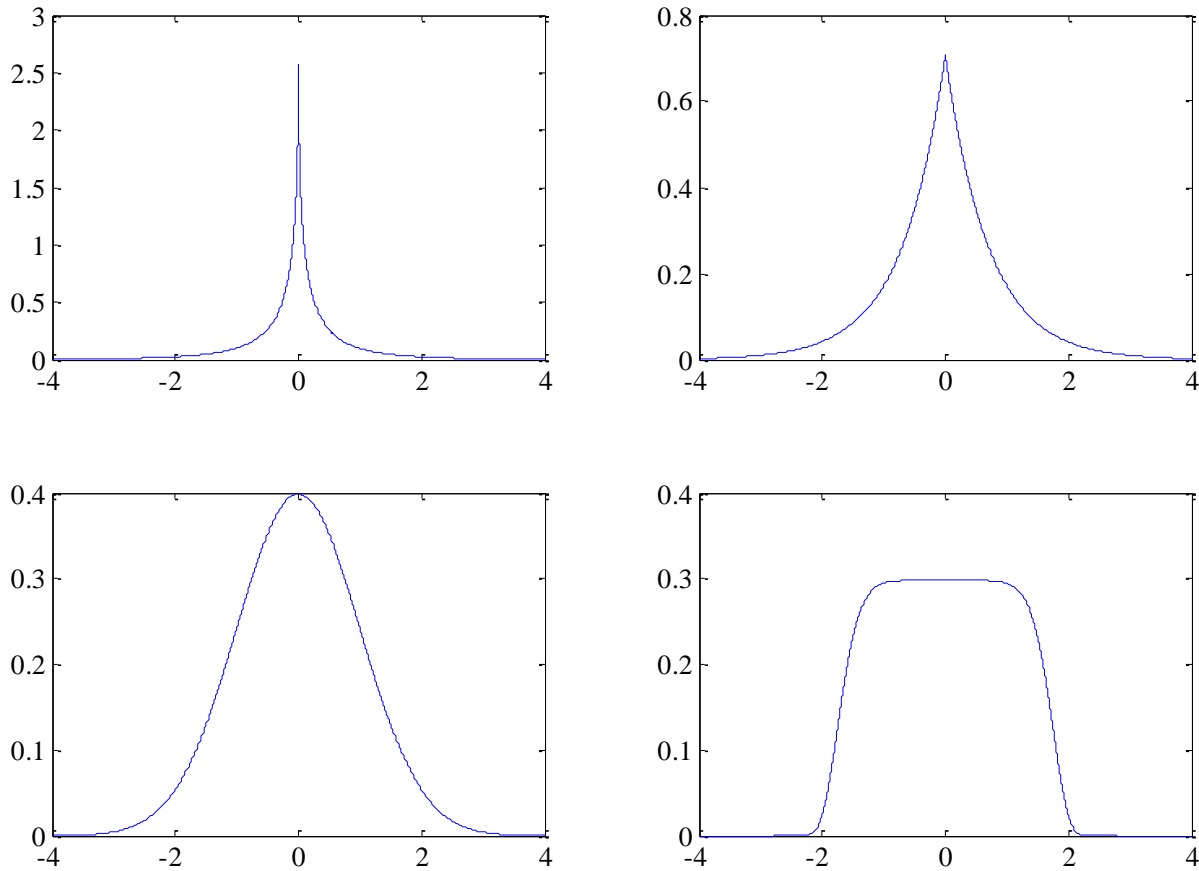


Figure 3-1 Generalized Gaussian Distribution; Top Left: $\beta = 0.5$; Top Right: $\beta = 1$ (Laplace distribution); Bottom Left: $\beta = 2$ (normal distribution); Bottom Right: $\beta = 8$.
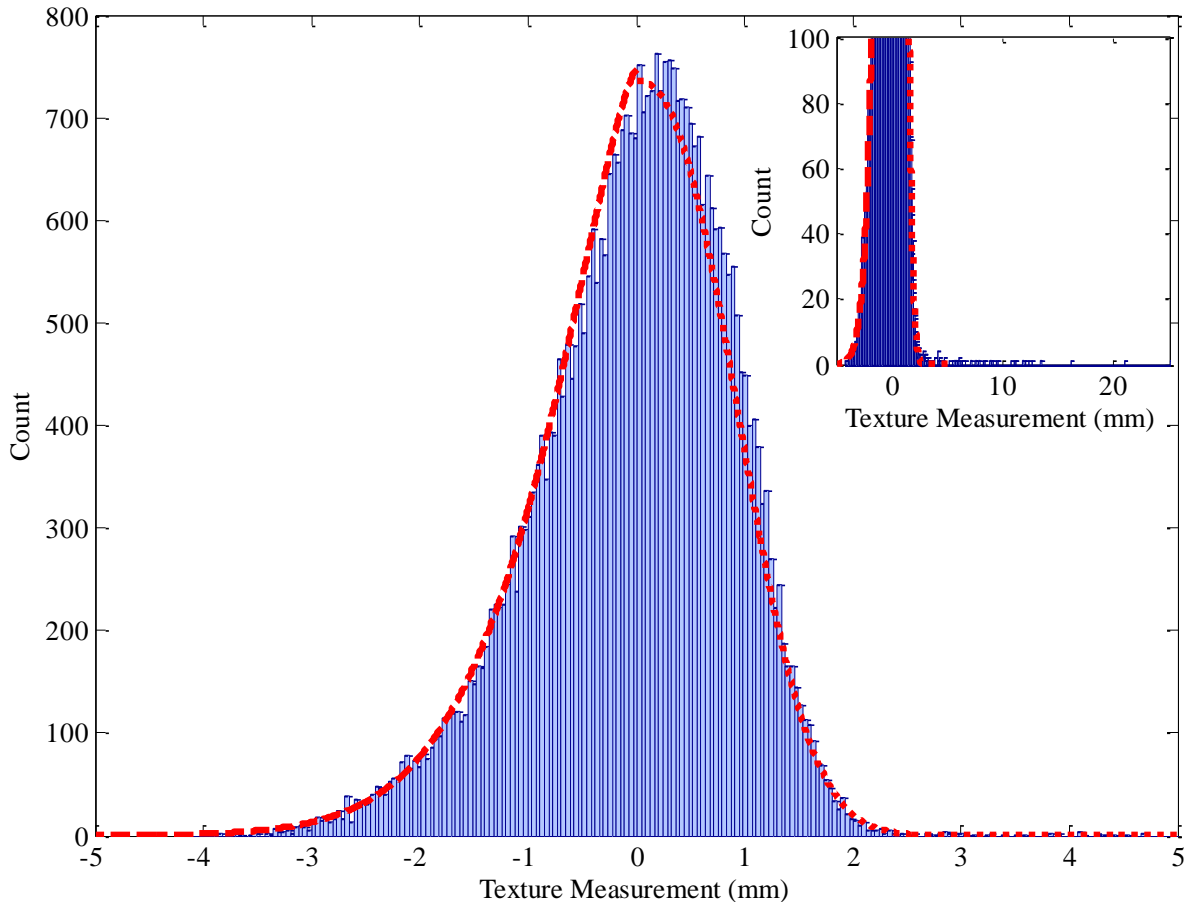
Figure 3-2 Distribution of texture measurements and GGD fit to positive and negative texture measurements. Note that the GDD is fit to the extreme ends of the histogram because the tails of the distribution determined which measurements are outliers. Inset: texture distribution details showing outliers.

Outlier Detection Threshold

Once the distribution is determined, a threshold to identify outliers needs to be applied to remove the spikes in the data. To give a simple explanation of threshold selection, suppose the normal distribution was found to fit the texture distribution. A popular choice of threshold might be 2 sigma (which approximately covers 95 % of the distribution) or 3 sigma (about 99 %). While these choices seem reasonable based on "standard practice" in pavement research, they fail to address one crucial aspect of high speed texture measurement – the large amount of data collected. For example, in a 20 m pavement section, collecting data at an interval of 0.5 mm will result in 40,000 measurements. Suppose the distribution of these measurements is normal and that none of the measurements is affected with spikes; using a 2 sigma threshold to identify spikes (outliers), on average, 2,000 of the collected measurements will be identified as spikes. Even with using 3 sigma as a threshold, 400 measurements will be identified (when actually none of the measurements is an outlier). Clearly this choice of threshold is not appropriate.

A possible adjustment to the threshold is to use a Bonferroni correction. The Bonferroni correction consists of dividing the p-value of the significance test by the number of observations. For example, for the 95% interval, the p-value is 0.05; with 40,000 measurements, Bonferroni correction adjusts the p-value of 0.05 to 0.00000125 (=0.05/40,000). While this will solve the problem of wrongly identifying outliers, it will miss detecting outliers that are just under the Bonferroni threshold. Figure 3-3

illustrates situations that are problematic for the 2-sigma approach and the Bonferroni approach with 40,000 measurements from a normal distribution with and without outliers. In the case without outliers, the 2-sigma approach will on average wrongly identify 2,000 outliers. The Bonferroni correction will result in a threshold of 4.71 and in general identify no outliers (there is a 0.05 probability that one or more measurements are flagged as outliers using the Bonferroni correction). In the case with 2,000 outliers at a threshold of 4.5, the 2-sigma approach will identify all the outliers (along with many non-outliers) while the Bonferroni approach will not identify any outlier (because of the 4.71 threshold). To address the shortcomings of the 2-sigma and the Bonferroni correction, we use the False Discovery Rate (FDR) approach which adapts to the data, to determine the threshold. Figure 3-3 shows that in the case in which there are no outliers, the FDR threshold is high (actually equal to the Bonferroni threshold in this case) while for the case in which there are outliers, the FDR threshold is low so that these outliers are identified. We present the FDR method in the following section.
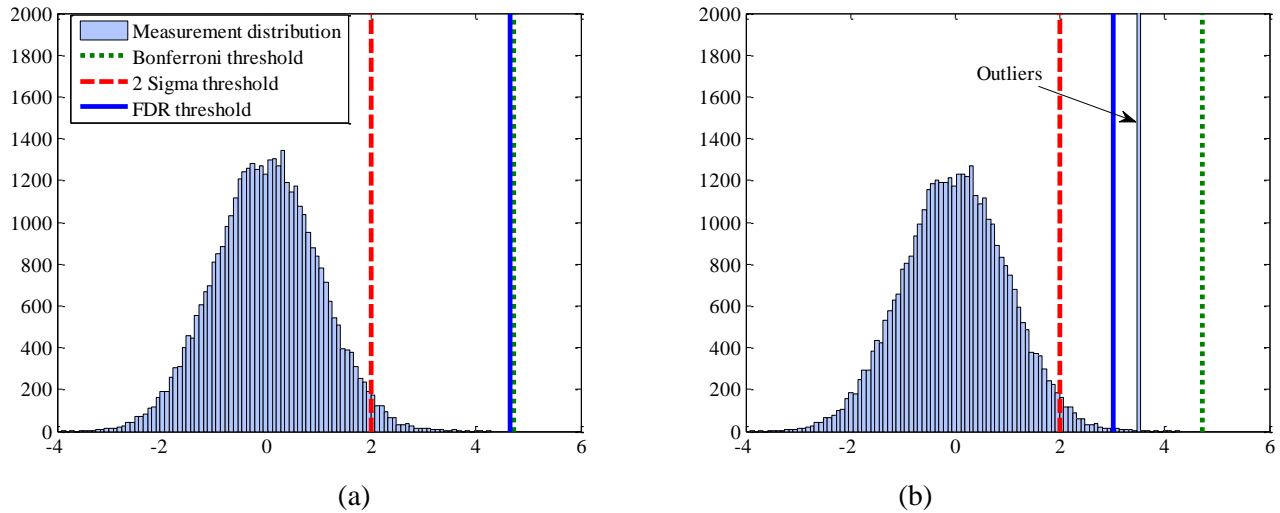


Figure 3-3 Threshold selection based on 2 sigma, Bonferroni correction, and FDR for distributions: (a) without outliers and (b) with outliers. The 2 sigma and Bonferroni thresholds are constant while the FDR threshold adapts to the measurements

**False Discovery Rate (FDR)**

The false discovery method of threshold selection was proposed by Benjamini and Hochberg *(9)* to address the case of multiple measurements as an alternative to the Bonferroni procedure. Instead of controlling the rate of false positive (type I error), the FDR control the proportion of false discoveries among all discoveries. In the case of the texture measurements that we are addressing in this paper, a discovery is a measurement that is flagged as a spike. As such, Bonferroni correction controls the probability of having one or more wrongly identified spikes, while the FDR method controls the proportion of wrongly identified spikes among all identified spikes. Since its introduction in 1995, the FDR criterion has become widely used in the medical field of gene expression studies (Efron et al. 2001 *(10)*; Storey and Tibshirani 2003a *(11)*, 2003b *(12)*, 2003c *(13)*; Benjamini et al. 2001 *(14)*; Reiner et al. 2003) *(15)*. Part of the attractiveness of the FDR is that is simple to implement as shown in the Benjamini and Hochberg procedure *(9),* as follows:

1. Given $n$ measurements of which $n_0$ are not spikes and 1-$n_0$ are spikes, using the determined distribution of texture measurements, calculate the p-values of all $n$ measurements
2. Reorder the p-values in increasing order ( $p_1 \leq ... \leq p_i \leq ... \leq p_n$ )

3. Select a $q$ value at which to control the FDR (e.g. 0.01, 0.05, or 0.1)
4. Let $k$ be the maximum $i$ such that:

$$p_i \leq \frac{i}{n} q$$

Eq. 3.2.

5. Spikes are identified as all measurements whose p-value is $\leq p_k$

Benjamini and Hochberg (1995) *(9)* proved this procedure controls the FDR at the preselected level q; more precisely:

$$FDR \leq \frac{n_0}{n} q \leq q.$$

Eq. 3.3.

In the implementation of the procedure of spike removal, we have selected $q = 0.1$.

**Calculation of MPD**

After the analysis of the data with the proposed method a new set of denoised data is obtained, and on this the MPD analysis is performed according to the ASTM E1845-09 *(16),* which applies a 2.5 mm moving average low-pass filter before the MPD calculation. The results are presented every 100 mm along the whole dataset and the relative slope was also removed before the actual MPD calculation.

**Sites**

The Virginia Smart Road, A 2.2-mile, controlled-access test track, located at the VTTI was chosen for the experimentation. The variety of pavement sections makes this a key facility for the significance of this study; Figure 3-4 below shows an aerial view of the Virginia Smart Road with the sections' location, more information about The Smart Road can be found on the VTTI Web page *(17).* Table 3-1 shows detailed information for each measured and analyzed section.

The experimented segment on the Smart Road have 14 different sections representing 9 different pavement mixes. All fourteen section were measured and analyzed showing consistent results for the comparison and validation; however, the results are presented for only nine sections (in order to decrease the number of figures in the paper) that encompasses all the pavement types (the nine bolded sections in Table 3-1 below). Therefore, as sections B, E, F, G and H are similar SM-9.5D mix, the results for this type of mix will be represented by Section E; the same for Sections D and I (SM-9.5A), the results will be represented by section I.
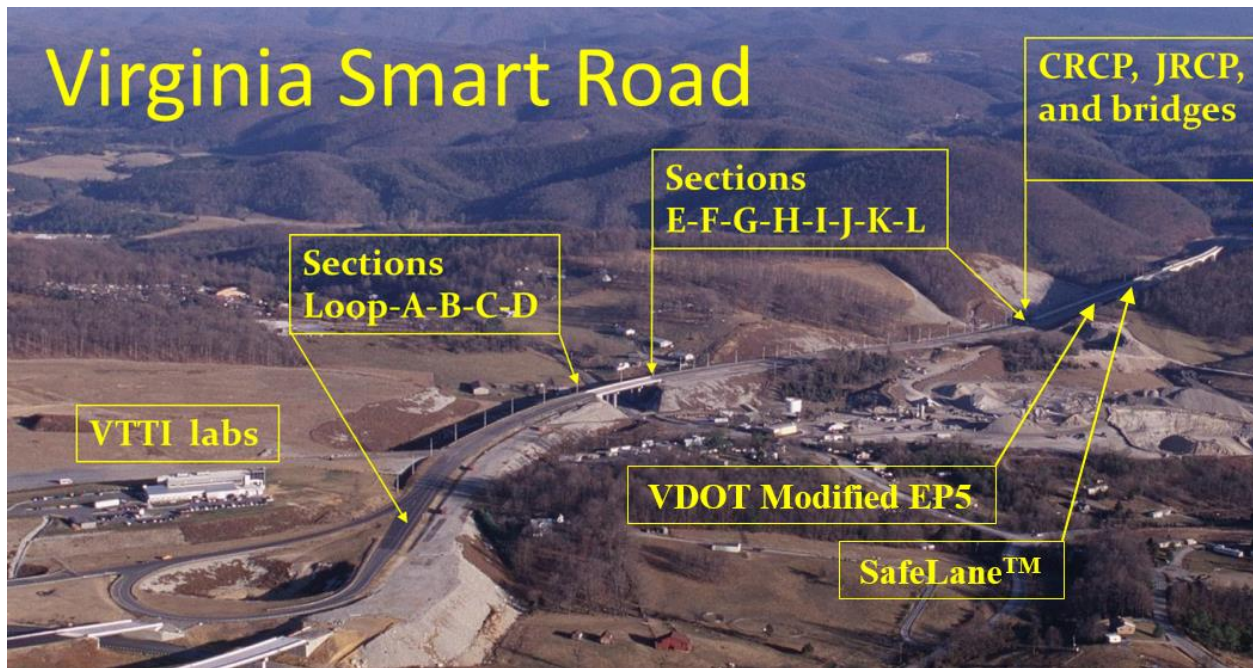
Figure 3-4 test locations on the Virginia Smart Road

Table 3-1 Smart Road Sections

| Section | Mix | Binder | Approx. length meters (ft.) |
|---|---|---|---|
| A | SM-12.5D | PG 70-22 | 106 (347) |
| B | SM-9.5D | PG 70-22 | 88 (289) |
| C | SM-9.5E | PG 76-22 | 89 (292) |
| D | SM-9.5A | PG 64-22 | 124 (407) |
| E | SM-9.5D | PG 70-22 | 82 (268) |
| F | SM-9.5D | PG 70-22 | 92 (302) |
| G | SM-9.5D | PG 70-22 | 93 (304) |
| H | SM-9.5D | PG 70-22 | 89 (292) |
| I | SM-9.5A | PG 64-22 | 103 (338) |
| J | SM-9.5D | PG 70-22 | 85 (280) |
| K | OGFC | PG 76-22 | 92 (302) |
| L | SMA-12.5D | PG 70-22 | 99 (326) |
| VDOT Modified EP-5 * | Epoxi-(Silica, Basalt) concrete overlay | epoxy | 30 (100) |
| SafeLane ™ * | 3/8-in-think polymer-Limestone concrete overlay | epoxy | 30 (100) |

* Further Information about these special surfaces can be found on Sprinkel et al. report *(18).*

**Equipment and Field Data Collection**

Two different sets of data were collected for this study: (1) Static measurements that provided the control data, and (2) dynamic measurements using a high speed laser device (HSLD) that provided the data to be used as a basis to test the proposed denoising methodology.

The CTMeter was adopted as the reference device to gather the "control" texture measurements, which were used to compare with the HSLD results. This is a standardized methodology, and this type of measurements is widely accepted.

Two CTMeter devices (Figure 3-5a) were used for repeatability purposes, and the measurements and analysis were made following ASTM E2157 *(19)*. Moreover, a pre-calibration (checking the proper functioning with the calibration plate) with successful results was performed for both devices in order to assure the reliability of the control measurements and therefore the validation of the HSLD measurements. Figure 3-5c shows the calibration plate used for this experiment. Ten measurements with each static device were made for every section along the left wheel path, and every MPD measurement from each of the eight sectors was considered individually, further explanation of this approach is presented in the results section of this paper.

An HSLD (Figure 3-5b) capable of collecting measurements at speeds between 25 and 65 mph (40 and 105 km/h) was used to gather the dynamic measurements, The HSLD has a laser spot with diameter of 0.2 mm and a sampling frequency of 64 kHz; more detailed information about this dynamic device can be found on the referenced document *(8)*. A total of 10 runs at 50 mph along the left wheel path (same as the CTMeter measurements) were performed over all fourteen sections; these measurements are the basis to test the proposed denoising methodology.



| a) | b) | c) |
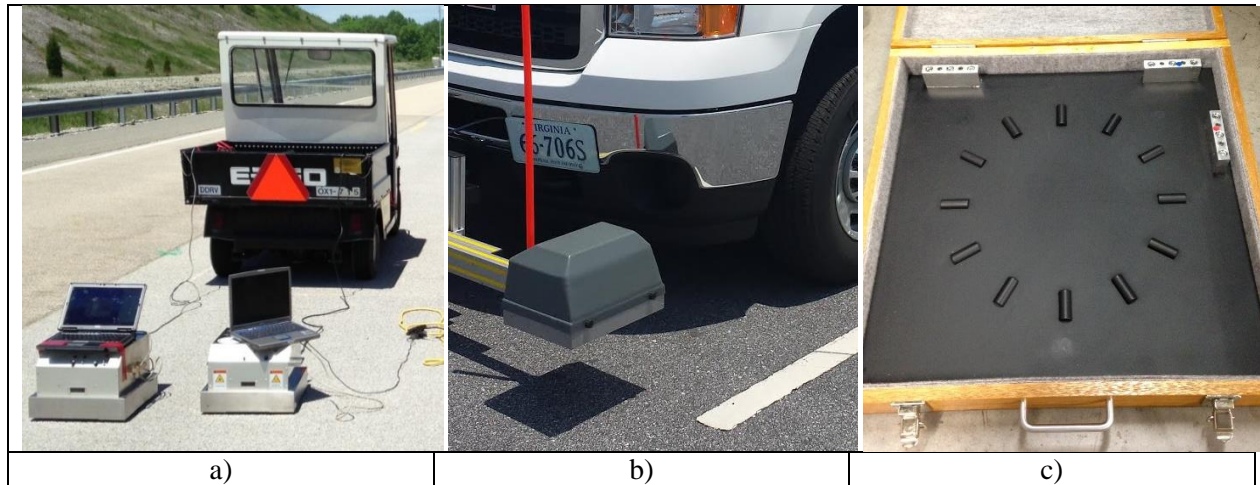
Figure 3-5 a) CTMeter devices, b) HSLD, and c) CTMeter calibration plate

**RESULTS**

An analysis of variance (ANOVA) performed for CTMeter measurements on the Virginia Smart Road and presented elsewhere in *(2)* showed that: for CTMeter measurements over an specific section, the observed variability over the following three variables is <u>not statistically significant</u>: (a) any transversal offsetting, (b) the relative longitudinal position along the wheel path, and (c) the MPD measurements from the eight different sectors of the device. In other words, for the same pavement section, the location in which we place the CTMeter (neither transversally, nor longitudinally) in not a factor of influence in the final results. The same is true for the sectors within the CTMeter.

As mentioned before, ten randomly taken measurements with each CTMeter were made for every section along the left wheel path. The MPD measurement from each of the eight segments (CTMeter segments A, B …, H) were considered individually to avoid the smoothing effect of the averaging. This resulted in a total number of 80 MPD measurements for each device per section.

The statistical MPD results for the CTMeter devices are presented in Figure 3-9 through Figure 3-11. It is important to note that all dynamic runs (ten runs) were analyzed with the proposed methodology and the analysis produced similar results; only five runs will be presented in order to reduce the number of figures with repetitive data.

The dynamic measurements were processed using the proposed denoising methodology, with a chosen False Discovery Rate of 0.1, and a range of 0.9 to 0.95 of the correspondent values of the tail obtained in the texture measurements distribution. It is important to clarify that the FDR = 0.1 value was chosen after a sensitivity analysis and experimentation, by looking which FDR value gives the highest positive difference of correctly identified spikes minus wrongly identified spikes, in other words maximizing the correctly identified outliers over the wrongly identified spikes. Figure 3-6 shows an example of both profile measurements (the original laser profile in blue, and the denoised laser measurements in green) for one of the ten runs (run 3). It is noticeable that the denoising method successfully removes (at least most of) the spikes from the original dataset.

In this example, the analysis found 6,034 spikes in a total number of 4,517,952 measurements, which corresponds to 0.13% of the data. Similar percentages were found for the other runs. This means that the denoising method found on average one significant spike for approximately every 750 data points (every 300 to 400 mm). In other words the method successfully removes spikes that otherwise would affect, on average, one third of the calculated continuous MPD results.
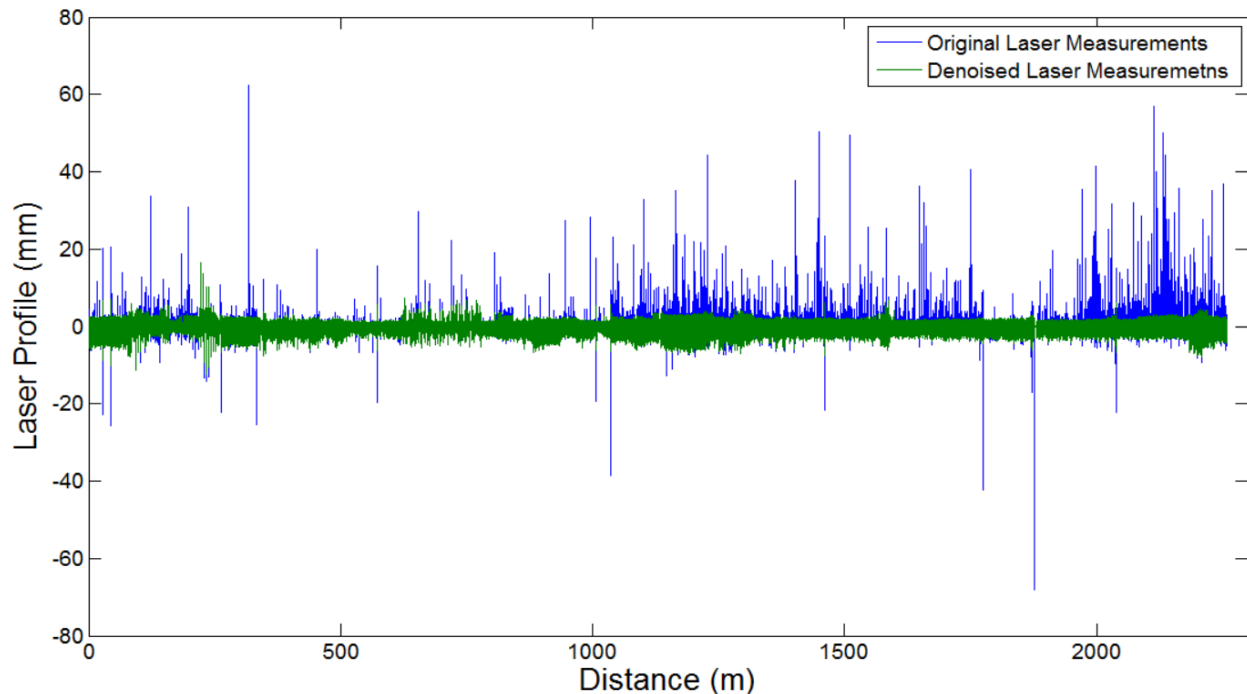


Figure 3-6 Profile Measurements from the HSLD, with and without Spikes (e.g. run 3)

The MPD calculations using the ASTM E1845-09 *(16)* and using the laser profile without spikes are expected to result in accurate texture values. Figure 3-7 illustrates this point; in this figure we spot the calculated MPD measurements (one value every 100 mm) from the same run 3 calculated from the original profile (in blue) and from the denoised profile (in green).
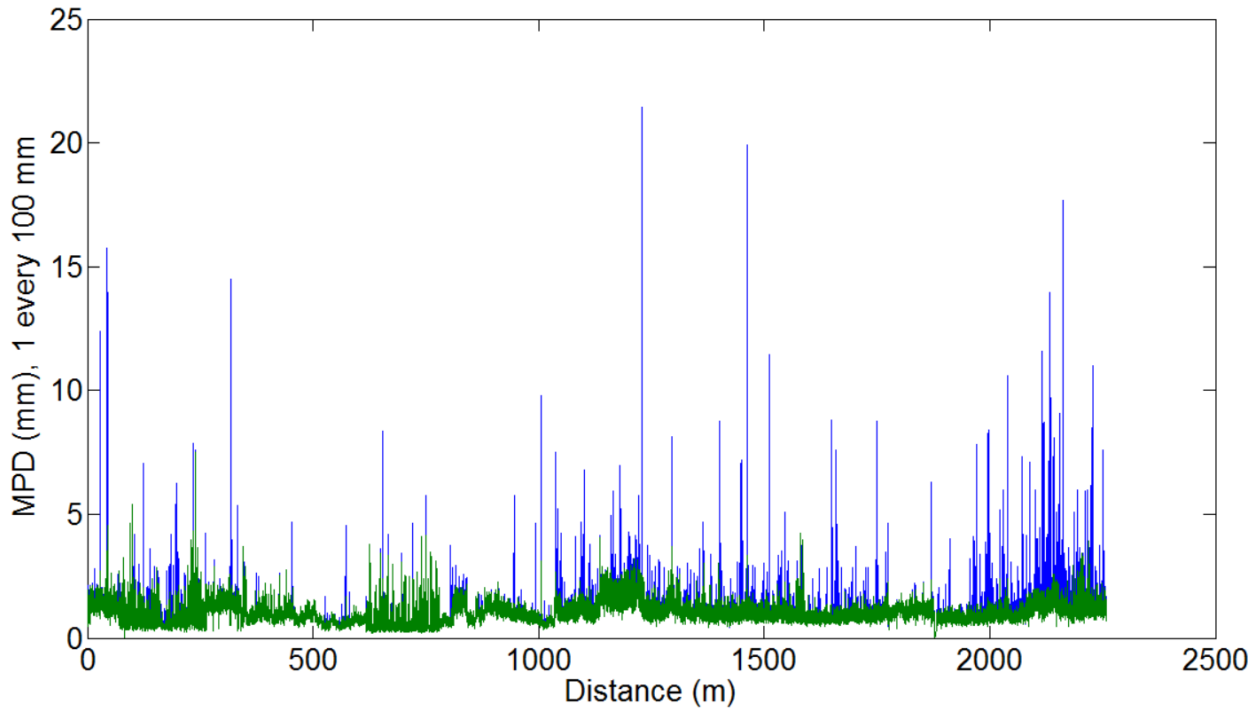
Figure 3-7 MPD values calculated with the original (blue) and denoised (green) data (e.g. run 3)

Figure 3-8 depicts the continuous MPD results for the 14 sections along the analyzed Smart Road. This intermediate step was used to define the relative location for each section in order to isolate the sections and proceed to the MPD analysis for each one. Those results were then compared with the control data (CTMeter results) for the validation of the proposed denoising methodology. Figure 3-9 though Figure 3-11 compare the MPD statistics for the control measurements and the dynamic results.
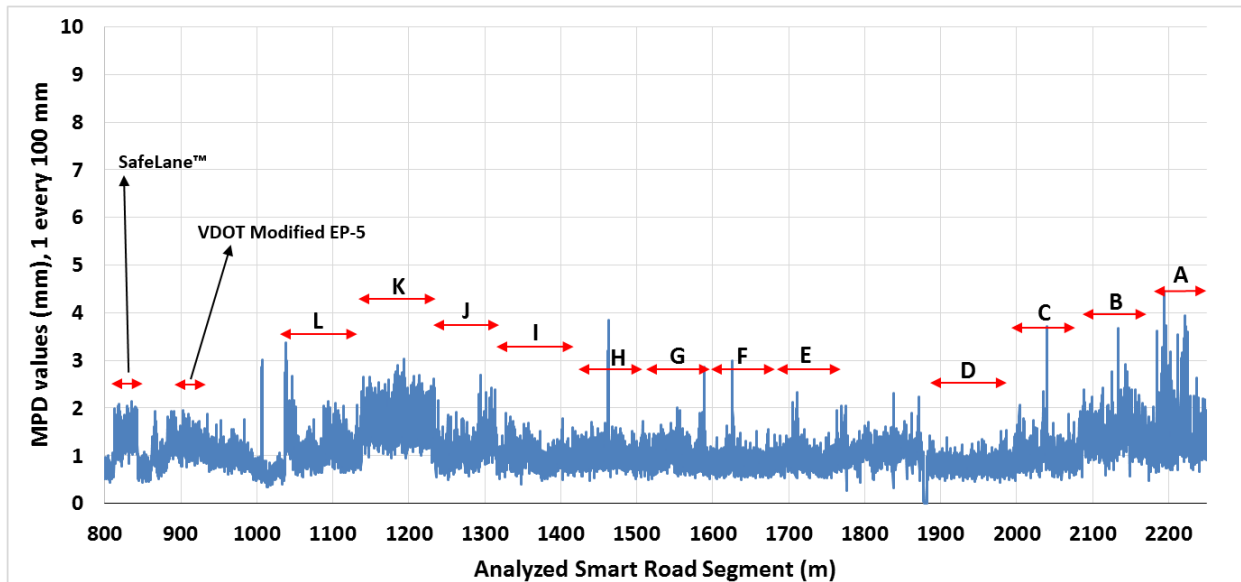


Figure 3-8 Evaluated Sections for Comparison with the Control Device (e.g. run 3 for the HSLD)

35
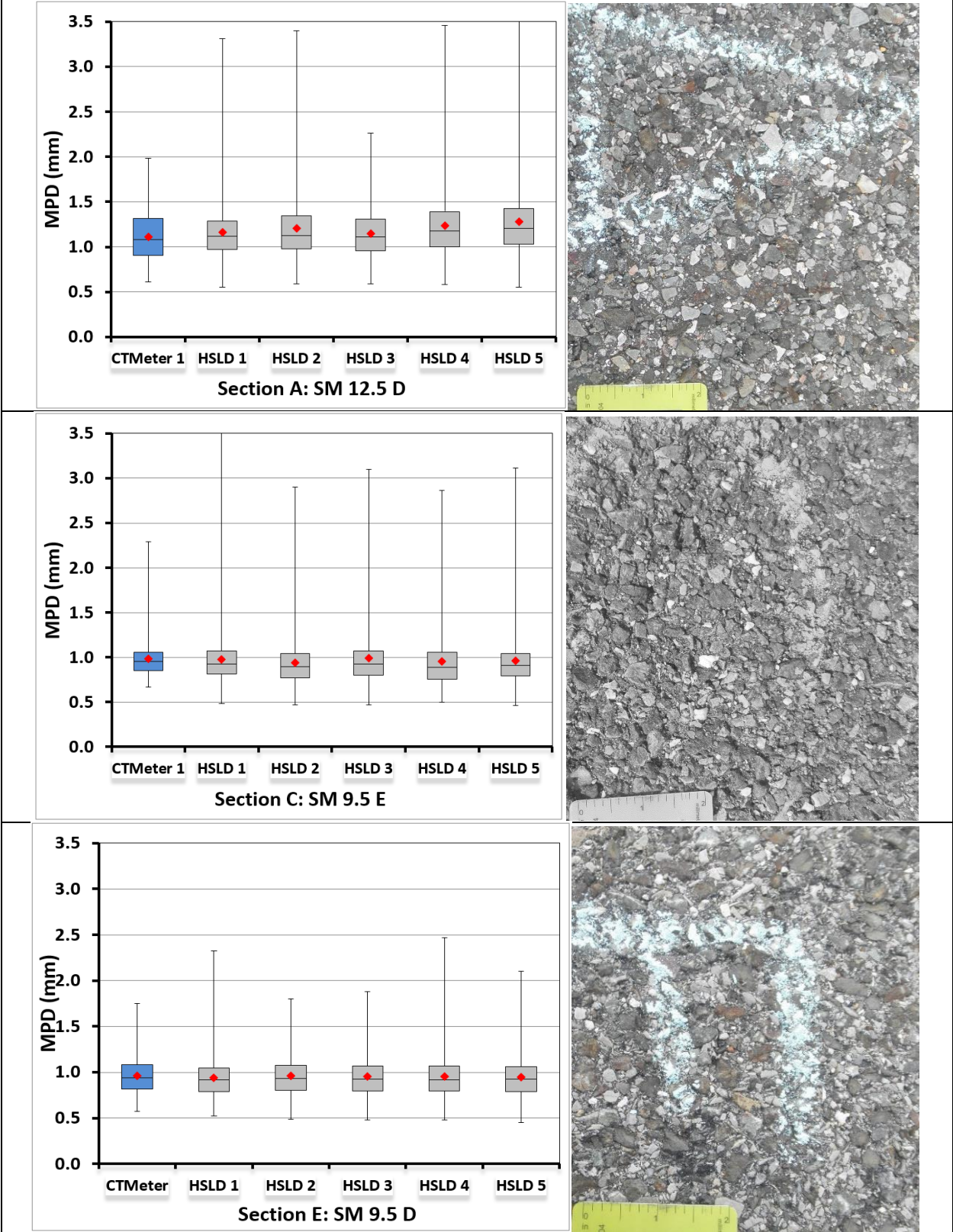
Figure 3-9 Texture Measurements: SM12.5D, SM9.5E, and SM9.5D
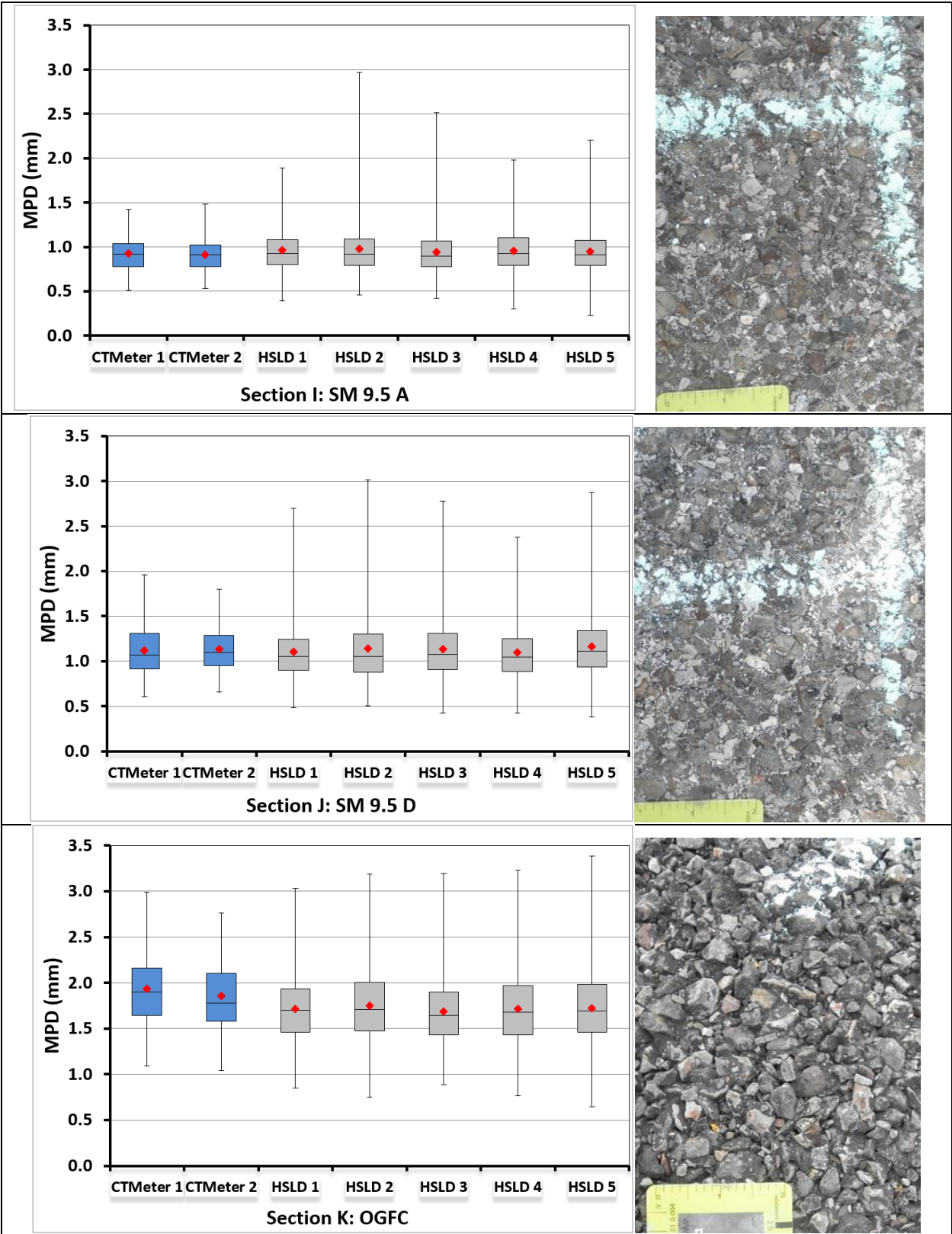
Figure 3-10 Texture Measurements: SM 9.5A, SM 9.5D, and OGFC
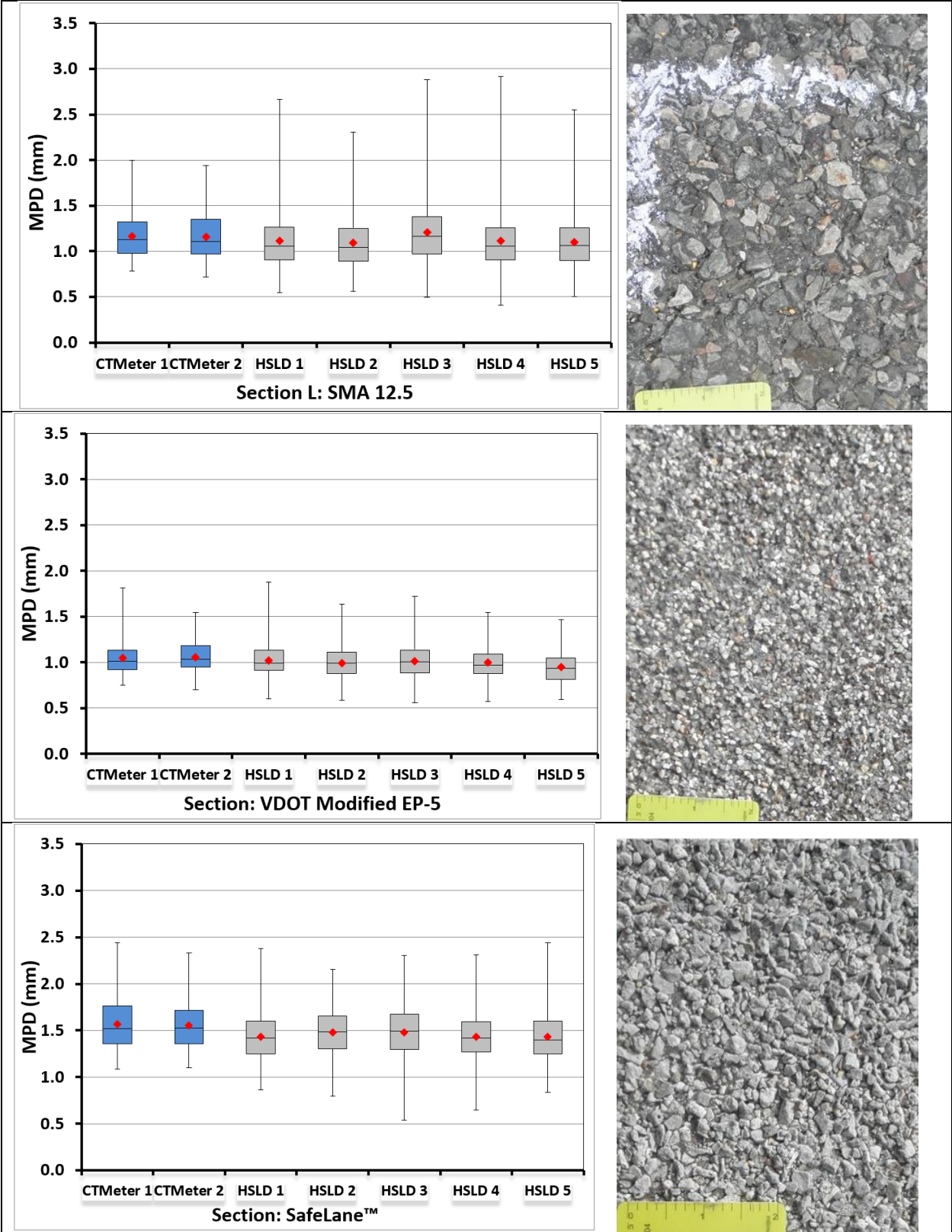
Figure 3-11 Texture Measurements: SMA 12.5, VDOT Modified EP-5, and SafeLane™

## SUMMARY AND CONCLUSIONS

The research described in this paper can be summarized as follows:

- The paper proposed an innovative and robust methodology for removing spikes from texture measurements gathered with an HSLD; this a significant step towards the development of standardized procedures that allow the use of these devices for texture investigation at network level.
- The test of the proposed methodology using a substantial amount of data collected over several and different pavement surfaces confirmed the reliability of the method on surfaces with different texture distributions, macrotexture depth, connectedness, porosity, etc.
- For all HSLD measurements, the proposed methodology was able to effectively remove (at least most of) the spikes from the texture profile on all the surfaces investigated.
- The validation of the method showed that the MPD results obtained with denoised dynamic measurements are comparable to MPD results from the control devices on all the pavement sections investigated.

The following conclusions can be drawn from the experiment:

- The use of two CTMeter devices, properly pre-calibrated, and the significant amount of control data points taken with this reference device on all of the analyzed sections, increases the confidence of the reference or control measurements.
- The GGD is a flexible parametric family of continuous distributions that allows the statistical representation of a wide range of pavement texture measurements distribution.
- FDR control allows for an adaptive threshold selection that differentiates between valid measurements and spikes (outliers). The FDR control value gives a value for the expected number of wrongly identified spikes.
- The "wider" ranges of variability shown for the HSLD measurements (compared to the CTMeter ranges) are due to the significantly higher number of data points taken by the dynamic device (relative to the CTMeter measurements). Since the HSLD measurements are continuous along the whole section, this higher variability should not be considered as a drawback in the proposed methodology.

## REFERENCES

[1] Flintsch, G. W., E. De Leon, K. K. McGhee, and I. L. Al-Qadi. Pavement Surface Macrotexture Measurement and Applications.In, National Research Council, 2003. pp. 168-177.

[2] Mogrovejo, D., Katicha, S., Flintsch, G., de León Izeppi, E. Latest Development in the Processing of Pavement Macrotexture Measurements of High Speed Laser Devices. 9th International Conference on Managing Pavement Assets, 2014.

[3] Perera, R. M., M; Orthmeyer, R. De León Izeppi, E. AFD 90, Group III Texture Measurements and useof Work, 2013.

[4] Goubert, L. B. A. About the reproducibility of texture profiles and the problem of spikes. Surf 0079, 2012.

[5] Flintsch, G. W., M. Huang, and K. McGhee. Harmonization of macrotexture measuring devices. Journal of ASTM International, Vol. 2, No. 9, 2005, pp. 101-112.

[6] Perera, R. K., S. . Issues in Pavement Smoothness, A Summary Report. Transportation Research Board, 2002.

[7] Sayers, M. K., S. Interpretation of Road Roughness Profile Data.In, Federal Highway Administration, 1996.

[8] LMI-Technologies. Selcom Optocator User's manual.In, LMI Technologies INC., Sweden, 2013.

[9] Benjamini, Y., and Y. Hochberg. Controlling the False Discovery Rate: A Practical and Powerful Approach to Multiple Testing. Journal of the Royal Statistical Society. Series B (Methodological), Vol. 57, No. 1, 1995, pp. 289-300.

[10] Efron, B., R. Tibshirani, J. D. Storey, and V. Tusher. Empirical Bayes Analysis of a Microarray Experiment. Journal of the American Statistical Association, Vol. 96, No. 456, 2001, pp. 1151-1160.

[11] Storey, J. D., and R. Tibshirani. Statistical significance for genomewide studies. Proc Natl Acad Sci U S A, Vol. 100, No. 16, 2003, pp. 9440-9445.

[12] Storey, J. D., and R. Tibshirani. Statistical methods for identifying differentially expressed genes in DNA microarrays. Methods in molecular biology (Clifton, N.J.), Vol. 224, 2003, pp. 149-157.

[13] Storey, J., and R. Tibshirani. SAM Thresholding and False Discovery Rates for Detecting Differential Gene Expression in DNA Microarrays.In The Analysis of Gene Expression Data, Springer New York, 2003. pp. 272-290.

[14] Benjamini, Y., D. Drai, G. Elmer, N. Kafkafi, and I. Golani. Controlling the false discovery rate in behavior genetics research. Behavioural Brain Research, Vol. 125, No. 1–2, 2001, pp. 279-284.

[15] Reiner, A., D. Yekutieli, and Y. Benjamini. Identifying differentially expressed genes using false discovery rate controlling procedures. Bioinformatics, Vol. 19, No. 3, 2003, pp. 368-375.

[16] International, A. ASTM E1845-09 Standard Practice for Calculating Pavement Macrotexture Mean Profile Depth.In, ASTM International, PA 19428-2959. United States, 2009.

[17] VTTI. Virginia Smart Road. https://www.vtti.vt.edu/smart-road/virginia-smart-road.html Accessed July 7th, 2014, 2014.

[18] Sprinkel, M. M., Roosevelt, Daniel S., Flintsch, Gerardo W., de León, and E. Izeppi, Mokarem, David W. . Evaluation of the Cargill SafeLane TM Surface Overlay.In, Charlottesville, 2009. p. 55.

[19] International, A. ASTM E2157-09 Standard Test Method for Measuring Pavement Macrotexture Properties Using the Circular Track Meter In, ASTM International, PA 19428-2959. United States, 2009.

# Chapter 4 ENHANCING PAVEMENT SURFACE MACROTEXTURE CHARACTERIZATION BY USING THE EFFECTIVE AREA FOR WATER EVACUATION[3]

## ABSTRACT

Adequate macrotexture characterization is an essential objective for transportation practitioners since primary pavement surface characteristics like friction, tire/pavement noise, splash and spray, and rolling resistance are significantly influenced by pavement macrotexture.

This study proposes an enhanced macrotexture characterization index based on the effective area for water evacuation (EAWE) that (a) estimates the potential of the pavement to drain water better than currently use indices, and (b) provides stronger correlations with two pavement surface properties affected by macrotexture: friction and noise.

A three-step methodology is proposed to compute the index: (1) a spike removal procedure that assures the reliability of the texture profile data; (2) an enveloping profile calculation, which is necessary to delimit the area between the tire and the pavement when contact occurs; and (3) a definition of the EAWE, which will be the (multiple representation) index to characterize macrotexture.

Comparisons of current (MPD) and proposed (EAWE) macrotexture characterization indices using 32 sections confirmed that MPD overestimates the effective area for water evacuation significantly.

Correlations for MPD and EAWE indices with the main pavement surface characteristics were also performed. Improvements in correlations with friction and noise were achieved.
Results show that it is possible to define a promising index based on the EAWE that features improvements when compared with MPD.

---

[3] This manuscript has not been submitted for publication at the time of submission of the Dissertation. Co-authors include Samer Katicha, Gerardo W. Flintsch, and Edgar D. de León Izeppi.

## INTRODUCTION

### Background

According to International Organization for Standardization (ISO) 13473-5:2009, pavement texture is the "deviation of a pavement surface from a true planar surface, with a texture wavelength (λ) less than 0.5 m, for texture wavelengths over 0.5 m these deviations are known as unevenness or roughness" *(1)*.

The World Road Association (PIARC) has established standard categories of texture (Microtexture, Macrotexture, and Megatexture) and roughness (Unevenness) and their effects on pavement surface properties *(2, 3)*. Specifically, this categorization states that macrotexture is defined in the range of 0.5 mm < λ < 50 mm, and it may be the most influential category over most of pavement–surface interactions (e.g., friction, tire/pavement noise, splash and spray, and rolling resistance).

Even though the use of the Circular Track Meter (or Circular Texture Meter, CTMeter), and its reported mean profile depth (MPD) index is the most widely accepted procedure among practitioners for macrotexture characterization, it is known that significant limitations are involved with this methodology, as explained in the problem statement section.

With the aim of improving texture measurements and overcoming the limitations of the static methods (time consuming procedures, provides localized results, needs traffic control, etc.), dynamic methods (e.g. using High Frequency Laser Equipment [HFLE]) have also been developed for texture measurements *(4-6)*. With these HFLE, significant resolution of texture measurements has been achieved even at highway speeds; however, two difficulties are still to be solved: a) most of the methods still report MPD that presents limitations as well as explained later, and b) standard procedures for dynamic methods are still not yet available.

On the other hand, interesting approaches are being studied, mainly by European institutions, for texture modeling. The potential implementation of enveloping profiles (representing the actual profile of the tire when it rolls over the pavement surface) to better explain texture correlations with other parameters is an example *(7)*. A study conducted by Kleim and Hamet proposes enveloping profiles for noise prediction based on texture *(8)*. Sandberg et al. propose the use of enveloping to improve the modeling of rolling resistance *(9)*.

Based on this research, the Virginia Tech Transportation Institute (VTTI) considered several of these models with the goal of applying the enveloping profile to macrotexture characterization rather than to texture–noise and texture–rolling resistance modeling. Three models were revised and evaluated: the Clapp's envelopment procedure based on a physical model that consists of evaluating the contact between a rigid body and a semi-infinite elastic body *(8);* the INRETS model based on calculation of vertical displacement of the border of an elastic medium under the influence of a vertical force *(8, 10)*; and the von Meier model based on a mathematical-mechanistic approach based on the mathematical limitation of the second-order derivative of the discretized texture sample *(8, 9, 11)*. This last model resulted in a better fit for the purpose of macrotexture characterization due its versatility and customizable settings (as detailed in the methodology section of this paper).

### Problem Statement

The CTMeter procedure and the resulting MPD value may not be the best approach for macrotexture characterization since significant limitations arise. For example, being a static method, its implementation at the network level is not feasible. Moreover, significant variations within the eight CTMeter sectors are found *(12)*. While these shortcomings could be addressed by dynamic methods that report MPD, such as the VTTI method *(4)*, additional limitations can also be detailed for this index. For instance, a single MPD value should not be used for characterizing an entire section of road since important variations can be present in the pavement. Moreover, by definition MPD is calculated using the peaks of the profile, and thus this value may not represent the actual potential of the pavement to drain water, which may be the

most desired safety feature of the pavement. What is more, strong correlations of MPD with the main surface characteristics of the pavement are not well defined.

All of these problems justify the need for a better approach to macrotexture characterization. Thus, the use of an improved (multiple representation) index is proposed in this study and detailed following.

## OBJECTIVE

The objective of this study is to propose an enhanced macrotexture characterization index that (a) estimates the Effective Area for Water Evacuation (EAWE) better than current Mean Profile Depth method, and (b) provides stronger correlations with the corresponding pavement surface properties affected by macrotexture (friction and rolling noise).

## METHODOLOGY

### Sites

Thirty-two sections of road were selected for this study, covering most of the pavement types used in Virginia, including both dense and porous mixes and also combinations of different aggregate sizes, different binders, and mixes with rubber additions.

Twelve of the thirty-two sections were selected from the Virginia Smart Road, a 2.2-mile, controlled-access test track, located at VTTI facilities in Blacksburg, Virginia *(13) (22)*. Figure 4-1 shows an aerial view of the Virginia Smart Road, with pictures of the chosen sections and their details.

The remaining 20 of the 32 sections were chosen from three demonstration projects of the Virginia Quiet Pavement Implementation Program (VQPIP). These projects are located on State Route 199 west of Williamsburg, Virginia, on State Route 286 in Fairfax, Virginia, and on State Route 288 near Chester, Virginia *(14)*. Figure 4-2 below shows the diagrams for these projects and the sections, as well as the corresponding pictures and details for each pavement type.

### Equipment and Field Data Collection

*Equipment*

Measurements for macrotexture, friction, and noise were performed for this study under the basis that friction and noise are the main pavement surface characteristics that are influenced by macrotexture and its wavelength range (0.5 mm $< \lambda < 50$ mm).

For texture measurements, two different sets of data were collected: (a) static measurements using the CTMeter, and (b) dynamic measurements using a high-speed laser device (HSLD) that provided the data to be used for deriving both MPD and the proposed index based on the EAWE.

On the Smart Road sections, two CTMeter devices (Figure 4-3a) were used for repeatability purposes. The measurements and analysis were made in accordance to ASTM E2157 *(15)*. Before the static measurements, a pre-calibration that included checking for the proper functioning of the calibration plate was performed for both devices with successful results. For the VQPIP sections, one CTMeter was used. One HSLD (Figure 4-3b) capable of collecting measurements at different speeds (between 25 and 65 mph [40 and 105 km/h]) was used to gather the dynamic measurements on all sites (Smart Road and VQPIP sections). This HSLD uses a laser spot with diameter of 0.2 mm and a sampling frequency of 64 kHz *(4, 5)*; more detailed information about this device can be found in the Selcom Optocator User's Manual *(16)*.

For the friction measurements, a GripTester device that operates at a constant slip (16% slip) was used at all sites. A speed of 40 mph was chosen. Figure 4-3c shows the GripTester.

| A–SMA-12.5D PG 70-22 Section length: 106 m (347 ft.) | B–SM-9.5D PG 70-22 Section length: 88 m (289 ft.) | C–SM-9.5E PG 76-22 Section length: 89 m (292 ft.) | D–SM-9.5A PG 64-22 Section length: 124 m (407 ft.) | E–SM-9.5D PG 70-22 Section length: 82 m (268 ft.) | F–SM-9.5D PG 70-22 Section length: 92 m (302 ft.) |
| --- | --- | --- | --- | --- | --- |
| G-SM-9.5D PG 70-22 Section length: 93 m (304 ft.) | H-SM-9.5D PG 70-22 Section length: 89 m (292 ft.) | I–SM-9.5A PG 64-22 Section length: 103 m (338 ft.) | J–SM-9.5D PG 70-22 Section length: 85 m (280 ft.) | K–OGFC PG 76-22 Section length: 92 m (302 ft.) | L–SMA-12.5D PG 70-22 Section length: 99 m (326 ft.) |

Figure 4-1 Smart Road test sections.

| SMA 9.5 Stone matrix asphalt pavement, PG: 76-22, 1.5" thick, maximum aggregate size: 9.5 mm, 165 lbs./sy | AR-PFC 9.5 Asphalt rubber – porous friction course, 1" thick, maximum aggregate size: 9.5 mm, 90 lbs./sy | PFC 9.5 Porous friction course, PG: 70-28, 1" thick, maximum aggregate size: 9.5 mm, 90 lbs./sy | PFC 12.5 Porous friction course, PG: 70-28, 1.5" thick, maximum aggregate size: 12.5 mm 180 lbs./sy in SR-199, 135 lbs./sy in SR-288 | SMA 12.5 Stone matrix asphalt pavement, PG: 76-22, maximum aggregate size: 12.5 mm | AR-PFC 12.5 Asphalt rubber – porous friction course, maximum aggregate size: 12.5 mm |
|---|---|---|---|---|---|
| Section names: | | | | | |
| SR-199 SMA 9.5 – E<br>SR-199 SMA 9.5 – W<br>SR-288 SMA 9.5 – N<br>SR-288 SMA 9.5 – S | SR-199 AR-PFC 9.5 – E<br>SR-199 AR-PFC 9.5 – W<br>SR-288 AR-PFC 9.5 – N<br>SR-288 AR-PFC 9.5 – S | SR-199 PFC 9.5 – E<br>SR-199 PFC 9.5 – W<br>SR-288 PFC 9.5 – N<br>SR-288 PFC 9.5 – S | SR-199 PFC 12.5 – E<br>SR-199 PFC 12.5 – W<br>SR-288 PFC 12.5 – N<br>SR-288 PFC 12.5 – S | SR-286 SMA 12.5 – N<br>SR-286 SMA 12.5 – S | SR-286 AR-PFC 12.5 – N<br>SR-286 AR-PFC 12.5 – S |

Figure 4-2 VQPIP test sections.

|                           |                        |
|:-------------------------:|:----------------------:|
| (a) CTMeter *(4)*         | (b) HSLD *(4)*         |
| (c) GripTester            | (d) OBSI *(18)*       |
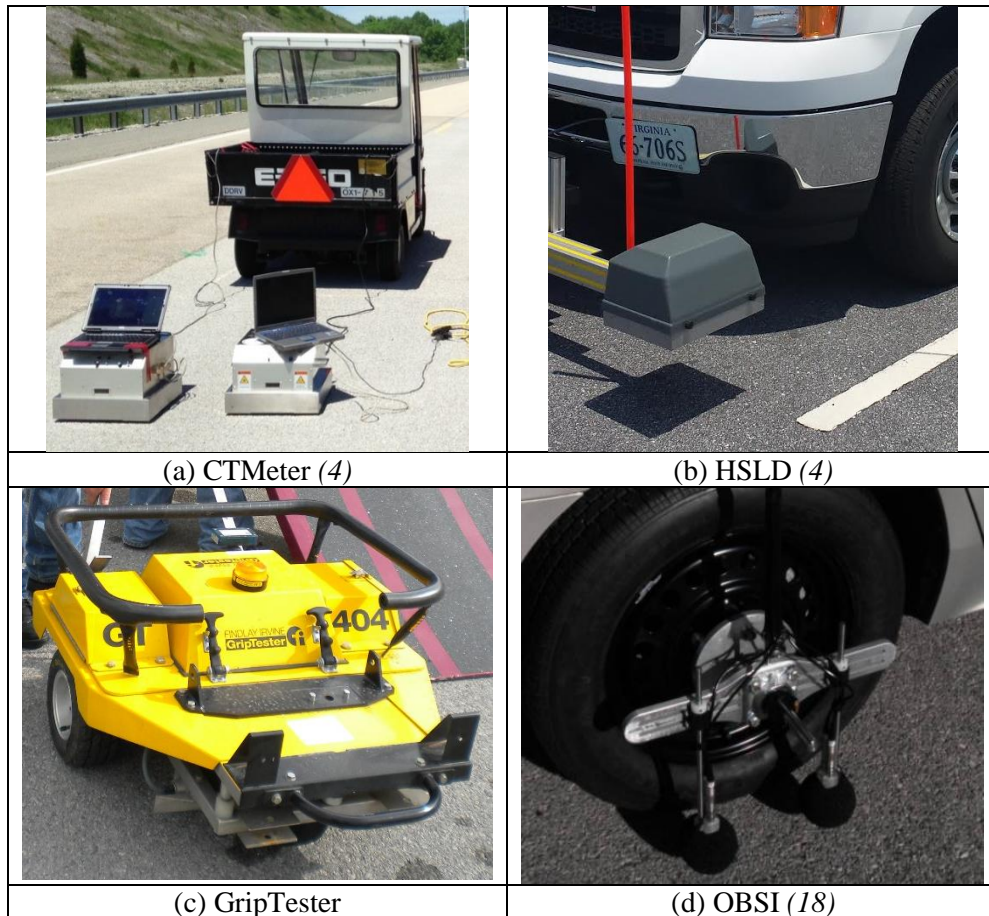
Figure 4-3 Equipment used for the analysis.


Tire/pavement noise was measured following the American Association of State Highway and Transportation Officials (AASHTO) standard TP 76-12, "Measurement of Tire/Pavement Noise Using the On-Board Sound Intensity (OBSI) Method" *(17)*. VTTI's OBSI equipment (shown in Figure 4-3d) was used for all sites *(18)*

*Field Data Collection*
The following measurements were collected for the CTMeter, HSLD, GripTester, and OBSI:
　　　**CTMeter** – At least 10 measurements with each CTMeter were performed for each section on the Virginia Smart Road since it is closed to traffic (which means at least 20 CTMeter measurements for each section to calculate an average MPD). For the VQPIP sections, traffic control was necessary since these are state routes with annual average daily traffic (AADT) counts between 23,000 and 41,000. At least five measurements for each section (e.g., SMA 9.5), in each direction (e.g., northbound), and for each location (e.g., SR-199), were performed. Every single CTMeter measurement (considering 1 measure for every one of the 8 CTMeter's sectors) was included in the results to account for variability more accurately.
　　　**HSLD** – Ten runs at 50 mph (80.5 km/h) were performed on the Virginia Smart Road sections and three runs (at the same speed) for the VQPIP sections (giving a total of 180 runs to analyze). Raw data were collected at a frequency of 64 kHz and analyzed every 0.5 mm. A de-spiking procedure *(4)* was performed over every single set of raw data prior to both calculating the MPD and finding the enveloping profile to be used for the proposed index based on the EAWE (explained below).

**GripTester** – For the Virginia Smart Road sections, 12 runs were performed using the GripTester. Three runs were performed for the VQPIP sections. Data collection was performed at 40 mph, with a 16% slip speed. The data were collected every 3 ft. along the entire length of every section.

**OBSI** – Tire/pavement measurements on the Virginia Smart Road were performed as follows: 2 valid runs for Section K (minimum number of valid runs according to AASHTO standard TP 76-12), 3 valid runs over Sections L and A, 5 valid runs over Section B, and 7 valid runs over Sections E, F, G, and H. In the case of the VQPIP sections, at least 3 valid runs were performed for each section. A run was considered valid if it met all four criteria stated in the standard for coherence, pressure-intensity (PI) index, direction of the sound intensity vector, and standard deviation. Detailed information about this validation can be found in Mogrovejo et al. *(14)*.

## Calculating the Proposed Index Based on EAWE

An enhanced pavement surface texture analysis is proposed in this study by using a novel index for macrotexture characterization: the EAWE index (in mm$^2$). Three crucial steps structure the proposed methodology for computing the index:
1) A mandatory spike-removal process over the HSLD raw data;
2) The finding the enveloping profile, which is the profile that the tire creates when in contact with the surface of the pavement, and
3) The definition of the EAWE index (and the correspondent effective depth for water evacuation [EDWE]).

*Step 1. Spike Removal*
It is widely known that all HSLD measurements have "noise" in the data in the form of spikes that *must* be removed before any further analysis *(4, 5, 19)*. In this study, in order to correctly calculate the proposed indices for macrotexture characterization, a spike-removal method developed by the authors and published elsewhere, "Adaptive Spike Removal Method for High Speed Pavement Macrotexture Measurements by Controlling the False Discovery Rate" *(4),* was applied to the gathered raw data. This is therefore considered the first step in the proposed methodology.

The spike-removal method basically consists of a two-step algorithm. First, the algorithm determines the distribution of texture measurements (after high-pass filtering of the raw data for slope removal) by using the family of Generalized Gaussian Distributions (GGDs), which allows for the tail of the distribution to be heavier or thinner than the normal distribution. Second, the algorithm uses the False Discovery Rate (FDR) method to control the proportion of wrongly identified spikes among all identified spikes. The FDR control allows for an adaptive threshold selection that differentiates between valid measurements and spikes.

*Step 2. Enveloping Profile Calculation*
As stated in the background section, a number of envelopment procedures are being studied, mainly by European organizations, to better understand texture *(8)*. For this study, the envelopment procedure developed by von Meier, van Blokland, and Descornet was chosen on the basis that this mathematical–empirical model allows the adjustment of the resulting enveloping profile according to the tire stiffness (a required feature for comparison of the EAWE and MPD as explained and depicted in the results following). This procedure limits (or reduces) the second-order derivative of the profile to a given limit value, $d^*$, which is a measure for the elasticity of the tire rubber expressed in mm/mm$^2$ (or mm$^{-1}$). Empirical measurements of the deformation of a tire pressed onto various idealized profiles made of steel rods with different diameters and spacing were performed by von Meier et al. to find $d^*$ values; in their work, enveloping profiles with $d^*$ values of 0.1, 0.054, 0.027 are presented *(20)*.

A revised version of the von Meier et al. model (including "form" corrections made by Goubert *(7)* and restructured by VTTI to fit MATLAB codification) was used for the enveloping profile calculations. The restructured model is diagrammed in Figure 4-4 .

**Start**

For i = 2 : n-1

$d = e_{(i)} - (e_{(i-1)} + e_{(i+1)})/2$

$d - d^* > 0$  — **yes** / **no**

**yes** path:
$(e_{(i-1)} - e_{(i)} + d^*) <= 0$ — **yes** / **no**

**no** path (d - d* > 0 = no):
$d + d^* < 0$ — **yes** / **no**

**yes** (d + d* < 0):
$e_{(i)} = e_{(i)} - d - d^*$

**yes** branch:
$(e_{(i+1)} - e_{(i)} + d^*) > 0$ — **yes** / (no)

**no** branch:
$e_{(i+1)} = e_{(i+1)} + 2(d - d^*)$

**yes** (leftmost):
$e_{(i-1)} = e_{(i-1)} + 2(d - d^*)$

$e_{(i-1)} = e_{(i)} - d^*$
$e_{(i+1)} = e_{(i)} - d^*$

**End**
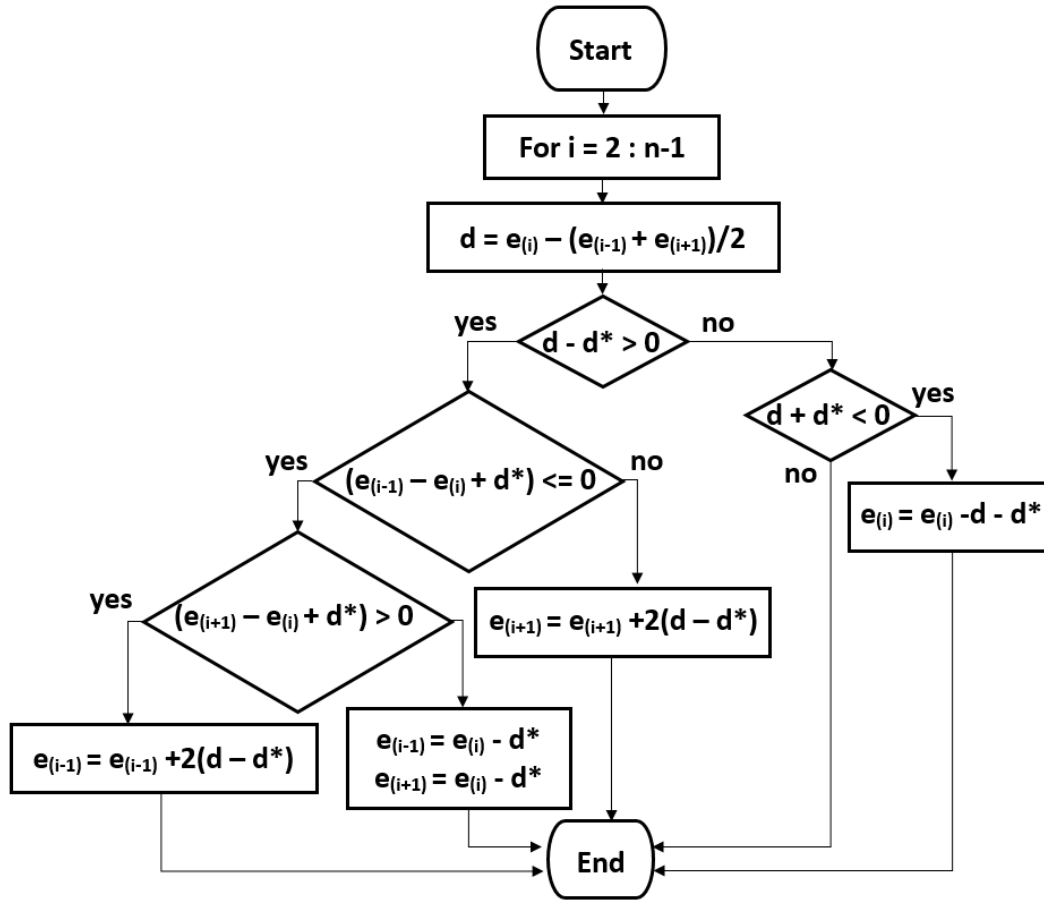
Where:

$n$ = number of data points from the original pavement texture profile obtained with the HSLD
$d^*$ = given maximum value (e.g. d* = 0.054 mm/mm$^2$) representing the elasticity of the tire rubber
$d$ = changing aid variable
**e** = resulting enveloping profile (vector)

Figure 4-4 Diagram for enveloping profile calculation.

*Step 3. Effective Area and Effective Depth for Water (and/or Air) Evacuation*
As explained in the objective at the beginning of the article, the proposed index for pavement surface macrotexture characterization is EAWE (in mm$^2$), which represents the area that will be occupied by the water that is pushed away through macrotexture during tire/pavement contact. EAWE is defined in this study as the area between the resulting enveloping profile and the actual pavement texture profile when tire/pavement contact occurs.

EAWE (in mm$^2$) can be reported in three different ways:

**1.** As a vector of values $\widehat{EAWE}$, which means one value for every data point in the profile. This vector is arranged as follows:

$$\widehat{EAWE} = [EAWE_1, EAWE_2, ..., EAWE_i, ..., EAWE_n] \qquad \text{Eq. 4.1.}$$

Where:

$n$ is the number of data points in the texture profile, and

49

$$EAWE_i = \left(\frac{b_i + b_{i+1}}{2} * h\right)$$ Eq. 4.2.

Where:

$b_i$ = the difference of the $i^{th}$ data point in the enveloping profile minus the $i^{th}$ data point in the original pavement profile,

$h$ = 0.5 mm, which is the spacing between data points in the profiles.

**2.** As a vector of accumulated values with base length 100 mm ($\widehat{EAWE}_{100}$), which means one value for every 100 mm (every 200 data points) in the profile. The 100 mm base length was chosen to be consisted with MPD base length when analyzed with the HSLD, and thus allow point-by-point comparison of this 2 indices. This vector is arranged as follows

$$\widehat{EAWE}_{100} = \left[EAWE_{100_1}, EAWE_{100_2}, \dots, EAWE_{100_m}\right]$$ Eq. 4.3.

Where:

$$EAWE_{100_1} = \sum_{j=1}^{200} EAWE_j, EAWE_{100_2} = \sum_{j=201}^{400} EAWE_j, \dots, EAWE_{100_m} = \sum_{j=n-199}^{200m} EAWE_j$$ Eq. 4.4.

**3.** As a scalar value (*EAWE*), which means a single average value with a 100-mm baseline that represents the whole section, calculated as follows:

$$EAWE = \frac{\sum_{j=1}^{m} EAWE_{100_j}}{m}$$ Eq. 4.5.

Finally the correspondent Effective Depth for Water Evacuation (EDWE, in mm) is defined and can be reported as a scalar value (*EDWE*), which means a single average value with a 100-mm baseline that represents the whole section, calculated as follows:

$$EDWE = \frac{EAWE}{100}$$ Eq. 4.6.

The vector representations of EAWE allow every single location in the section to be analyzed (for example, to find significant variation of texture, section changes, critical spots [relatively low EAWE], etc.). When compared with MPD, which really is just a single value for an entire section, it is evident that EAWE represents an improvement for macrotexture characterization. However, even though it is also possible to report MPD vectors with values every 100 mm, as shown by Katicha et al. *(4)*, there are additional advantages in reporting macrotexture characterization as EAWE instead of MPD, which are shown in the results below.

**RESULTS**
The results for each step involved in calculating the EAWE index are shown as follows.

**Step 1. Spike Removal**

Spike removal was performed over all HSLD raw data for every single run and for all the analyzed sections (180 runs in total for all 32 sections). A snapshot of the beginning of a random section is presented in Figure 4-5 .
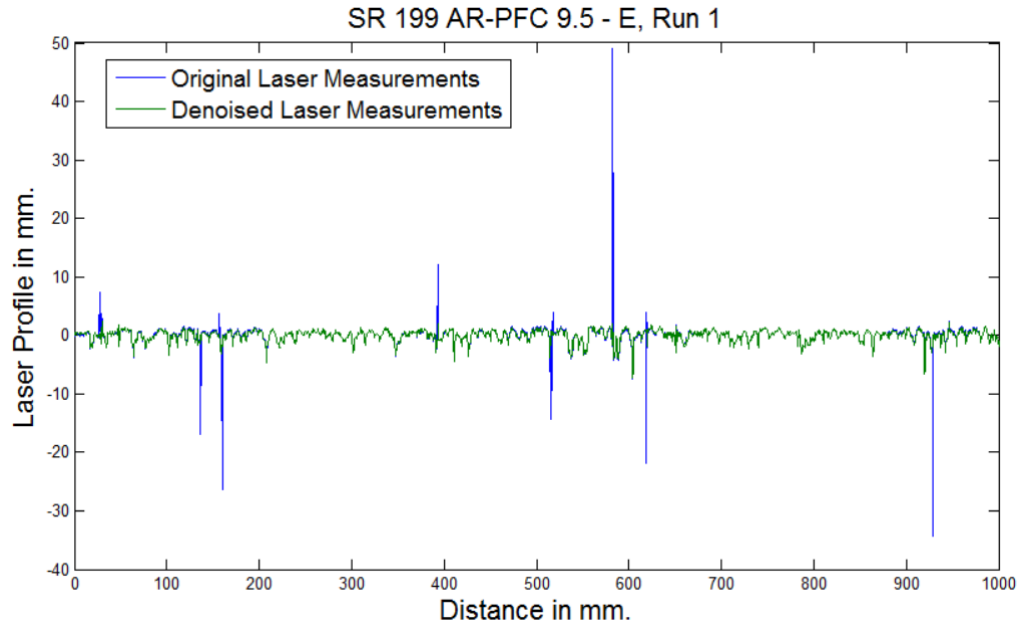
Figure 4-5 HSLD Measurements, with and without spikes (1st meter of Section B-SM-9.5D).


## Step 2. Enveloping Profile Calculation

For the chosen enveloping profile method, d* is defined as a measure for the elasticity of the tire rubber. Different values for $d*$ (0.054, 0.027, 0.01) in mm/mm$^2$ were obtained by von-Meier during his empirical experimentation with different artificial surfaces (containing peaks and valleys with different amplitude and longitude).

The larger the value of $d*$ is, the more the enveloped profile will follow the original pavement profile, meaning that high d* values represent soft rubber tires, and low d* values represent stiff tires. For this study, very small values for $d*$ (e.g., 0.001, representing significantly stiffer rubber tires) are also used in addition to the $d*$ values used by von Meier et al. to test the hypothesis about overestimation of the EAWE when using MPD (indicated in Step 3).

Therefore, the enveloping profile analysis was performed for all 180 denoised profiles using four different $d*$ values (0.054, 0.027, 0.01, 0.001, which can be related to medium soft, medium hard, stiff, and significantly stiff tires, respectively), giving a total of 720 calculated enveloping profiles to be used for calculation of the proposed index (EAWE) in the last step. This significantly large amount of data guarantees the confidence of the results.

For the enveloping profile calculation, since we are interested in the pavement macrotexture, rather than the geometric properties of the tire, a smooth tire is assumed in this study.

Examples of the resulting enveloping profiles, for different tire stiffnesses, are presented in Figure 4-6  and Figure 4-7 , which show the results for a dense and a porous mix, respectively. It is noted that, as expected, for these two sections (as well as for all 32 analyzed sections) the higher the tire stiffness (which corresponds to smaller the $d*$ values), the higher the EAWE.

51
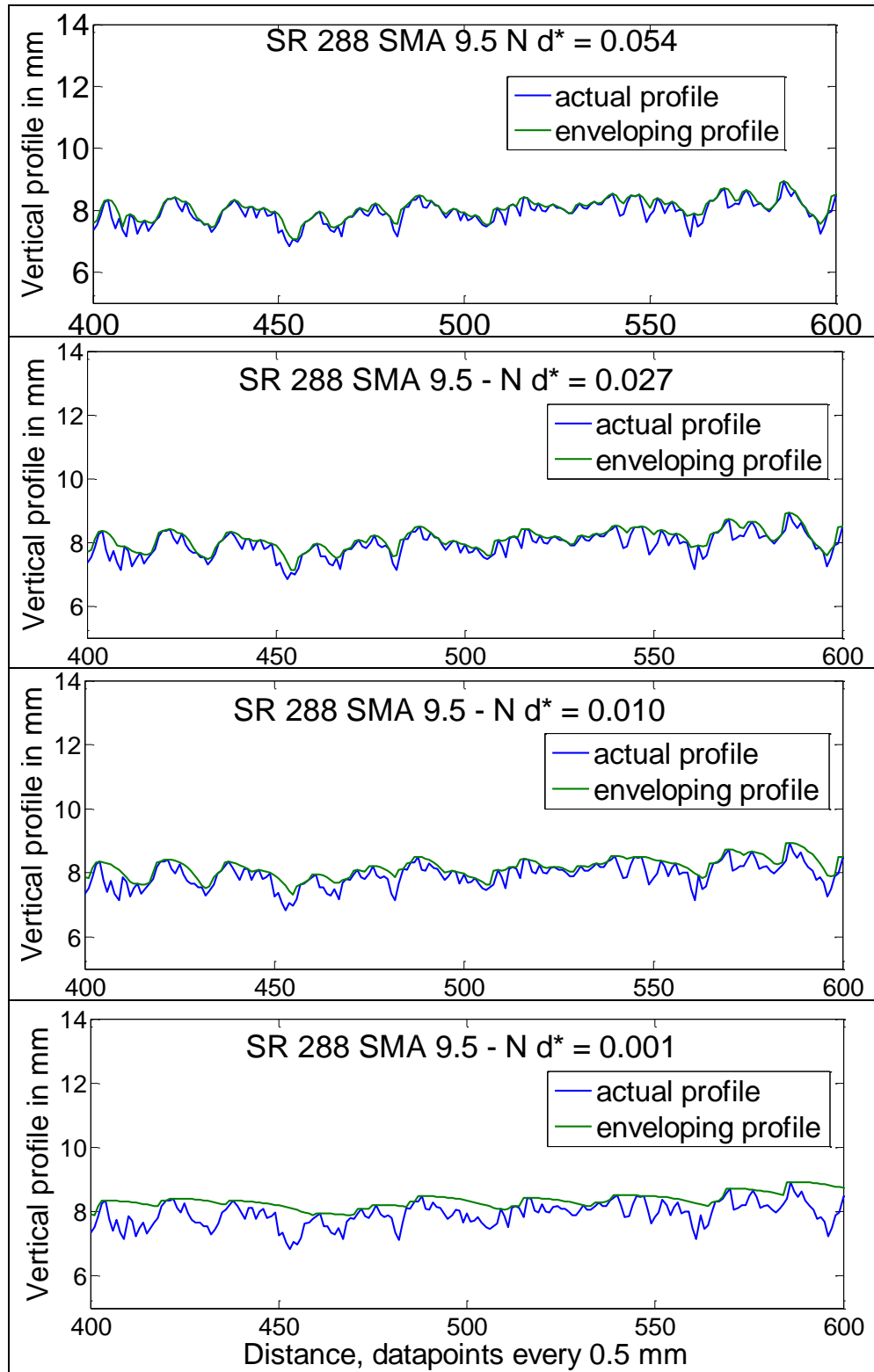
Figure 4-6 Enveloping profile illustration calculated for different tire stiffnesses for a dense asphalt mix (e.g., 100 mm for Section SR-288 SMA 9.5 N).
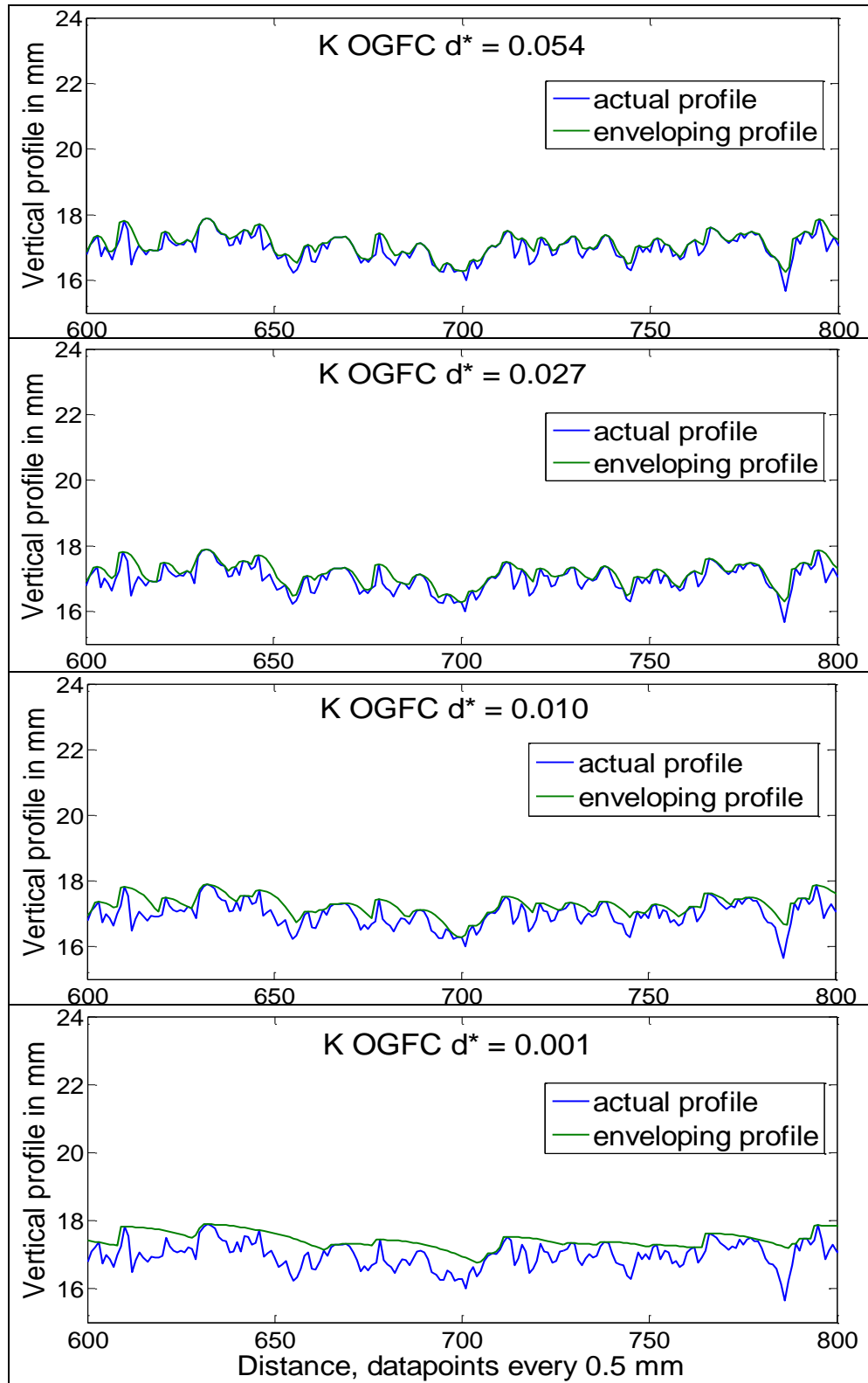
Figure 4-7 Enveloping profile illustration calculated for different tire stiffnesses for a porous asphalt mix (e.g., 100 mm for Section K - OGFC).

**Step 3. EAWE and EDWE Calculation and Its Potential Improvement.**

As explained in the problem statement, MPD by definition may not be the best indicator of the real potential that pavement macrotexture have to evacuate water (or air). Actually, since the MPD is calculated as the average of the peak levels on each half of the baseline minus the average level (which means using the peaks by definition), then MPD is believed to overestimate the EAWE that the pavement may have. This hypothesis is confirmed in the following analysis.

For all of the 32 analyzed sections, Figure 4-8 clearly depicts how Mean Profile Depth (MPD) overestimates the potential of the pavement for evacuating water, since, these mean depths (function of the peaks by definition) are higher in magnitude than the average effective depth of the resulting area between the tire and the pavement (represented by EDWE), this is confirmed for both, CTMeter-MPD and HSLD-MPD.

Considering the fact that, the lower the tire stiffness, the higher the tire rubber deformation, and the lower the effective area for water evacuation. A sensitivity analysis (varying tire stiffness) confirms the hypothesis, since it shows that MPD models the area similar to EAWE only when relatively no tire rubber deformation is allowed which is not what really happens. The EDWE index tends to compare with MPD in magnitude only when a relatively small $d^*$ value of 0.001 is used (theoretically representing a significantly stiff tire).
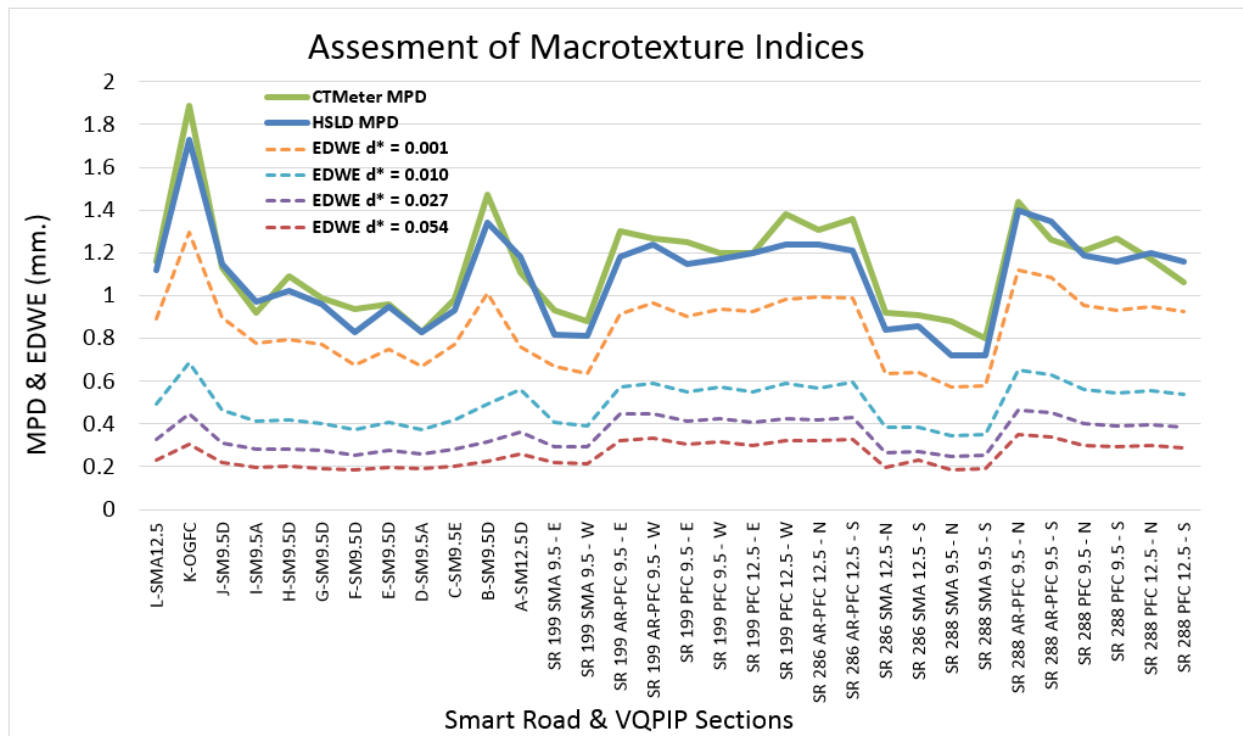


Figure 4-8 Comparison of macrotexture characterization indices.

Furthermore, correlations with friction and tire/pavement noise, which are the main pavement surface characteristics influenced by the texture wavelength (0.5 mm $< \lambda <$ 50 mm) corresponding to macrotexture *(2, 3)*, also improve when using the EAWE instead of MPD for all tire stiffnesses, even when compared with two different sets of MPD (CTMeter MPD and HSLD MPD).

Table 4-1 represents a summary of 340 CTMeter runs for texture (CTMeter-MPD); 180 HSLD runs for texture (HSLD-MPD); 720 HSLD runs for texture (EAWE); 204 GripTester runs for friction (grip number [GN]); and 101 OBSI runs for noise (intensity level [IL]) that were used for the correlation analysis.

54

Table 4-1 Summary of Texture, Friction, and Noise Indices

| Sections | Macrotexture | | | | | | | | | | Friction | Noise |
|---|---|---|---|---|---|---|---|---|---|---|---|---|
| | MPD (mm) | | EAWE (mm) | | | | EDWE (mm) | | | | GN | IL |
| | CTMeter | HSLD | 0.054 | 0.027 | 0.010 | 0.001 | 0.054 | 0.027 | 0.010 | 0.001 | | dBA |
| L-SMA12.5 | 1.16 | 1.12 | 23.29 | 33.09 | 49.14 | 89.33 | 0.23 | 0.33 | 0.49 | 0.89 | 0.53 | 101.1 |
| K-OGFC | 1.89 | 1.73 | 30.54 | 44.56 | 68.43 | 129.49 | 0.31 | 0.45 | 0.68 | 1.29 | | 99.7 |
| J-SM9.5D | 1.13 | 1.15 | 21.92 | 31.30 | 46.52 | 89.85 | 0.22 | 0.31 | 0.47 | 0.90 | 0.57 | |
| I-SM9.5A | 0.92 | 0.97 | 19.72 | 28.14 | 41.34 | 77.78 | 0.20 | 0.28 | 0.41 | 0.78 | 0.66 | |
| H-SM9.5D | 1.09 | 1.02 | 20.00 | 28.34 | 41.75 | 79.58 | 0.20 | 0.28 | 0.42 | 0.80 | | 102.3 |
| G-SM9.5D | 0.99 | 0.96 | 19.15 | 27.44 | 40.40 | 77.07 | 0.19 | 0.27 | 0.40 | 0.77 | | 102.3 |
| F-SM9.5D | 0.94 | 0.83 | 18.42 | 25.65 | 37.10 | 67.40 | 0.18 | 0.26 | 0.37 | 0.67 | | 102.3 |
| E-SM9.5D | 0.96 | 0.95 | 19.72 | 27.86 | 40.73 | 74.95 | 0.20 | 0.28 | 0.41 | 0.75 | | 102.3 |
| D-SM9.5A | 0.83 | 0.83 | 18.98 | 26.09 | 37.59 | 66.83 | 0.19 | 0.26 | 0.38 | 0.67 | 0.52 | |
| C-SM9.5E | 0.98 | 0.93 | 20.47 | 28.41 | 42.00 | 77.35 | 0.20 | 0.28 | 0.42 | 0.77 | 0.56 | |
| B-SM9.5D | 1.47 | 1.34 | 22.53 | 31.80 | 49.59 | 100.88 | 0.23 | 0.32 | 0.50 | 1.01 | 0.67 | 101.1 |
| A-SM12.5D | 1.11 | 1.18 | 25.89 | 36.32 | 56.38 | 75.82 | 0.26 | 0.36 | 0.56 | 0.76 | 0.61 | 100.7 |
| SR 199 SMA 9.5 - E | 0.93 | 0.82 | 21.85 | 29.43 | 40.62 | 67.25 | 0.22 | 0.29 | 0.41 | 0.67 | 0.65 | 102 |
| SR 199 SMA 9.5 - W | 0.88 | 0.81 | 21.30 | 29.18 | 39.33 | 63.62 | 0.21 | 0.29 | 0.39 | 0.64 | 0.64 | 102.2 |
| SR 199 AR-PFC 9.5 - E | 1.3 | 1.18 | 32.06 | 44.75 | 57.38 | 91.31 | 0.32 | 0.45 | 0.57 | 0.91 | 0.72 | 99.2 |
| SR 199 AR-PFC 9.5 - W | 1.27 | 1.24 | 33.34 | 44.87 | 58.89 | 96.59 | 0.33 | 0.45 | 0.59 | 0.97 | | 99.3 |
| SR 199 PFC 9.5 - E | 1.25 | 1.15 | 30.56 | 41.60 | 55.08 | 90.43 | 0.31 | 0.42 | 0.55 | 0.90 | 0.73 | |
| SR 199 PFC 9.5 - W | 1.2 | 1.17 | 31.58 | 42.56 | 57.41 | 94.00 | 0.32 | 0.43 | 0.57 | 0.94 | 0.68 | 100.1 |
| SR 199 PFC 12.5 - E | 1.2 | 1.2 | 30.20 | 40.72 | 54.97 | 92.36 | 0.30 | 0.41 | 0.55 | 0.92 | 0.67 | |
| SR 199 PFC 12.5 - W | 1.38 | 1.24 | 32.08 | 42.51 | 58.84 | 98.31 | 0.32 | 0.43 | 0.59 | 0.98 | 0.68 | 100.9 |
| SR 286 AR-PFC 12.5 - N | 1.31 | 1.24 | 31.98 | 42.06 | 56.74 | 99.33 | 0.32 | 0.42 | 0.57 | 0.99 | | 98.7 |
| SR 286 AR-PFC 12.5 - S | 1.36 | 1.21 | 32.94 | 43.18 | 59.54 | 98.90 | 0.33 | 0.43 | 0.60 | 0.99 | 0.68 | 97.5 |
| SR 286 SMA 12.5 -N | 0.92 | 0.84 | 19.68 | 26.51 | 38.66 | 63.32 | 0.20 | 0.27 | 0.39 | 0.63 | 0.67 | 103.1 |
| SR 286 SMA 12.5 - S | 0.91 | 0.86 | 23.06 | 26.91 | 38.77 | 64.28 | 0.23 | 0.27 | 0.39 | 0.64 | 0.62 | 103.2 |
| SR 288 SMA 9.5 - N | 0.88 | 0.72 | 18.60 | 24.89 | 34.32 | 57.51 | 0.19 | 0.25 | 0.34 | 0.58 | 0.66 | 103.3 |
| SR 288 SMA 9.5 - S | 0.8 | 0.72 | 18.89 | 25.30 | 34.94 | 58.09 | 0.19 | 0.25 | 0.35 | 0.58 | 0.60 | 103 |
| SR 288 AR-PFC 9.5 - N | 1.44 | 1.4 | 35.10 | 46.46 | 65.28 | 111.98 | 0.35 | 0.46 | 0.65 | 1.12 | 0.67 | 100.9 |
| SR 288 AR-PFC 9.5 - S | 1.26 | 1.35 | 33.88 | 45.22 | 63.21 | 108.40 | 0.34 | 0.45 | 0.63 | 1.08 | 0.70 | 101.2 |
| SR 288 PFC 9.5 - N | 1.21 | 1.19 | 30.17 | 40.10 | 56.14 | 95.18 | 0.30 | 0.40 | 0.56 | 0.95 | 0.69 | 101.7 |
| SR 288 PFC 9.5 - S | 1.27 | 1.16 | 29.35 | 39.00 | 54.60 | 93.03 | 0.29 | 0.39 | 0.55 | 0.93 | 0.67 | 102.2 |
| SR 288 PFC 12.5 - N | 1.17 | 1.2 | 30.06 | 39.86 | 55.65 | 94.84 | 0.30 | 0.40 | 0.56 | 0.95 | 0.70 | 101.2 |
| SR 288 PFC 12.5 - S | 1.06 | 1.16 | 28.98 | 38.53 | 53.96 | 92.65 | 0.29 | 0.39 | 0.54 | 0.93 | 0.64 | 100.6 |

*Empty spaces: data not collected due to different circumstances.

Figure 4-9  and Figure 4-10 show the improvement in correlations with friction and noise, respectively, when using the EAWE instead of MPD.
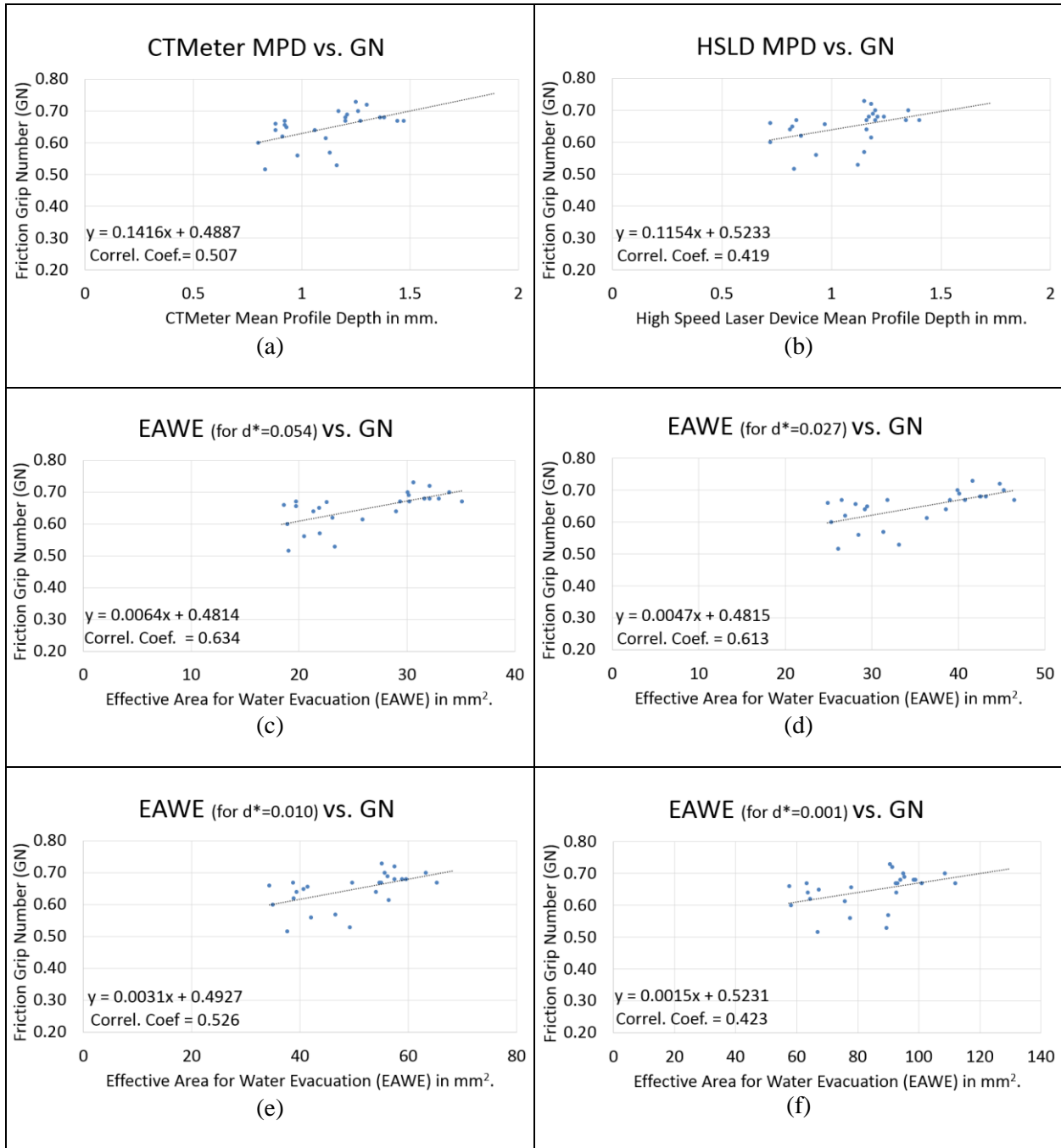


Figure 4-9 Macrotexture vs. friction - correlations.
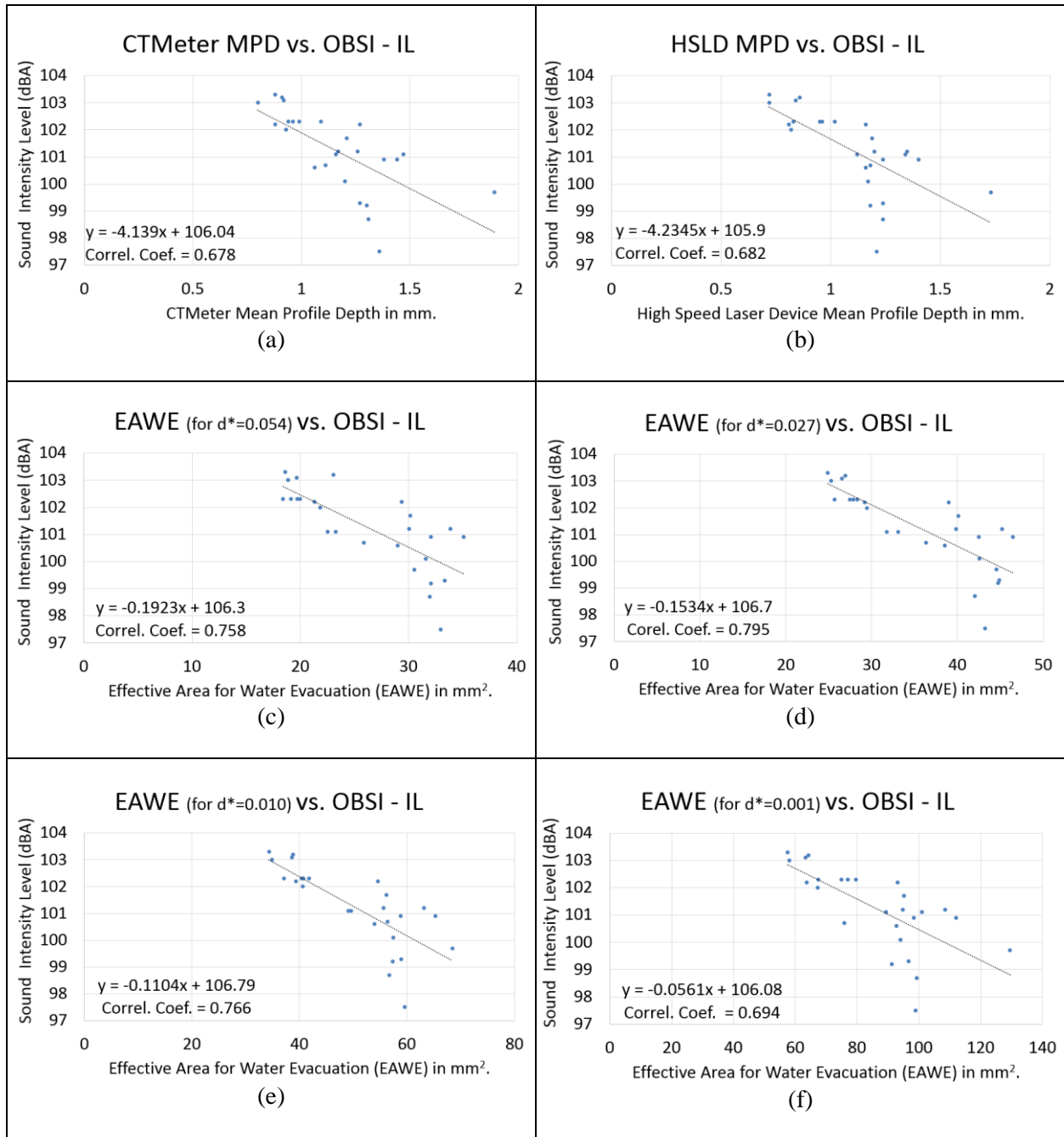
Figure 4-10 Macrotexture vs. noise - correlations.

The corresponding correlation coefficients are summarized in Table 4-2 . Besides the reasonable improvement in correlations with friction and noise, when using EAWE (at any tire stiffness) instead of MPD (CTMeter MPD or HSLD MPD), it is noticeable also that EAWE correlations tend to decrease while tire stiffness increases. Both correlations, EAWE vs. friction and EAWE vs. noise, get worse and become comparable with the correspondent MPD correlations only when working with significantly high tire-stiffness values (e.g. $d* = 0.001$). This confirms the fact that characterizing macrotexture in the "peaks" range (as MPD does by definition) is not the more appropriate approach.

Table 4-2 Goodness of Correlations for All Comparisons

| Indices | | Correlation Coefficient | |
|---|---|---|---|
| | | Friction | Noise |
| MPD (mm) | CTMeter | 0.507 | 0.678 |
| | HSLD | 0.419 | 0.682 |
| EDWE (mm) | d* = 0.054 | **0.634** | **0.758** |
| | d* = 0.027 | **0.613** | **0.795** |
| | d* = 0.01 | **0.526** | **0.766** |
| | d* = 0.001 | **0.423** | **0.694** |

It must be noticed that some of the sections with the highest macrotexture values are measured on porous surfaces, which absorb some of noise generated at the tire-pavement interface. Therefore, this confounding effect may have impact on the high correlation between macrotexture and noise.

The improvements on the correlations when using EAWE instead of MPD, and MPD overestimation of the ability of the pavement to drain water, can be physically explained by the following: by definition, MPD is an index that is calculated taking into account only 2 data points every 100 mm base-length (the highest peak for each 50 mm half base-length). The MPD is somehow equivalent to 2 stages of a rigid and flat tire only making contact in the two highest peaks; thus, the corresponding predicted area (voids between the tire and the pavement) is too large. On the other hand, the EAWE takes into account all data points (not only 2 peaks) along the whole section, not only 100 mm base-length (although, EAWE results can be presented for any base-length including 100 mm), and predicts better the tire rubber deformation over the pavement profile (MPD does not predict tire deformation at all). Therefore, the EAWE modeling leads to a better estimation of the actual area between that tire and the pavement. The conclusion of this interpretation is that MPD represent a more simplistic model when compared with EAWE modeling that is more complex but it is closer to what really happens at tire-pavement contact. Consequently, the use of the proposed EAWE index is recommended.

**SUMMARY AND CONCLUSIONS**

The research described in this paper can be summarized as follows:

- This paper proposes an innovative and robust three-step methodology to compute a novel index for macrotexture characterization.

- The significant number of macrotexture, friction, and noise measurements over 32 sections ensure the confidence of the results. The proposed three-step methodology (spike removal, enveloping profile calculation, and EAWE definition) was robust and reliable for all 32

sections, which provided a variety of different profile distributions, texture depths, connectedness, porosity, etc.

- Comparisons of current (MPD) and proposed (EAWE) macrotexture characterization indices were performed.

- Correlations for MPD and EAWE indices with the main pavement surface characteristics influenced by macrotexture wavelength were established.

The following conclusions can be drawn from the results:

- It was possible to define a promising index for macrotexture characterization based on the EAWE that appears to be improvement when compared with MPD.

- A comprehensive comparison between MPD and EAWE (with different tire configurations) involving a significant amount of different asphalt sections confirms that MPD overestimates the ability of the pavement to drain water under a real tire.

- The macrotexture values computed using the EAWE (for all tire stiffnesses tested) instead of MPD (either calculated using CTMeter or HSLD) correlate better with friction and noise measurements.

- The use of a continuous HSLD to measure texture, and the consequent possibility of presenting macrotexture data for every single location along the analyzed section (e.g., $\widehat{EAWE}$, $\widehat{EAWE}_{100}$, $\widehat{EDWE}$, or $\widehat{EDWE}_{100}$), also represents a significant improvement for macrotexture characterization. This feature may represent a step toward macrotexture characterization, not just at the project level but also at the network level.

# REFERENCES

[1] International Organization for Standardization. Characterization of pavement texture by use of surface profiles 2009  [cited 1/21/2015]; Available from: https://www.iso.org/obp/ui/#iso:std:iso:13473:-5:ed-1:v1:en

[2] Rasmussen RO. Pavement texture fundamentals. CE News 2013;25(7):pp 48-50.

[3] Loprencipe G, Cantisani, G. Unified Analysis of Road Pavement Profiles for Evaluation of Surface Characteristics. Canadian Center of Science and Education 2013;7.

[4] Katicha S, Mogrovejo, D., Flintsch, G., de León Izeppi, E. Adaptive Spike Removal Method for High Speed Pavement Macrotexture Measurements by Controlling the False Discovery Rate. Transportation Research Board 2015.

[5] Mogrovejo, D., Katicha, S., Flintsch, G., de León Izeppi, E. Latest Development in the Processing of Pavement Macrotexture Measurements of High Speed Laser Devices. 9th International Conference on Managing Pavement Assets 2014.

[6] McGhee KK, Flintsch GW. High-Speed Texture Measurement of Pavements. United States; 2003.

[7] Goubert L. Road Surface Texture and Traffic Noise.  NPRA workshop Texture and Road traffic noise; 2007; Oslo; 2007.

[8] Kleim P, Hamet Jean-Fran¸cois. Road texture and rolling noise - An envelopment procedure for tire-road contact. 2004.

[9] Sandberg U, Bergiers, A., Ejsmont, J., Goubert, L., Karlsson, R., Zoller, M. Road Surface Influence and Tyre/Road Rolling Resistance. In: MIRIAM, editor.; 2011.

[10] Hamet J, Klein, P., Anfosso, F., Duhamel, D., Fadavi, A., Beguet, B. Road Profile Texture and Tire Noise. 2002.

[11] von Meier A, van Blokland, G., Descornet, G. The Influence of texture and Sound Absorption on the Noise of Porous road Surfaces

[12] Perera RM, M; Orthmeyer, R. De León Izeppi, E. AFD 90, Group III Texture Measurements and use; 2013.

[13] VTTI. Virginia Smart Road.  2014  [cited 2014 July 7th, 2014]; Available from: https://www.vtti.vt.edu/smart-road/virginia-smart-road.html

[14] Mogrovejo DE, Flintsch GW, De León E, McGhee KK, Burdisso R. Short-Term Effect of Pavement Surface Aging on Tire/Pavement Noise Measured with On-Board Sound Intensity Methodology. Transportation Research Board 2014.

[15] ASTM. ASTM E2157-09 Standard Test Method for Measuring Pavement Macrotexture Properties Using the Circular Track Meter PA 19428-2959. United States: ASTM International; 2009.

[16] LMI-Technologies. Selcom Optocator User's manual. Sweden: LMI Technologies INC.; 2013.

[17] AASHTO. Standard Method of Test for Measurement of Tire/Pavement Noise Using the On-Board Sound Intensity (OBSI) Method (Draft).  AASHTO Designation: TP 76-13. Washington, 444 North Capitol Street N.W., Suite 249, D.C., United States of America: American Association of State Highway and Transportation Officials; 2012.

[18] Mogrovejo Carrasco DE. Effect of Air Temperature, Vehicle Speed, and Pavement Surface Aging on Tire/Pavement Noise Measured with On-Board Sound Intensity Methodology. Blacksburg: Virginia Tech; 2012.

[19] Goubert L, Bergiers A. About The Reproducibility Of Texture Profiles And The Problem of Spikes. SURF 2012 2012.

[20] von-Meier A, van-Blokland, G., Descornet, G. . The influence of texture and Sound Absorption on the Noise of Porous Road Surfaces. 1992.

# Chapter 5 –CONCLUSIONS, AND RECOMMENDATIONS FOR FUTURE RESEARCH

## SUMMARY

This dissertation presented the analysis and results for two spike removal methodologies, applicable for texture measurements obtained with HSLD, along with a proposed multi-representation macrotexture index that better characterizes the pavement potential to evacuate water out of the tire pavement contact patch, a key safety feature desired on all pavement surfaces.

The first and second manuscripts addressed the problem of spikes (that current equipment/ software fail to remove) in the texture measurements gathered with HSLD.

The first manuscript proposes a denoising methodology based on an alternative representation of the texture profile, the following steps summarize the methodology:

a) Calculate the discrete wavelet transform for the raw measurements,

b) Detect and remove the "spikes" from the obtained wavelet coefficients (that represent the differences on amplitude along the original texture profile) by fitting an accurate distribution of this differences, and by defining the correspondent threshold and boundary, and subsequent spike removal,

c) After removing all wavelet coefficients that are defined as outliers, the method then recomposes the processed wavelet coefficients using the inverse discrete wavelet transform to finally obtain correct MPD measurements by using the denoised texture profile.

The Comparison of MPD vales with and without spikes was also performed. Finally, the proposed method was validated by contrasting the calculated MPD with MPD measurements obtained with the CTMeter.

The second manuscript builds on the method proposed in the previous one, and proposes a more robust methodology that uses an adaptive threshold approach. The method is summarized below:

a) The distribution definition is less subjective, since the actual distribution fit is automated and performed only over the significant range of values in the distribution tails.

b) The threshold for outliers delimitation is not fixed, instead, the threshold adapts to the data by accounting for the large amount of data, and by controlling the proportion of wrongly identified outliers among all identified spikes using the false discovery rate method,

c) A sensitivity analysis for the proportion at which the false discovery rate is controlled was made in order to optimize the threshold selection and maximize the difference between the correctly identified spikes minus the wrongly identified spikes.

The third manuscript addresses the limitation of current macrotexture characterization procedures by proposing an enhanced multi-representation macrotexture index (based on the pavement potential to evacuate water). This method improves texture correlations with two pavement surface characteristics: friction and noise. The method used for the calculation of the proposed index can be summarized as follows:

a) Applies a spike removal procedure (consistent with the methodology presented on the second manuscript), which assures the reliability of the texture profile data is performed.

b) Conducts a delimitation of the area between the tire and the pavement where the contact occurs by calculating the tire enveloping profile with a variation of the Von-Meiers enveloping method.

c) Computes the proposed index (EAWE) as a function of this delimitated area.

Comparison of the proposed index with MPD confirmed that MPD's overestimates the pavement potential to drain water. Furthermore, improvements are found with friction and noise measurements; the EAWE correlates slightly better than MPD.

## FINDINGS

Some of the findings of this work can be summarized as follows:

- An analysis of variance (ANOVA) for the CTMeter measurements performed and presented in the first manuscript showed that the relative location of the CTMeter within the analyzed section do not influence the final average MPD, nor the differences found between MPD values for the eight CTMeter sectors. This finding allowed for better comparisons of MPD calculated with control devices and MPD calculated using the proposed denoising methodologies.

- Current software implemented on high speed texture measurement devices fail to successfully remove all the spikes in the laser measurements; some spikes remain even after traditional filtering and dropout removal performed by the manufacturer software. The proposed methodologies addresses this problem and make measurements reliable for further macrotexture indices calculation.

- The recommended methodologies for denoising texture measurements are applicable for all of the studied sections (wide range of typical asphalt sections). The proposed new macrotexture characterization index resulted to be applicable for all studied sections as well.

- A possible limitation was found in terms of automation for the spike removal process when using the wavelet transform method (presented in the first manuscript). The definition of the threshold is dependent on the particular modeling of the distribution for the wavelet coefficients for each surface to be analyzed. This particular process cannot be generalized for all sections and must be done for each section in order to correctly define the threshold for outlier definition. The false discovery rate method (presented in the second manuscript) addresses this limitation by automatically fitting the data using the Generalized Gaussian distribution (GGD) approach.

- Comparison of MPD values calculated with raw and denoised data shows that spikes do affect the results significantly. The MPD values calculated with the original texture data were on average 50% higher that the values calculated with denoised data.

- The test of this methodologies, especially the one based on the false discovery rate over a substantial amount of real data (wide range of asphalt pavement surfaces) confirms its reliability to successfully discover the spikes to be removed out of the collected data.

## CONCLUSIONS

The following are the main conclusions obtained in the study:

- Two innovative and robust denoising methodologies are proposed in this work; both methods demonstrated to objectively define spikes and remove them from the original texture profile. The first method based on discrete wavelet transform depends on modeling the distribution of the wavelet coefficients of texture measurements to correctly define the appropriate threshold to

define outliers (which can be interpreted as a limitation). The second method uses an automated distribution fit on the significant range of values (at the tails proximity) plus an adaptive threshold approach based on the false discovery rate control, which eliminates the subjective dependence of the distribution definition. The comparison of MPD values obtained from the denoised data (analyzed with the proposed spike removal methods) vs MPD values calculated with the control device (CTMeter), detected no statistical differences between the results from both methods and the reference measurements.

- A three step method that involves: spike removal, enveloping profile calculation, and effective area for water evacuation definition, was developed to compute a new index (EAWE) that better characterize macrotexture. The proposed index, based on the actual potential of the pavement to evacuate water out of the tire-pavement contact area, features the following *improvements* when compared with MPD:

    a) A comprehensive comparison between MPD and EAWE involving a significant amount of different asphalt sections suggested that MPD overestimates the effective area for water evacuation significantly

    b) Macrotexture values quantified using EAWE correlated better with friction and texture measurements than using MPD. The analysis yielded EAWE vs friction correlations as high as 0.634 and EAWE vs noise correlations as high as 0.795.


## SIGNIFICANCE AND IMPACT

Each manuscript represents a contribution to the field of pavement surface properties, the impact of its contents has already started strong, since its contents are being presented/published on the most important peer-reviewed transportation journals and conferences.

From the engineering point of view: direct application of additional techniques and models is expected, the improvements on the texture measurement analysis, with the automated FDR method for spike removal, and its ongoing practical implementation in manufacturer's software; constitute a significant step towards reliable macrotexture characterization when using HSLD. The resulting benefits of employing HSLD (now with adequate reliability), like: reduction in time for field measurements, eliminating the need of traffic control, eliminating the presence of personnel on the road, among others, represent a huge positive impact on safety, efficiency and budget. Practical implementation of the new index is perfectly possible too.

From the scientific point of view: the comprehensive texture profile study, the development of the spike removal methods, and the definition and proposal of an enhanced macrotexture index; represents the main scientific contribution of this dissertation, since a better understanding of the pavement macrotexture and its influence on pavement surface characteristics was achieved.

## RECOMMENDATIONS

The following recommendations for *testing* can be made:

- It is recommended the testing of the FDR denoising method, and the subsequent calculation of EAWE with different laser configurations/devices, other than the single point laser device used in this study (e.g. beam transversal lasers) that allows transversal measurements, and therefore the possibility of including sections with longitudinal grinding and/or grooving (e.g. longitudinal diamond grinding concrete surfaces, next regeneration concrete surfaces, etc.), and so broaden the spectrum of analyzed surfaces. It will help to generalize the conclusions.

- The implementation of both, the FDR denoising method, and the EAWE calculation, on manufacturer's software is recommended, it will contribute significantly on achieving accurate macrotexture characterization; this will represent a huge step towards network level macrotexture analysis.

The following recommendations for *future research* are expended to lead the path for advances in the measurement and characterization of macrotexture:

- After the implementation of the proposed denoising methods on manufacturer's devices/software, and after significant amount of field testing; a sensitivity analysis looking for the best base lengths for results presentation should be made, considering both: a representative macrotexture value (or set of values) for the analyzed section(s); and, at the same time looking for the optimum (minimum) usage of computer memory and space. This will help to implement an optimized way of macrotexture measurements at a network level.

- In terms of: the enveloping methodology implemented in the EAWE index definition, its reported d* values, and the fact that this d* values were obtained by experimentation over artificial surfaces; it will be remarkable to experimentally investigate and obtain different d* values over real pavement surfaces, and its relationship with actual reference tires (different stiffness, different tread paths, etc.). It will make the methodology more robust and well based to be considered for implementation on standards, practitioners' manuals, DOTs, etc.

- It will be interesting also to investigate another enveloping methodologies as they become available, (e.g. INRETS method), to see for example if better correlations with the main pavement surface characteristics can be achieved.

- The implementation of the spike removal methodology on measurements gathered with 3D laser devices is recommended for future research, as resolution and speed on laser technology improves and become more available. Furthermore with planar texture measurements (possible with 3D lasers), and with the EAWE as basis, a totally new index based on the Effective Volume for Water evacuation (EVWE) can be studied and developed.

# APPENDICES

## Appendix A: Field Test Results for Chapter 2

*CTMeter Field Results:*

### Section B - Run 1 - Wheel Path:

| | | | | | | | | |
|---|---|---|---|---|---|---|---|---|
| [1] | A: 0.95( 0%)[1.20] | B: 1.50( 0%)[1.35] | C: 1.49( 0%)[1.50] | D: 0.97( 0%)[0.98] | E: 0.90( 0%)[0.68] | F: 1.27( 0%)[0.76] | G: 1.29( 1%)[0.96] | H: 0.89( 2%)[0.60] | Ave: 1.16( 0%)[1.00] |
| [2] | A: 0.94( 1%)[1.20] | B: 1.47( 0%)[1.34] | C: 1.48( 0%)[1.49] | D: 1.00( 0%)[0.98] | E: 0.89( 1%)[0.67] | F: 1.27( 2%)[0.76] | G: 1.25( 1%)[0.96] | H: 0.87( 2%)[0.61] | Ave: 1.15( 1%)[1.00] |
| [3] | A: 0.94( 0%)[1.21] | B: 1.50( 0%)[1.38] | C: 1.49( 0%)[1.52] | D: 0.97( 1%)[1.00] | E: 0.90( 0%)[0.69] | F: 1.26( 1%)[0.76] | G: 1.29( 1%)[0.99] | H: 0.87( 2%)[0.61] | Ave: 1.15( 1%)[1.02] |
| [4] | A: 0.94( 1%)[1.23] | B: 1.52( 0%)[1.39] | C: 1.49( 1%)[1.52] | D: 0.99( 1%)[1.01] | E: 0.91( 0%)[0.67] | F: 1.25( 0%)[0.77] | G: 1.24( 1%)[0.96] | H: 0.89( 2%)[0.64] | Ave: 1.15( 1%)[1.02] |
| [5] | A: 0.97( 0%)[1.22] | B: 1.49( 0%)[1.37] | C: 1.48( 2%)[1.51] | D: 0.99( 0%)[1.01] | E: 0.91( 0%)[0.68] | F: 1.28( 0%)[0.76] | G: 1.26( 1%)[0.98] | H: 0.88( 0%)[0.62] | Ave: 1.16( 0%)[1.02] |
| [6] | A: 0.94( 2%)[1.22] | B: 1.48( 0%)[1.37] | C: 1.50( 0%)[1.52] | D: 0.99( 0%)[1.01] | E: 0.92( 0%)[0.68] | F: 1.26( 0%)[0.77] | G: 1.26( 1%)[0.98] | H: 0.89( 2%)[0.63] | Ave: 1.15( 1%)[1.02] |
| Ave | A: 0.95( 1%)[1.21] | B: 1.49( 0%)[1.37] | C: 1.49( 1%)[1.51] | D: 0.99( 0%)[1.00] | E: 0.91( 0%)[0.68] | F: 1.27( 1%)[0.76] | G: 1.27( 1%)[0.97] | H: 0.88( 2%)[0.62] | Ave: 1.16( 1%)[1.02] |

### Section B - Run 1 – Offset Path:

| | | | | | | | | |
|---|---|---|---|---|---|---|---|---|
| [1] | A: 1.36( 2%)[1.08] | B: 1.61( 0%)[1.54] | C: 1.57( 0%)[1.46] | D: 1.80( 2%)[1.65] | E: 1.27( 4%)[1.10] | F: 1.18( 1%)[1.03] | G: 1.06( 0%)[0.70] | H: 0.86( 0%)[0.62] | Ave: 1.34( 1%)[1.15] |
| [2] | A: 1.37( 2%)[1.09] | B: 1.61( 0%)[1.54] | C: 1.55( 0%)[1.45] | D: 1.79( 0%)[1.65] | E: 1.25( 3%)[1.10] | F: 1.17( 1%)[1.01] | G: 1.12( 2%)[0.74] | H: 0.88( 0%)[0.62] | Ave: 1.34( 1%)[1.15] |
| [3] | A: 1.37( 2%)[1.07] | B: 1.59( 1%)[1.51] | C: 1.53( 0%)[1.43] | D: 1.82( 0%)[1.65] | E: 1.84( 5%)[2.19] | F: 1.21( 1%)[1.12] | G: 1.10( 2%)[0.72] | H: 0.86( 0%)[0.61] | Ave: 1.42( 1%)[1.29] |
| [4] | A: 1.36( 2%)[1.07] | B: 1.56( 0%)[1.51] | C: 1.52( 0%)[1.43] | D: 1.82( 0%)[1.65] | E: 1.25( 2%)[1.10] | F: 1.19( 1%)[1.00] | G: 1.07( 1%)[0.72] | H: 0.86( 0%)[0.61] | Ave: 1.33( 1%)[1.14] |
| [5] | A: 1.36( 4%)[1.08] | B: 1.58( 0%)[1.51] | C: 1.57( 0%)[1.43] | D: 1.80( 0%)[1.65] | E: 1.24( 3%)[1.09] | F: 1.17( 2%)[0.99] | G: 1.05( 0%)[0.72] | H: 0.88( 0%)[0.61] | Ave: 1.33( 1%)[1.14] |
| [6] | A: 1.37( 5%)[1.09] | B: 1.59( 0%)[1.51] | C: 1.49( 0%)[1.45] | D: 1.79( 0%)[1.63] | E: 1.24( 2%)[1.11] | F: 1.18( 2%)[0.99] | G: 1.10( 1%)[0.72] | H: 0.88( 0%)[0.61] | Ave: 1.33( 1%)[1.14] |
| Ave | A: 1.37( 3%)[1.08] | B: 1.59( 0%)[1.52] | C: 1.54( 0%)[1.44] | D: 1.80( 0%)[1.65] | E: 1.35( 3%)[1.28] | F: 1.18( 1%)[1.02] | G: 1.08( 1%)[0.72] | H: 0.87( 0%)[0.61] | Ave: 1.35( 1%)[1.17] |

### Section B - Run 2 - Wheel Path:

| | | | | | | | | |
|---|---|---|---|---|---|---|---|---|
| [1] | A: 1.43( 2%)[1.32] | B: 1.50( 5%)[1.26] | C: 1.71( 0%)[1.23] | D: 1.49( 2%)[1.25] | E: 1.00( 1%)[0.82] | F: 1.32( 1%)[1.25] | G: 1.20( 0%)[1.20] | H: 1.11( 1%)[0.89] | Ave: 1.35( 2%)[1.15] |
| [2] | A: 1.48( 2%)[1.32] | B: 1.39( 3%)[1.19] | C: 1.68( 0%)[1.20] | D: 1.51( 2%)[1.23] | E: 1.03( 2%)[0.81] | F: 1.34( 2%)[1.24] | G: 1.21( 0%)[1.21] | H: 1.12( 0%)[0.88] | Ave: 1.35( 1%)[1.14] |
| [3] | A: 1.45( 1%)[1.34] | B: 1.39( 3%)[1.20] | C: 1.66( 0%)[1.18] | D: 1.56( 2%)[1.22] | E: 1.00( 1%)[0.82] | F: 1.35( 1%)[1.25] | G: 1.27( 1%)[1.20] | H: 1.09( 0%)[0.86] | Ave: 1.35( 1%)[1.13] |
| [4] | A: 1.46( 0%)[1.31] | B: 1.64( 1%)[1.61] | C: 1.68( 0%)[1.19] | D: 1.47( 3%)[1.24] | E: 0.99( 1%)[0.80] | F: 1.31( 1%)[1.23] | G: 1.20( 1%)[1.17] | H: 1.08( 0%)[0.86] | Ave: 1.35( 1%)[1.18] |
| [5] | A: 1.40( 2%)[1.30] | B: 1.40( 2%)[1.21] | C: 1.69( 0%)[1.19] | D: 1.52( 2%)[1.22] | E: 1.01( 1%)[0.82] | F: 1.34( 2%)[1.25] | G: 1.20( 1%)[1.18] | H: 1.08( 0%)[0.86] | Ave: 1.33( 1%)[1.13] |
| [6] | A: 1.39( 0%)[1.31] | B: 1.40( 0%)[1.19] | C: 1.68( 0%)[1.18] | D: 1.48( 2%)[1.19] | E: 1.03( 1%)[0.81] | F: 1.32( 2%)[1.23] | G: 1.20( 1%)[1.18] | H: 1.08( 0%)[0.86] | Ave: 1.32( 1%)[1.12] |
| Ave | A: 1.44( 1%)[1.32] | B: 1.45( 2%)[1.28] | C: 1.68( 0%)[1.20] | D: 1.51( 2%)[1.23] | E: 1.01( 1%)[0.81] | F: 1.33( 2%)[1.24] | G: 1.21( 1%)[1.19] | H: 1.09( 0%)[0.87] | Ave: 1.34( 1%)[1.14] |

### Section B - Run 2 – Offset Path:

| | | | | | | | | |
|---|---|---|---|---|---|---|---|---|
| [1] | A: 1.15( 1%)[0.94] | B: 1.67( 1%)[2.03] | C: 1.24( 3%)[1.21] | D: 0.99( 2%)[1.01] | E: 0.97( 0%)[1.04] | F: 2.56( 2%)[1.55] | G: 1.30( 1%)[1.06] | H: 1.35( 0%)[0.94] | Ave: 1.40( 1%)[1.22] |
| [2] | A: 1.14( 1%)[0.93] | B: 1.14( 2%)[1.19] | C: 1.21( 2%)[1.18] | D: 0.99( 2%)[0.99] | E: 1.07( 0%)[1.03] | F: 2.59( 2%)[1.55] | G: 1.32( 2%)[1.08] | H: 1.33( 0%)[0.93] | Ave: 1.35( 1%)[1.11] |
| [3] | A: 1.13( 0%)[0.90] | B: 1.10( 2%)[1.16] | C: 1.24( 2%)[1.19] | D: 1.04( 0%)[1.01] | E: 1.07( 0%)[1.03] | F: 2.57( 2%)[1.55] | G: 1.29( 1%)[1.05] | H: 1.38( 0%)[0.94] | Ave: 1.35( 1%)[1.10] |
| [4] | A: 1.16( 1%)[0.92] | B: 1.15( 2%)[1.16] | C: 1.20( 3%)[1.18] | D: 1.02( 2%)[0.98] | E: 1.01( 0%)[1.01] | F: 2.54( 2%)[1.53] | G: 1.34( 2%)[1.06] | H: 1.34( 1%)[0.93] | Ave: 1.35( 2%)[1.10] |
| [5] | A: 1.16( 0%)[0.92] | B: 1.15( 2%)[1.14] | C: 1.26( 3%)[1.19] | D: 1.01( 2%)[0.99]` | E: 1.01( 0%)[1.01] | F: 2.56( 2%)[1.52] | G: 1.26( 1%)[1.04] | H: 1.35( 0%)[0.92] | Ave: 1.35( 1%)[1.09] |
| [6] | A: 1.17( 1%)[0.92] | B: 1.15( 3%)[1.14] | C: 1.23( 0%)[1.18] | D: 1.05( 2%)[0.98] | E: 1.00( 0%)[1.00] | F: 2.51( 2%)[1.51] | G: 2.15( 2%)[2.45] | H: 1.35( 1%)[0.93] | Ave: 1.45( 1%)[1.26] |
| Ave | A: 1.15( 1%)[0.92] | B: 1.23( 2%)[1.30] | C: 1.23( 2%)[1.19] | D: 1.02( 2%)[0.99] | E: 1.02( 0%)[1.02] | F: 2.56( 2%)[1.54] | G: 1.44( 2%)[1.29] | H: 1.35( 0%)[0.93] | Ave: 1.38( 1%)[1.15] |

## Section B - Run 3 - Wheel Path:

| | | | | | | | | |
|---|---|---|---|---|---|---|---|---|
| [1] | A: 1.20( 2%)[0.78] | B: 1.52( 2%)[1.33] | C: 1.53( 0%)[1.36] | D: 1.28( 2%)[1.33] | E: 1.58( 0%)[1.67] | F: 1.63( 4%)[1.37] | G: 1.11( 0%)[0.80] | H: 1.69( 0%)[1.38] | Ave: 1.44( 1%)[1.25] |
| [2] | A: 1.23( 2%)[0.77] | B: 1.61( 2%)[1.32] | C: 1.51( 0%)[1.35] | D: 1.28( 2%)[1.34] | E: 1.59( 0%)[1.66] | F: 1.53( 5%)[1.32] | G: 1.10( 0%)[0.82] | H: 1.67( 0%)[1.38] | Ave: 1.44( 1%)[1.25] |
| [3] | A: 1.21( 2%)[0.77] | B: 1.56( 0%)[1.30] | C: 1.53( 2%)[1.32] | D: 1.25( 2%)[1.30] | E: 1.56( 0%)[1.66] | F: 1.59( 1%)[1.33] | G: 1.14( 0%)[0.82] | H: 1.69( 0%)[1.36] | Ave: 1.44( 1%)[1.23] |
| [4] | A: 1.22( 2%)[0.76] | B: 1.60( 1%)[1.31] | C: 1.53( 0%)[1.32] | D: 1.27( 2%)[1.32] | E: 1.60( 0%)[1.66] | F: 1.58( 3%)[1.33] | G: 1.12( 0%)[0.81] | H: 1.67( 2%)[1.37] | Ave: 1.45( 1%)[1.24] |
| [5] | A: 1.19( 4%)[0.73] | B: 1.59( 1%)[1.27] | C: 1.50( 1%)[1.25] | D: 1.26( 5%)[1.22] | E: 1.55( 0%)[1.58] | F: 1.60( 3%)[1.27] | G: 1.12( 0%)[0.74] | H: 1.69( 2%)[1.32] | Ave: 1.44( 2%)[1.17] |
| [6] | A: 1.18( 2%)[0.72] | B: 1.57( 2%)[1.23] | C: 1.50( 0%)[1.20] | D: 1.25( 2%)[1.18] | E: 1.55( 0%)[1.54] | F: 1.47( 3%)[1.17] | G: 1.11( 0%)[0.71] | H: 1.67( 0%)[1.28] | Ave: 1.41( 1%)[1.13] |
| Ave | A: 1.21( 2%)[0.76] | B: 1.58( 1%)[1.29] | C: 1.52( 1%)[1.30] | D: 1.27( 3%)[1.28] | E: 1.57( 0%)[1.63] | F: 1.57( 3%)[1.30] | G: 1.12( 0%)[0.78] | H: 1.68( 1%)[1.35] | Ave: 1.44( 1%)[1.21] |

## Section B - Run 3 – Offset Path:

| | | | | | | | | |
|---|---|---|---|---|---|---|---|---|
| [1] | A: 1.24( 2%)[0.90] | B: 0.79( 0%)[0.93] | C: 1.23( 0%)[0.80] | D: 1.50( 0%)[1.02] | E: 1.22( 0%)[0.84] | F: 1.52( 0%)[1.36] | G: 1.64( 0%)[1.04] | H: 1.44( 0%)[0.89] | Ave: 1.32( 0%)[0.97] |
| [2] | A: 1.22( 1%)[0.89] | B: 0.79( 0%)[0.91] | C: 1.23( 0%)[0.80] | D: 1.51( 0%)[1.01] | E: 1.18( 0%)[0.84] | F: 1.49( 0%)[1.38] | G: 1.64( 1%)[1.08] | H: 1.42( 0%)[0.89] | Ave: 1.31( 0%)[0.98] |
| [3] | A: 1.25( 1%)[0.90] | B: 0.78( 0%)[0.92] | C: 1.29( 0%)[0.79] | D: 1.48( 0%)[1.01] | E: 1.20( 0%)[0.86] | F: 1.50( 0%)[1.38] | G: 1.63( 0%)[1.06] | H: 1.41( 0%)[0.90] | Ave: 1.32( 0%)[0.98] |
| [4] | A: 1.24( 2%)[0.89] | B: 0.79( 0%)[0.92] | C: 1.29( 0%)[0.80] | D: 1.48( 1%)[0.99] | E: 1.20( 0%)[0.84] | F: 1.47( 0%)[1.37] | G: 1.65( 0%)[1.08] | H: 1.40( 0%)[0.88] | Ave: 1.32( 0%)[0.97] |
| [5] | A: 1.24( 0%)[0.89] | B: 0.80( 0%)[0.91] | C: 1.19( 0%)[0.78] | D: 1.51( 0%)[1.02] | E: 1.17( 0%)[0.85] | F: 1.50( 0%)[1.41] | G: 1.66( 0%)[1.07] | H: 1.42( 0%)[0.90] | Ave: 1.31( 0%)[0.98] |
| [6] | A: 1.24( 0%)[0.89] | B: 0.82( 0%)[0.92] | C: 1.24( 0%)[0.79] | D: 1.51( 0%)[1.01] | E: 1.20( 0%)[0.86] | F: 1.50( 0%)[1.38] | G: 1.60( 0%)[1.06] | H: 1.43( 0%)[0.90] | Ave: 1.32( 0%)[0.98] |
| Ave | A: 1.24( 1%)[0.89] | B: 0.80( 0%)[0.92] | C: 1.25( 0%)[0.79] | D: 1.50( 0%)[1.01] | E: 1.20( 0%)[0.85] | F: 1.50( 0%)[1.38] | G: 1.64( 0%)[1.07] | H: 1.42( 0%)[0.89] | Ave: 1.32( 0%)[0.98] |

## Section B - Run 4 - Wheel Path:

| | | | | | | | | |
|---|---|---|---|---|---|---|---|---|
| [1] | A: 1.65( 2%)[1.37] | B: 1.30( 0%)[1.15] | C: 1.19( 0%)[0.97] | D: 1.41( 3%)[0.99] | E: 1.27( 3%)[0.85] | F: 1.78( 0%)[1.42] | G: 1.21( 1%)[1.15] | H: 1.43( 0%)[1.20] | Ave: 1.41( 1%)[1.14] |
| [2] | A: 1.64( 2%)[1.36] | B: 1.29( 0%)[1.16] | C: 1.22( 1%)[0.98] | D: 1.46( 2%)[1.07] | E: 1.22( 2%)[0.84] | F: 1.71( 2%)[1.38] | G: 1.14( 0%)[1.05] | H: 1.42( 0%)[1.21] | Ave: 1.39( 1%)[1.13] |
| [3] | A: 1.67( 2%)[1.38] | B: 1.29( 1%)[1.12] | C: 1.20( 0%)[0.94] | D: 1.51( 4%)[1.09] | E: 1.23( 2%)[0.82] | F: 1.81( 1%)[1.41] | G: 1.17( 2%)[1.06] | H: 1.41( 0%)[1.18] | Ave: 1.41( 2%)[1.13] |
| [4] | A: 1.65( 2%)[1.34] | B: 1.35( 1%)[1.13] | C: 1.17( 0%)[0.94] | D: 1.41( 2%)[0.98] | E: 1.19( 2%)[0.84] | F: 1.78( 0%)[1.42] | G: 1.14( 2%)[1.07] | H: 1.40( 0%)[1.20] | Ave: 1.39( 1%)[1.12] |
| [5] | A: 1.60( 3%)[1.33] | B: 1.31( 0%)[1.11] | C: 1.18( 1%)[0.91] | D: 1.41( 5%)[0.95] | E: 1.22( 4%)[0.84] | F: 1.82( 0%)[1.42] | G: 1.16( 3%)[1.07] | H: 1.39( 0%)[1.16] | Ave: 1.39( 2%)[1.10] |
| [6] | A: 1.63( 2%)[1.32] | B: 1.29( 1%)[1.11] | C: 1.21( 1%)[0.92] | D: 1.34( 4%)[0.94] | E: 1.19( 2%)[0.83] | F: 1.69( 2%)[1.35] | G: 1.17( 2%)[1.10] | H: 1.39( 0%)[1.17] | Ave: 1.36( 2%)[1.09] |
| [7] | A: 1.67( 3%)[1.49] | B: 1.27( 1%)[1.24] | C: 1.19( 0%)[1.04] | D: 1.36( 5%)[1.03] | E: 1.24( 2%)[0.89] | F: 1.82( 1%)[1.50] | G: 1.16( 0%)[1.19] | H: 1.41( 0%)[1.27] | Ave: 1.39( 2%)[1.21] |
| Ave | A: 1.64( 2%)[1.37] | B: 1.30( 1%)[1.15] | C: 1.19( 0%)[0.96] | D: 1.41( 4%)[1.01] | E: 1.22( 2%)[0.84] | F: 1.77( 1%)[1.41] | G: 1.16( 1%)[1.10] | H: 1.41( 0%)[1.20] | Ave: 1.39( 1%)[1.13] |

## Section B - Run 4 – Offset Path:

| | | | | | | | | |
|---|---|---|---|---|---|---|---|---|
| [1] | A: 1.51( 2%)[0.96] | B: 1.77( 1%)[1.21] | C: 1.69( 0%)[1.17] | D: 1.19( 1%)[0.93] | E: 1.05( 0%)[0.71] | F: 1.92( 1%)[1.41] | G: 1.12( 3%)[0.69] | H: 0.97( 0%)[0.66] | Ave: 1.40( 1%)[0.97] |
| [2] | A: 1.48( 2%)[0.94] | B: 1.76( 1%)[1.21] | C: 1.69( 0%)[1.19] | D: 1.20( 1%)[0.93] | E: 1.07( 0%)[0.69] | F: 1.94( 1%)[1.41] | G: 1.15( 0%)[0.68] | H: 0.99( 0%)[0.68] | Ave: 1.41( 1%)[0.97] |
| [3] | A: 1.54( 3%)[0.95] | B: 1.78( 2%)[1.19] | C: 1.71( 0%)[1.17] | D: 1.20( 0%)[0.93] | E: 1.05( 0%)[0.69] | F: 1.93( 1%)[1.38] | G: 1.13( 3%)[0.67] | H: 1.00( 0%)[0.69] | Ave: 1.42( 1%)[0.96] |
| [4] | A: 1.46( 2%)[0.93] | B: 1.81( 1%)[1.19] | C: 1.72( 0%)[1.18] | D: 1.21( 0%)[0.92] | E: 1.06( 2%)[0.69] | F: 1.93( 0%)[1.38] | G: 1.12( 0%)[0.66] | H: 0.99( 0%)[0.68] | Ave: 1.41( 1%)[0.95] |
| [5] | A: 1.48( 0%)[0.94] | B: 1.79( 2%)[1.20] | C: 1.69( 0%)[1.18] | D: 1.22( 0%)[0.90] | E: 1.07( 1%)[0.69] | F: 1.92( 0%)[1.40] | G: 1.15( 0%)[0.66] | H: 1.00( 0%)[0.69] | Ave: 1.42( 0%)[0.96] |
| [6] | A: 1.47( 2%)[0.93] | B: 1.79( 1%)[1.18] | C: 1.70( 0%)[1.16] | D: 1.23( 0%)[0.92] | E: 1.04( 0%)[0.69] | F: 1.91( 0%)[1.37] | G: 1.14( 0%)[0.66] | H: 0.97( 0%)[0.68] | Ave: 1.41( 0%)[0.95] |
| Ave | A: 1.49( 2%)[0.94] | B: 1.78( 1%)[1.20] | C: 1.70( 0%)[1.18] | D: 1.21( 0%)[0.92] | E: 1.06( 1%)[0.69] | F: 1.93( 1%)[1.39] | G: 1.14( 1%)[0.67] | H: 0.99( 0%)[0.68] | Ave: 1.41( 1%)[0.96] |

## Section B - Run 5 - Wheel Path:

| | A | B | C | D | E | F | G | H | Ave |
|---|---|---|---|---|---|---|---|---|---|
| [1] | 2.05( 0%)[2.15] | 1.66( 2%)[1.49] | 1.35( 0%)[2.28] | 1.16( 3%)[1.11] | 1.31( 0%)[0.82] | 1.13( 0%)[0.89] | 1.42( 0%)[0.94] | 1.52( 0%)[1.06] | 1.45( 1%)[1.34] |
| [2] | 2.03( 0%)[2.12] | 1.62( 2%)[1.44] | 1.43( 2%)[2.27] | 1.18( 2%)[1.11] | 1.28( 0%)[0.84] | 1.10( 2%)[0.86] | 1.46( 0%)[0.94] | 1.53( 0%)[1.05] | 1.45( 1%)[1.33] |
| [3] | 2.06( 0%)[2.10] | 1.64( 1%)[1.44] | 1.37( 2%)[2.26] | 1.19( 2%)[1.10] | 1.29( 0%)[0.83] | 1.17( 4%)[0.87] | 1.43( 0%)[0.92] | 1.51( 0%)[1.05] | 1.46( 1%)[1.32] |
| [4] | 2.11( 0%)[2.11] | 1.67( 1%)[1.46] | 1.37( 2%)[2.24] | 1.17( 2%)[1.11] | 1.30( 0%)[0.82] | 1.14( 0%)[0.89] | 1.44( 0%)[0.93] | 1.53( 0%)[1.07] | 1.47( 1%)[1.33] |
| [5] | 1.94( 0%)[2.09] | 1.63( 1%)[1.44] | 1.38( 2%)[2.24] | 1.20( 2%)[1.11] | 1.31( 0%)[0.83] | 1.15( 3%)[0.86] | 1.45( 1%)[0.92] | 1.55( 0%)[1.07] | 1.45( 1%)[1.32] |
| [6] | 2.10( 0%)[2.12] | 1.64( 0%)[1.44] | 1.33( 2%)[2.23] | 1.21( 3%)[1.10] | 1.29( 0%)[0.81] | 1.15( 2%)[0.86] | 1.43( 0%)[0.91] | 1.51( 0%)[1.05] | 1.46( 1%)[1.32] |
| Ave | 2.05( 0%)[2.12] | 1.64( 1%)[1.45] | 1.37( 2%)[2.25] | 1.19( 2%)[1.11] | 1.30( 0%)[0.83] | 1.14( 2%)[0.87] | 1.44( 0%)[0.93] | 1.53( 0%)[1.06] | 1.46( 1%)[1.33] |

## Section B - Run 5 – Offset Path:

| | A | B | C | D | E | F | G | H | Ave |
|---|---|---|---|---|---|---|---|---|---|
| [1] | 1.30( 0%)[0.87] | 1.32( 3%)[1.89] | 1.00( 0%)[0.61] | 1.31( 2%)[0.93] | 1.47( 0%)[0.93] | 1.75( 0%)[0.91] | 1.33( 2%)[1.10] | 1.97( 3%)[1.14] | 1.43( 1%)[1.05] |
| [2] | 1.31( 0%)[0.86] | 1.28( 4%)[1.86] | 1.03( 1%)[0.60] | 1.32( 2%)[0.94] | 1.42( 0%)[0.94] | 1.77( 0%)[0.92] | 1.31( 0%)[1.10] | 1.97( 2%)[1.15] | 1.43( 1%)[1.05] |
| [3] | 1.26( 0%)[0.85] | 1.31( 5%)[1.84] | 1.05( 0%)[0.62] | 1.36( 1%)[0.96] | 1.50( 0%)[0.94] | 1.84( 0%)[0.93] | 1.42( 1%)[1.12] | 1.96( 2%)[1.16] | 1.46( 1%)[1.05] |
| [4] | 1.27( 0%)[0.86] | 1.28( 3%)[1.85] | 0.97( 2%)[0.60] | 1.34( 0%)[0.95] | 1.43( 2%)[0.92] | 1.80( 0%)[0.91] | 1.43( 0%)[1.10] | 2.13( 2%)[1.27] | 1.46( 1%)[1.06] |
| [5] | 1.30( 0%)[0.87] | 1.33( 4%)[1.85] | 1.03( 1%)[0.60] | 1.35( 1%)[0.95] | 1.40( 0%)[0.92] | 1.77( 0%)[0.89] | 1.45( 0%)[1.09] | 1.98( 4%)[1.15] | 1.45( 1%)[1.04] |
| [6] | 1.28( 0%)[0.86] | 1.28( 5%)[1.82] | 1.00( 1%)[0.60] | 1.34( 1%)[0.94] | 1.38( 0%)[0.90] | 1.80( 0%)[0.93] | 1.39( 0%)[1.10] | 1.96( 2%)[1.15] | 1.43( 1%)[1.04] |
| Ave | 1.29( 0%)[0.86] | 1.30( 4%)[1.85] | 1.01( 1%)[0.61] | 1.34( 1%)[0.95] | 1.43( 0%)[0.93] | 1.79( 0%)[0.92] | 1.39( 1%)[1.10] | 2.00( 3%)[1.17] | 1.44( 1%)[1.05] |

## Section B - Run 6 - Wheel Path:

| | A | B | C | D | E | F | G | H | Ave |
|---|---|---|---|---|---|---|---|---|---|
| [1] | 1.60( 1%)[1.10] | 1.12( 1%)[0.88] | 1.53( 0%)[1.97] | 1.41( 0%)[1.01] | 1.01( 0%)[0.87] | 1.47( 3%)[0.90] | 1.66( 4%)[0.95] | 1.41( 2%)[0.80] | 1.40( 1%)[1.06] |
| [2] | 1.63( 0%)[1.07] | 1.13( 2%)[0.89] | 1.32( 0%)[0.70] | 1.46( 0%)[1.02] | 1.01( 2%)[0.86] | 1.44( 5%)[0.89] | 1.69( 3%)[0.95] | 1.47( 2%)[0.81] | 1.39( 2%)[0.90] |
| [3] | 1.61( 1%)[1.08] | 1.17( 2%)[0.88] | 1.38( 0%)[1.00] | 1.50( 0%)[1.02] | 1.02( 4%)[0.86] | 1.42( 4%)[0.86] | 1.70( 2%)[0.96] | 1.40( 2%)[0.80] | 1.40( 2%)[0.93] |
| [4] | 1.63( 2%)[1.10] | 1.15( 2%)[0.86] | 1.30( 0%)[0.71] | 1.45( 0%)[1.01] | 0.99( 0%)[0.86] | 1.42( 4%)[0.87] | 1.65( 2%)[0.95] | 1.45( 2%)[0.80] | 1.38( 2%)[0.90] |
| [5] | 1.66( 0%)[1.09] | 1.14( 2%)[0.84] | 1.26( 0%)[0.69] | 1.46( 0%)[1.02] | 1.05( 3%)[0.88] | 1.45( 3%)[0.86] | 1.62( 2%)[0.93] | 1.22( 2%)[0.79] | 1.36( 2%)[0.89] |
| [6] | 1.63( 1%)[1.07] | 1.10( 2%)[0.85] | 1.28( 0%)[0.70] | 1.47( 0%)[1.02] | 1.01( 0%)[0.87] | 1.45( 4%)[0.89] | 1.68( 3%)[0.95] | 1.22( 1%)[0.80] | 1.36( 1%)[0.89] |
| Ave | 1.63( 1%)[1.09] | 1.14( 2%)[0.87] | 1.35( 0%)[0.96] | 1.46( 0%)[1.02] | 1.02( 2%)[0.87] | 1.44( 4%)[0.88] | 1.67( 3%)[0.95] | 1.36( 2%)[0.80] | 1.38( 2%)[0.93] |

## Section B - Run 6 – Offset Path:

| | A | B | C | D | E | F | G | H | Ave |
|---|---|---|---|---|---|---|---|---|---|
| [1] | 1.47( 0%)[1.02] | 1.59( 2%)[1.14] | 1.52( 1%)[1.89] | 2.05( 0%)[1.47] | 1.22( 2%)[0.91] | 0.88( 1%)[1.21] | 1.84( 0%)[1.36] | 1.51( 0%)[1.52] | 1.51( 1%)[1.32] |
| [2] | 1.44( 0%)[1.01] | 1.60( 2%)[1.12] | 1.55( 1%)[1.88] | 2.07( 0%)[1.47] | 1.26( 2%)[0.92] | 0.91( 0%)[1.21] | 1.83( 1%)[1.36] | 1.51( 0%)[1.51] | 1.52( 1%)[1.31] |
| [3] | 1.47( 0%)[1.02] | 1.60( 1%)[1.13] | 1.57( 1%)[1.88] | 2.04( 0%)[1.47] | 1.27( 2%)[0.90] | 0.89( 0%)[1.20] | 1.74( 2%)[1.33] | 1.49( 0%)[1.51] | 1.51( 1%)[1.31] |
| [4] | 1.46( 1%)[1.02] | 1.58( 1%)[1.16] | 1.48( 1%)[1.88] | 2.07( 0%)[1.48] | 1.29( 5%)[0.91] | 0.86( 1%)[1.18] | 1.85( 0%)[1.36] | 1.48( 0%)[1.50] | 1.51( 1%)[1.31] |
| [5] | 1.49( 0%)[1.02] | 1.59( 1%)[1.11] | 1.52( 1%)[1.87] | 2.01( 0%)[1.47] | 1.22( 2%)[0.89] | 0.90( 0%)[1.21] | 1.74( 2%)[1.32] | 1.53( 0%)[1.52] | 1.50( 1%)[1.30] |
| [6] | 1.44( 1%)[1.03] | 1.56( 2%)[1.11] | 1.47( 1%)[1.86] | 2.04( 0%)[1.45] | 1.27( 3%)[0.90] | 0.97( 0%)[1.21] | 1.80( 1%)[1.34] | 1.53( 0%)[1.52] | 1.51( 1%)[1.30] |
| Ave | 1.46( 0%)[1.02] | 1.59( 2%)[1.13] | 1.52( 1%)[1.88] | 2.05( 0%)[1.47] | 1.26( 3%)[0.91] | 0.90( 0%)[1.20] | 1.80( 1%)[1.35] | 1.51( 0%)[1.51] | 1.51( 1%)[1.31] |

**Appendix B: Field Test Results for Chapter 3**

CTMeters & HSLD – MPD for Smart Road Sections - Box and Whiskers Plots per Section:

| Section A | CTMeter 1 | HSLD Ave. |
|---|---|---|
| Count | 80 | 3236 |
| **Mean** | **1.11** | **1.21** |
| SD | 0.27 | 0.34 |
| Min | 0.6 | 0.6 |
| Q1 | 0.9 | 1.0 |
| Median | 1.1 | 1.1 |
| Q3 | 1.3 | 1.4 |
| Max | 2.0 | 3.3 |
| Bottom | 0.9 | 1.0 |
| 2Q box | 0.173 | 0.159 |
| 3Q box | 0.233 | 0.204 |
| Whisker - | 0.298 | 0.415 |
| Whisker + | 0.668 | 1.986 |
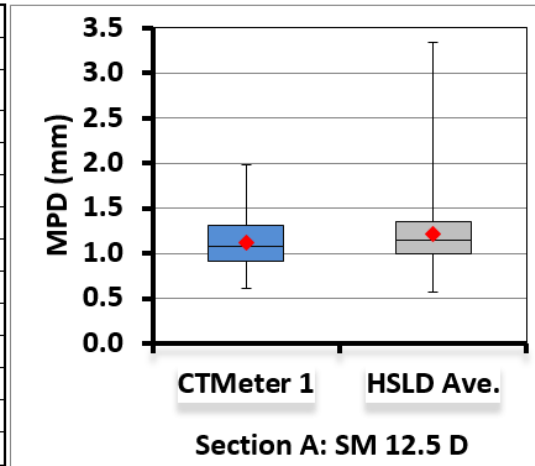


MPD Statistics - Section A

| Section B | CTMeter | HSLD Ave. |
|---|---|---|
| Count | 80 | 5105 |
| **Mean** | **1.47** | **1.38** |
| SD | 0.35 | 0.38 |
| Min | 0.9 | 0.4 |
| Q1 | 1.2 | 1.1 |
| Median | 1.4 | 1.3 |
| Q3 | 1.7 | 1.6 |
| Max | 2.3 | 3.0 |
| Bottom | 1.2 | 1.1 |
| 2Q box | 0.263 | 0.225 |
| 3Q box | 0.230 | 0.269 |
| Whisker - | 0.258 | 0.687 |
| Whisker + | 0.650 | 1.441 |
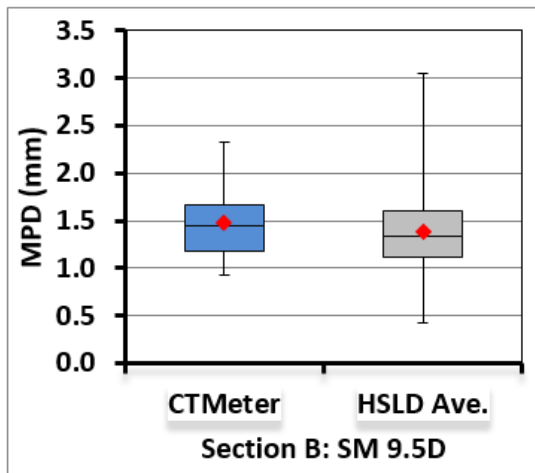


MPD Statistics - Section B

| Section C | CTMeter 1 | HSLD Ave. |
|---|---|---|
| Count | 80 | 2755 |
| **Mean** | **0.98** | **0.96** |
| SD | 0.23 | 0.29 |
| Min | 0.7 | 0.5 |
| Q1 | 0.8 | 0.8 |
| Median | 1.0 | 0.9 |
| Q3 | 1.1 | 1.1 |
| Max | 2.3 | 3.1 |
| Bottom | 0.8 | 0.8 |
| 2Q box | 0.108 | 0.121 |
| 3Q box | 0.105 | 0.150 |
| Whisker - | 0.178 | 0.310 |
| Whisker + | 1.230 | 2.078 |
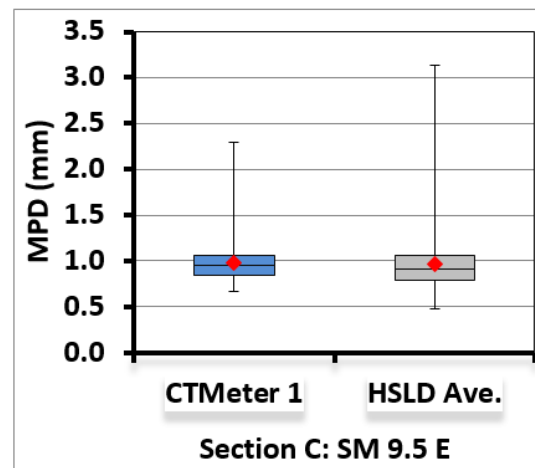


MPD Statistics - Section C

| Section D | CTMeter | HSLD Ave. |
|---|---|---|
| Count | 96 | 6255 |
| **Mean** | **0.83** | **0.83** |
| SD | 0.16 | 0.18 |
| Min | 0.5 | 0.4 |
| Q1 | 0.7 | 0.7 |
| Median | 0.8 | 0.8 |
| Q3 | 0.9 | 0.9 |
| Max | 1.3 | 1.9 |
| Bottom | 0.7 | 0.7 |
| 2Q box | 0.130 | 0.098 |
| 3Q box | 0.103 | 0.120 |
| Whisker - | 0.190 | 0.282 |
| Whisker + | 0.358 | 0.977 |
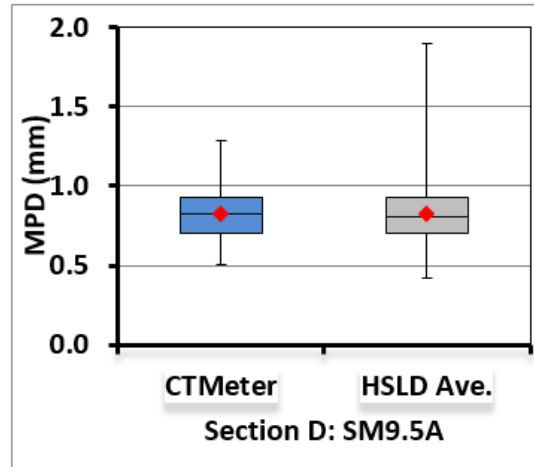


MPD Statistics - Section D

| Section E | CTMeter | HSLD Ave. |
|---|---|---|
| Count | 80 | 4150 |
| **Mean** | **0.96** | **0.95** |
| SD | 0.23 | 0.22 |
| Min | 0.6 | 0.5 |
| Q1 | 0.8 | 0.8 |
| Median | 0.9 | 0.9 |
| Q3 | 1.1 | 1.1 |
| Max | 1.8 | 2.1 |
| Bottom | 0.8 | 0.8 |
| 2Q box | 0.123 | 0.130 |
| 3Q box | 0.145 | 0.140 |
| Whisker - | 0.248 | 0.308 |
| Whisker + | 0.665 | 1.052 |
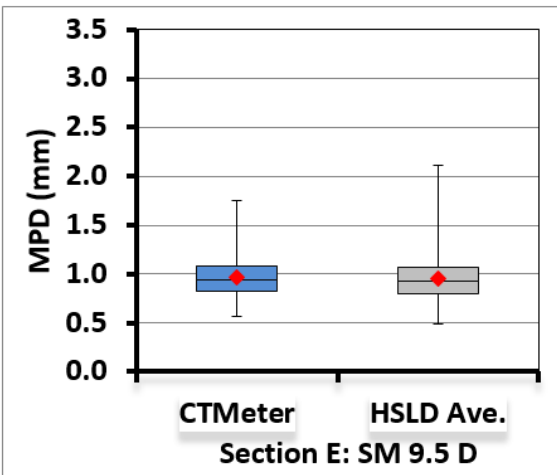


MPD Statistics - Section E

| Section F | CTMeter | HSLD Ave. |
|---|---|---|
| Count | 80 | 4500 |
| **Mean** | **0.94** | **0.84** |
| SD | 0.21 | 0.18 |
| Min | 0.6 | 0.5 |
| Q1 | 0.8 | 0.7 |
| Median | 0.9 | 0.8 |
| Q3 | 1.0 | 0.9 |
| Max | 1.8 | 1.9 |
| Bottom | 0.8 | 0.7 |
| 2Q box | 0.108 | 0.100 |
| 3Q box | 0.140 | 0.115 |
| Whisker - | 0.238 | 0.257 |
| Whisker + | 0.775 | 0.994 |
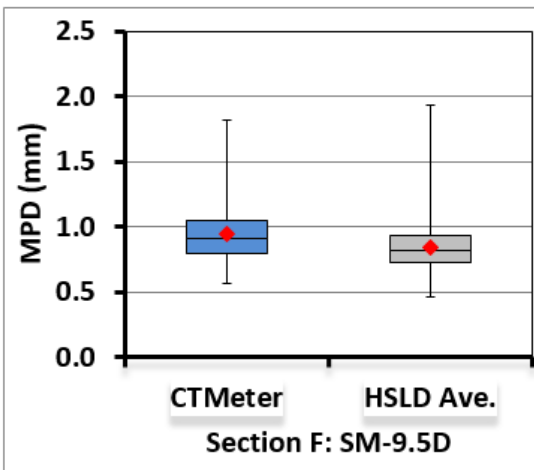


MPD Statistics - Section F

| Section G | CTMeter | HSLD Ave. |
|---|---|---|
| Count | 80 | 4500 |
| **Mean** | **0.99** | **0.99** |
| SD | 0.23 | 0.28 |
| Min | 0.6 | 0.5 |
| Q1 | 0.8 | 0.8 |
| Median | 0.9 | 0.9 |
| Q3 | 1.1 | 1.1 |
| Max | 1.8 | 3.0 |
| Bottom | 0.8 | 0.8 |
| 2Q box | 0.110 | 0.137 |
| 3Q box | 0.180 | 0.175 |
| Whisker - | 0.220 | 0.310 |
| Whisker + | 0.700 | 1.862 |
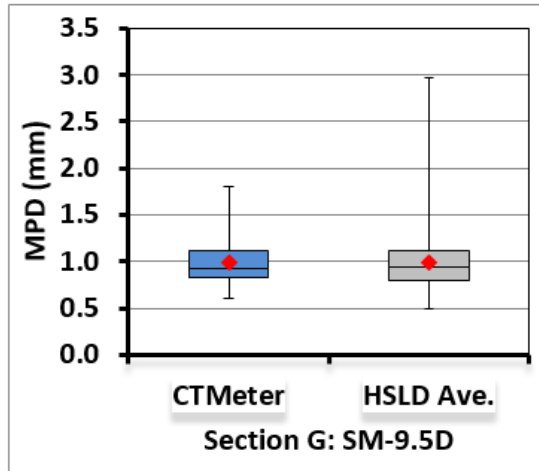


MPD Statistics - Section G

| Section H | CTMeter | HSLD Ave. |
|---|---|---|
| Count | 80 | 4255 |
| **Mean** | **1.09** | **1.03** |
| SD | 0.27 | 0.26 |
| Min | 0.7 | 0.5 |
| Q1 | 0.9 | 0.9 |
| Median | 1.0 | 1.0 |
| Q3 | 1.2 | 1.2 |
| Max | 2.0 | 2.8 |
| Bottom | 0.9 | 0.9 |
| 2Q box | 0.093 | 0.140 |
| 3Q box | 0.243 | 0.171 |
| Whisker - | 0.248 | 0.349 |
| Whisker + | 0.728 | 1.677 |
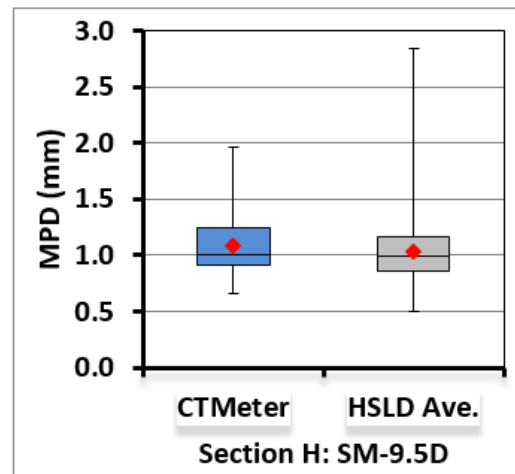


MPD Statistics - Section H

| Section I | CTMeter 1 | CTMeter 2 | HSLD Ave. |
|---|---|---|---|
| Count | 80 | 80 | 4755 |
| **Mean** | **0.92** | **0.91** | **0.96** |
| SD | 0.17 | 0.18 | 0.24 |
| Min | 0.5 | 0.5 | 0.4 |
| Q1 | 0.8 | 0.8 | 0.8 |
| Median | 0.9 | 0.9 | 0.9 |
| Q3 | 1.0 | 1.0 | 1.1 |
| Max | 1.4 | 1.5 | 2.3 |
| Bottom | 0.8 | 0.8 | 0.8 |
| 2Q box | 0.140 | 0.130 | 0.125 |
| 3Q box | 0.120 | 0.113 | 0.168 |
| Whisker - | 0.270 | 0.250 | 0.431 |
| Whisker + | 0.380 | 0.458 | 1.227 |
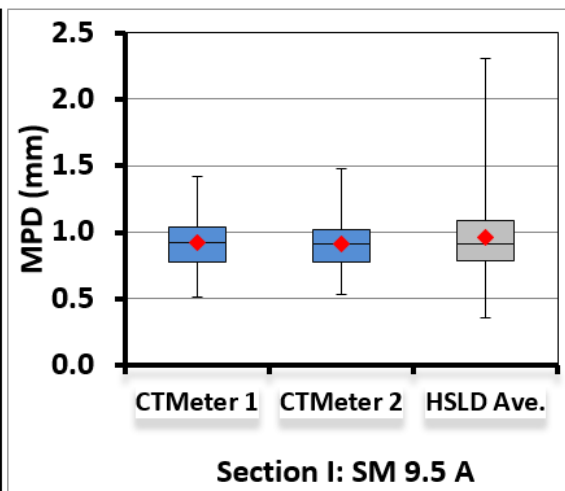


MPD Statistics - Section I

| Section J | CTMeter 1 | CTMeter 2 | HSLD Ave. |
|---|---|---|---|
| Count | 80 | 80 | 3805 |
| **Mean** | **1.12** | **1.13** | **1.13** |
| SD | 0.30 | 0.25 | 0.33 |
| Min | 0.6 | 0.7 | 0.4 |
| Q1 | 0.9 | 1.0 | 0.9 |
| Median | 1.1 | 1.1 | 1.1 |
| Q3 | 1.3 | 1.3 | 1.3 |
| Max | 2.0 | 1.8 | 2.7 |
| Bottom | 0.9 | 1.0 | 0.9 |
| 2Q box | 0.148 | 0.140 | 0.167 |
| 3Q box | 0.245 | 0.195 | 0.218 |
| Whisker - | 0.308 | 0.295 | 0.457 |
| Whisker + | 0.650 | 0.510 | 1.460 |
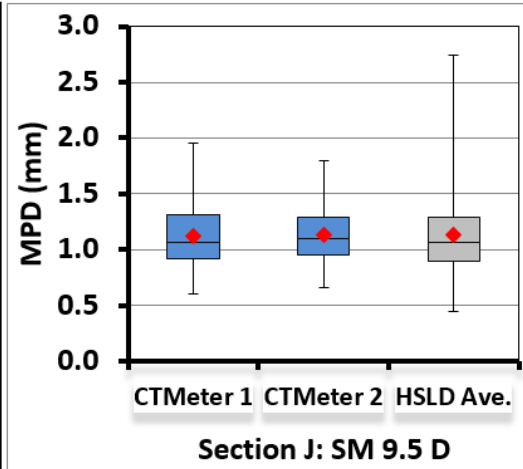


MPD Statistics - Section J

| Section K | CTMeter 1 | CTMeter 2 | HSLD Ave. |
|---|---|---|---|
| Count | 80 | 80 | 4505 |
| **Mean** | **1.93** | **1.85** | **1.72** |
| SD | 0.41 | 0.39 | 0.38 |
| Min | 1.1 | 1.0 | 0.8 |
| Q1 | 1.6 | 1.6 | 1.5 |
| Median | 1.9 | 1.8 | 1.7 |
| Q3 | 2.2 | 2.1 | 2.0 |
| Max | 3.0 | 2.8 | 3.2 |
| Bottom | 1.6 | 1.6 | 1.5 |
| 2Q box | 0.260 | 0.200 | 0.234 |
| 3Q box | 0.263 | 0.323 | 0.272 |
| Whisker - | 0.550 | 0.540 | 0.670 |
| Whisker + | 0.828 | 0.658 | 1.247 |
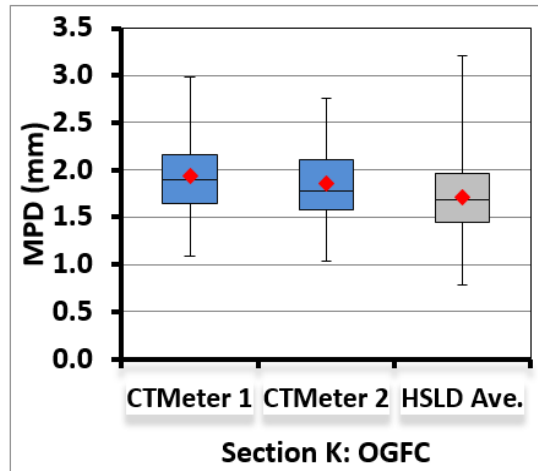


MPD Statistics - Section K

| Section L | CTMeter 1 | CTMeter 2 | HSLD Ave. |
|---|---|---|---|
| Count | 80 | 80 | 4755 |
| **Mean** | **1.16** | **1.16** | **1.13** |
| SD | 0.25 | 0.27 | 0.30 |
| Min | 0.8 | 0.7 | 0.5 |
| Q1 | 1.0 | 1.0 | 0.9 |
| Median | 1.1 | 1.1 | 1.1 |
| Q3 | 1.3 | 1.4 | 1.3 |
| Max | 2.0 | 1.9 | 2.7 |
| Bottom | 1.0 | 1.0 | 0.9 |
| 2Q box | 0.145 | 0.135 | 0.163 |
| 3Q box | 0.198 | 0.245 | 0.206 |
| Whisker - | 0.200 | 0.250 | 0.410 |
| Whisker + | 0.678 | 0.590 | 1.380 |
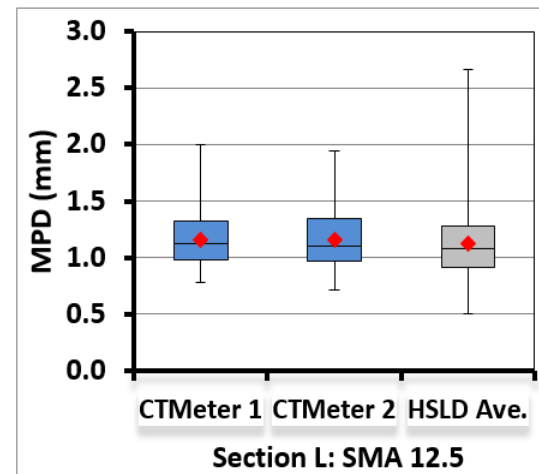


MPD Statistics - Section L

| Section EP5 | CTMeter 1 | CTMeter 2 | HSLD Ave. |
|---|---|---|---|
| Count | 80 | 80 | 1610 |
| **Mean** | **1.05** | **1.06** | **0.99** |
| SD | 0.19 | 0.19 | 0.17 |
| Min | 0.8 | 0.7 | 0.6 |
| Q1 | 0.9 | 0.9 | 0.9 |
| Median | 1.0 | 1.0 | 1.0 |
| Q3 | 1.1 | 1.2 | 1.1 |
| Max | 1.8 | 1.5 | 1.6 |
| Bottom | 0.9 | 0.9 | 0.9 |
| 2Q box | 0.093 | 0.088 | 0.107 |
| 3Q box | 0.123 | 0.145 | 0.123 |
| Whisker - | 0.168 | 0.248 | 0.290 |
| Whisker + | 0.678 | 0.360 | 0.546 |



Section: VDOT Modified EP-5
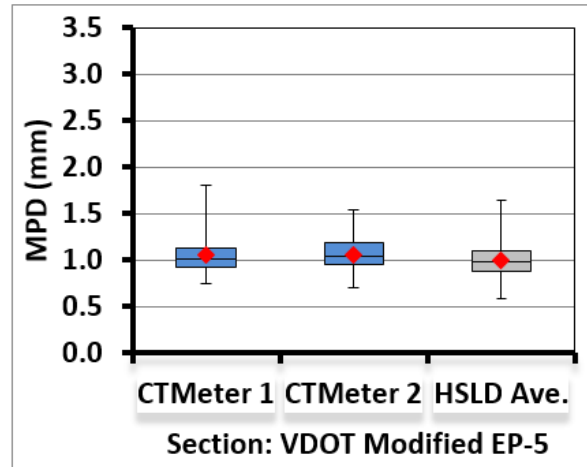
MPD Statistics - Section EP5

| Section SafeLane | CTMeter 1 | CTMeter 2 | HSLD Ave, |
|---|---|---|---|
| Count | 80 | 80 | 1355 |
| **Mean** | **1.57** | **1.55** | **1.45** |
| SD | 0.29 | 0.25 | 0.28 |
| Min | 1.1 | 1.1 | 0.7 |
| Q1 | 1.4 | 1.4 | 1.3 |
| Median | 1.5 | 1.5 | 1.4 |
| Q3 | 1.8 | 1.7 | 1.6 |
| Max | 2.4 | 2.3 | 2.3 |
| Bottom | 1.4 | 1.4 | 1.3 |
| 2Q box | 0.160 | 0.173 | 0.173 |
| 3Q box | 0.243 | 0.188 | 0.181 |
| Whisker - | 0.270 | 0.258 | 0.536 |
| Whisker + | 0.678 | 0.613 | 0.692 |



Section: SafeLane™
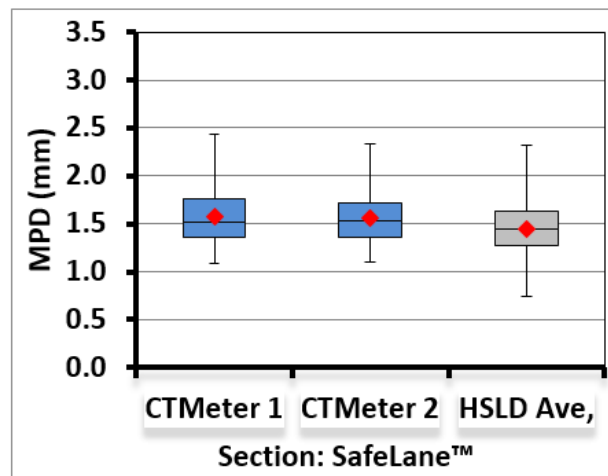
MPD Statistics - Section Cargill

*HSLD – MPD for Smart Road Sections - Box and Whiskers Plots per Run:*
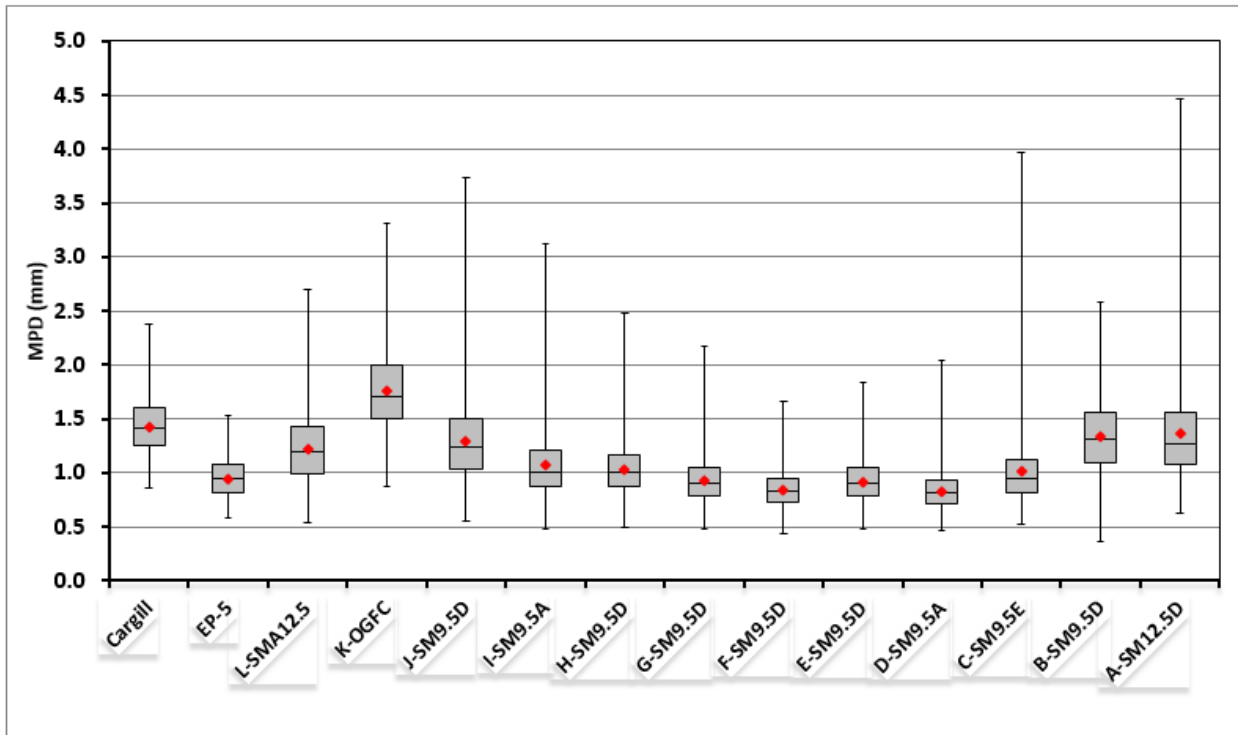


HSLD - MPD Box and Whiskers - Run 1
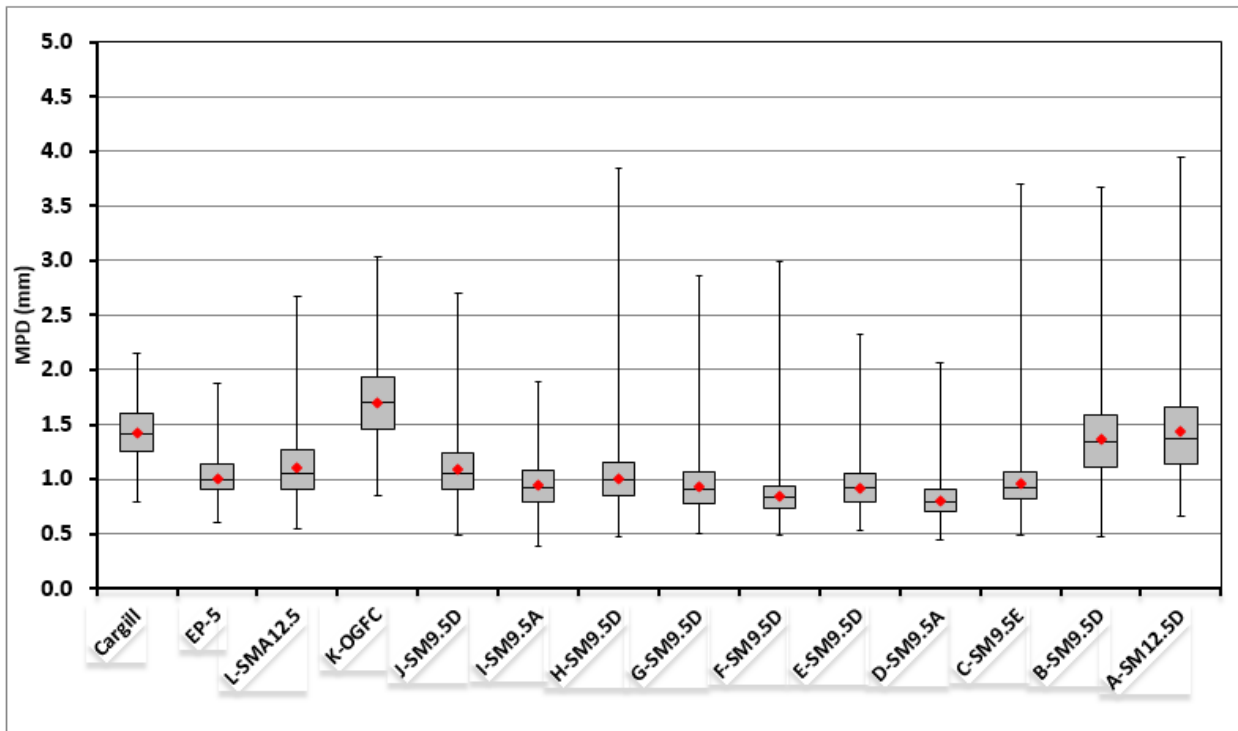


HSLD - MPD Box and Whiskers - Run 2

74
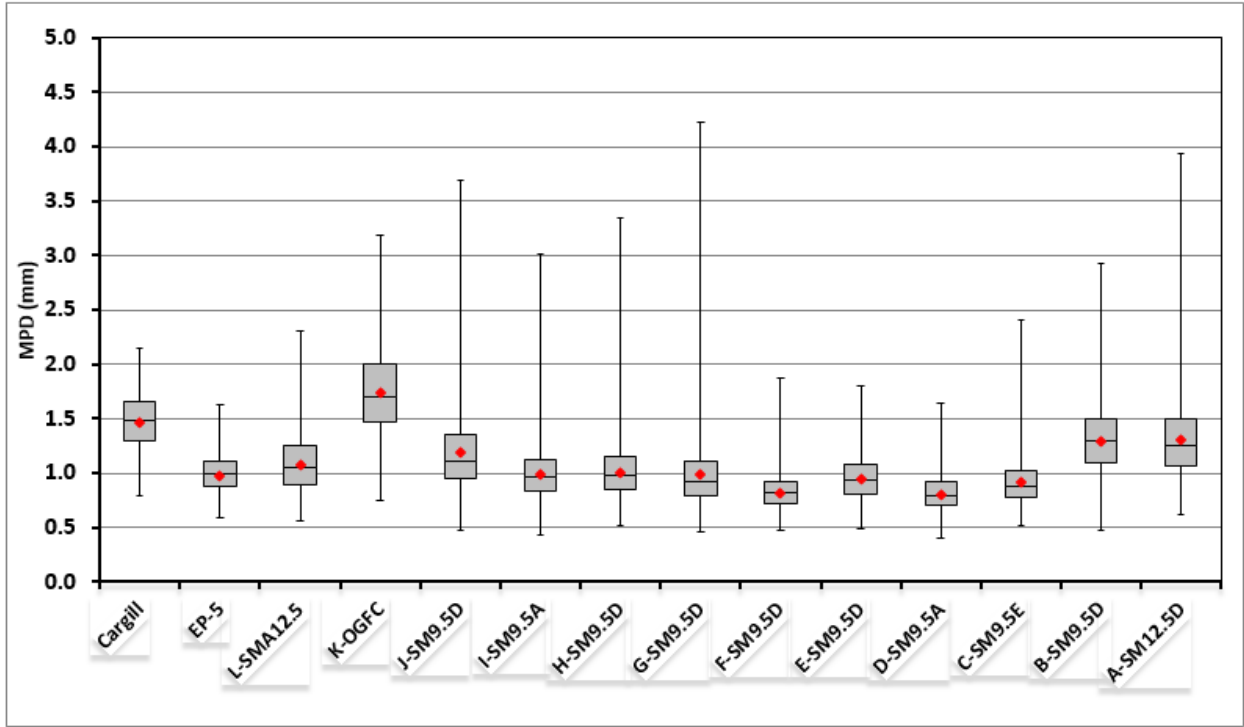
HSLD - MPD Box and Whiskers - Run 3
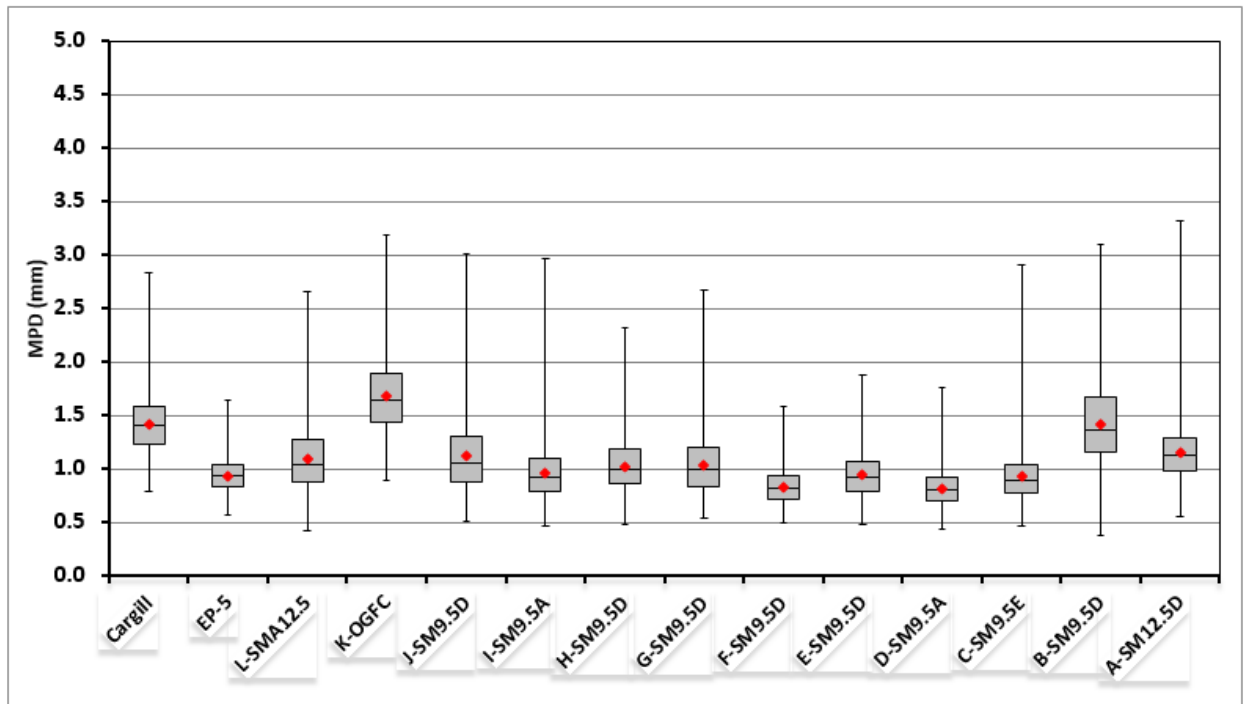


HSLD - MPD Box and Whiskers - Run 4
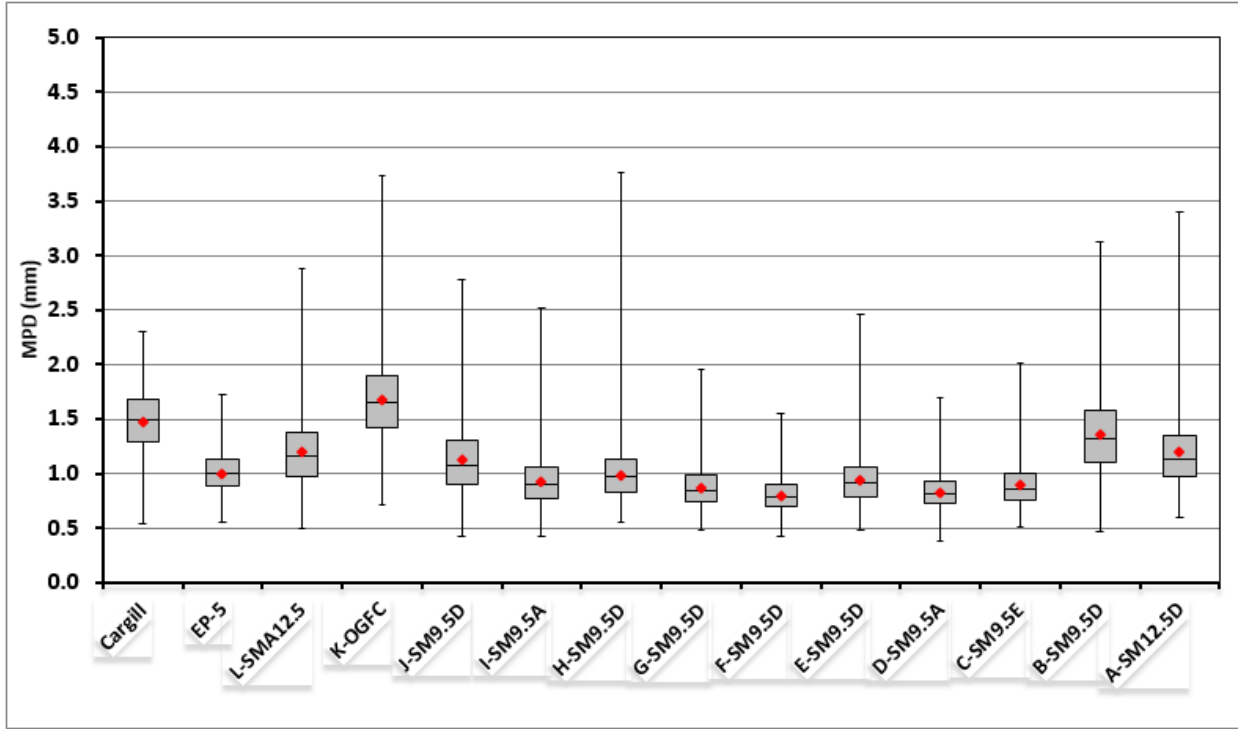
HSLD - MPD Box and Whiskers - Run 5
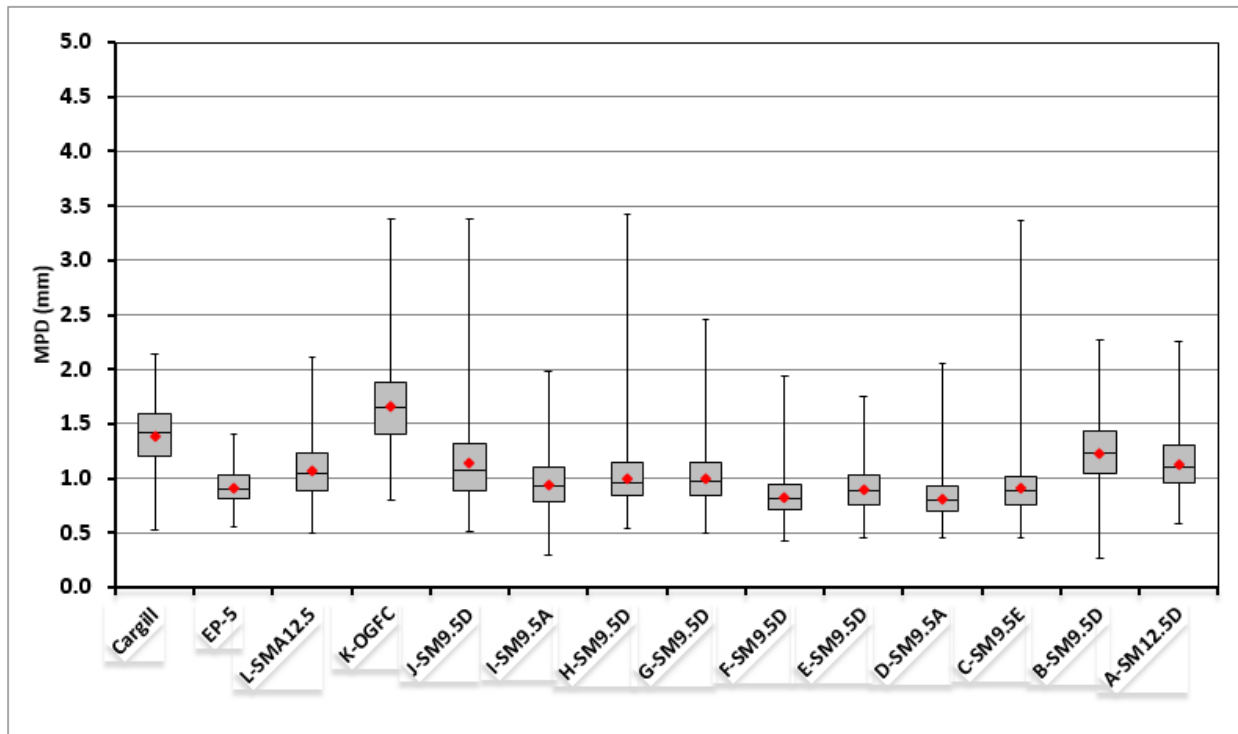


HSLD - MPD Box and Whiskers - Run 6
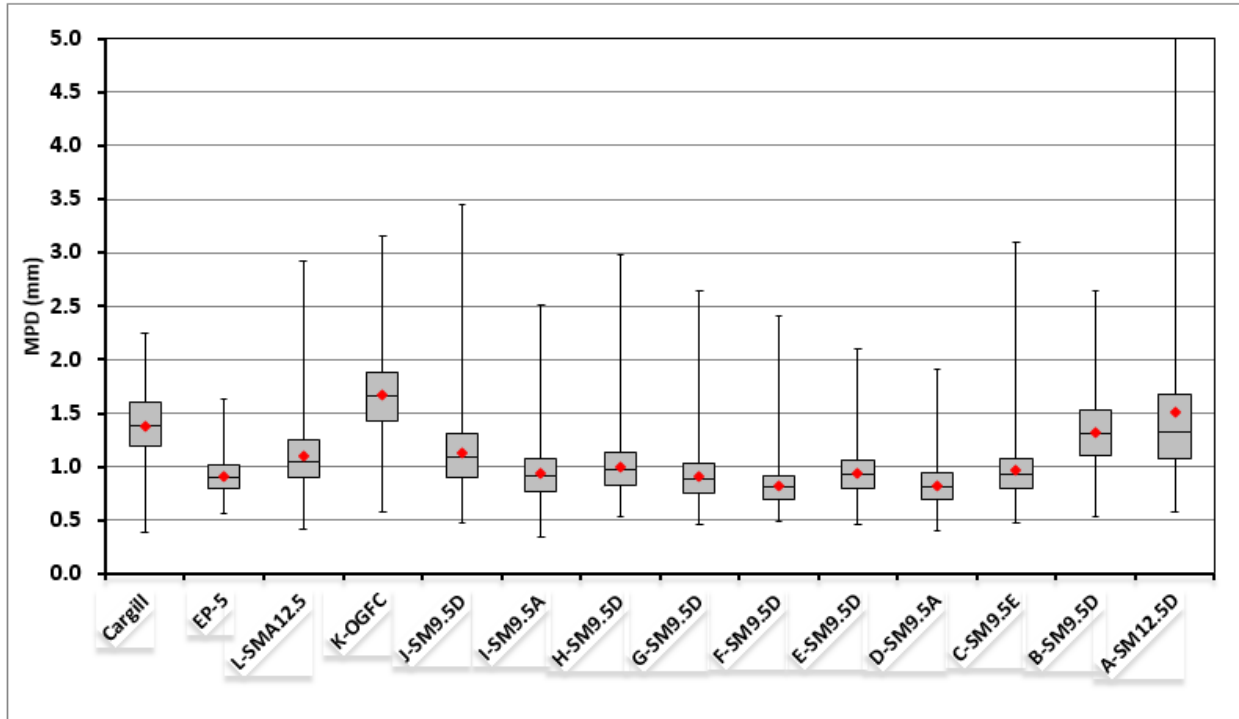
HSLD - MPD Box and Whiskers - Run 7
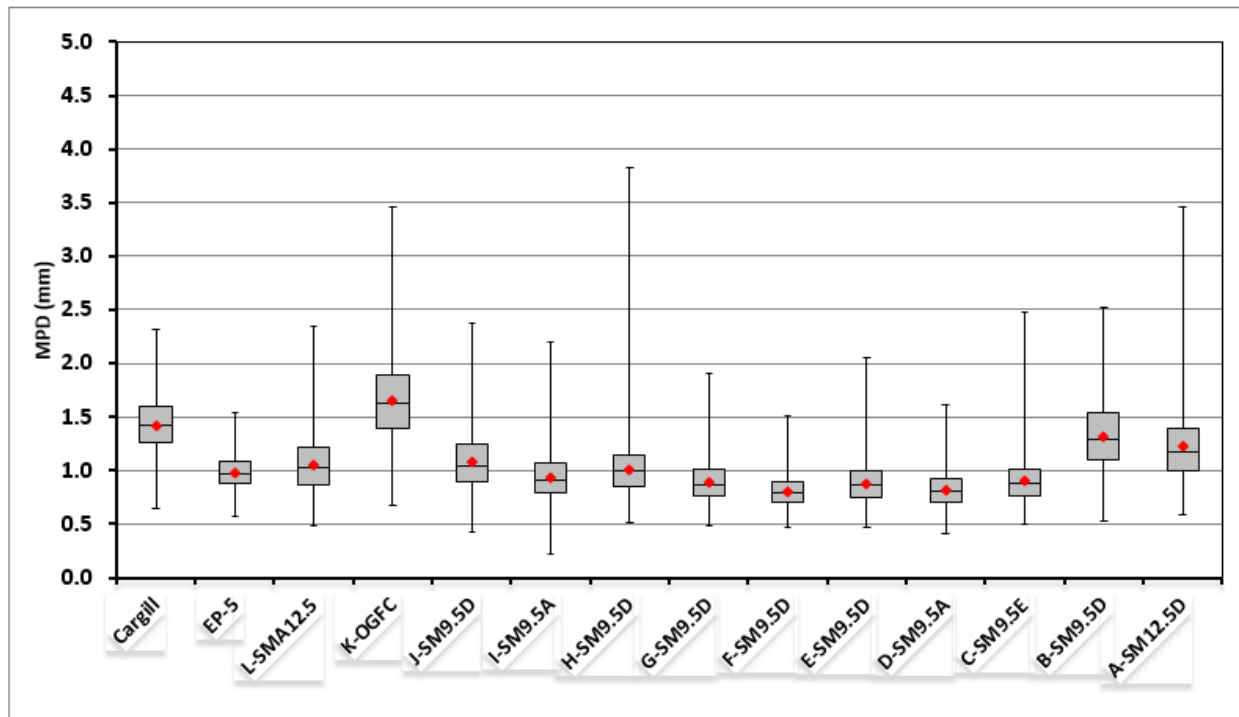


HSLD - MPD Box and Whiskers - Run 8
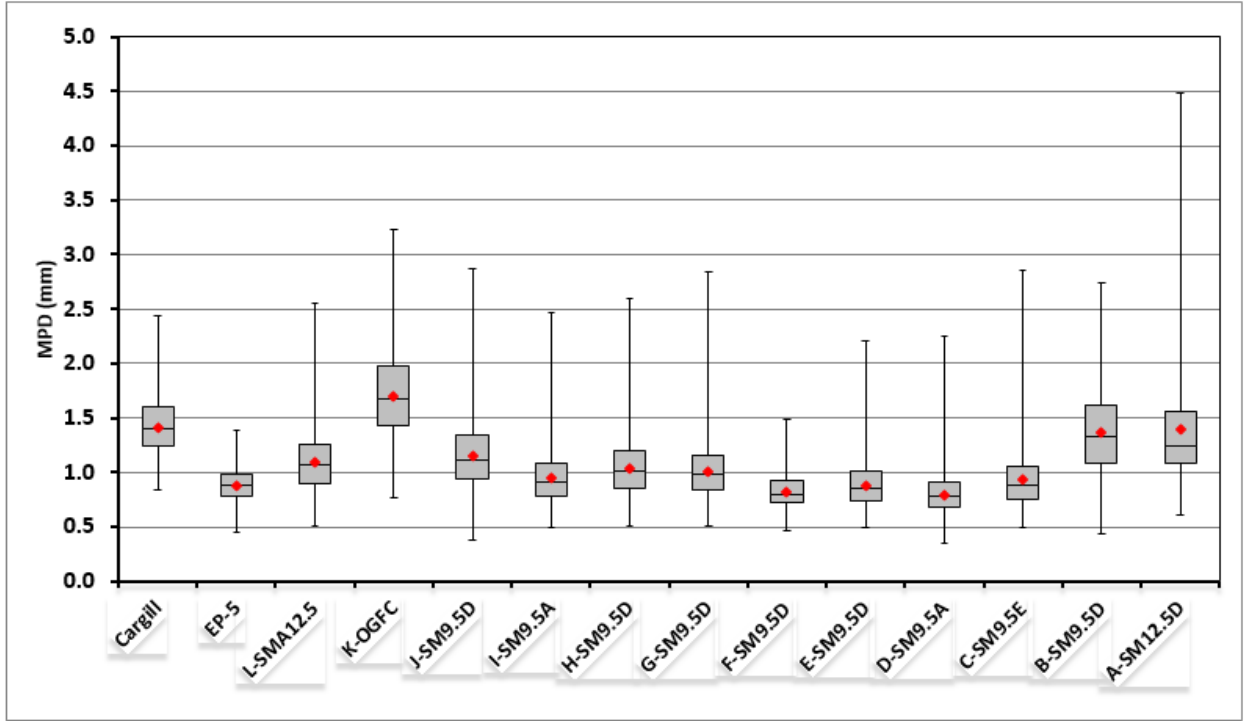
HSLD - MPD Box and Whiskers - Run 9
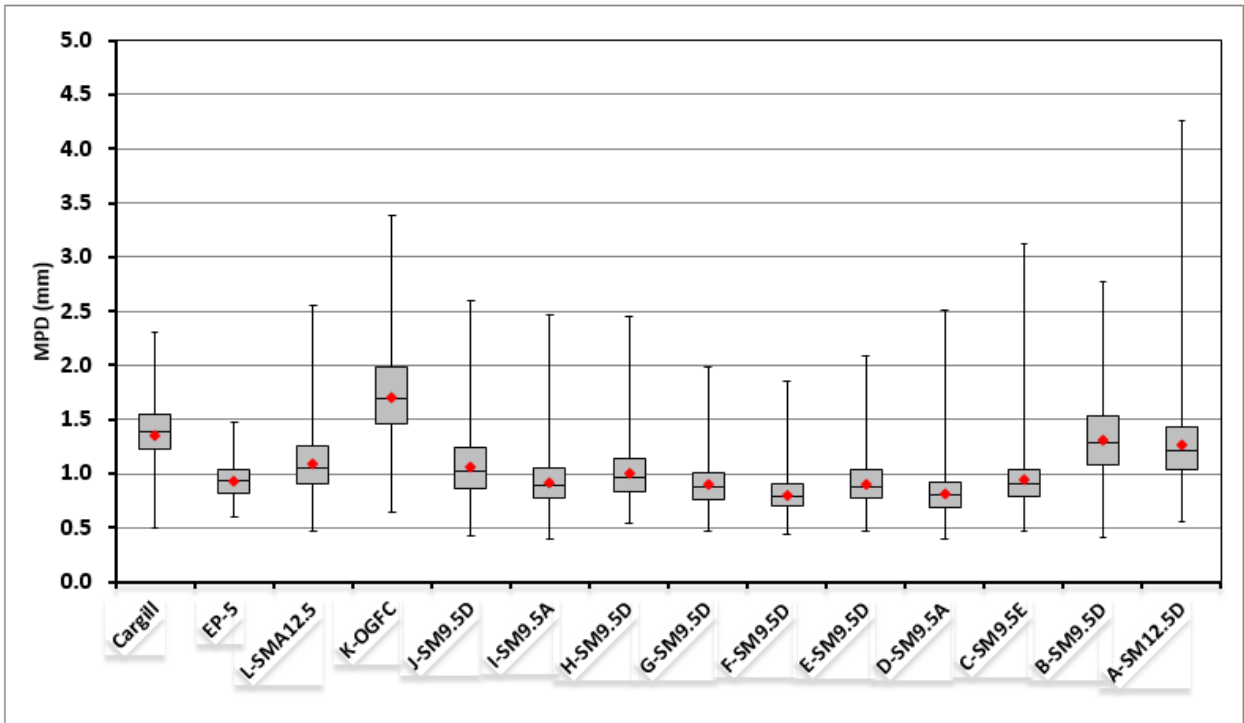


HSLD - MPD Box and Whiskers - Run 10

## Appendix C: Robustness of FDR method based on its successful applicability over different high speed laser devices

The FDR method was applied for 2 different HSLD, the first one, a Long-Term Pavement Performance (LTPP) laser device; and the second, a VTTI-HSLD believed to have a defective laser.
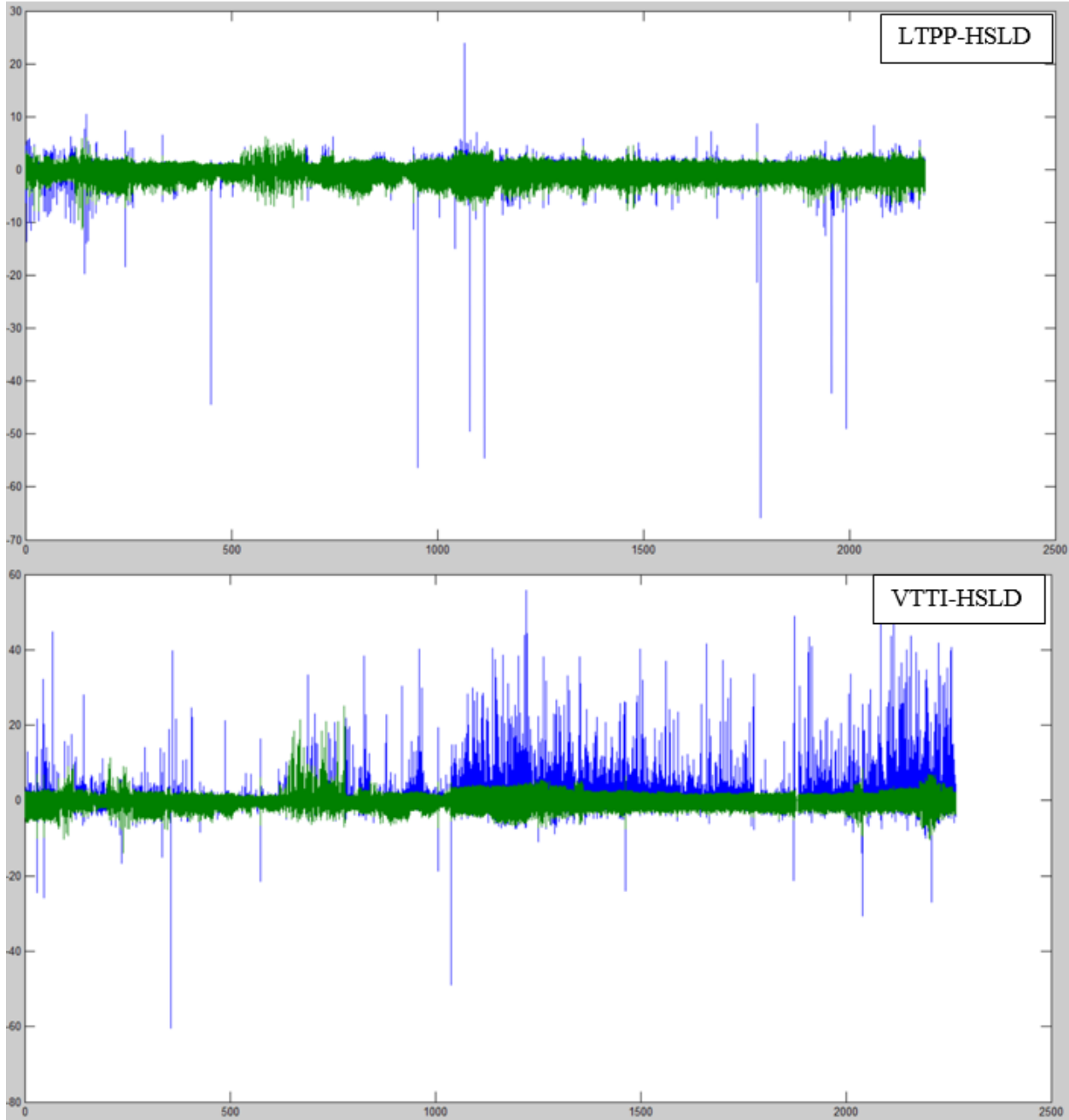


Original data (blue) and denoised data using the FDR method (green) for 2 different HSLDs

Notice the significantly higher number (and magnitude) of spikes for the second HSLD. Even though, the similarity on the denoised results, using the same FDR proportion (q = 0.1 for both), is evident.

Moreover, the same trend is observed for the calculated MPD presented below; again, similar MPD results are obtained after applying the FDR spike removal method.
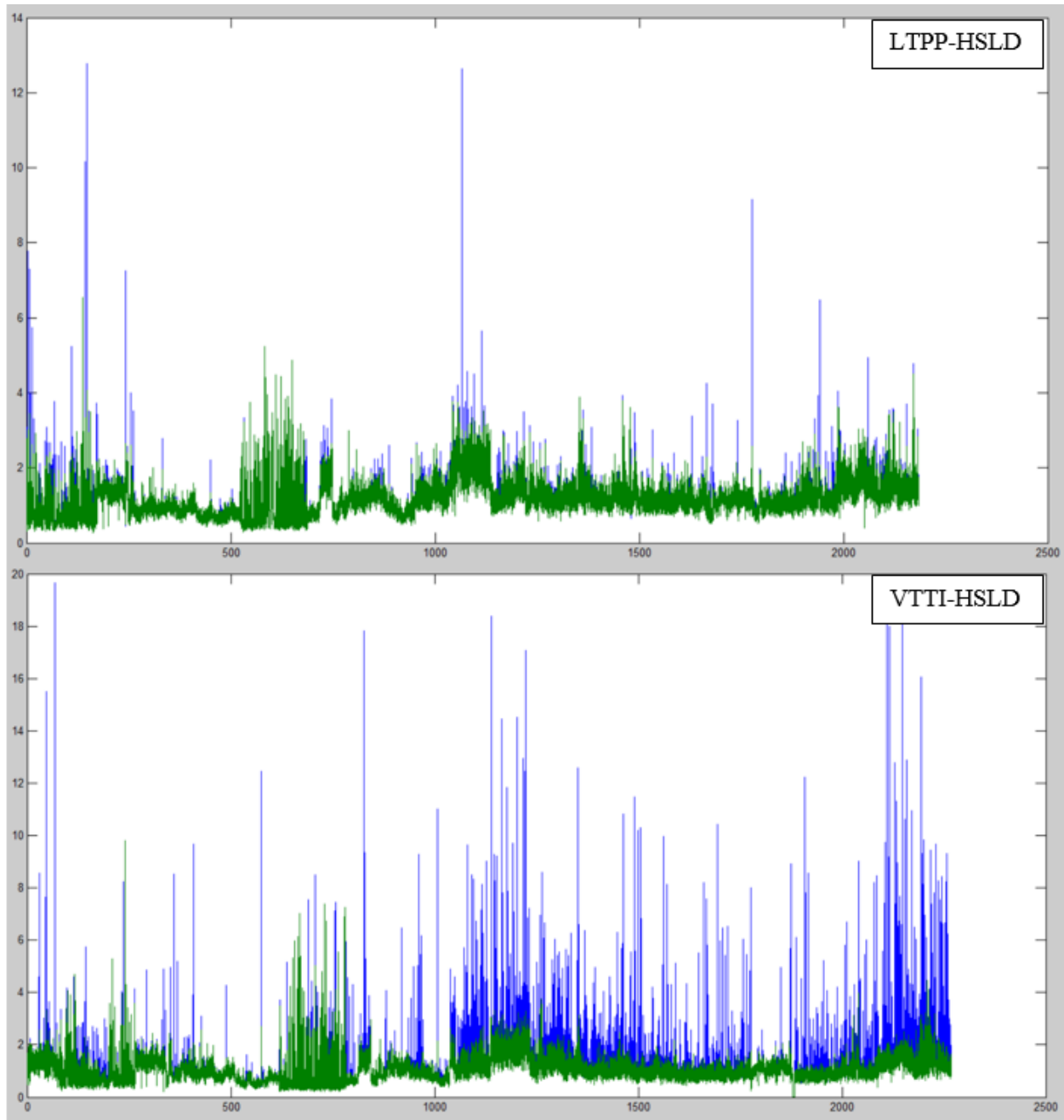


MPD calculated, with original data (blue) and denoised data using the FDR method (green)

More detailed MPD results, now presented by section, are depicted below:
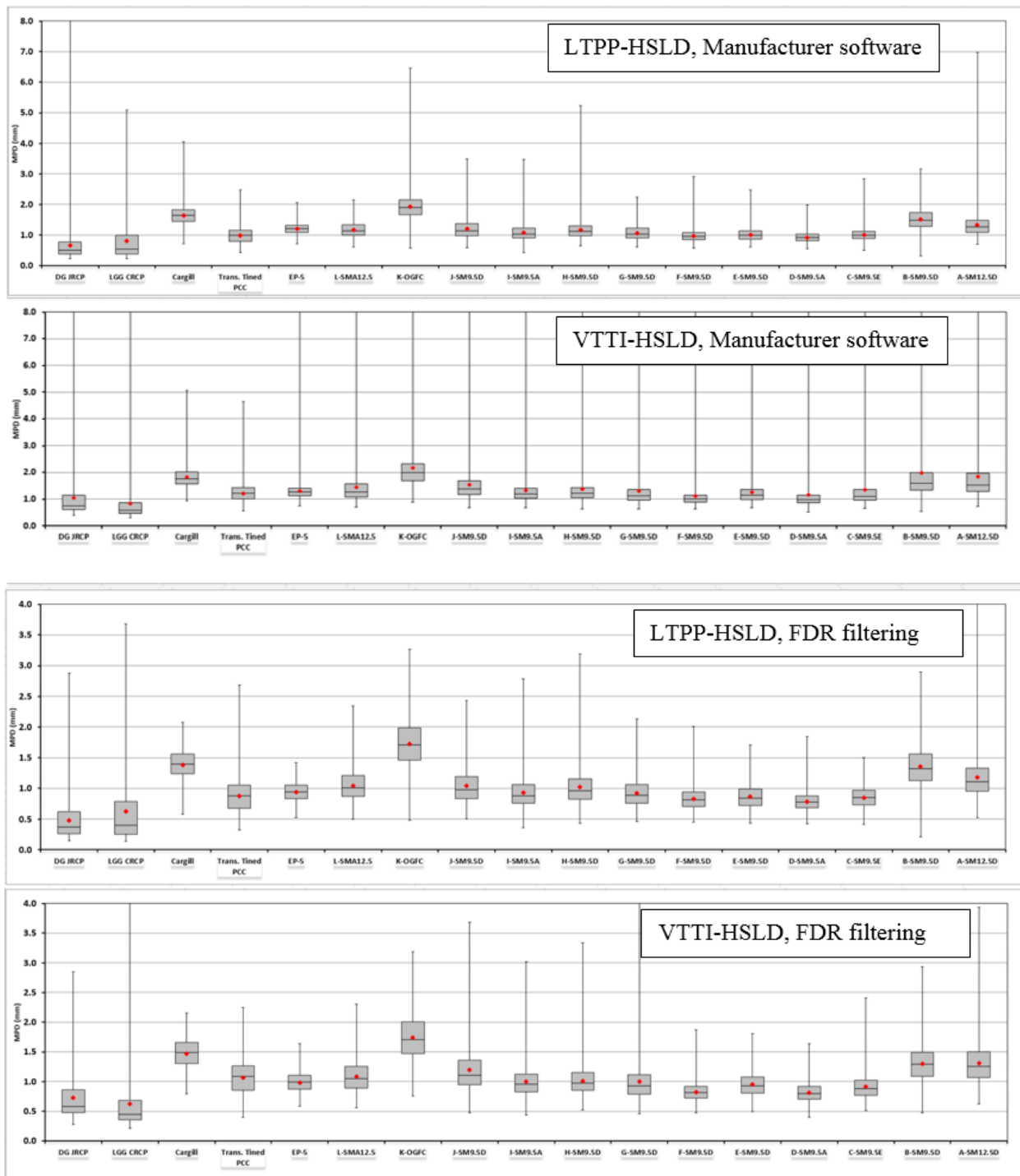
MPD results per section, for both devices, using manufacture's software and FRD method

On this figure, the MPD results for both the LTPP and the VTTI profiler systems are shown in the first two plots, using the manufacturer's software to compute the MPD values. These MPD values are very high in magnitude as shown by the box-plot diagrams, and have very high extreme values caused by the computations without despiking the data.

Using the FDR method for both data sets (bottom plots on figure above), some extreme values are still high for both MPD computations, but now the mean, median and quartile values are very similar for all sections computed. More importantly, both agree closely with the two CT Meter values.
Finally, a closer comparison is made of a particular section in the next figure:
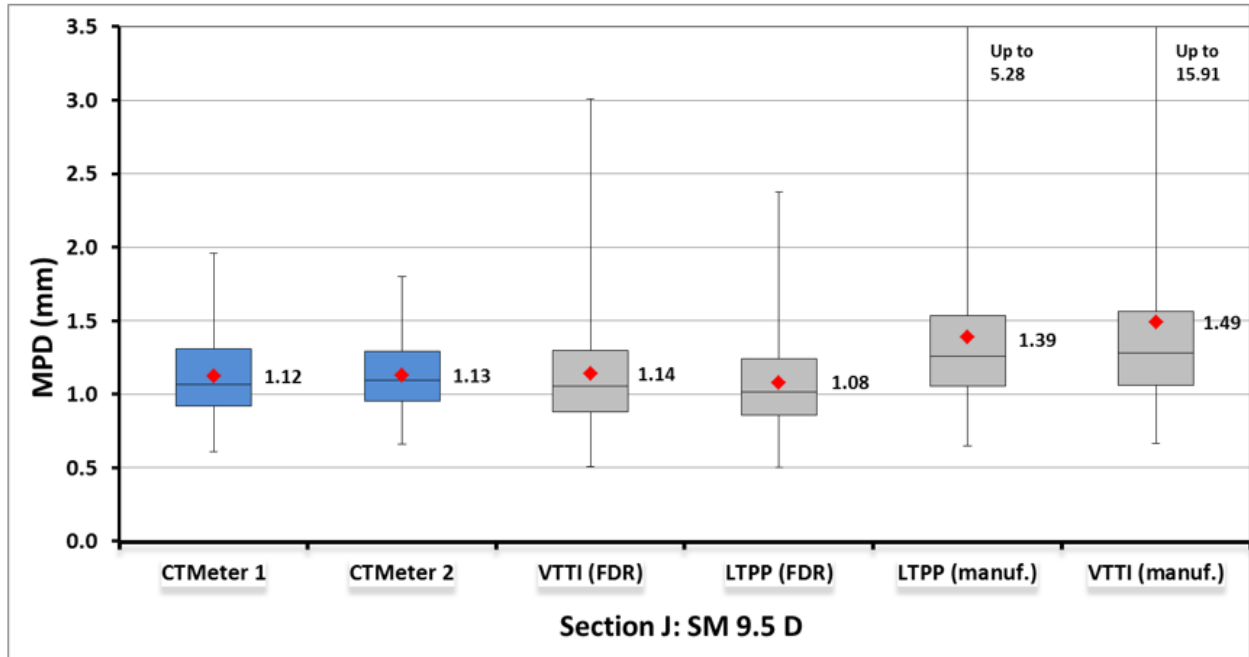


MPD results comparison for a particular section (e.g. section J)

As can be seen, both of the MPD results with the FDR method agree very well with the two CT Meter values, but not so if the manufacturer's software is used. It is also noticed that the method works for both devices even considering one of them as defective in terms of spikes present on the data.

**Appendix D: FDR method, selection of the proportion "q" optimizing correctly identified spikes**

The generalized Gaussian distribution represents the distribution of the texture measurements and is considered the null distribution. Spikes are measurements that are not originating from the null distribution and the FDR control procedure aims at identifying these spikes by controlling the expected proportion of wrongly rejected measurements. Table D.1 shows the possible outcomes of the FDR procedure. The first row represents measurements that come from the null distribution while the second row represents the measurements that are spikes. The total number of measurements is $m$ with $m_0$ coming from the null distribution and $m-m_0$ spikes. When the FDR procedure is applied, T observations coming from the null distribution are wrongly identified as spikes while V observations coming from the null distribution are correctly classified as null with $m = V+T$. for the case of spikes, U observations are correctly identified as spikes while S observations are wrongly identified as null with $m-m_0 = S+U$. The total number of identified spikes is $R = T+U$ and the false discovery proportion is defined as FDP = T/R with the FDP = 0 when R = 0. The FDR is defined as the expected value of the FDP.

| | Accept Hypothesis Meaning --> no spikes | Reject hypothesis (discovery) Meaning --> spikes | |
|---|---|---|---|
| TRUE | V | T | mo |
| FALSE | S | U | m-mo |
| | x | R | m |



Blue: histogram of actual texture data
Red: histogram of spikes
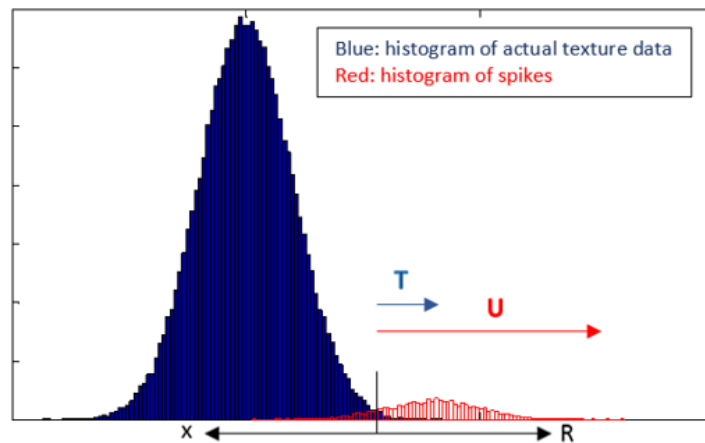
With the FDR method, Instead of controlling the rate of false positive (type I error), the FDR controls the proportion of false discoveries (T) among all discoveries (R):

$$FDP = T/R. \leftrightarrow FDR = \text{Expected FDP} < q$$

Where:

    R: represents all the identified spikes,
    U: represents the correctly identified spikes (actually belongs to the histogram of spikes), this is the one we want to maximize,
    T: is the wrongly identifies spikes (actually belong to the histogram of actual texture data, not a spike), but it is identified as spike, so, we want to minimize "T", and
    q: is the proportion at which we want to control the FDR.

As Explained in the results section on chapter 3, the proportion at which to control the False Discovery Rate was chosen after a sensitivity analysis by looking which "q" value gives the highest positive difference of correctly identified spikes minus wrongly identified spikes, maximizing the correctly identified spikes. Below 2 screen shots depicting the number of spikes found as a function of the chosen FDR value, and a summary table showing a sensitive analysis for different FDR values.



```
Editor - C:\VT\VTTI\Ph.D\TEXTURE\2nd paper (TRB2015)\Matlab\dspsmrtrdrun3.m
dspsmrtrdrun3.m   ×   +
2 -     load SR3
3
4 -     y = robustdsp(VTTISR3Texture,40000,'fdr',0.005);
5 -     n = length(y);
6 -     x = linspace(0,2259,n);
7
8 -     plot(x,VTTISR3Texture-mvaveragec(VTTISR3Texture,100),x,y-mvaverag
9
10 -    mtd = zeros(ceil(n/200),1);
11
12 -    for i=1:length(mtd)
13 -        strt = 1+(i-1)*200;
```

Matlab Script showing the chosen FDR value (e.g. q = 0.005) for run 3.



| Workspace | |
|---|---|
| Name ▲ | Value |
| i | 22590 |
| last | 4517952 |
| mtd | 22590x2 double |
| n | 4517952 |
| NumberOfSpikes | 5222 |
| PercentageOfSpikes | 0.0012 |
| strt | 4517801 |
| VectorOfSpikes | 4517952x1 double |
| VTTISR3Texture | 4517952x1 double |
| x | 1x4517952 double |
| X | 1x22590 double |
| y | 4517952x1 double |

Matlab Workspace showing results (including number of spikes) for the same run 3

Below, the sensitivity analysis for "q", maximizing the correctly identified spikes minus the wrongly identified spikes (U – T)), therefore defining the optimum range of FDR (q) values.

Optimum range for FDR value (q)

| Proportion (q) | All Spikes found (R) | Wrongly identified (T) | Correctly identified (U) | U - T |
|---|---|---|---|---|
| 0.005 | 5222 | 26 | 5196 | 5170 |
| 0.01 | 5613 | 56 | 5557 | 5501 |
| 0.05 | 7207 | 360 | 6847 | 6486 |
| 0.1 | 8652 | 865 | 7787 | 6922 |
| 0.15 | 9934 | 1490 | 8444 | 6954 |
| 0.2 | 11763 | 2353 | 9410 | 7058 |
| 0.25 | 12530 | 3133 | 9398 | 6265 |
| 0.3 | 13850 | 4155 | 9695 | 5540 |

84

For this example, the chosen proportion (q) of wrongly identified Spikes can be around 10 % to 20%. (0.1 < q < 0.2).

Notice that the final choice of "q" within the calculated range (10% to 20% for this specific example) doesn't affect significantly the subsequent MPD calculation, due to the small percentage of spikes, and its small variability (e.g. 0.1532 % for q=0.1, 0.1539 for q=0.15, 0.1562% for q=0.2) compared with the number of data points (n =4,517,952 measurements).

**Appendix E: Field Test Results for Chapter 4**

*CTMeter - MPD Results per Section*

Note: CTMeter results for the Smart Road Section are presented in Appendix B, below the remaining results for the VQPIP sections:

| Section | SR 199 1E |
|---|---|
| Count | 40 |
| Mean | 0.93 |
| SD | 0.21 |
| Min | 0.6 |
| Q1 | 0.8 |
| Median | 0.9 |
| Q3 | 1.0 |
| Max | 1.4 |
| Bottom | 0.8 |
| 2Q box | 0.118 |
| 3Q box | 0.138 |
| Whisker - | 0.158 |
| Whisker + | 0.368 |

CTMeter - MPD Statistics – SR-199 SMA 9.5 – E

| Section | SR 199 2E |
|---|---|
| Count | 40 |
| Mean | 1.30 |
| SD | 0.29 |
| Min | 0.7 |
| Q1 | 1.1 |
| Median | 1.3 |
| Q3 | 1.5 |
| Max | 2.2 |
| Bottom | 1.1 |
| 2Q box | 0.245 |
| 3Q box | 0.158 |
| Whisker - | 0.365 |
| Whisker + | 0.703 |

CTMeter - MPD Statistics – SR-199 AR-PFC 9.5 – E

| Section | SR 199 3E |
|---|---|
| Count | 40 |
| Mean | 1.25 |
| SD | 0.27 |
| Min | 0.9 |
| Q1 | 1.0 |
| Median | 1.2 |
| Q3 | 1.4 |
| Max | 2.3 |
| Bottom | 1.0 |
| 2Q box | 0.138 |
| 3Q box | 0.218 |
| Whisker - | 0.178 |
| Whisker + | 0.858 |
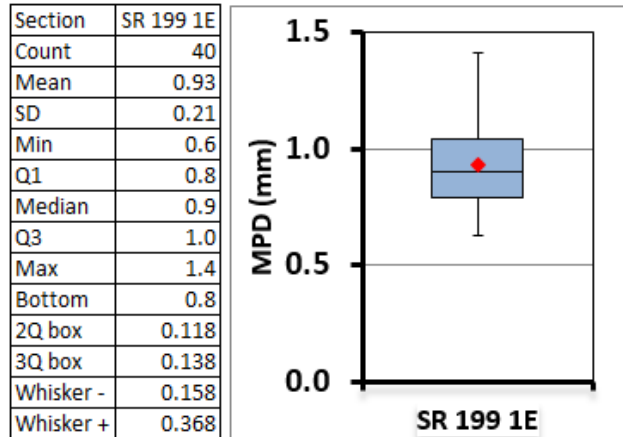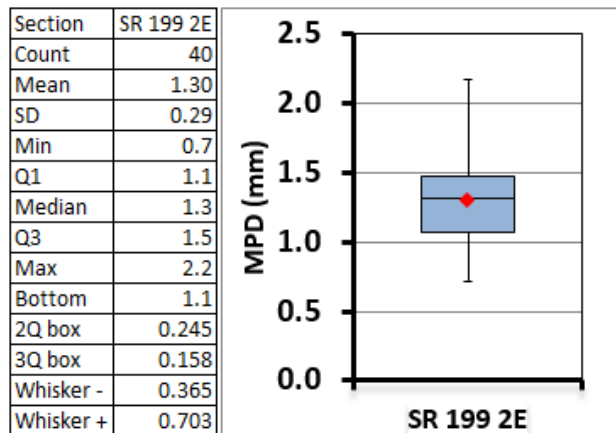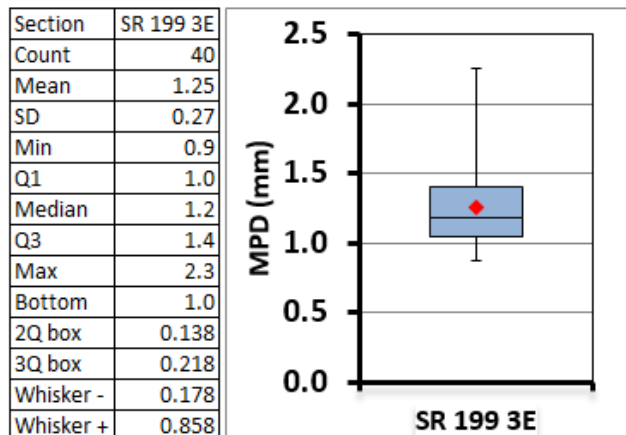
CTMeter - MPD Statistics SR-199 PFC 9.5 – E

| Section | SR 199 4E |
|---|---|
| Count | 40 |
| Mean | 1.20 |
| SD | 0.25 |
| Min | 0.8 |
| Q1 | 1.0 |
| Median | 1.2 |
| Q3 | 1.4 |
| Max | 1.9 |
| Bottom | 1.0 |
| 2Q box | 0.195 |
| 3Q box | 0.143 |
| Whisker - | 0.215 |
| Whisker + | 0.518 |
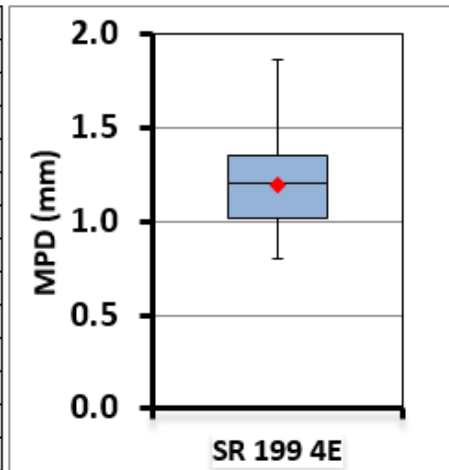
CTMeter - MPD Statistics SR-199 PFC 12.5 – E

| Section | SR 199 1W |
|---|---|
| Count | 40 |
| Mean | 0.88 |
| SD | 0.22 |
| Min | 0.5 |
| Q1 | 0.8 |
| Median | 0.9 |
| Q3 | 1.0 |
| Max | 1.3 |
| Bottom | 0.8 |
| 2Q box | 0.100 |
| 3Q box | 0.110 |
| Whisker - | 0.260 |
| Whisker + | 0.370 |
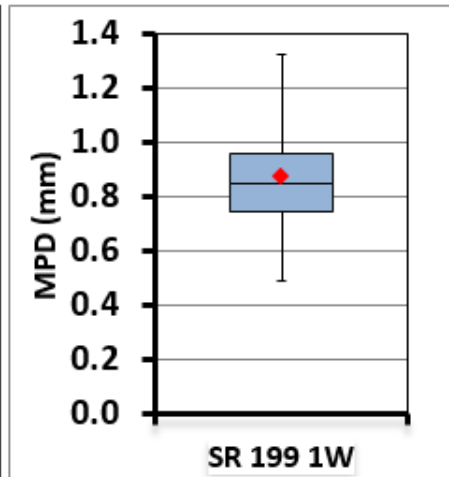
CTMeter - MPD Statistics SR-199 SMA 9.5 – W

| Section | SR 199 2W |
|---|---|
| Count | 40 |
| Mean | 1.27 |
| SD | 0.28 |
| Min | 0.7 |
| Q1 | 1.1 |
| Median | 1.2 |
| Q3 | 1.4 |
| Max | 2.1 |
| Bottom | 1.1 |
| 2Q box | 0.093 |
| 3Q box | 0.180 |
| Whisker - | 0.478 |
| Whisker + | 0.630 |
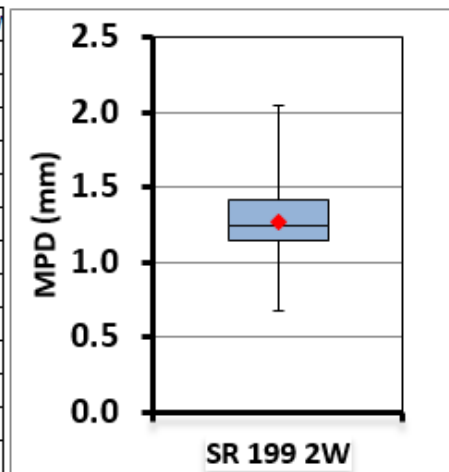
CTMeter - MPD Statistics SR-199 AR-PFC 9.5 – W

| Section | SR 199 3W |
|---|---|
| Count | 40 |
| Mean | 1.21 |
| SD | 0.23 |
| Min | 0.7 |
| Q1 | 1.1 |
| Median | 1.2 |
| Q3 | 1.3 |
| Max | 1.8 |
| Bottom | 1.1 |
| 2Q box | 0.085 |
| 3Q box | 0.118 |
| Whisker - | 0.370 |
| Whisker + | 0.478 |
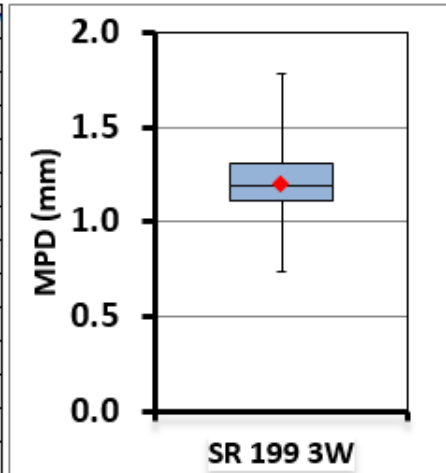


CTMeter - MPD Statistics SR-199 PFC 9.5 – W

| Section | SR 199 4W |
|---|---|
| Count | 40 |
| Mean | 1.38 |
| SD | 0.35 |
| Min | 0.8 |
| Q1 | 1.1 |
| Median | 1.3 |
| Q3 | 1.7 |
| Max | 2.1 |
| Bottom | 1.1 |
| 2Q box | 0.205 |
| 3Q box | 0.365 |
| Whisker - | 0.320 |
| Whisker + | 0.440 |
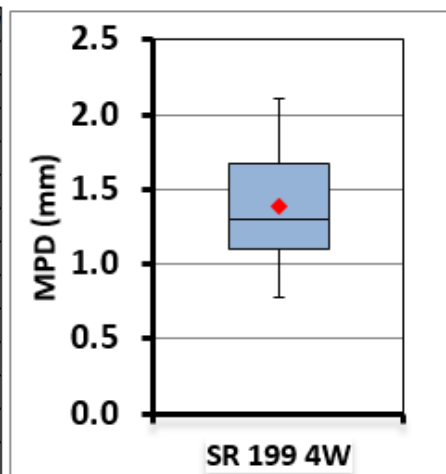


CTMeter - MPD Statistics SR-199 PFC 12.5 – W

| Section | SR 288 1N |
|---|---|
| Count | 40 |
| Mean | 0.87 |
| SD | 0.31 |
| Min | 0.4 |
| Q1 | 0.7 |
| Median | 0.9 |
| Q3 | 1.0 |
| Max | 1.7 |
| Bottom | 0.7 |
| 2Q box | 0.165 |
| 3Q box | 0.160 |
| Whisker - | 0.340 |
| Whisker + | 0.625 |
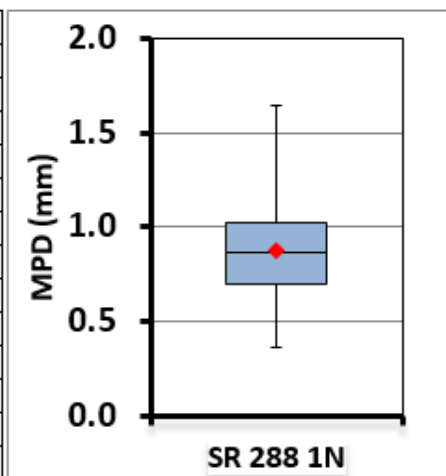


CTMeter - MPD Statistics SR-288 SMA 9.5 – N

| Section | SR 288 2N |
|---|---|
| Count | 40 |
| Mean | 1.44 |
| SD | 0.47 |
| Min | 0.8 |
| Q1 | 1.1 |
| Median | 1.3 |
| Q3 | 1.7 |
| Max | 2.6 |
| Bottom | 1.1 |
| 2Q box | 0.213 |
| 3Q box | 0.390 |
| Whisker - | 0.318 |
| Whisker + | 0.920 |
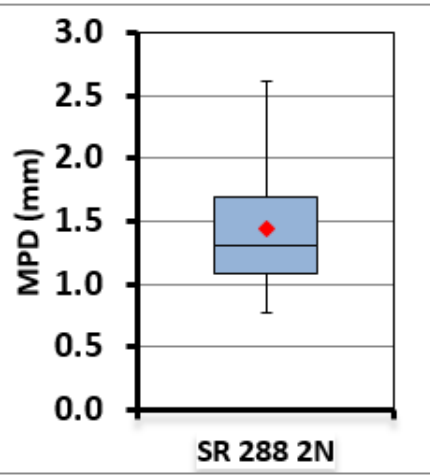
CTMeter - MPD Statistics SR-288 AR-PFC 9.5 – N

| Section | SR 288 3N |
|---|---|
| Count | 40 |
| Mean | 1.21 |
| SD | 0.23 |
| Min | 0.8 |
| Q1 | 1.1 |
| Median | 1.2 |
| Q3 | 1.3 |
| Max | 1.8 |
| Bottom | 1.1 |
| 2Q box | 0.082 |
| 3Q box | 0.183 |
| Whisker - | 0.298 |
| Whisker + | 0.468 |
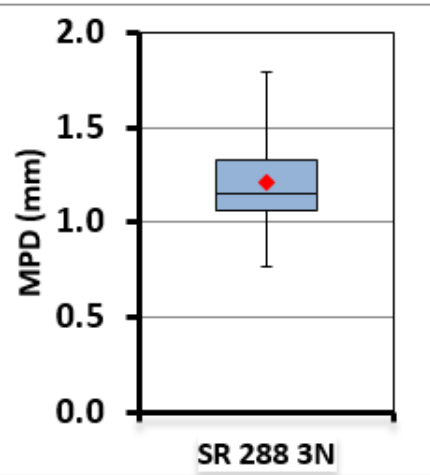
CTMeter - MPD Statistics SR-288 PFC 9.5 – N

| Section | SR 288 4N |
|---|---|
| Count | 40 |
| Mean | 1.17 |
| SD | 0.28 |
| Min | 0.7 |
| Q1 | 1.0 |
| Median | 1.1 |
| Q3 | 1.3 |
| Max | 1.9 |
| Bottom | 1.0 |
| 2Q box | 0.105 |
| 3Q box | 0.195 |
| Whisker - | 0.265 |
| Whisker + | 0.565 |
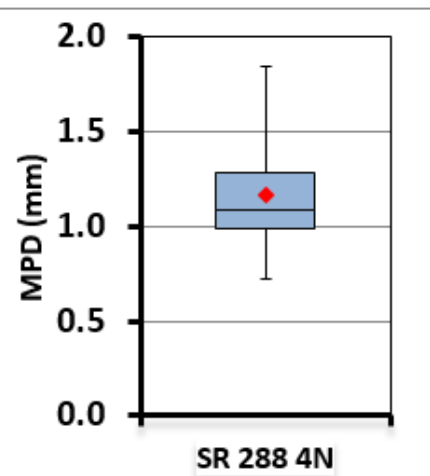
CTMeter - MPD Statistics SR-288 PFC 12.5 – N

| Section | SR 288 1S |
|---|---|
| Count | 40 |
| Mean | 0.80 |
| SD | 0.21 |
| Min | 0.5 |
| Q1 | 0.6 |
| Median | 0.8 |
| Q3 | 0.9 |
| Max | 1.4 |
| Bottom | 0.6 |
| 2Q box | 0.108 |
| 3Q box | 0.153 |
| Whisker - | 0.138 |
| Whisker + | 0.473 |
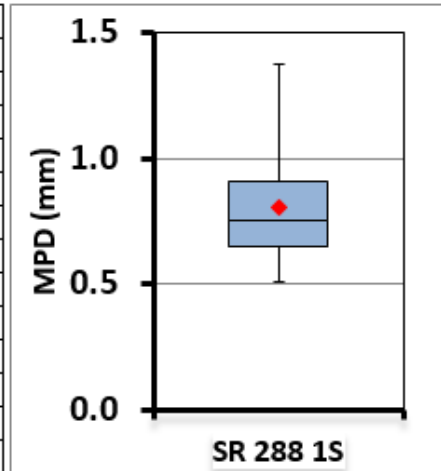
CTMeter - MPD Statistics SR-288 SMA 9.5 – S

| Section | SR 288 2S |
|---|---|
| Count | 40 |
| Mean | 1.26 |
| SD | 0.20 |
| Min | 0.9 |
| Q1 | 1.1 |
| Median | 1.2 |
| Q3 | 1.4 |
| Max | 1.8 |
| Bottom | 1.1 |
| 2Q box | 0.125 |
| 3Q box | 0.135 |
| Whisker - | 0.185 |
| Whisker + | 0.425 |
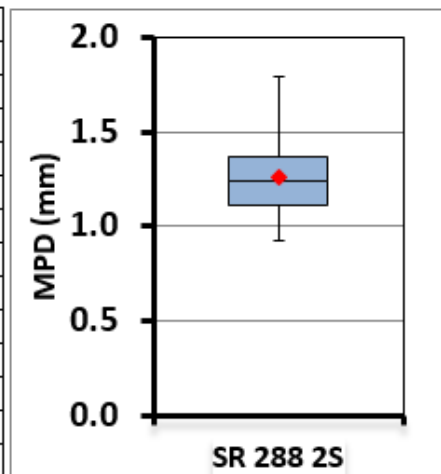
CTMeter - MPD Statistics SR-288 AR-PFC 9.5 – S

| Section | SR 288 3S |
|---|---|
| Count | 40 |
| Mean | 1.27 |
| SD | 0.29 |
| Min | 0.8 |
| Q1 | 1.0 |
| Median | 1.2 |
| Q3 | 1.5 |
| Max | 1.9 |
| Bottom | 1.0 |
| 2Q box | 0.190 |
| 3Q box | 0.248 |
| Whisker - | 0.230 |
| Whisker + | 0.393 |
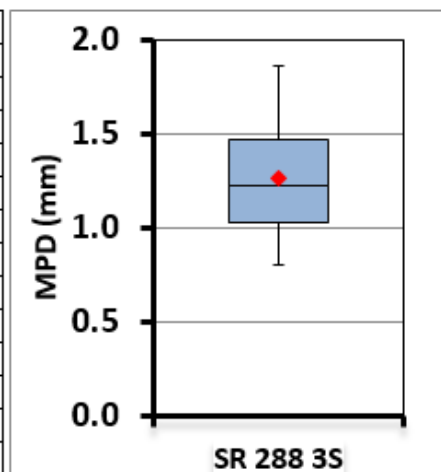
CTMeter - MPD Statistics SR-288 PFC 9.5 – S

| Section | SR 288 4S |
|---|---|
| Count | 40 |
| Mean | 1.06 |
| SD | 0.22 |
| Min | 0.6 |
| Q1 | 0.9 |
| Median | 1.1 |
| Q3 | 1.2 |
| Max | 1.5 |
| Bottom | 0.9 |
| 2Q box | 0.163 |
| 3Q box | 0.143 |
| Whisker - | 0.308 |
| Whisker + | 0.348 |
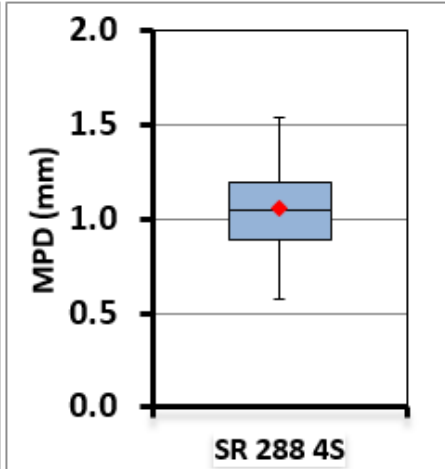
CTMeter - MPD Statistics SR-288 PFC 12.5 – S

| Section | SR 286 1N |
|---|---|
| Count | 40 |
| Mean | 0.92 |
| SD | 0.25 |
| Min | 0.5 |
| Q1 | 0.7 |
| Median | 0.9 |
| Q3 | 1.1 |
| Max | 1.7 |
| Bottom | 0.7 |
| 2Q box | 0.175 |
| 3Q box | 0.140 |
| Whisker - | 0.235 |
| Whisker + | 0.610 |
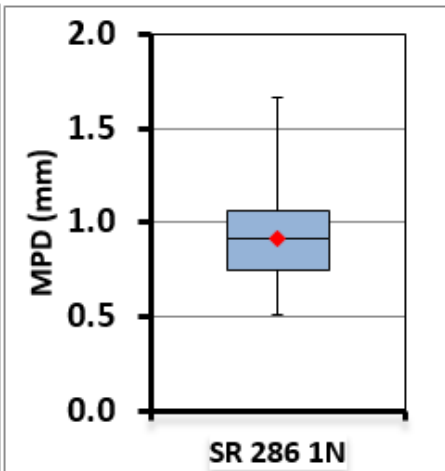
CTMeter - MPD Statistics SR-286 SMA 12.5 – N

| Section | SR 286 2N |
|---|---|
| Count | 40 |
| Mean | 1.31 |
| SD | 0.35 |
| Min | 0.7 |
| Q1 | 1.0 |
| Median | 1.3 |
| Q3 | 1.4 |
| Max | 2.3 |
| Bottom | 1.0 |
| 2Q box | 0.238 |
| 3Q box | 0.163 |
| Whisker - | 0.378 |
| Whisker + | 0.863 |
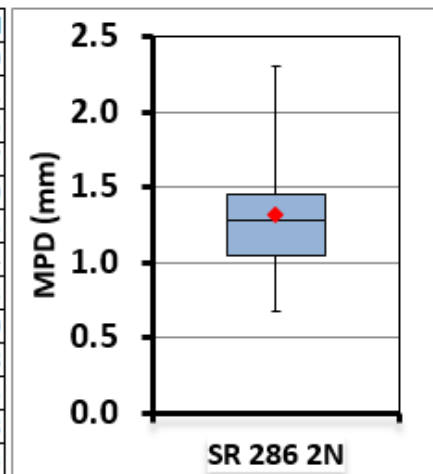
CTMeter - MPD Statistics SR-286 AR-PFC 12.5 – N

| Section | SR 286 1S |
|---|---|
| Count | 40 |
| Mean | 0.92 |
| SD | 0.20 |
| Min | 0.6 |
| Q1 | 0.8 |
| Median | 0.9 |
| Q3 | 1.1 |
| Max | 1.3 |
| Bottom | 0.8 |
| 2Q box | 0.097 |
| 3Q box | 0.205 |
| Whisker - | 0.198 |
| Whisker + | 0.220 |
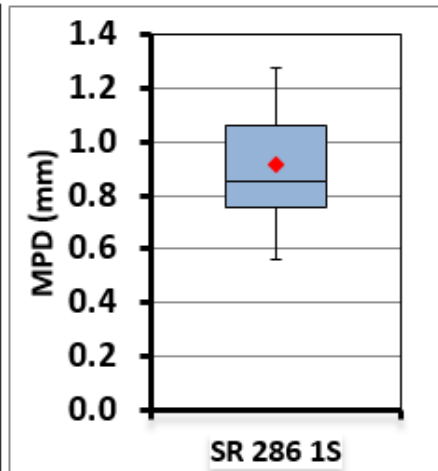


CTMeter - MPD Statistics SR-286 SMA 12.5 – S

| Section | SR 286 2S |
|---|---|
| Count | 40 |
| Mean | 1.36 |
| SD | 0.35 |
| Min | 0.8 |
| Q1 | 1.1 |
| Median | 1.2 |
| Q3 | 1.6 |
| Max | 2.4 |
| Bottom | 1.1 |
| 2Q box | 0.118 |
| 3Q box | 0.315 |
| Whisker - | 0.348 |
| Whisker + | 0.830 |
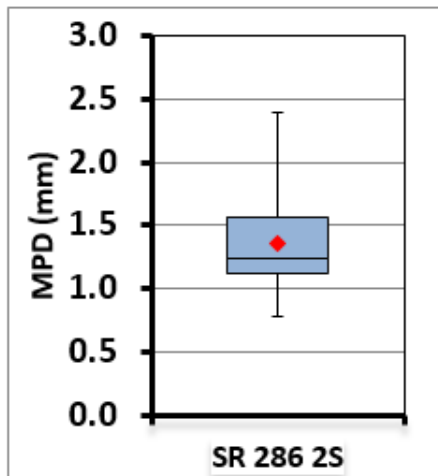


CTMeter - MPD Statistics SR-286 AR-PFC 12.5 – S

Note: HSLD results for the Smart Road Section are presented in Appendix B, below the remaining results for the VQPIP sections:
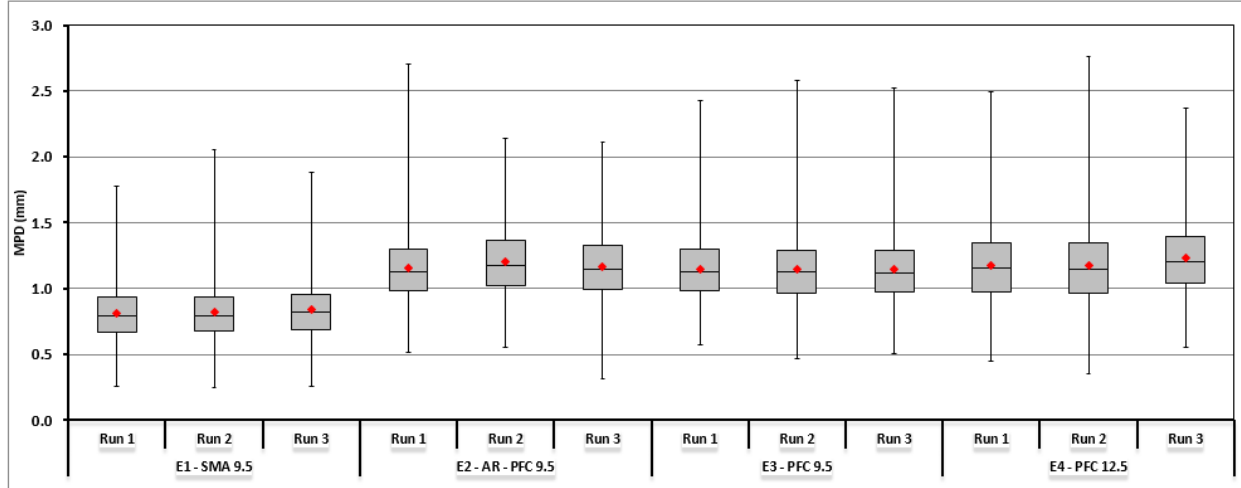


| SR199 | E1 - SMA 9.5 | | | E2 - AR - PFC 9.5 | | | E3 - PFC 9.5 | | | E4 - PFC 12.5 | | |
|---|---|---|---|---|---|---|---|---|---|---|---|---|
| | Run 1 | Run 2 | Run 3 | Run 1 | Run 2 | Run 3 | Run 1 | Run 2 | Run 3 | Run 1 | Run 2 | Run 3 |
| Count | 1654 | 1626 | 1673 | 1510 | 1617 | 1543 | 1654 | 1701 | 1668 | 1722 | 1660 | 1526 |
| Mean | 0.81 | 0.82 | 0.84 | 1.16 | 1.21 | 1.17 | 1.15 | 1.14 | 1.14 | 1.18 | 1.17 | 1.23 |
| SD | 0.20 | 0.21 | 0.21 | 0.25 | 0.26 | 0.25 | 0.24 | 0.24 | 0.25 | 0.28 | 0.29 | 0.27 |
| Min | 0.3 | 0.2 | 0.3 | 0.5 | 0.6 | 0.3 | 0.6 | 0.5 | 0.5 | 0.5 | 0.3 | 0.6 |
| Median | 0.8 | 0.8 | 0.8 | 1.1 | 1.2 | 1.1 | 1.1 | 1.1 | 1.1 | 1.2 | 1.1 | 1.2 |
| Max | 1.8 | 2.1 | 1.9 | 2.7 | 2.1 | 2.1 | 2.4 | 2.6 | 2.5 | 2.5 | 2.8 | 2.4 |
| Average of the mean | 0.82 | | | 1.18 | | | 1.15 | | | 1.20 | | |

HSLD - MPD Statistics – SR-199 – E
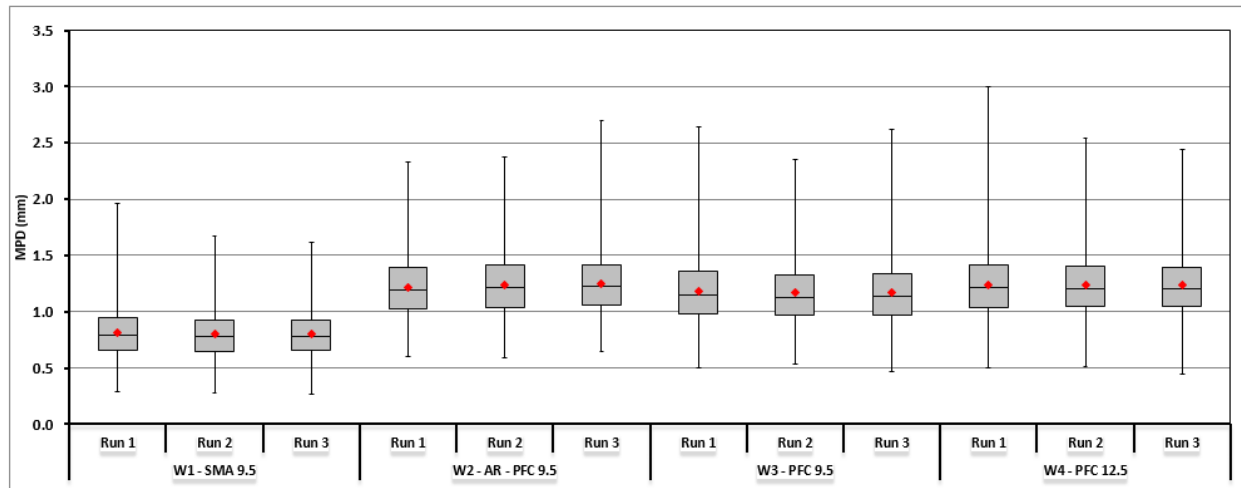


| SR199 | W1 - SMA 9.5 | | | W2 - AR - PFC 9.5 | | | W3 - PFC 9.5 | | | W4 - PFC 12.5 | | |
|---|---|---|---|---|---|---|---|---|---|---|---|---|
| | Run 1 | Run 2 | Run 3 | Run 1 | Run 2 | Run 3 | Run 1 | Run 2 | Run 3 | Run 1 | Run 2 | Run 3 |
| Count | 1416 | 1836 | 1715 | 1637 | 1690 | 1492 | 1738 | 1640 | 1622 | 1823 | 1543 | 1627 |
| Mean | 0.82 | 0.80 | 0.81 | 1.22 | 1.24 | 1.25 | 1.19 | 1.17 | 1.17 | 1.24 | 1.24 | 1.23 |
| SD | 0.22 | 0.22 | 0.20 | 0.28 | 0.28 | 0.27 | 0.29 | 0.28 | 0.29 | 0.29 | 0.28 | 0.27 |
| Min | 0.3 | 0.3 | 0.3 | 0.6 | 0.6 | 0.6 | 0.5 | 0.5 | 0.5 | 0.5 | 0.5 | 0.4 |
| Median | 0.8 | 0.8 | 0.8 | 1.2 | 1.2 | 1.2 | 1.1 | 1.1 | 1.1 | 1.2 | 1.2 | 1.2 |
| Max | 2.0 | 1.7 | 1.6 | 2.3 | 2.4 | 2.7 | 2.6 | 2.4 | 2.6 | 3.0 | 2.5 | 2.4 |
| Average of the mean | 0.81 | | | 1.24 | | | 1.17 | | | 1.24 | | |

HSLD - MPD Statistics – SR-199 – W
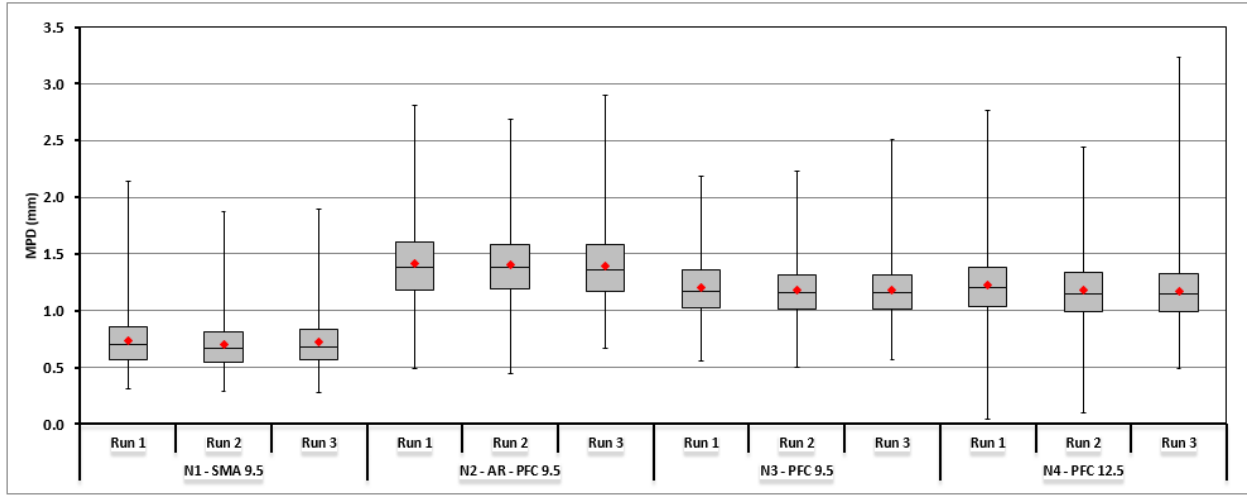
| SR288 | N1 - SMA 9.5 | | | N2 - AR - PFC 9.5 | | | N3 - PFC 9.5 | | | N4 - PFC 12.5 | | |
|---|---|---|---|---|---|---|---|---|---|---|---|---|
| | Run 1 | Run 2 | Run 3 | Run 1 | Run 2 | Run 3 | Run 1 | Run 2 | Run 3 | Run 1 | Run 2 | Run 3 |
| Count | 1651 | 1657 | 1509 | 1899 | 1824 | 1658 | 1504 | 1843 | 1676 | 1631 | 1630 | 4000 |
| Mean | **0.73** | **0.70** | **0.72** | **1.41** | **1.40** | **1.39** | **1.20** | **1.18** | **1.18** | **1.23** | **1.19** | **1.17** |
| SD | 0.22 | 0.22 | 0.22 | 0.33 | 0.31 | 0.32 | 0.25 | 0.24 | 0.24 | 0.28 | 0.27 | 0.26 |
| Min | 0.3 | 0.3 | 0.3 | 0.5 | 0.4 | 0.7 | 0.6 | 0.5 | 0.6 | 0.0 | 0.1 | 0.5 |
| Median | 0.7 | 0.7 | 0.7 | 1.4 | 1.4 | 1.4 | 1.2 | 1.2 | 1.2 | 1.2 | 1.2 | 1.1 |
| Max | 2.1 | 1.9 | 1.9 | 2.8 | 2.7 | 2.9 | 2.2 | 2.2 | 2.5 | 2.8 | 2.4 | 3.2 |
| Average of the mean | **0.72** | | | **1.40** | | | **1.19** | | | **1.20** | | |

HSLD - MPD Statistics – SR-288 – N
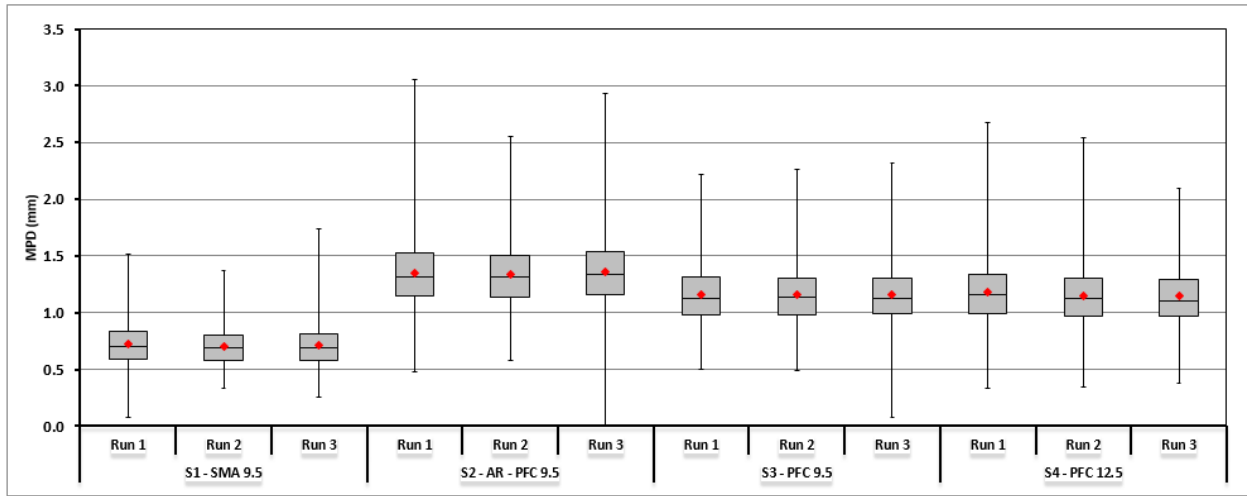


| SR288 | S1 - SMA 9.5 | | | S2 - AR - PFC 9.5 | | | S3 - PFC 9.5 | | | S4 - PFC 12.5 | | |
|---|---|---|---|---|---|---|---|---|---|---|---|---|
| | Run 1 | Run 2 | Run 3 | Run 1 | Run 2 | Run 3 | Run 1 | Run 2 | Run 3 | Run 1 | Run 2 | Run 3 |
| Count | 1649 | 1683 | 1648 | 1844 | 1687 | 1821 | 1756 | 1806 | 1651 | 2294 | 1656 | 1674 |
| Mean | **0.73** | **0.71** | **0.72** | **1.35** | **1.34** | **1.36** | **1.16** | **1.16** | **1.16** | **1.18** | **1.15** | **1.14** |
| SD | 0.19 | 0.18 | 0.19 | 0.30 | 0.28 | 0.30 | 0.24 | 0.25 | 0.24 | 0.27 | 0.26 | 0.25 |
| Min | 0.1 | 0.3 | 0.3 | 0.5 | 0.6 | 0.0 | 0.5 | 0.5 | 0.1 | 0.3 | 0.3 | 0.4 |
| Median | 0.7 | 0.7 | 0.7 | 1.3 | 1.3 | 1.3 | 1.1 | 1.1 | 1.1 | 1.2 | 1.1 | 1.1 |
| Max | 1.5 | 1.4 | 1.7 | 3.0 | 2.6 | 2.9 | 2.2 | 2.3 | 2.3 | 2.7 | 2.5 | 2.1 |
| Average of the mean | **0.72** | | | **1.35** | | | **1.16** | | | **1.16** | | |

HSLD - MPD Statistics – SR-288 – S

94
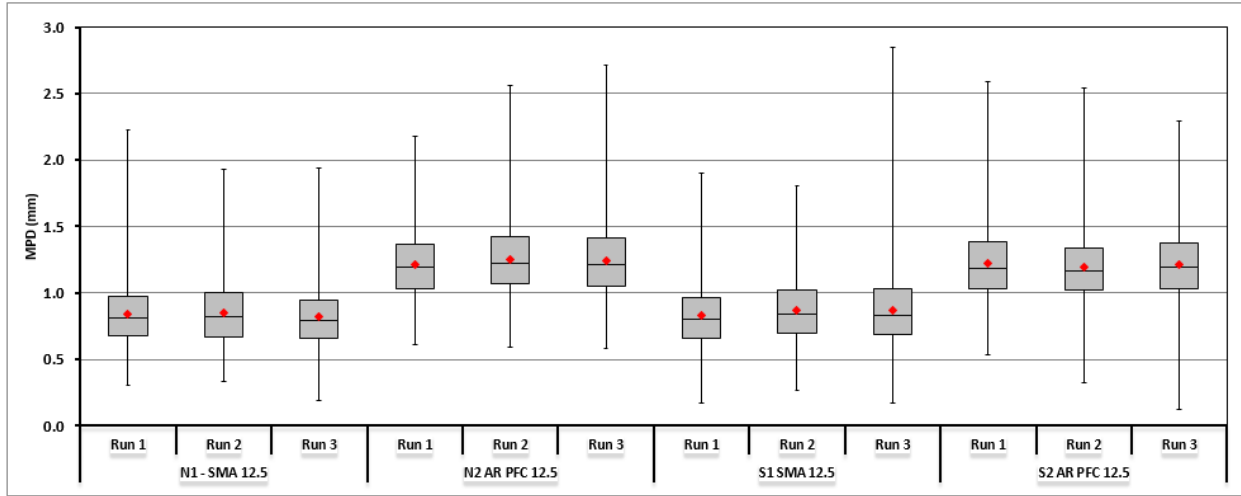
| SR286 | N1 - SMA 12.5 | | | N2 AR PFC 12.5 | | | S1 SMA 12.5 | | | S2 AR PFC 12.5 | | |
|---|---|---|---|---|---|---|---|---|---|---|---|---|
| | Run 1 | Run 2 | Run 3 | Run 1 | Run 2 | Run 3 | Run 1 | Run 2 | Run 3 | Run 1 | Run 2 | Run 3 |
| Count | 1683 | 1652 | 1691 | 1653 | 1810 | 2197 | 1753 | 1691 | 1721 | 1859 | 1745 | 1935 |
| Mean | 0.84 | 0.85 | 0.82 | 1.21 | 1.25 | 1.24 | 0.83 | 0.87 | 0.87 | 1.23 | 1.19 | 1.22 |
| SD | 0.22 | 0.25 | 0.22 | 0.25 | 0.27 | 0.27 | 0.24 | 0.24 | 0.26 | 0.27 | 0.26 | 0.26 |
| Min | 0.3 | 0.3 | 0.2 | 0.6 | 0.6 | 0.6 | 0.2 | 0.3 | 0.2 | 0.5 | 0.3 | 0.1 |
| Median | 0.8 | 0.8 | 0.8 | 1.2 | 1.2 | 1.2 | 0.8 | 0.8 | 0.8 | 1.2 | 1.2 | 1.2 |
| Max | 2.2 | 1.9 | 1.9 | 2.2 | 2.6 | 2.7 | 1.9 | 1.8 | 2.8 | 2.6 | 2.5 | 2.3 |
| Average of the mean | 0.84 | | | 1.24 | | | 0.86 | | | 1.21 | | |

HSLD - MPD Statistics – SR-286 – N & S

*EAWE Results per Section*

EAWE & EDWE for all Sections (3 runs shown) – d* = 0.054

| Tire:medium soft | EAWE (mm²) | | | | EDWE (mm) |
|---|---|---|---|---|---|
| d* = 0.054 | Run 1 | Run 2 | Run 3 | average | EAWE/100 |
| L-SMA12.5 | 23.75 | 23.84 | 23.10 | 23.29 | 0.23 |
| K-OGFC | 31.22 | 31.77 | 30.27 | 30.54 | 0.31 |
| J-SM9.5D | 23.00 | 22.70 | 21.79 | 21.92 | 0.22 |
| I-SM9.5A | 20.34 | 20.45 | 20.01 | 19.72 | 0.20 |
| H-SM9.5D | 20.62 | 20.16 | 20.46 | 20.00 | 0.20 |
| G-SM9.5D | 19.45 | 19.82 | 20.03 | 19.15 | 0.19 |
| F-SM9.5D | 19.06 | 18.38 | 18.47 | 18.42 | 0.18 |
| E-SM9.5D | 20.03 | 20.19 | 20.29 | 19.72 | 0.20 |
| D-SM9.5A | 19.30 | 19.23 | 19.00 | 18.98 | 0.19 |
| C-SM9.5E | 21.14 | 20.43 | 20.37 | 20.47 | 0.20 |
| B-SM9.5D | 23.44 | 22.95 | 23.02 | 22.53 | 0.23 |
| A-SM12.5D | 29.54 | 26.16 | 25.77 | 25.89 | 0.26 |
| SMA 9.5 - E | 21.68 | 21.71 | 22.16 | 21.85 | 0.22 |
| SMA 9.5 - W | 21.74 | 20.95 | 21.22 | 21.30 | 0.21 |
| AR-PFC 9.5 - E | 31.28 | 32.59 | 32.33 | 32.06 | 0.32 |
| AR-PFC 9.5 - W | 32.44 | 33.45 | 34.12 | 33.34 | 0.33 |
| PFC 9.5 - E | 30.62 | 30.18 | 30.89 | 30.56 | 0.31 |
| PFC 9.5 - W | 31.69 | 31.60 | 31.46 | 31.58 | 0.32 |
| PFC 12.5 - E | 29.71 | 29.91 | 30.99 | 30.20 | 0.30 |
| PFC 12.5 - W | 31.79 | 32.24 | 32.21 | 32.08 | 0.32 |
| AR-PFC 12.5 - N | 31.25 | 32.15 | 32.53 | 31.98 | 0.32 |
| AR-PFC 12.5 - S | 33.55 | 32.55 | 32.73 | 32.94 | 0.33 |
| SMA 12.5 -N | 19.16 | 20.60 | 19.30 | 19.68 | 0.20 |
| SMA 12.5 - S | 22.74 | 23.03 | 23.41 | 23.06 | 0.23 |
| SMA 9.5 - N | 18.5795 | 18.4501 | 18.7683 | 18.60 | 0.19 |
| SMA 9.5 - S | 18.9976 | 18.9125 | 18.7727 | 18.89 | 0.19 |
| AR-PFC 9.5 - N | 35.1807 | 35.042 | 35.0692 | 35.10 | 0.35 |
| AR-PFC 9.5 - S | 33.9071 | 33.8631 | 33.8682 | 33.88 | 0.34 |
| PFC 9.5 - N | 30.4211 | 30.0809 | 30.0107 | 30.17 | 0.30 |
| PFC 9.5 - S | 29.6673 | 29.192 | 29.1779 | 29.35 | 0.29 |
| PFC 12.5 - N | 30.7264 | 29.6763 | 29.7885 | 30.06 | 0.30 |
| PFC 12.5 - S | 29.8258 | 28.6084 | 28.5085 | 28.98 | 0.29 |

Note: For the Smart Road Sections (A through L), only 3 of the 9 runs are shown due to space constraints, Average results corresponds to all runs.

EAWE & EDWE for all Sections (3 runs shown) – d* = 0.027

| Tire:medium hard | EAWE (mm²) | | | | EDWE (mm) |
| d* = 0.027 | Run 1 | Run 2 | Run 3 | average | EAWE/100 |
|---|---|---|---|---|---|
| L-SMA12.5 | 33.3675 | 33.3641 | 32.5383 | 33.09 | 0.33 |
| K-OGFC | 44.6526 | 45.6352 | 43.4036 | 44.56 | 0.45 |
| J-SM9.5D | 31.7551 | 31.7602 | 30.387 | 31.30 | 0.31 |
| I-SM9.5A | 28.135 | 28.4421 | 27.8305 | 28.14 | 0.28 |
| H-SM9.5D | 28.5985 | 27.991 | 28.4411 | 28.34 | 0.28 |
| G-SM9.5D | 26.9224 | 27.5701 | 27.8314 | 27.44 | 0.27 |
| F-SM9.5D | 26.276 | 25.2344 | 25.4384 | 25.65 | 0.26 |
| E-SM9.5D | 27.6841 | 27.9422 | 27.9548 | 27.86 | 0.28 |
| D-SM9.5A | 26.4462 | 26.2925 | 26.0489 | 26.09 | 0.26 |
| C-SM9.5E | 29.361 | 28.3973 | 28.3076 | 28.41 | 0.28 |
| B-SM9.5D | 33.1302 | 32.1497 | 32.6355 | 31.80 | 0.32 |
| A-SM12.5D | 41.1387 | 36.7243 | 35.7001 | 36.32 | 0.36 |
| SMA 9.5 - E | 28.9524 | 29.7296 | 29.6114 | 29.43 | 0.29 |
| SMA 9.5 - W | 29.1238 | 28.0393 | 30.3683 | 29.18 | 0.29 |
| AR-PFC 9.5 - E | 45.0774 | 44.725 | 44.4617 | 44.75 | 0.45 |
| AR-PFC 9.5 - W | 44.2298 | 44.8528 | 45.5293 | 44.87 | 0.45 |
| PFC 9.5 - E | 41.8749 | 41.0656 | 41.8479 | 41.60 | 0.42 |
| PFC 9.5 - W | 42.7606 | 42.46 | 42.4612 | 42.56 | 0.43 |
| PFC 12.5 - E | 40.1448 | 40.3508 | 41.6705 | 40.72 | 0.41 |
| PFC 12.5 - W | 42.2053 | 42.6938 | 42.639 | 42.51 | 0.43 |
| AR-PFC 12.5 - N | 40.6422 | 42.5053 | 43.0189 | 42.06 | 0.42 |
| AR-PFC 12.5 - S | 43.93 | 42.6899 | 42.9346 | 43.18 | 0.43 |
| SMA 12.5 -N | 25.9274 | 27.5604 | 26.0422 | 26.51 | 0.27 |
| SMA 12.5 - S | 26.2832 | 26.9646 | 27.4825 | 26.91 | 0.27 |
| SMA 9.5 - N | 24.9369 | 24.6213 | 25.1165 | 24.89 | 0.25 |
| SMA 9.5 - S | 25.5033 | 25.2595 | 25.1285 | 25.30 | 0.25 |
| AR-PFC 9.5 - N | 46.6221 | 46.3062 | 46.445 | 46.46 | 0.46 |
| AR-PFC 9.5 - S | 45.0356 | 44.6992 | 45.9305 | 45.22 | 0.45 |
| PFC 9.5 - N | 40.5556 | 39.9353 | 39.7945 | 40.10 | 0.40 |
| PFC 9.5 - S | 39.3013 | 38.8186 | 38.8849 | 39.00 | 0.39 |
| PFC 12.5 - N | 40.8151 | 39.3811 | 39.3765 | 39.86 | 0.40 |
| PFC 12.5 - S | 39.5792 | 38.0844 | 37.9266 | 38.53 | 0.39 |

Note: For some of the Smart Road Sections (A through D), only 3 of the 9 runs are shown due to space constraints, Average results corresponds to all runs.

EAWE & EDWE for all Sections (3 runs shown) – d* = 0.010

| Tire: stiff | EAWE (mm$^2$) | | | | EDWE (mm) |
|---|---|---|---|---|---|
| d* = 0.01 | Run 1 | Run 2 | Run 3 | average | EAWE/100 |
| L-SMA12.5 | 49.6243 | 49.2943 | 48.5063 | 49.14 | 0.49 |
| K-OGFC | 68.48 | 70.0855 | 66.7254 | 68.43 | 0.68 |
| J-SM9.5D | 46.9551 | 47.4597 | 45.1438 | 46.52 | 0.47 |
| I-SM9.5A | 41.2292 | 41.9538 | 40.8292 | 41.34 | 0.41 |
| H-SM9.5D | 42.0672 | 41.2354 | 41.9396 | 41.75 | 0.42 |
| G-SM9.5D | 39.4334 | 40.5572 | 41.2077 | 40.40 | 0.40 |
| F-SM9.5D | 38.1182 | 36.3918 | 36.7756 | 37.10 | 0.37 |
| E-SM9.5D | 40.3844 | 40.863 | 40.9336 | 40.73 | 0.41 |
| D-SM9.5A | 37.7622 | 37.5957 | 37.4072 | 37.59 | 0.38 |
| C-SM9.5E | 43.0327 | 41.5696 | 41.4069 | 42.00 | 0.42 |
| B-SM9.5D | 50.4352 | 48.3929 | 49.9332 | 49.59 | 0.50 |
| A-SM12.5D | 61.7046 | 55.2322 | 52.2029 | 56.38 | 0.56 |
| SMA 9.5 - E | 40.0364 | 40.7595 | 41.0557 | 40.62 | 0.41 |
| SMA 9.5 - W | 38.4777 | 38.9584 | 40.5645 | 39.33 | 0.39 |
| AR-PFC 9.5 - E | 57.9217 | 57.421 | 56.8098 | 57.38 | 0.57 |
| AR-PFC 9.5 - W | 57.1343 | 59.2949 | 60.239 | 58.89 | 0.59 |
| PFC 9.5 - E | 55.2863 | 54.5589 | 55.3878 | 55.08 | 0.55 |
| PFC 9.5 - W | 57.6925 | 57.2483 | 57.2762 | 57.41 | 0.57 |
| PFC 12.5 - E | 54.0795 | 54.4954 | 56.3406 | 54.97 | 0.55 |
| PFC 12.5 - W | 58.522 | 59.1224 | 58.8794 | 58.84 | 0.59 |
| AR-PFC 12.5 - N | 53.9881 | 56.3527 | 59.8767 | 56.74 | 0.57 |
| AR-PFC 12.5 - S | 60.4276 | 58.9077 | 59.2991 | 59.54 | 0.60 |
| SMA 12.5 -N | 38.197 | 39.6171 | 38.1557 | 38.66 | 0.39 |
| SMA 12.5 - S | 37.9653 | 38.9475 | 39.3924 | 38.77 | 0.39 |
| SMA 9.5 - N | 34.5936 | 33.8199 | 34.5557 | 34.32 | 0.34 |
| SMA 9.5 - S | 35.3522 | 34.7813 | 34.6774 | 34.94 | 0.35 |
| AR-PFC 9.5 - N | 65.5541 | 65.0997 | 65.1773 | 65.28 | 0.65 |
| AR-PFC 9.5 - S | 63.0929 | 62.5373 | 63.9853 | 63.21 | 0.63 |
| PFC 9.5 - N | 56.8338 | 55.8506 | 55.7208 | 56.14 | 0.56 |
| PFC 9.5 - S | 54.8792 | 54.3227 | 54.5921 | 54.60 | 0.55 |
| PFC 12.5 - N | 57.0711 | 55.0076 | 54.8775 | 55.65 | 0.56 |
| PFC 12.5 - S | 55.3755 | 53.4166 | 53.0767 | 53.96 | 0.54 |

EAWE & EDWE for all Sections (3 runs shown) – d* = 0.001

| Tire: Super stiff | EAWE (mm²) | | | | EDWE (mm) |
| d* = 0.001 | Run 1 | Run 2 | Run 3 | average | EAWE/100 |
|---|---|---|---|---|---|
| L-SMA12.5 | 90.8142 | 88.5345 | 88.6336 | 89.33 | 0.89 |
| K-OGFC | 129.5518 | 133.1697 | 125.7552 | 129.49 | 1.29 |
| J-SM9.5D | 89.2935 | 92.7345 | 87.5219 | 89.85 | 0.90 |
| I-SM9.5A | 77.3876 | 79.006 | 76.9503 | 77.78 | 0.78 |
| H-SM9.5D | 80.0052 | 78.6685 | 80.0647 | 79.58 | 0.80 |
| G-SM9.5D | 74.1877 | 77.6219 | 79.4073 | 77.07 | 0.77 |
| F-SM9.5D | 69.3365 | 65.9509 | 66.9011 | 67.40 | 0.67 |
| E-SM9.5D | 74.5359 | 75.1896 | 75.1194 | 74.95 | 0.75 |
| D-SM9.5A | 67.0192 | 67.0338 | 66.4353 | 66.83 | 0.67 |
| C-SM9.5E | 79.6023 | 76.2511 | 76.1889 | 77.35 | 0.77 |
| B-SM9.5D | 102.502 | 97.44 | 102.7028 | 100.88 | 1.01 |
| A-SM12.5D | 120.1558 | 10.8823 | 96.4164 | 75.82 | 0.76 |
| SMA 9.5 - E | 66.4962 | 67.1128 | 68.1356 | 67.25 | 0.67 |
| SMA 9.5 - W | 60.8781 | 65.1305 | 64.8599 | 63.62 | 0.64 |
| AR-PFC 9.5 - E | 88.7885 | 93.2877 | 91.852 | 91.31 | 0.91 |
| AR-PFC 9.5 - W | 93.5913 | 97.1867 | 98.9811 | 96.59 | 0.97 |
| PFC 9.5 - E | 90.7983 | 89.9278 | 90.5653 | 90.43 | 0.90 |
| PFC 9.5 - W | 94.6192 | 93.5887 | 93.7814 | 94.00 | 0.94 |
| PFC 12.5 - E | 90.5826 | 91.3402 | 95.1584 | 92.36 | 0.92 |
| PFC 12.5 - W | 98.0483 | 98.7786 | 98.1075 | 98.31 | 0.98 |
| AR-PFC 12.5 - N | 98.1024 | 99.4539 | 100.4213 | 99.33 | 0.99 |
| AR-PFC 12.5 - S | 99.8549 | 98.2266 | 98.6126 | 98.90 | 0.99 |
| SMA 12.5 -N | 62.9832 | 64.6195 | 62.3703 | 63.32 | 0.63 |
| SMA 12.5 - S | 62.901 | 64.6598 | 65.2651 | 64.28 | 0.64 |
| SMA 9.5 - N | 58.3061 | 56.454 | 57.7686 | 57.51 | 0.58 |
| SMA 9.5 - S | 58.8139 | 57.635 | 57.8228 | 58.09 | 0.58 |
| AR-PFC 9.5 - N | 113.1581 | 111.3946 | 111.4022 | 111.98 | 1.12 |
| AR-PFC 9.5 - S | 108.4328 | 107.3283 | 109.4497 | 108.40 | 1.08 |
| PFC 9.5 - N | 96.5198 | 94.4661 | 94.5414 | 95.18 | 0.95 |
| PFC 9.5 - S | 93.2522 | 92.9382 | 92.9079 | 93.03 | 0.93 |
| PFC 12.5 - N | 97.2632 | 93.7689 | 93.4807 | 94.84 | 0.95 |
| PFC 12.5 - S | 94.7564 | 92.3119 | 90.8769 | 92.65 | 0.93 |

Fiction for Smart Road Sections

| Section | Run 1 | Run 2 | Run 3 | Run 4 | Run 5 | Run 6 | Run 7 | Run 8 | Run 9 | Run 10 | Run 11 | Run 12 | Ave. |
|---|---|---|---|---|---|---|---|---|---|---|---|---|---|
| A | 0.61 | 0.66 | 0.61 | 0.57 | 0.59 | 0.60 | 0.70 | 0.65 | 0.60 | 0.59 | 0.61 | 0.59 | 0.61 |
| B | 0.66 | 0.67 | 0.62 | 0.68 | 0.62 | 0.63 | 0.71 | 0.64 | 0.61 | 0.61 | 0.62 | 0.96 | 0.67 |
| C | 0.54 | 0.58 | 0.57 | 0.57 | 0.58 | 0.54 | 0.59 | 0.56 | 0.56 | 0.57 | 0.55 | 0.54 | 0.56 |
| D | 0.53 | 0.52 | 0.51 | 0.50 | 0.51 | 0.50 | 0.52 | 0.51 | 0.55 | 0.51 | 0.52 | 0.50 | 0.52 |
| I | 0.67 | 0.69 | 0.67 | 0.62 | 0.70 | 0.68 | 0.70 | 0.62 | 0.67 | 0.63 | 0.62 | 0.62 | 0.66 |
| J | 0.53 | 0.59 | 0.62 | 0.64 | 0.60 | 0.53 | 0.58 | 0.57 | 0.56 | 0.58 | 0.49 | 0.55 | 0.57 |
| L | 0.51 | 0.55 | 0.56 | 0.54 | 0.51 | 0.53 | 0.59 | 0.53 | 0.54 | 0.48 | 0.54 | 0.48 | 0.53 |

Fiction for VQPIP Sections (average of 3 runs)

| Project | Direction | SMA 9.5 | SMA 12.5 | AR PFC 9.5 | AR PFC 12.5 | PFC 9.5 | PFC 12.5 |
|---|---|---|---|---|---|---|---|
| Rt 286 Fairfax | NORTH | | 0.67 | | 0.60 | | |
| | SOUTH | | 0.62 | | 0.68 | | |
| Rt 288 Chesterfield | NORTH | 0.66 | | 0.67 | | 0.69 | 0.70 |
| | SOUTH | 0.60 | | 0.70 | | 0.67 | 0.64 |
| Rt 199 Williamsburg | EAST | 0.65 | | 0.72 | | 0.73 | 0.67 |
| | WEST | 0.64 | | 0.65 | | 0.68 | 0.68 |

SR199, SR288, SR 286, Summary Average Overall IL Measured & Normalized for temperature (dBA)

| | Project | Measured | | Normalized | |
|---|---|---|---|---|---|
| | **SR 199** | **E** | **W** | **E** | **W** |
| 1 | SMA 9.5 | 101.7 | 101.9 | 102.0 | 102.2 |
| 2 | AR-PFC 9.5 | 98.9 | 99 | 99.2 | 99.3 |
| 3 | PFC 9.5 | 103 | 99.8 | 103.3 | 100.1 |
| 4 | PFC 12.5 | 103 | 100.6 | 103.3 | 100.9 |
| | **SR 288** | **N** | **S** | **N** | **S** |
| 1 | SMA 9.5 | 102.8 | 102.5 | 103.3 | 103.0 |
| 2 | AR-PFC 9.5 | 100.4 | 100.7 | 100.9 | 101.2 |
| 3 | PFC 9.5 | 101.2 | 101.7 | 101.7 | 102.2 |
| 4 | PFC 12.5 | 100.7 | 100.1 | 101.2 | 100.6 |
| | **SR 286** | **N** | **S** | **N** | **S** |
| 1 | SMA 12.5 | 103.1 | 103.2 | 103.1 | 103.2 |
| 2 | AR - PFC 12.5 | 98.7 | 97.5 | 98.7 | 97.5 |

State Route 199, west of Williamsburg (SMA 9.5) 1 E

| Freq. [Hz] | 1st - Intensity Level [dBA] (re. 1 pW/m²) | 2nd - Intensity Level [dBA] (re. 1 pW/m²) | 3rd - Intensity Level [dBA] (re. 1 pW/m²) | Average Intensity Level [dBA] (re. 1 pW/m²) |
|---|---|---|---|---|
| 400 | 79.3 | 78.5 | 79.1 | 79 |
| 500 | 82.8 | 82.6 | 82.6 | 82.7 |
| 630 | 86.6 | 86.3 | 86.4 | 86.4 |
| 800 | 94.3 | 94.1 | 94.2 | 94.2 |
| 1000 | 96.3 | 96.5 | 96.6 | 96.5 |
| 1250 | 94.2 | 94.1 | 94.7 | 94.3 |
| 1600 | 93 | 93.3 | 93.1 | 93.1 |
| 2000 | 91.4 | 91.7 | 91.7 | 91.6 |
| 2500 | 87.7 | 88 | 87.8 | 87.9 |
| 3150 | 82.9 | 83 | 82.7 | 82.9 |
| 4000 | 78.6 | 78.8 | 78.5 | 78.6 |
| 5000 | 75.5 | 75.6 | 75.4 | 75.5 |
| Overall IL [dBA] | 101.6 | 101.7 | 101.8 | 101.7 |

1 E
Overall IL [dBA]: 101.7
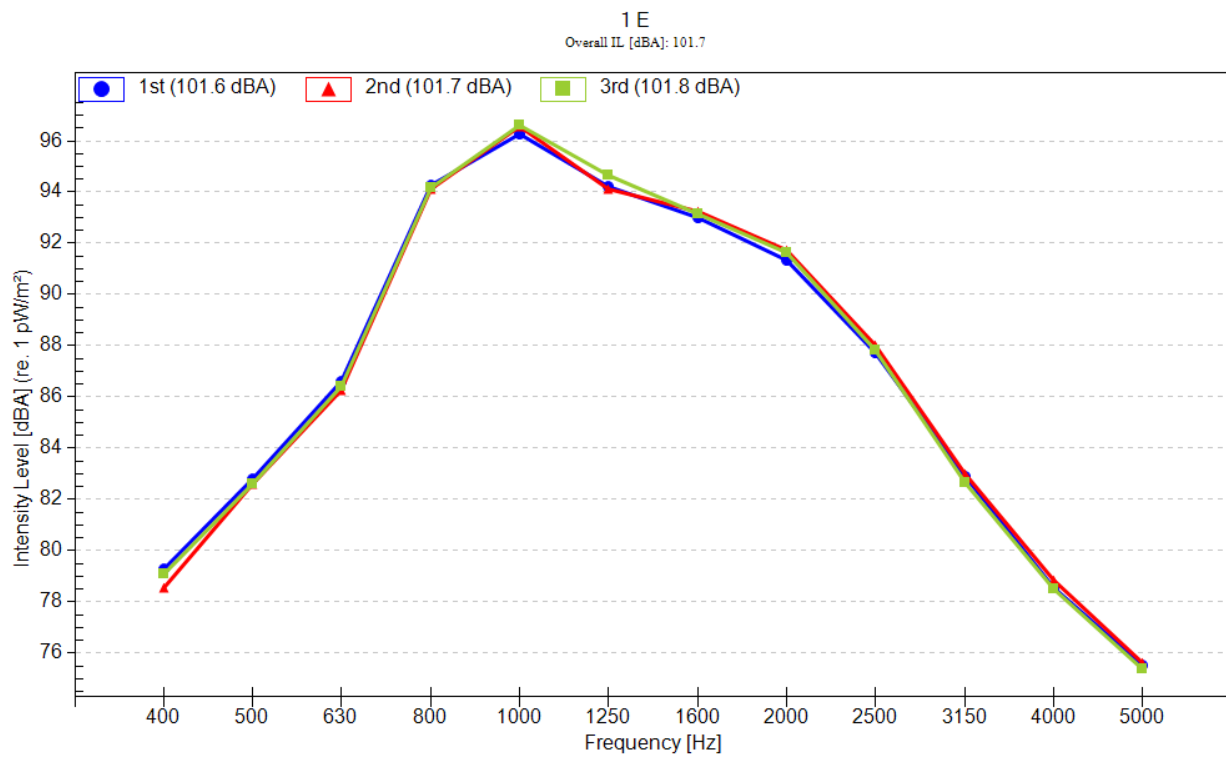
State Route 199, west of Williamsburg (AR-PFC 9.5) 2 E

| Freq. [Hz] | 1st - Intensity Level [dBA] (re. 1 pW/m²) | 2nd - Intensity Level [dBA] (re. 1 pW/m²) | 3rd - Intensity Level [dBA] (re. 1 pW/m²) | Average Intensity Level [dBA] (re. 1 pW/m²) |
|---|---|---|---|---|
| 400 | 81.8 | 81.8 | 81.7 | 81.8 |
| 500 | 88.2 | 88.5 | 88.3 | 88.3 |
| 630 | 90.5 | 91.5 | 91.4 | 91.1 |
| 800 | 93.6 | 94.2 | 94.2 | 94 |
| 1000 | 91.5 | 92.1 | 92.1 | 91.9 |
| 1250 | 87.3 | 87.3 | 86.9 | 87.2 |
| 1600 | 85 | 85.2 | 85 | 85.1 |
| 2000 | 85.1 | 85.7 | 85.6 | 85.5 |
| 2500 | 82.5 | 82.9 | 83.1 | 82.8 |
| 3150 | 79.3 | 79.5 | 79.3 | 79.4 |
| 4000 | 74.7 | 75 | 74.8 | 74.9 |
| 5000 | 71.3 | 71.7 | 71.4 | 71.5 |
| Overall IL [dBA] | 98.5 | 99.1 | 99 | 98.9 |



2 E
Overall IL [dBA]: 98.9

State Route 199, west of Williamsburg (PFC 9.5) 3 E

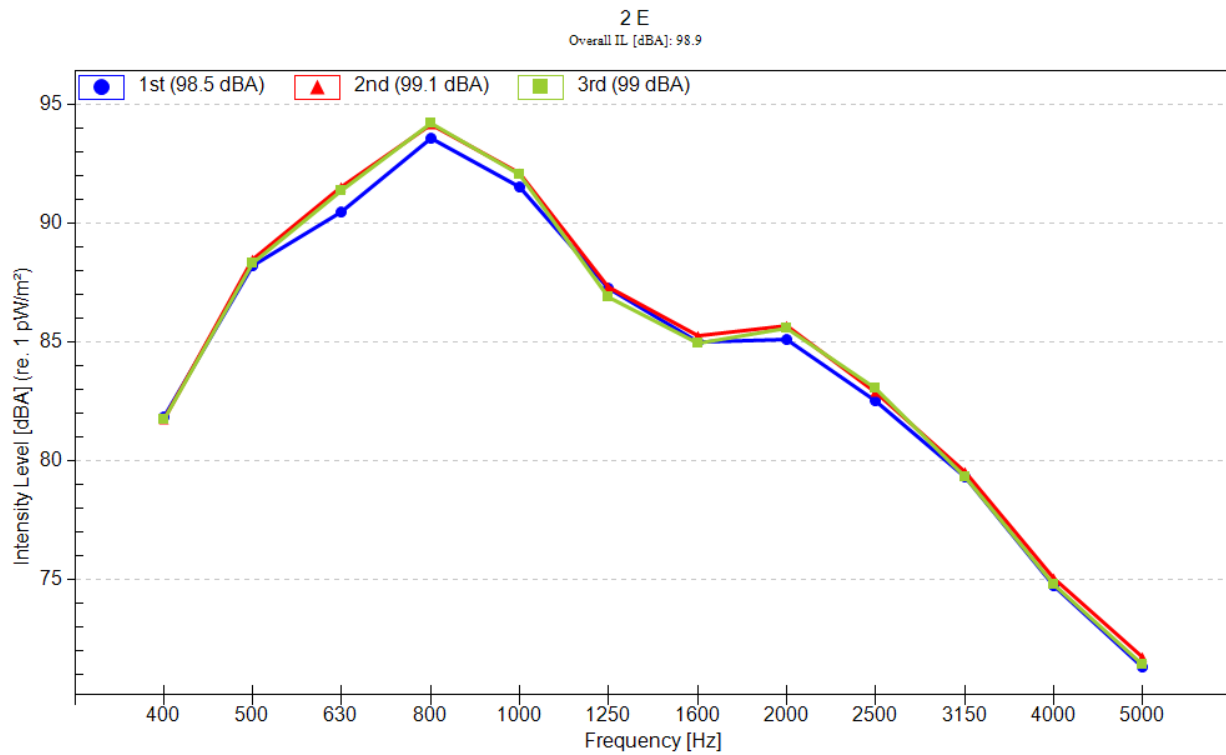| Freq. [Hz] | 1st - Intensity Level [dBA] (re. 1 pW/m²) | 2nd - Intensity Level [dBA] (re. 1 pW/m²) | Average Intensity Level [dBA] (re. 1 pW/m²) |
|---|---|---|---|
| 400 | 84.1 | 84.5 | 84.3 |
| 500 | 89.9 | 90.8 | 90.4 |
| 630 | 94.2 | 95.1 | 94.6 |
| 800 | 98.1 | 98.8 | 98.5 |
| 1000 | 97.3 | 97.8 | 97.6 |
| 1250 | 93.5 | 93.8 | 93.6 |
| 1600 | 86.8 | 87.4 | 87.1 |
| 2000 | 81.9 | 82.7 | 82.3 |
| 2500 | 78.8 | 77.9 | 78.4 |
| 3150 | 77.8 | 76.2 | 77 |
| 4000 | 74.4 | 73.3 | 73.9 |
| 5000 | 71.1 | 70.5 | 70.8 |
| Overall IL [dBA] | 102.7 | 103.4 | 103 |



3 E
Overall IL [dBA]: 103

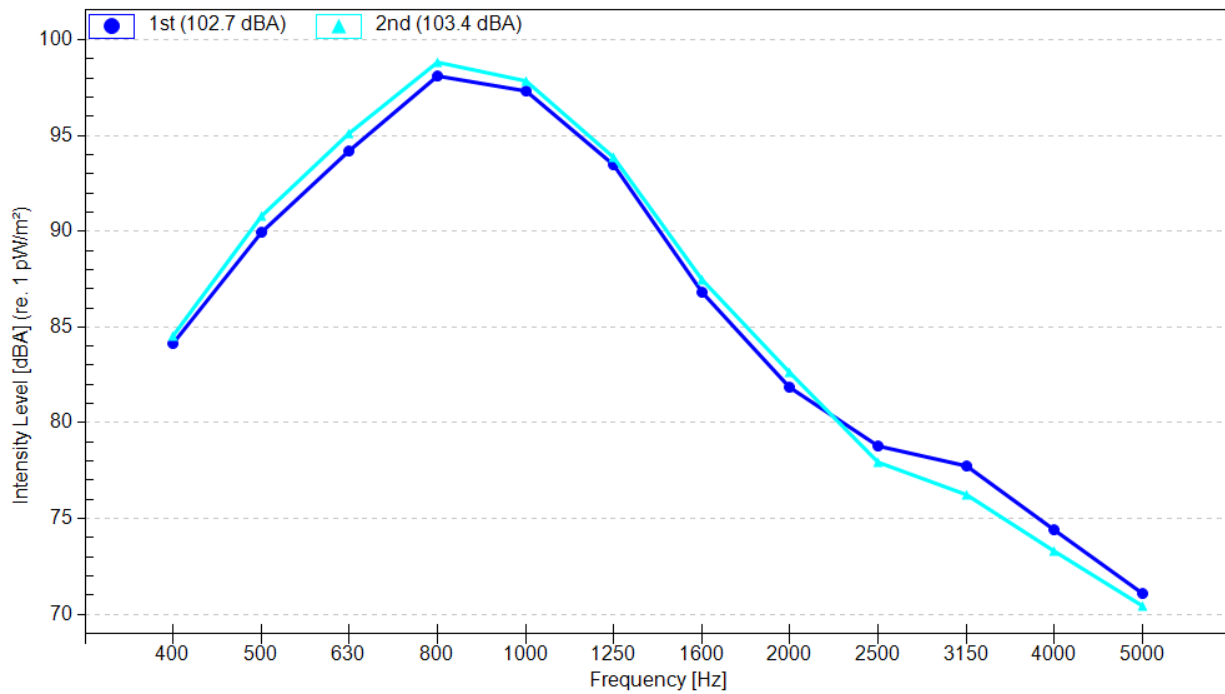State Route 199, west of Williamsburg (PFC 12.5) 4 E

| Freq. [Hz] | 1st - Intensity Level [dBA] (re. 1 pW/m²) | 2nd - Intensity Level [dBA] (re. 1 pW/m²) | 3rd - Intensity Level [dBA] (re. 1 pW/m²) | Average Intensity Level [dBA] (re. 1 pW/m²) |
|---|---|---|---|---|
| 400 | 82.9 | 83.3 | 83.4 | 83.2 |
| 500 | 89.9 | 89.4 | 90.7 | 90 |
| 630 | 94.8 | 94.3 | 95.2 | 94.7 |
| 800 | 98.7 | 98.7 | 98.5 | 98.6 |
| 1000 | 97 | 97.7 | 96.6 | 97.1 |
| 1250 | 92.6 | 93.6 | 91.6 | 92.6 |
| 1600 | 88.1 | 88.6 | 86.8 | 87.8 |
| 2000 | 85.8 | 86.3 | 85.4 | 85.9 |
| 2500 | 82.8 | 83 | 82.9 | 82.9 |
| 3150 | 79.5 | 79.7 | 79.3 | 79.5 |
| 4000 | 74.9 | 75.2 | 74.6 | 74.9 |
| 5000 | 71.9 | 72.1 | 71.4 | 71.8 |
| Overall IL [dBA] | 102.9 | 103.2 | 102.8 | 103 |



4 E
Overall IL [dBA]: 103
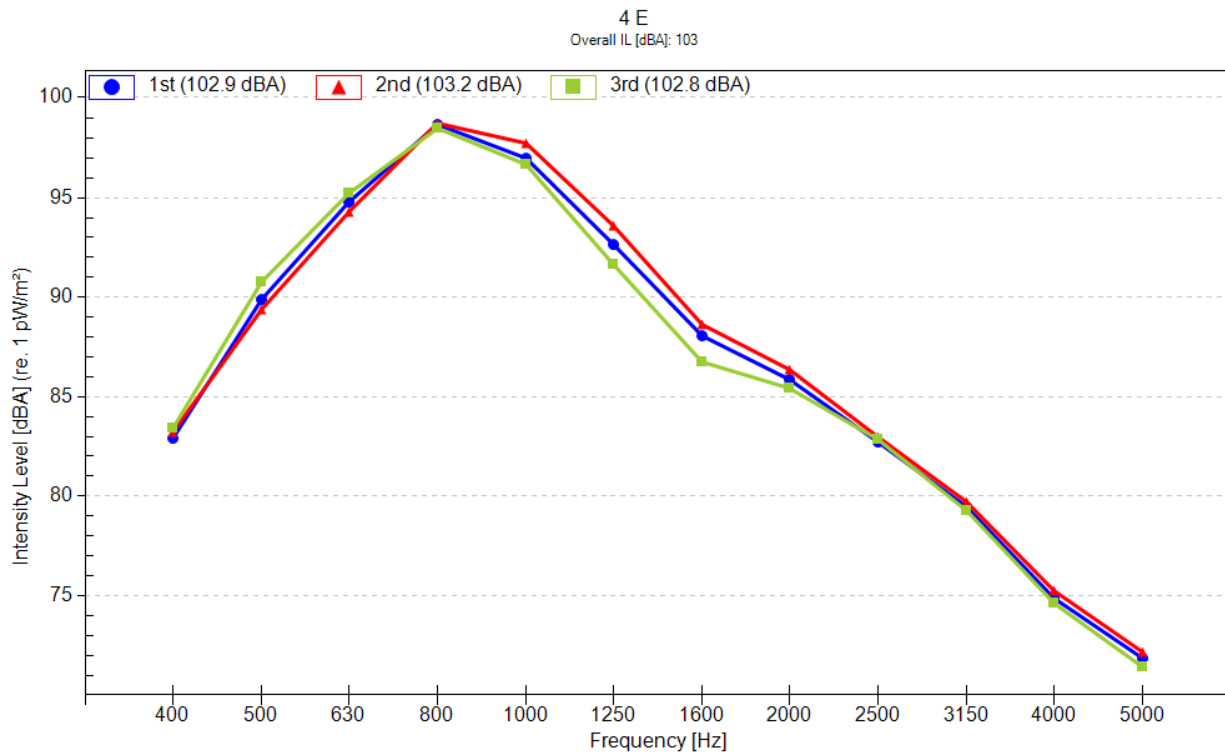
State Route 199, west of Williamsburg (SMA 9.5) 1 W

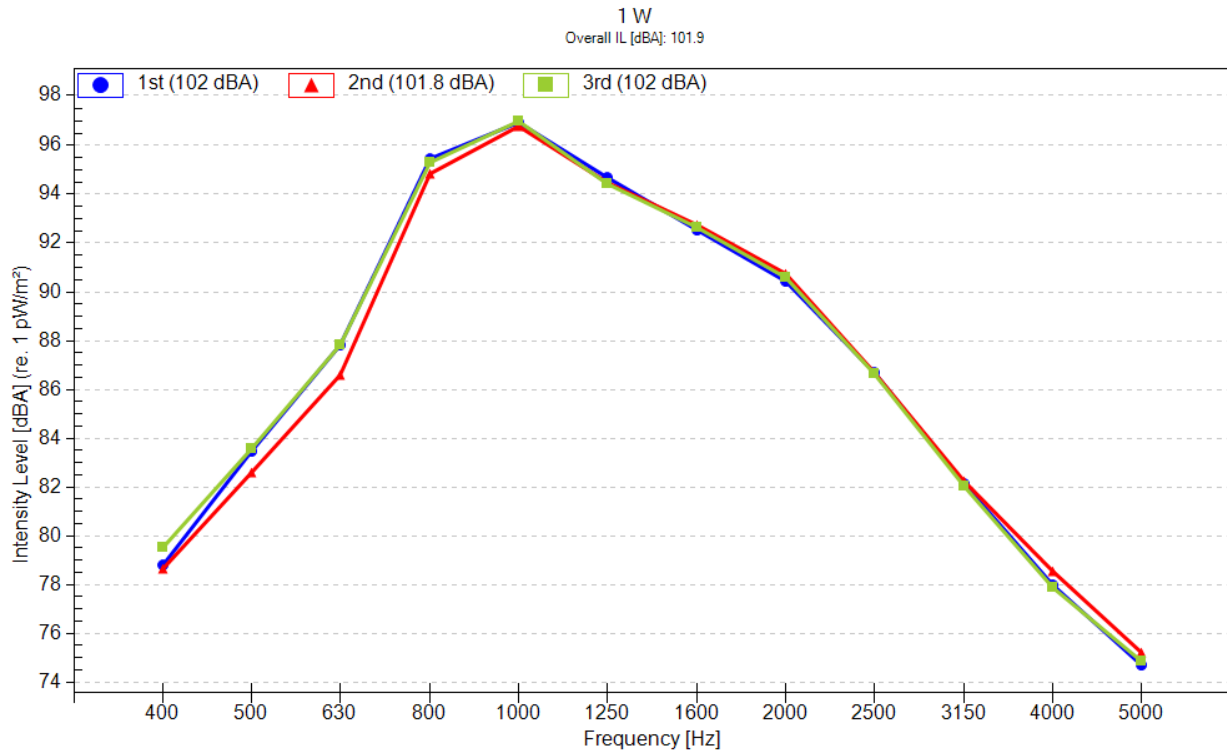| Freq. [Hz] | 1st - Intensity Level [dBA] (re. 1 pW/m²) | 2nd - Intensity Level [dBA] (re. 1 pW/m²) | 3rd - Intensity Level [dBA] (re. 1 pW/m²) | Average Intensity Level [dBA] (re. 1 pW/m²) |
|---|---|---|---|---|
| 400 | 78.8 | 78.7 | 79.5 | 79 |
| 500 | 83.4 | 82.6 | 83.6 | 83.2 |
| 630 | 87.8 | 86.6 | 87.8 | 87.4 |
| 800 | 95.4 | 94.8 | 95.3 | 95.2 |
| 1000 | 96.9 | 96.8 | 97 | 96.9 |
| 1250 | 94.7 | 94.5 | 94.4 | 94.5 |
| 1600 | 92.5 | 92.7 | 92.6 | 92.6 |
| 2000 | 90.4 | 90.8 | 90.6 | 90.6 |
| 2500 | 86.7 | 86.7 | 86.7 | 86.7 |
| 3150 | 82.1 | 82.2 | 82 | 82.1 |
| 4000 | 78 | 78.5 | 77.9 | 78.1 |
| 5000 | 74.7 | 75.2 | 74.9 | 74.9 |
| Overall IL [dBA] | 102 | 101.8 | 102 | 101.9 |



1 W
Overall IL [dBA]: 101.9

State Route 199, west of Williamsburg (AR-PFC - 9.5) 2 W

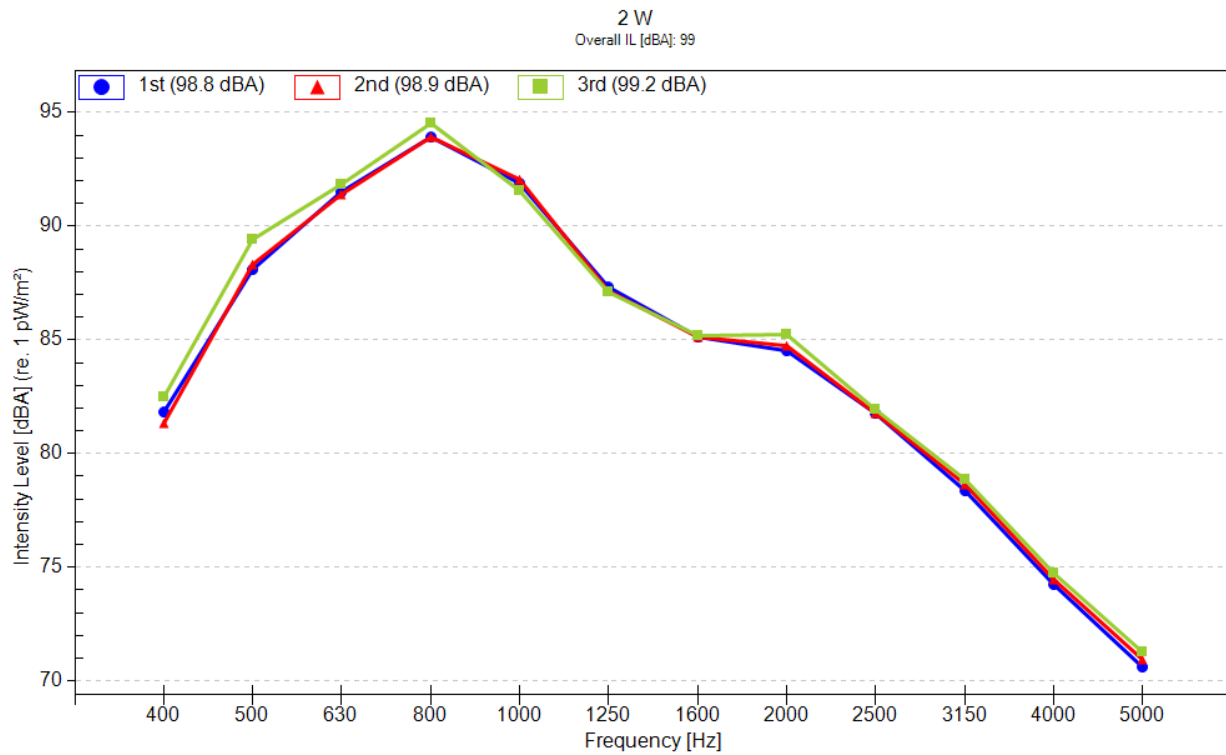| Freq. [Hz] | 1st - Intensity Level [dBA] (re. 1 pW/m²) | 2nd - Intensity Level [dBA] (re. 1 pW/m²) | 3rd - Intensity Level [dBA] (re. 1 pW/m²) | Average Intensity Level [dBA] (re. 1 pW/m²) |
|---|---|---|---|---|
| 400 | 81.8 | 81.4 | 82.5 | 81.9 |
| 500 | 88.1 | 88.3 | 89.4 | 88.6 |
| 630 | 91.5 | 91.4 | 91.8 | 91.6 |
| 800 | 93.9 | 93.9 | 94.5 | 94.1 |
| 1000 | 91.9 | 92.1 | 91.5 | 91.8 |
| 1250 | 87.3 | 87.2 | 87.1 | 87.2 |
| 1600 | 85.1 | 85.1 | 85.2 | 85.1 |
| 2000 | 84.5 | 84.8 | 85.2 | 84.8 |
| 2500 | 81.8 | 81.8 | 82 | 81.8 |
| 3150 | 78.4 | 78.6 | 78.9 | 78.6 |
| 4000 | 74.2 | 74.4 | 74.7 | 74.5 |
| 5000 | 70.6 | 70.9 | 71.2 | 70.9 |
| Overall IL [dBA] | 98.8 | 98.9 | 99.2 | 99 |

State Route 199, west of Williamsburg (PFC 9.5) 3 W

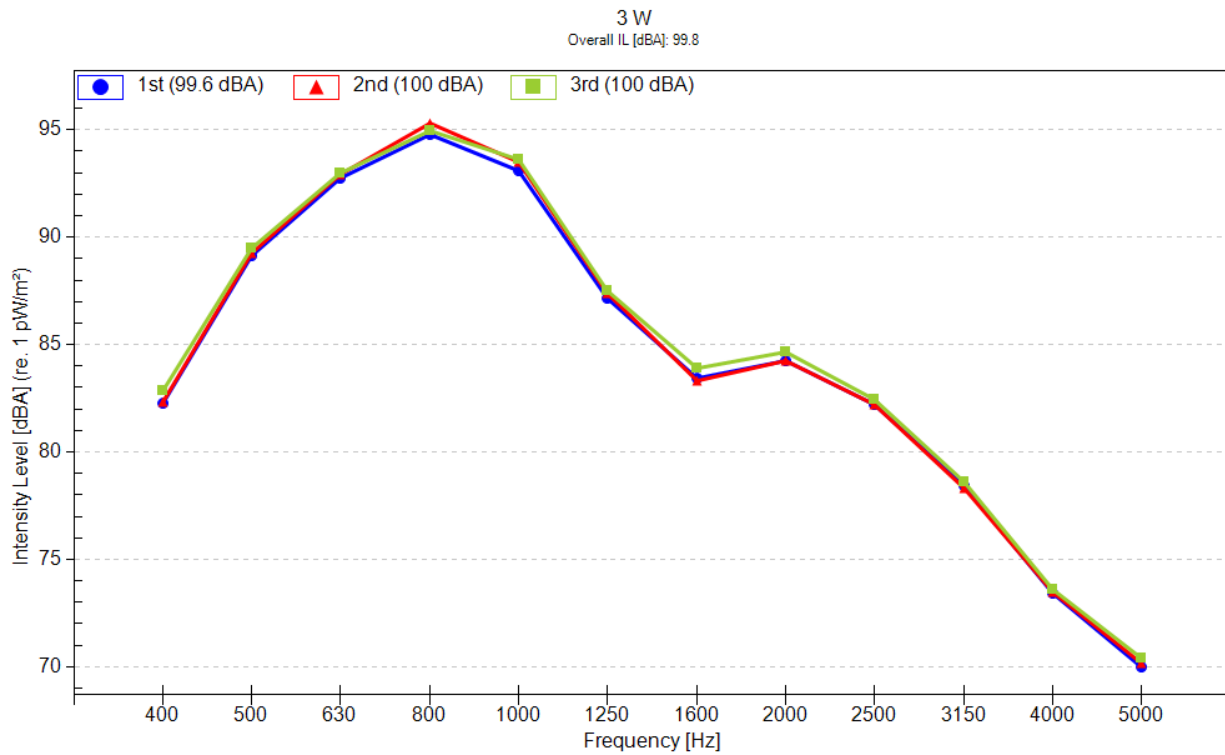| Freq. [Hz] | 1st - Intensity Level [dBA] (re. 1 pW/m²) | 2nd - Intensity Level [dBA] (re. 1 pW/m²) | 3rd - Intensity Level [dBA] (re. 1 pW/m²) | Average Intensity Level [dBA] (re. 1 pW/m²) |
|---|---|---|---|---|
| 400 | 82.3 | 82.3 | 82.8 | 82.5 |
| 500 | 89.1 | 89.3 | 89.5 | 89.3 |
| 630 | 92.8 | 92.9 | 93 | 92.9 |
| 800 | 94.8 | 95.3 | 94.9 | 95 |
| 1000 | 93.1 | 93.5 | 93.6 | 93.4 |
| 1250 | 87.2 | 87.4 | 87.5 | 87.4 |
| 1600 | 83.4 | 83.3 | 83.9 | 83.6 |
| 2000 | 84.2 | 84.2 | 84.6 | 84.4 |
| 2500 | 82.2 | 82.2 | 82.4 | 82.3 |
| 3150 | 78.4 | 78.3 | 78.6 | 78.4 |
| 4000 | 73.4 | 73.5 | 73.6 | 73.5 |
| 5000 | 70 | 70.1 | 70.4 | 70.2 |
| Overall IL [dBA] | 99.6 | 100 | 100 | 99.8 |

3 W
Overall IL [dBA]: 99.8

State Route 199, west of Williamsburg (PFC 12.5) 4 W

| Freq. [Hz] | 1st - Intensity Level [dBA] (re. 1 pW/m²) | 2nd - Intensity Level [dBA] (re. 1 pW/m²) | 3rd - Intensity Level [dBA] (re. 1 pW/m²) | Average Intensity Level [dBA] (re. 1 pW/m²) |
|---|---|---|---|---|
| 400 | 84.4 | 83.5 | 84.1 | 84 |
| 500 | 92.2 | 90.3 | 91.4 | 91.3 |
| 630 | 94.3 | 92.7 | 93.8 | 93.6 |
| 800 | 95.6 | 94.9 | 95.4 | 95.3 |
| 1000 | 93.7 | 92.6 | 93.3 | 93.2 |
| 1250 | 89.3 | 89.7 | 89.1 | 89.3 |
| 1600 | 86.7 | 87.3 | 86.6 | 86.9 |
| 2000 | 86.1 | 86.8 | 86.2 | 86.4 |
| 2500 | 83.2 | 83.4 | 83.2 | 83.2 |
| 3150 | 79.8 | 80 | 79.7 | 79.8 |
| 4000 | 75.5 | 75.8 | 75.5 | 75.6 |
| 5000 | 71.9 | 72.4 | 72.1 | 72.1 |
| Overall IL [dBA] | 101 | 100.1 | 100.7 | 100.6 |



4 W
Overall IL [dBA]: 100.6
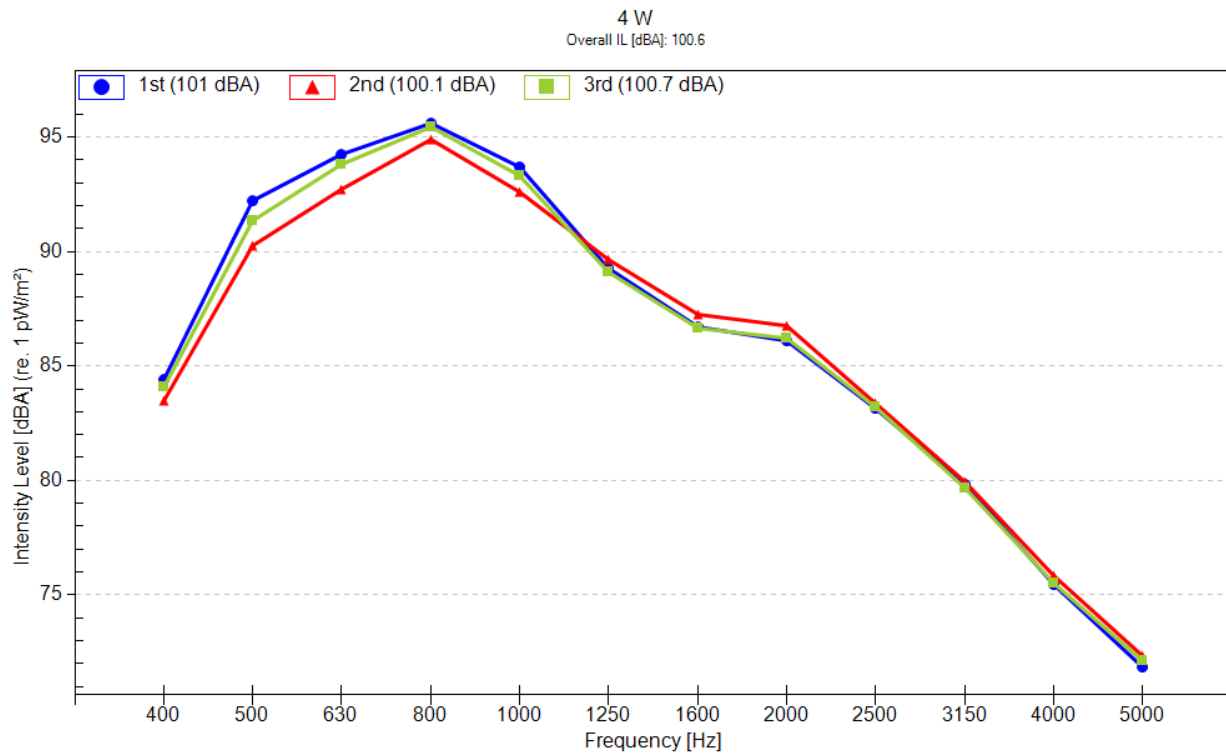
State Route 288 Summary Average Overall IL Measured & Normalized for temperature (dBA)
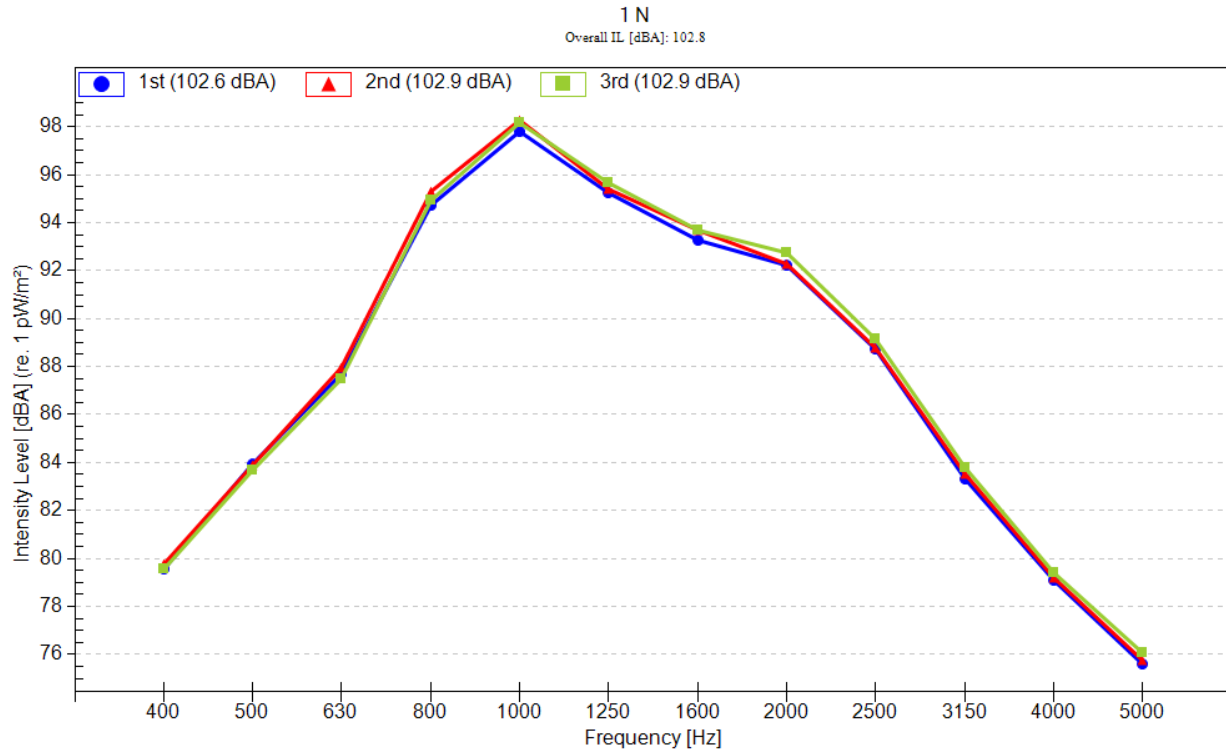
State Route 288, near Chester (SMA 9.5) 1 N

| Freq. [Hz] | 1st - Intensity Level [dBA] (re. 1 pW/m²) | 2nd - Intensity Level [dBA] (re. 1 pW/m²) | 3rd - Intensity Level [dBA] (re. 1 pW/m²) | Average Intensity Level [dBA] (re. 1 pW/m²) |
|---|---|---|---|---|
| 400 | 79.5 | 79.8 | 79.5 | 79.6 |
| 500 | 84 | 83.9 | 83.7 | 83.8 |
| 630 | 87.7 | 88 | 87.5 | 87.7 |
| 800 | 94.7 | 95.3 | 94.9 | 95 |
| 1000 | 97.8 | 98.3 | 98.2 | 98.1 |
| 1250 | 95.3 | 95.4 | 95.7 | 95.4 |
| 1600 | 93.3 | 93.7 | 93.7 | 93.6 |
| 2000 | 92.2 | 92.3 | 92.7 | 92.4 |
| 2500 | 88.7 | 88.8 | 89.1 | 88.9 |
| 3150 | 83.3 | 83.5 | 83.8 | 83.6 |
| 4000 | 79.1 | 79.2 | 79.4 | 79.2 |
| 5000 | 75.6 | 75.7 | 76.1 | 75.8 |
| Overall IL [dBA] | 102.6 | 102.9 | 102.9 | 102.8 |

1 N
Overall IL [dBA]: 102.8

State Route 288, near Chester (AR – PFC 9.5) 2 N

| Freq. [Hz] | 1st - Intensity Level [dBA] (re. 1 pW/m²) | 2nd - Intensity Level [dBA] (re. 1 pW/m²) | Average Intensity Level [dBA] (re. 1 pW/m²) |
|---|---|---|---|
| 400 | 82.9 | 82.6 | 82.7 |
| 500 | 90 | 90 | 90 |
| 630 | 93.2 | 93.1 | 93.2 |
| 800 | 96 | 95.8 | 95.9 |
| 1000 | 94.3 | 93.6 | 93.9 |
| 1250 | 87.7 | 87.5 | 87.6 |
| 1600 | 81.7 | 81.8 | 81.8 |
| 2000 | 83.7 | 83.8 | 83.7 |
| 2500 | 82.7 | 82.6 | 82.7 |
| 3150 | 79.4 | 79.3 | 79.4 |
| 4000 | 74.1 | 74 | 74.1 |
| 5000 | 70.1 | 69.9 | 70 |
| Overall IL [dBA] | 100.5 | 100.2 | 100.4 |



2 N
Overall IL [dBA]: 100.4

State Route 288, near Chester (PFC 9.5) 3 N

| Freq. [Hz] | 1st - Intensity Level [dBA] (re. 1 pW/m²) | 2nd - Intensity Level [dBA] (re. 1 pW/m²) | Average Intensity Level [dBA] (re. 1 pW/m²) |
|---|---|---|---|
| 400 | 82 | 82.5 | 82.3 |
| 500 | 88.8 | 88.3 | 88.6 |
| 630 | 92.6 | 92.7 | 92.6 |
| 800 | 96.6 | 96.9 | 96.8 |
| 1000 | 95.4 | 96 | 95.7 |
| 1250 | 91.1 | 91.5 | 91.3 |
| 1600 | 83.8 | 84.6 | 84.2 |
| 2000 | 82.5 | 82.1 | 82.3 |
| 2500 | 81.7 | 81.2 | 81.5 |
| 3150 | 79.8 | 79.5 | 79.7 |
| 4000 | 75.4 | 75.4 | 75.4 |
| 5000 | 71.3 | 71.2 | 71.2 |
| Overall IL [dBA] | 101.1 | 101.4 | 101.2 |



3 N
Overall IL [dBA]: 101.2

State Route 288, near Chester (PFC 12.5) 4 N

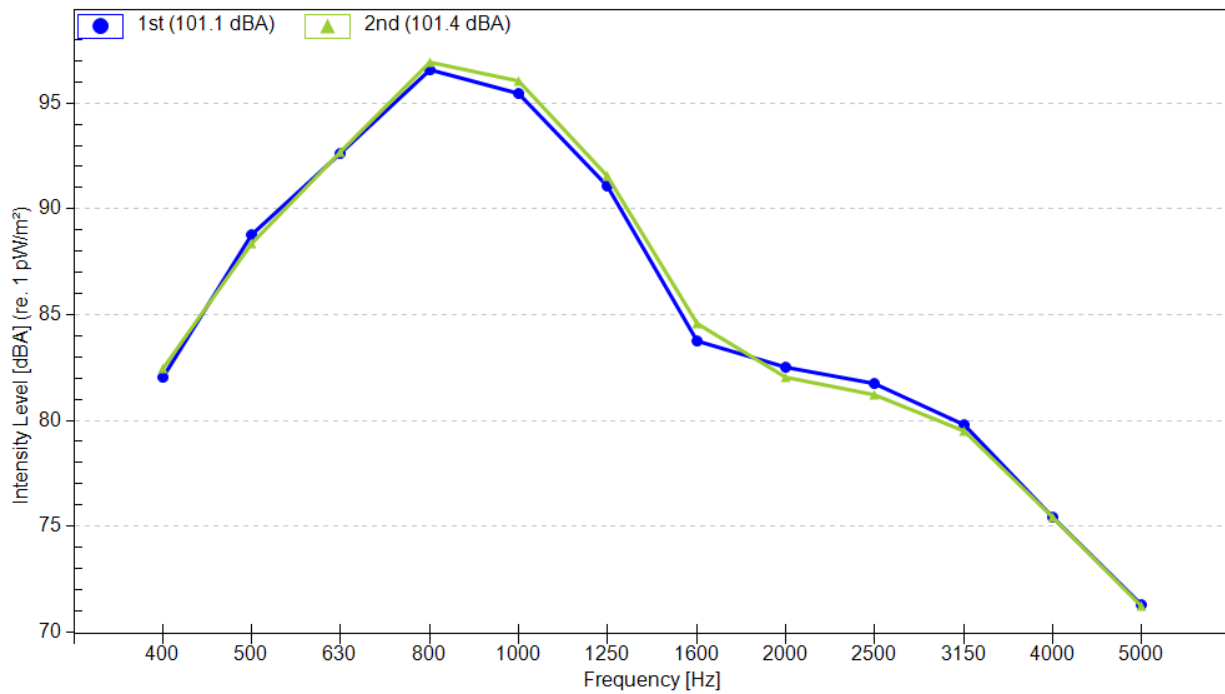| Freq. [Hz] | 1st - Intensity Level [dBA] (re. 1 pW/m²) | 2nd - Intensity Level [dBA] (re. 1 pW/m²) | Average Intensity Level [dBA] (re. 1 pW/m²) |
|---|---|---|---|
| 400 | 83.8 | 83.6 | 83.7 |
| 500 | 90.5 | 90.4 | 90.5 |
| 630 | 93.7 | 93.4 | 93.5 |
| 800 | 96.2 | 96.1 | 96.2 |
| 1000 | 93.3 | 92.9 | 93.1 |
| 1250 | 87.2 | 88.4 | 87.8 |
| 1600 | 85.9 | 87.3 | 86.6 |
| 2000 | 87 | 87.5 | 87.3 |
| 2500 | 84.6 | 84.6 | 84.6 |
| 3150 | 80.3 | 80.3 | 80.3 |
| 4000 | 75.4 | 75.7 | 75.5 |
| 5000 | 72 | 72.1 | 72.1 |
| Overall IL [dBA] | 100.8 | 100.7 | 100.7 |



4 N
Overall IL [dBA]: 100.7

State Route 288, near Chester (SMA 9.5) 1 S

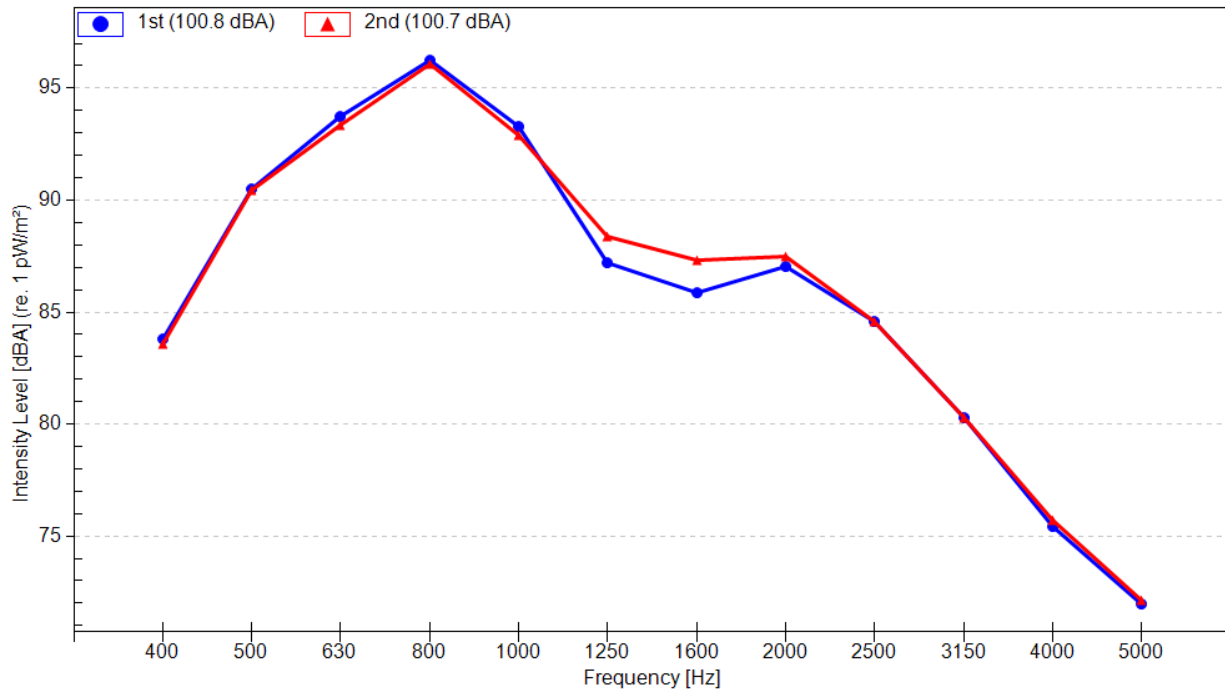| Freq. [Hz] | 1st - Intensity Level [dBA] (re. 1 pW/m²) | 2nd - Intensity Level [dBA] (re. 1 pW/m²) | 3rd - Intensity Level [dBA] (re. 1 pW/m²) | Average Intensity Level [dBA] (re. 1 pW/m²) |
|---|---|---|---|---|
| 400 | 79.6 | 78.7 | 78.7 | 79 |
| 500 | 82.1 | 82.3 | 82.3 | 82.2 |
| 630 | 85.4 | 85.4 | 85.6 | 85.5 |
| 800 | 92.8 | 93 | 93.2 | 93 |
| 1000 | 97.9 | 98.3 | 98.5 | 98.2 |
| 1250 | 95 | 95.1 | 95.2 | 95.1 |
| 1600 | 93 | 93 | 93.4 | 93.2 |
| 2000 | 92.4 | 92.8 | 93 | 92.8 |
| 2500 | 89 | 89.1 | 89.6 | 89.2 |
| 3150 | 83.5 | 83.8 | 84 | 83.8 |
| 4000 | 79.2 | 79.6 | 79.7 | 79.5 |
| 5000 | 75.6 | 76 | 76.3 | 76 |
| Overall IL [dBA] | 102.2 | 102.5 | 102.7 | 102.5 |



1 S
Overall IL [dBA]: 102.5
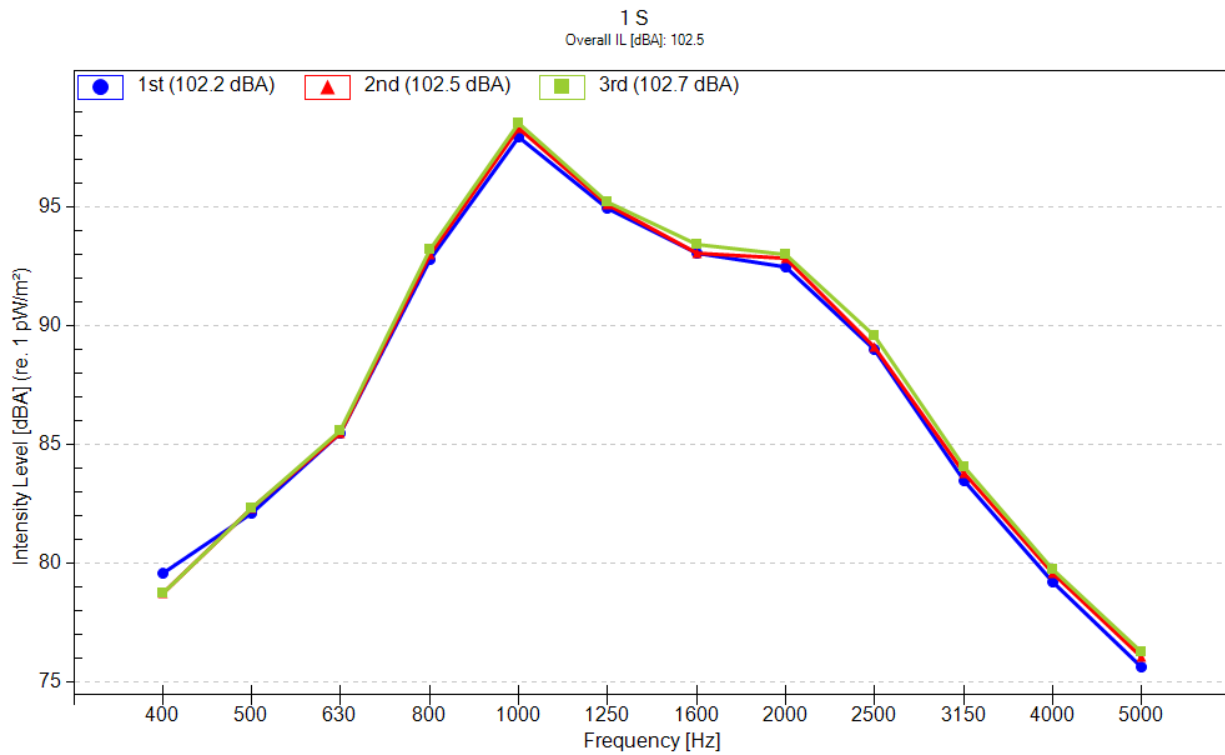
114

State Route 288, near Chester (AR – PFC 9.5) 2 S

| Freq. [Hz] | 1st - Intensity Level [dBA] (re. 1 pW/m²) | 2nd - Intensity Level [dBA] (re. 1 pW/m²) | Average Intensity Level [dBA] (re. 1 pW/m²) |
|---|---|---|---|
| 400 | 84.7 | 84.4 | 84.5 |
| 500 | 91.1 | 91 | 91.1 |
| 630 | 93.5 | 94 | 93.8 |
| 800 | 95.9 | 96.2 | 96 |
| 1000 | 93.8 | 94.1 | 93.9 |
| 1250 | 87.1 | 87.5 | 87.3 |
| 1600 | 81.8 | 81.5 | 81.6 |
| 2000 | 83.4 | 83 | 83.2 |
| 2500 | 82.2 | 82.1 | 82.2 |
| 3150 | 79 | 79.3 | 79.2 |
| 4000 | 73.7 | 74.1 | 73.9 |
| 5000 | 69.7 | 69.8 | 69.7 |
| Overall IL [dBA] | 100.5 | 100.8 | 100.7 |

2 S
Overall IL [dBA]: 100.7

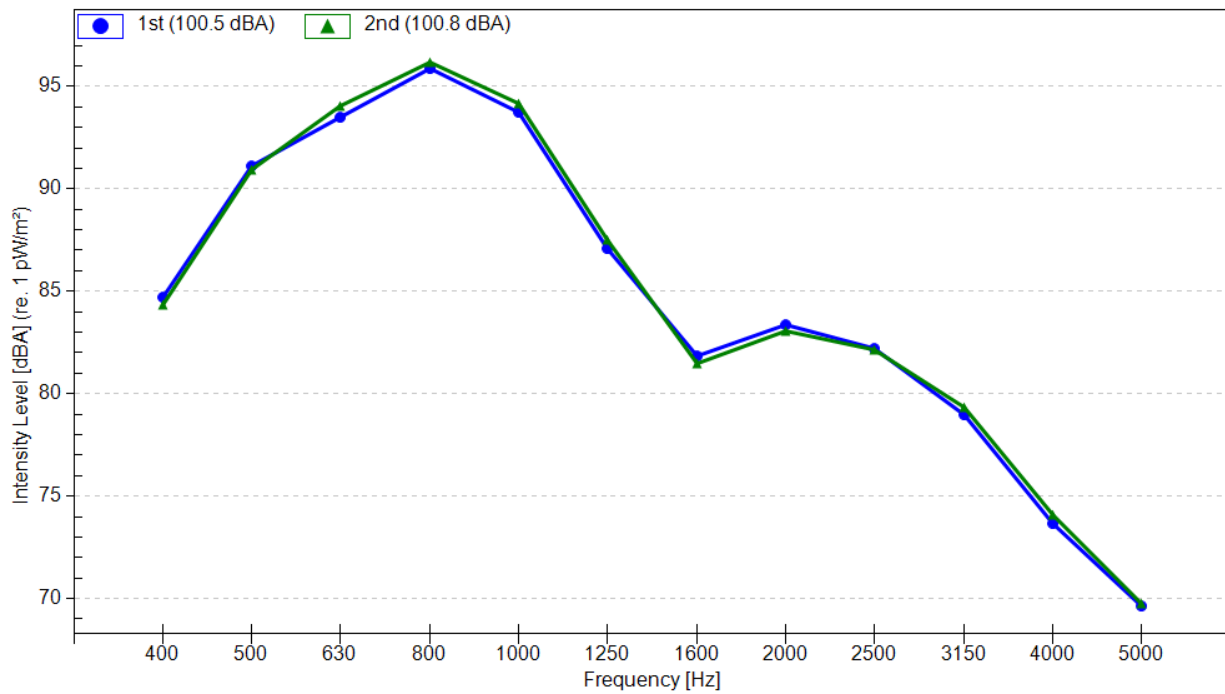State Route 288, near Chester (PFC 9.5) 3 S

| Freq. [Hz] | 1st - Intensity Level [dBA] (re. 1 pW/m²) | 2nd - Intensity Level [dBA] (re. 1 pW/m²) | 3rd - Intensity Level [dBA] (re. 1 pW/m²) | Average Intensity Level [dBA] (re. 1 pW/m²) |
|---|---|---|---|---|
| 400 | 82.7 | 82.8 | 82.7 | 82.7 |
| 500 | 88.8 | 88.9 | 88.8 | 88.8 |
| 630 | 93.7 | 92.4 | 93.4 | 93.2 |
| 800 | 97.6 | 96.8 | 97.2 | 97.2 |
| 1000 | 96.5 | 95.9 | 96.5 | 96.3 |
| 1250 | 92.6 | 91.8 | 92 | 92.1 |
| 1600 | 85.3 | 85.1 | 84.8 | 85.1 |
| 2000 | 82.1 | 81.7 | 81.8 | 81.9 |
| 2500 | 81.2 | 79.9 | 81.3 | 80.8 |
| 3150 | 79.4 | 78.3 | 79.4 | 79.1 |
| 4000 | 75.2 | 74.4 | 75.1 | 74.9 |
| 5000 | 71.4 | 70.4 | 71 | 71 |
| Overall IL [dBA] | 102 | 101.3 | 101.8 | 101.7 |

3 S
Overall IL [dBA]: 101.7



116

State Route 288, near Chester (PFC 12.5) 4 S

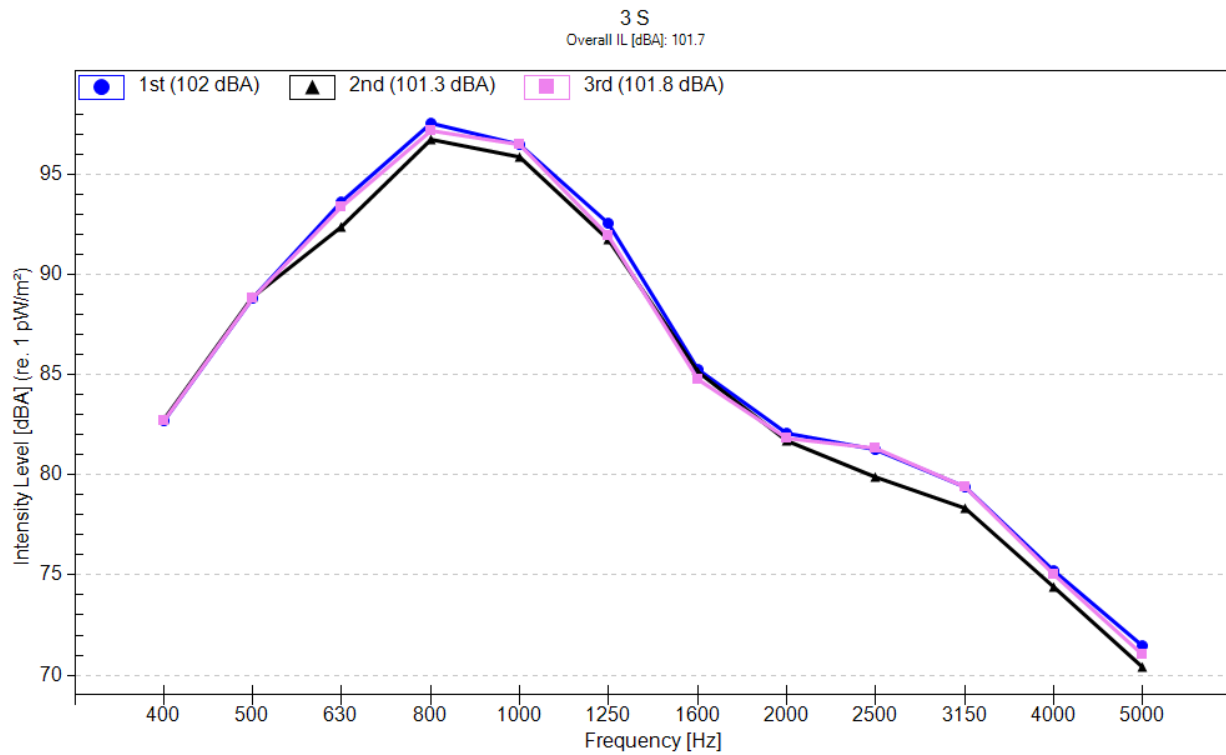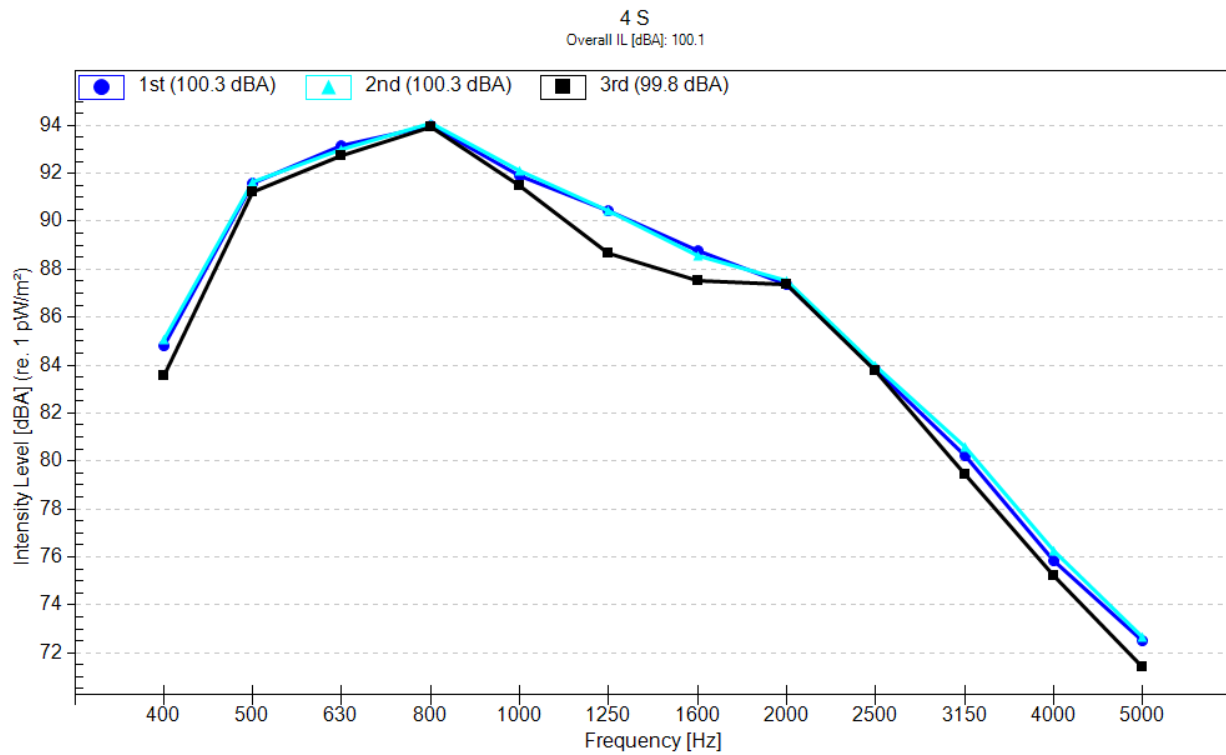| Freq. [Hz] | 1st - Intensity Level [dBA] (re. 1 pW/m²) | 2nd - Intensity Level [dBA] (re. 1 pW/m²) | 3rd - Intensity Level [dBA] (re. 1 pW/m²) | Average Intensity Level [dBA] (re. 1 pW/m²) |
|---|---|---|---|---|
| 400 | 84.8 | 85.1 | 83.6 | 84.5 |
| 500 | 91.6 | 91.6 | 91.2 | 91.5 |
| 630 | 93.2 | 93 | 92.7 | 93 |
| 800 | 94 | 94.1 | 93.9 | 94 |
| 1000 | 91.9 | 92.1 | 91.5 | 91.8 |
| 1250 | 90.4 | 90.4 | 88.7 | 89.9 |
| 1600 | 88.8 | 88.6 | 87.5 | 88.3 |
| 2000 | 87.4 | 87.5 | 87.4 | 87.4 |
| 2500 | 83.8 | 84 | 83.8 | 83.9 |
| 3150 | 80.2 | 80.6 | 79.4 | 80.1 |
| 4000 | 75.8 | 76.3 | 75.2 | 75.8 |
| 5000 | 72.5 | 72.7 | 71.4 | 72.2 |
| Overall IL [dBA] | 100.3 | 100.3 | 99.8 | 100.1 |



4 S
Overall IL [dBA]: 100.1

State Route 286 Summary Average Overall IL Measured & Normalized for temperature (dBA)

State Route 286, near Fairfax (SMA 12.5) 1 N

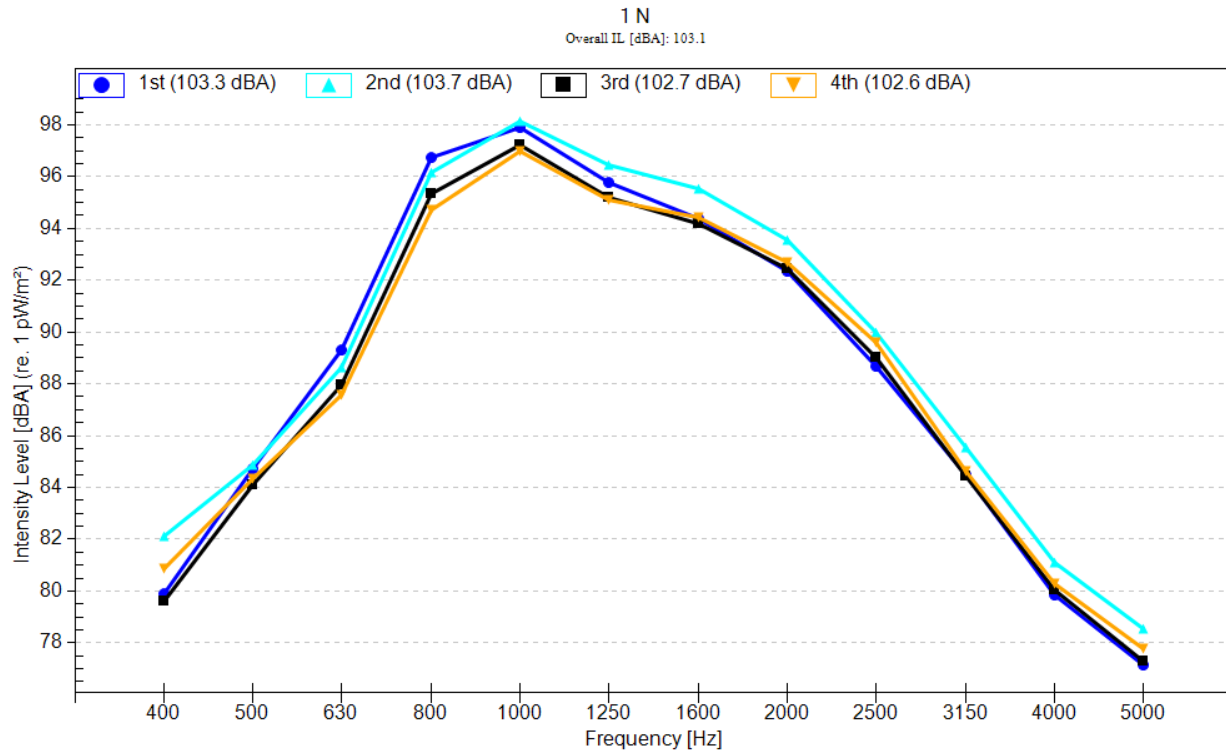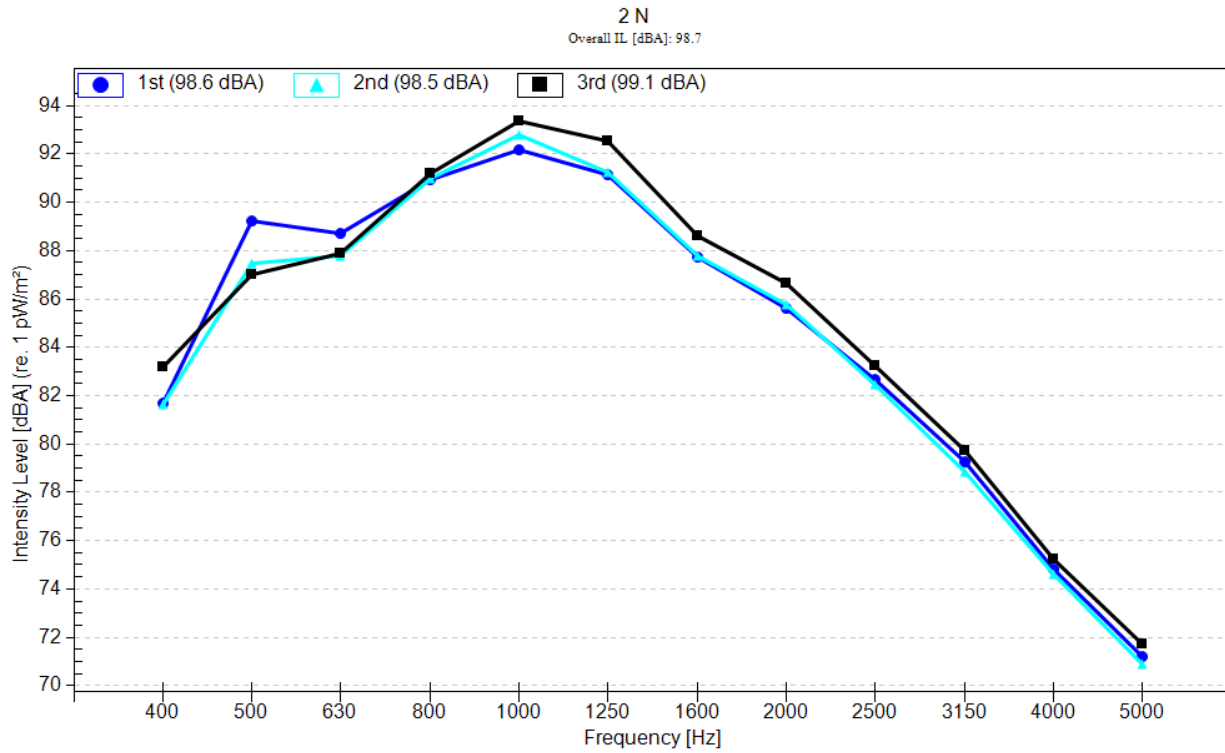| Freq. [Hz] | 1st - Intensity Level [dBA] (re. 1 pW/m²) | 2nd - Intensity Level [dBA] (re. 1 pW/m²) | 3rd - Intensity Level [dBA] (re. 1 pW/m²) | 4th - Intensity Level [dBA] (re. 1 pW/m²) | Average Intensity Level [dBA] (re. 1 pW/m²) |
|---|---|---|---|---|---|
| 400 | 79.9 | 82.1 | 79.6 | 80.8 | 80.6 |
| 500 | 84.7 | 84.9 | 84.1 | 84.3 | 84.5 |
| 630 | 89.3 | 88.6 | 87.9 | 87.6 | 88.4 |
| 800 | 96.8 | 96.2 | 95.3 | 94.7 | 95.7 |
| 1000 | 97.9 | 98.1 | 97.2 | 97 | 97.6 |
| 1250 | 95.8 | 96.4 | 95.2 | 95.1 | 95.6 |
| 1600 | 94.4 | 95.5 | 94.2 | 94.4 | 94.6 |
| 2000 | 92.4 | 93.6 | 92.4 | 92.7 | 92.8 |
| 2500 | 88.7 | 90 | 89 | 89.6 | 89.3 |
| 3150 | 84.5 | 85.5 | 84.4 | 84.6 | 84.8 |
| 4000 | 79.8 | 81.1 | 80 | 80.3 | 80.3 |
| 5000 | 77.2 | 78.5 | 77.3 | 77.8 | 77.7 |
| Overall IL [dBA] | 103.3 | 103.7 | 102.7 | 102.6 | 103.1 |

1 N
Overall IL [dBA]: 103.1

State Route 286, near Fairfax (AR-PFC 12.5) 2 N

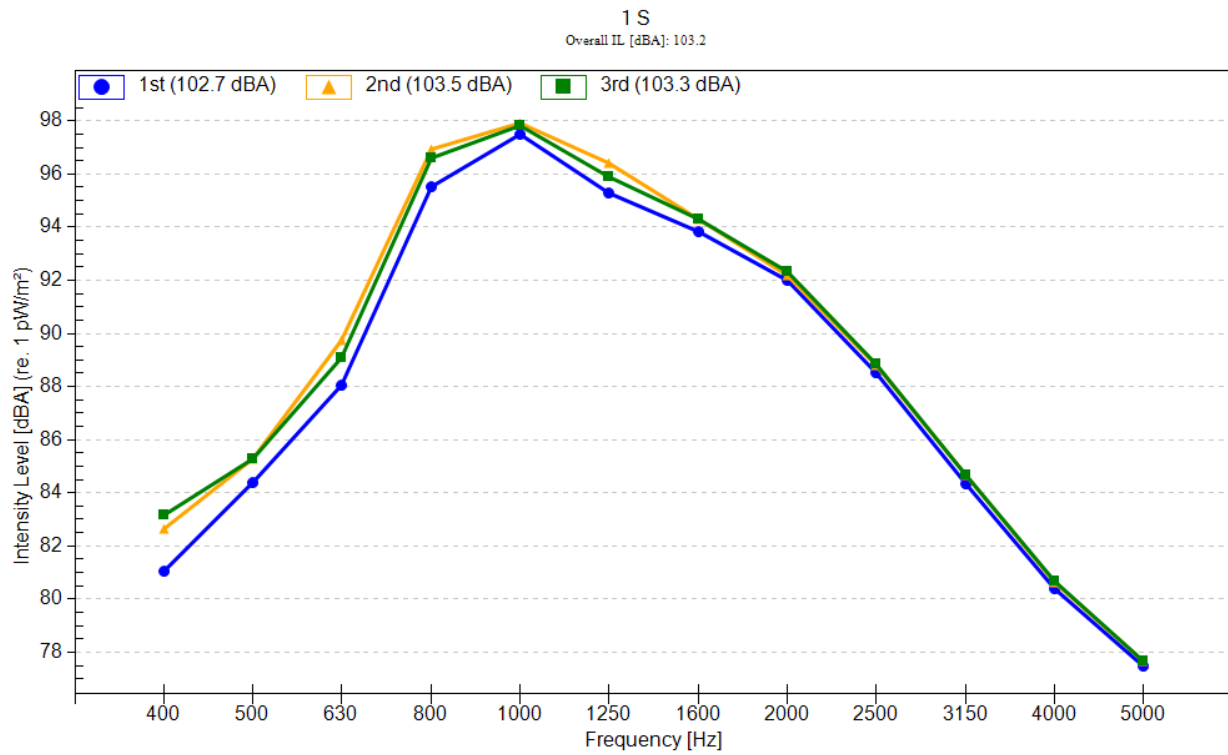| Freq. [Hz] | 1st - Intensity Level [dBA] (re. 1 pW/m²) | 2nd - Intensity Level [dBA] (re. 1 pW/m²) | 3rd - Intensity Level [dBA] (re. 1 pW/m²) | Average Intensity Level [dBA] (re. 1 pW/m²) |
|---|---|---|---|---|
| 400 | 81.7 | 81.7 | 83.2 | 82.2 |
| 500 | 89.2 | 87.4 | 87 | 87.9 |
| 630 | 88.7 | 87.8 | 87.9 | 88.1 |
| 800 | 90.9 | 91 | 91.2 | 91 |
| 1000 | 92.2 | 92.8 | 93.3 | 92.8 |
| 1250 | 91.1 | 91.3 | 92.5 | 91.6 |
| 1600 | 87.7 | 87.8 | 88.6 | 88 |
| 2000 | 85.6 | 85.7 | 86.6 | 86 |
| 2500 | 82.6 | 82.5 | 83.2 | 82.8 |
| 3150 | 79.3 | 78.9 | 79.7 | 79.3 |
| 4000 | 74.8 | 74.6 | 75.2 | 74.9 |
| 5000 | 71.2 | 70.9 | 71.7 | 71.3 |
| Overall IL [dBA] | 98.6 | 98.5 | 99.1 | 98.7 |



2 N
Overall IL [dBA]: 98.7

State Route 286, near Fairfax (SMA 12.5) 1 S

| Freq. [Hz] | 1st - Intensity Level [dBA] (re. 1 pW/m²) | 2nd - Intensity Level [dBA] (re. 1 pW/m²) | 3rd - Intensity Level [dBA] (re. 1 pW/m²) | Average Intensity Level [dBA] (re. 1 pW/m²) |
|---|---|---|---|---|
| 400 | 81 | 82.6 | 83.2 | 82.3 |
| 500 | 84.4 | 85.3 | 85.3 | 85 |
| 630 | 88 | 89.7 | 89.1 | 89 |
| 800 | 95.5 | 96.9 | 96.6 | 96.4 |
| 1000 | 97.5 | 97.9 | 97.8 | 97.7 |
| 1250 | 95.3 | 96.4 | 95.9 | 95.9 |
| 1600 | 93.8 | 94.3 | 94.3 | 94.1 |
| 2000 | 92 | 92.2 | 92.3 | 92.2 |
| 2500 | 88.5 | 88.8 | 88.9 | 88.7 |
| 3150 | 84.3 | 84.7 | 84.7 | 84.6 |
| 4000 | 80.4 | 80.6 | 80.7 | 80.6 |
| 5000 | 77.5 | 77.7 | 77.7 | 77.6 |
| Overall IL [dBA] | 102.7 | 103.5 | 103.3 | 103.2 |

1 S
Overall IL [dBA]: 103.2

State Route 286, near Fairfax (AR - PFC 12.5) 2 S

| Freq. [Hz] | 1st - Intensity Level [dBA] (re. 1 pW/m²) | 2nd - Intensity Level [dBA] (re. 1 pW/m²) | Average Intensity Level [dBA] (re. 1 pW/m²) |
|---|---|---|---|
| 400 | 82.7 | 82.8 | 82.7 |
| 500 | 88.1 | 88.5 | 88.3 |
| 630 | 87.4 | 87.7 | 87.5 |
| 800 | 88.7 | 88.9 | 88.8 |
| 1000 | 90.4 | 90.9 | 90.6 |
| 1250 | 89.4 | 90.5 | 89.9 |
| 1600 | 87.5 | 88.1 | 87.8 |
| 2000 | 85.4 | 85.9 | 85.7 |
| 2500 | 82.6 | 83 | 82.8 |
| 3150 | 79.4 | 80 | 79.7 |
| 4000 | 75 | 75.7 | 75.3 |
| 5000 | 71.6 | 72.4 | 72 |
| Overall IL [dBA] | 97.3 | 97.8 | 97.5 |

2 S
Overall IL [dBA]: 97.5
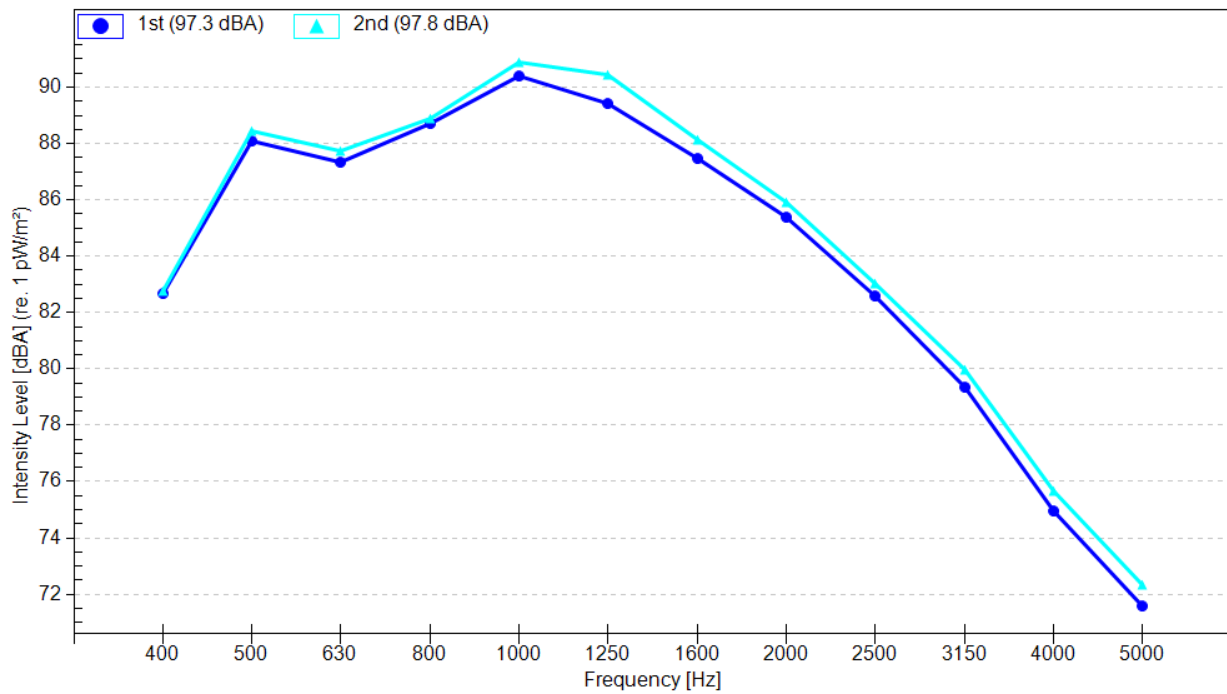
## Appendix F: Matlab Scripts for Chapter 2

```
%              CHOSING THE IDEAL DECOMPOSITION VALUE FOR SWT
% knowing that we define the stationary wavelet transform (SWT) only for
% signals of length divisible by 2^j, where j is the maximum decomposition
% level, we chose j=8 because 2^8 = 256 (data points every 0.5 mm) which
% means 256*0.5 = 128 mm (bigger than 100 mm, stated as the base length
% for MPD calculation in the ASTM E1845). With j=8 we remove the peaks
% relevant for this base length (relevant to macrotecture)
j = 8;
%                      RENAMING THE ORIGINAL DATA
OriginalData = columnA;
%                        EXTENDING THE DATA
% recalling again that we define the stationary wavelet transform (SWT)
% only for signals of length divisible by 2^j, we need to extend our
% original data points to a 2^j value, so we don't crop any valuable data at
% the end, later on after the SWT analysis we will crop the redundant data
% and we will have the actual original data (same number of data points)
% again.
% for this step we will recall the function: extend.m
%         function Y = extend(X)
%         Lx = length(X);
%         np2x = nextpow2(Lx);
%          L = 2^np2x-Lx;
%         if L>0
%              Left_extend = floor(L/2);
%              Right_extend = ceil(L/2);
%             Y = [X(1+Left_extend:-1:2); X; X(end-1:-1:end-Right_extend)];
%         else
%              Y = X;
%         end
% note: make sure the script with the function is in the same directory
TextData = extend(OriginalData);


%          CALCULATING THE UNIVERSAL THRESHOLD AND SIGMA
% In order to CORRECTLY calculate the boundaries for what we consider
% outliers, we will calculate the universal threshold, and sigma, using the
% original data (not the extended data), considering that the data follows
% a normal distribution, t = sqrt(2*log(n)). And sigma will be:
% sigma = 1.4826*mad, where mad is the median absolute deviation
% theory about mad: http://en.wikipedia.org/wiki/Median_absolute_deviation

n = length(OriginalData);
t = sqrt(2*log(n));


%          CALCULATING THE STATIONARTY WAVELET TRANSFORM
% ....introduce description and theory ...................
[swa,swd] = swt(TextData,j,'haar');


sigma = zeros(j,1); %filling with zeros a column vector sigma fro the
                    % following loop:

% for the following loop another function to inverse the extended data
% is used (as previously stated we want to calculate sigma only with the
```

```matlab
% actual original data).
% for this step we call the following function: inextend.m
%       function Y = iextend(X,L)
%       L = length(X)-L;
%       Left_limit = floor(L/2);
%       Right_limit = ceil(L/2);
%       Y = X(1+Left_limit:end-Right_limit);
% note: make sure the script with the fuction is in the same directory

for i=1:j
    SWD = iextend(swd(i,:),n);
    sigma(i) = 1.4826*mad(SWD,1);
end

%calculating the boundary:
ST = t*sigma;

%                   DENOISING THE DATA
% in order to get rid of the peaks that are outside the defined threshold
% we will equal to zero the details (swd's)n that are bigger the the
% boundary ST
for i=1:j
    b = swd(i,:);
    b(abs(b)>ST(i)) = 0;
    swd(i,:) = b;
end

%       RECOSTRUCTING THE (EXTENDED) TEXTURE DATA WITHOUT PEAKS
TextDataFiltered = iswt(swa,swd,'haar');

%       RECOSTRUCTING THE ORIGINAL TEXTURE DATA WITHOUT PEAKS
OriginalDataFiltered = iextend(TextDataFiltered',n);
%                   PLOTTING THE RESULTS
plot (OriginalData)
hold on
plot (OriginalDataFiltered)

%plotting histogram for data and for normal dist. (FOR THE FIRST LEVEL)
% hist(swd(1,:),2000);
% [h,c]=hist(swd(2,:),2000);
% [h,c]=hist(swd(1,:),2000);
% y=normpdf(c,0,ST(2)/t)/mean(diff(c))*length(swd(2,:));
% y=normpdf(c,0,ST(1)/t)*mean(diff(c))*length(swd(2,:));
% hold on
% plot(c,y);
```

**Appendix G: Matlab Scripts for Chapter 3**

Script 1 (dspsmrtmrtrdrun1.m)

```matlab
% Main Script

 %Loads the Raw data (e.g. SR10.mat) that must be in the same folder
 %with all 8 scripts, "SR10" will be changed below to match the raw
 % data file name that will be analyzed
load SR10
profile = VTTISR10Texture;
%(in this case SMARTRDU is the variable name from the RAWDATA.mat file,
% this name must be changed to match the name of the variable created when
%the Raw data file is loaded, CHANGE it in all four positions beow:
y = robustdsp(profile,40000,'fdr',0.1); %calls the robustdsp fuction
%x = SMARTRDU, Section_size = 40000, Method = fdr, FDR = 0.1
n = length(y);
x = linspace(0,1,n);

%plots both profiles without the terrain slope (with spikes: SMARTRDU, and
%without spikes: y)
%the slope is removed by substracting the moving average profile
%(mvaveragec
plot(x,profile-mvaveragec(profile,100),x,y-mvaveragec(y,100))

%below the subroutine for the MPD calculation:
%"MPD" and "mvaveragec" fuctions are called, slope is removed:
mtd = zeros(ceil(n/200),1);

for i=1:length(mtd)
    strt = 1+(i-1)*200;
    last = min(i*200,n);
    mtd(i,1) = MPD(mvaveragec(profile(strt:last),2),1);
    mtd(i,2) = MPD(mvaveragec(y(strt:last),2),1);
end

X = linspace(0,1,length(mtd));

%plots MPD results for both (with and without spikes, the resulting matrix
%called "mtd" contains: column1: MPD from original profile, and
% column 2: MPD data from profile without spikes.
figure
plot(X,mtd(:,1),X,mtd(:,2))
```

```matlab
function y = robustdsp(x,section_size,method,FDR,range,window)
 %nargin: returns the number of input arguments passed in the
 %call to the currently executing function,
 %window of 100 is defined and can be changed, 100 was chosed because of
 % the standard
 % FDR =0.1 is also changeable, 0.1 means that a 10% of the defined spikes
 % are considered to be wrongly defined as spikes
if nargin<6
    window = 100;
    if nargin<5
        range = 0.90:0.001:0.95;
        if nargin<4
            FDR = 0.1;
            if nargin<3
                method = 'universal';
                if nargin<2
                    section_size = 40000;
                end
            end
        end
    end
end

y = x;
M = length(x);
num_sections = ceil(M/section_size);

%despiking fuction is called:
for i=1:num_sections
    StartRange = 1+(i-1)*section_size;
    EndRange = min(i*section_size,M);
    y(StartRange:EndRange) =
despiking(x(StartRange:EndRange),method,FDR,range,window);
end
```

## Script 3 (`mvaveragec.m`)

```matlab
function y=mvaveragec(x,N)

%MVAVERAGEC    signal smoothing through the moving average method.
%   Y = MVAVERAGEC(X,N) Quickly smooths the signal X via averaging each
%   sampling with the previous and afterwards N samples.
%
%   Example:
%       t = 2*pi*linspace(-1,1);
%       xn = cos(x) + 0.25 - 0.5*rand(size(x));
%       xs = mvaveragec(xn,4);
%       plot(t,xn,t,xs), legend('noisy','smooth'), axis tight
%
%
s = size(x);
X = x(:);
X = [X(N+1:-1:2); X; X(end-1:-1:end-N)];
y0 = filter(ones(1,2*N+1)/(2*N+1),1,X);
y = reshape(y0(2*N+1:end),s(1),s(2));
```

## Script 4 (MPD.m)

```matlab
%calculates the MPD according to the standard, and also removes the slope
%using the "mvaveragec" function:
function M = MPD(P,type)

P = P-mvaveragec(P,min(50,length(P)-1));
if type == 1
    Half = floor(length(P)/2);
    M = (max(P(1:Half))+max(P(Half+1:end)))/2-mean(P);
elseif type == 2
    Third = floor(length(P)/3);
    M =
median([max(P(1:Third)),max(P(Third+1:2*Third)),max(P(2*Third+1:end))])-
mean(P);
else
    Fifth = floor(length(P)/5);
    M =
median([max(P(1:Fifth)),max(P(Fifth+1:2*Fifth)),max(P(2*Fifth+1:3*Fifth))...
        max(P(3*Fifth+1:4*Fifth)),max(P(4*Fifth+1:end))])-mean(P);
end
```

## Script 5 (gnorminv.m)

```matlab
function x = gnorminv(p,beta)

alpha = sqrt(gamma(1/beta)/gamma(3/beta));
if p<0.5
    x = -gammaincinv(1-2*p,1/beta).^(1/beta)*alpha;
else
    x = gammaincinv(2*p-1,1/beta).^(1/beta)*alpha;
end
```

## Script 6 (gnormcdf.m)

```
%Generalized Normal Cumuative Distribution function
function p = gnormcdf(x,beta)

alpha = sqrt(gamma(1/beta)/gamma(3/beta));
p = 0.5*(1+sign(x).*gammainc((abs(x)/alpha).^beta,1/beta));
```

## Script 7 (ggdistfit.m)

```matlab
function [nu, s, count] = ggdistfit(x,p1lim,p2lim,nulim)

Lower = nulim(1);
Upper = nulim(end);
Mid = (Lower+Upper)/2;
Mid1 = (Lower+Mid)/2;
Mid2 = (Upper+Mid)/2;
nuVals = [Lower Mid1 Mid Mid2 Upper];
sVals = zeros(1,5);
sdev = zeros(1,5);
count = 0;
while abs(Upper-Lower)>0.002
    for i=1:5
        b = gnorminv(p1lim,nuVals(i))./quantile(x,p2lim);
        sdev(i) = sqrt(mean(b.^2));
        sVals(i) = std(b)/mean(b);
    end
    ind = find(diff(sign(diff(sVals)))~=0);
    if isempty(ind)
        [~,ind] = min(sVals);
        if ind==1
            Lower = nuVals(1);
            Upper = nuVals(2);
        else
            Lower = nuVals(4);
            Upper = nuVals(5);
        end
    else
        Lower = nuVals(ind(1));
        Upper = nuVals(ind(1)+2);
    end
    nuVals(1) = Lower;
    nuVals(5) = Upper;
    nuVals(3) = (nuVals(1)+nuVals(5))/2;
    nuVals(2) = (nuVals(1)+nuVals(3))/2;
    nuVals(4) = (nuVals(3)+nuVals(5))/2;
    count = count+1;
end
[~,ind] = min(sVals);
nu = nuVals(ind);
s = 1/sdev(ind);
```

```matlab
%range is chosen to fit the tail of the distribution from the 90th to the
%95th persentile (range = 0.9:0.005:0.95)
function y = despiking(x,method,FDR,range,window)

if nargin<5
    window = 100;
    if nargin<4
        range = 0.9:0.005:0.95;
        if nargin<3
            FDR = 0.1;
            if nargin<2
                method = 'universal';
            end
        end
    end
end

%below the GGD is fitted by a narrowing iterative process:
%the following functions are called: "mvaveragec", "ggdistfit","gnorminv",
%"gnormcdf"
% a number of methods are avalible (i.e FDR method is the one defined in
% the main script), FDR method fits the General Normal continuous
% distribution, by calling the "gnormcdf" fuction.
method = lower(method);
m = length(x);

meanx = mvaveragec(x,window);
y = x-meanx;
my = median(y);
y = y-my;

[nu_p,s_p] = ggdistfit(y(y>0),1-(1-range)/2,range,[0.25 30]);
[nu_n,s_n] = ggdistfit(abs(y(y<0)),1-(1-range)/2,range,[0.25 30]);

switch method
    case 'universal'
        Tp = gnorminv(normcdf(sqrt(2*log(length(y(y>0))))),nu_p)*s_p;
        Tn = gnorminv(normcdf(sqrt(2*log(length(y(y<0))))),nu_n)*s_n;
        y(y>Tp) = 0;
        y(y<-Tn) = 0;
    case 'fdr'
        pp = 2*(1-gnormcdf(abs(y)/s_p,nu_p));
        pn = 2*(1-gnormcdf(abs(y)/s_n,nu_n));
        p = pp;
        p(y<0) = pn(y<0);
        k = (1:m)/m;
        k = reshape(k,size(x,1),size(x,2));
        p_sorted = sort(p);
        ind = find(p_sorted<=k*FDR);
        if ~isempty(ind)
            Th = max(p_sorted(ind));
            y(p<=Th) = 0;
        end
    case 'nonparam'
```

```
        th = nonparamoutlier(y,1.2);
        y(y<=th(1)) = 0;
        y(y>=th(2)) = 0;
    otherwise
        Tp = gnorminv(normcdf(sqrt(2*log(length(y(y>0))))),nu_p)*s_p;
        Tn = gnorminv(normcdf(sqrt(2*log(length(y(y<0))))),nu_n)*s_n;
        y(y>Tp) = 0;
        y(y<-Tn) = 0;
end

y = y+meanx+my;
```

## Appendix H: Matlab Scripts for Chapter 4

Script 1 (VTTI_SPIKE_REMOVAL_MAIN_SCRIPT_Plus_ENVELOPING_d0_054.m), e.g. for route sr7, third run, section 4 west:

```matlab
 % Main Script
clear
clc
 %Loads the Raw data (e.g. RAWDATA.mat) that must be in the same folder
 %with all 8 scripts, "RAWDATA" will be changed below to match the raw
 % data file name that will be analyzed
load 'sr7 t3 4w_Texture'
profile = sr7t34wTexture;
%(in this case SMARTRDU is the variable name from the RAWDATA.mat file,
% this name must be changed to match the name of the variable created when
%the Raw data file is loaded, CHANGE it in all four positions below:
y = robustdsp(profile,40000,'fdr',0.1); %calls the robustdsp fuction
%x = SMARTRDU, Section_size = 40000, Method = fdr, FDR = 0.1
n = length(y);
x = linspace(0,1,n);

%plots both profiles without the terrain slope (with spikes: SMARTRDU, and
%without spikes: y)
%the slope is removed by substracting the moving average profile
%(mvaveragec
plot(x,profile-mvaveragec(profile,100),x,y-mvaveragec(y,100))

%below the subroutine for the MPD calculation:
%"MPD" and "mvaveragec" fuctions are called, slope is removed:
mtd = zeros(ceil(n/200),1);

for i=1:length(mtd)
    strt = 1+(i-1)*200;
    last = min(i*200,n);
    mtd(i,1) = MPD(mvaveragec(profile(strt:last),2),1);
    mtd(i,2) = MPD(mvaveragec(y(strt:last),2),1);
end

X = linspace(0,1,length(mtd));

%plots MPD results for both (with and without spikes, the resulting matrix
%called "mtd" contains: column1: MPD from original profile, and
% column 2: MPD data from profile without spikes.
figure
plot(X,mtd(:,1),X,mtd(:,2))


% finding % of spikes
VectorOfSpikes=(profile-y);
NumberOfSpikes=length(find(VectorOfSpikes));
PercentageOfSpikes=(NumberOfSpikes/length(y));

          %Enveloping & Efective area for Water evacuation
```

```matlab
 % create the profile to be used for enveloping
original =y;
envelop = y;

number = length(envelop);

%choose the vertical deflection according to tire stiffness:
%Dprime = 0.1 (very soft tire)
%Dprime = 0.054(medium soft),
%Dprime = 0.027 (medium hard)
%Dprime = 0.01 (stiff tire).
dprime = 0.054;

for i = 2:number-1;
        d = envelop(i)-(envelop(i-1)+envelop(i+1))/2;
        if (d-dprime)>0
            if (envelop(i-1)-envelop(i)+dprime) <= 0
                if (envelop(i+1)-envelop(i)+dprime)> 0
                    envelop(i-1)=envelop(i-1)+2*(d-dprime);
                else envelop(i-1)= envelop(i)-dprime;
                        envelop(i+1)=envelop(i)-dprime;
                end
            else envelop(i+1)= envelop(i+1)+2*(d-dprime);
            end
        else
            if (d+dprime)<0
                envelop(i) = envelop(i)-d-dprime;
            else
            end
        end
end
 x = 1:number;
figure
plot(x,original,x,envelop);
xlabel('Distance, datapoints every 0.5 mm')
ylabel('Vertical profile in mm')
title('Tire Enveloping Profile')
legend('actual profile','enveloping profile')
%Efecctive area for water evacuation calculation (EAWE in mm2):
differences = envelop-original;
VectorofAreas(1:number-1) = zeros;

for j= 1:number-1;
VectorofAreas(1,j) = (((differences(j)+differences(j+1))/2)*0.5);
end;
MovAveVectorofAreas = mvaveragecEnv(VectorofAreas,100);
SingleAreasEvery100mm=MovAveVectorofAreas(101:201:end);
VectorofEAWEevery100mm = SingleAreasEvery100mm*200;
AverageEAWEfromWholeSection = mean(VectorofAreas)*200;
figure
boxplot_EAWE = boxplot(VectorofEAWEevery100mm);
xlabel('EAsWE for the whole Section')
ylabel('EAWE(mm2)')
title('Box Plot Effective Area for Water Evacuation')
cvVEAWE=(std(VectorofEAWEevery100mm))/(mean(VectorofEAWEevery100mm));
```

## Script 2 (robustdsp.m)

```matlab
function y = robustdsp(x,section_size,method,FDR,range,window)
 %nargin: returns the number of input arguments passed in the
 %call to the currently executing function,
 %window of 100 is defined and can be changed, 100 was chosed because of
 % the standard
 % FDR =0.1 is also changeable, 0.1 means that a 10% of the defined spikes
 % are considered to be wrongly defined as spikes
if nargin<6
    window = 100;
    if nargin<5
        range = 0.90:0.001:0.95;
        if nargin<4
            FDR = 0.1;
            if nargin<3
                method = 'universal';
                if nargin<2
                    section_size = 40000;
                end
            end
        end
    end
end

y = x;
M = length(x);
num_sections = ceil(M/section_size);

%despiking fuction is called:
for i=1:num_sections
    StartRange = 1+(i-1)*section_size;
    EndRange = min(i*section_size,M);
    y(StartRange:EndRange) =
despiking(x(StartRange:EndRange),method,FDR,range,window);
end
```

# Script 3 (vaveragecEnv.m)

```matlab
function y=mvaveragecEnv(x,N)

%MVAVERAGEC   signal smoothing through the moving average method.
%   Y = MVAVERAGEC(X,N) Quickly smooths the signal X via averaging each
%   sampling with the previous and afterwards N samples.
%
%   Example:
%      t = 2*pi*linspace(-1,1);
%      xn = cos(x) + 0.25 - 0.5*rand(size(x));
%      xs = mvaveragec(xn,4);
%      plot(t,xn,t,xs), legend('noisy','smooth'), axis tight
%

s = size(x);
X = x(:);
X = [X(N+1:-1:2); X; X(end-1:-1:end-N)];
y0 = filter(ones(1,2*N+1)/(2*N+1),1,X);
y = reshape(y0(2*N+1:end),s(1),s(2));
```

# Script 4 (vaveragec.m)

```matlab
function y=mvaveragec(x,N)

%MVAVERAGEC   signal smoothing through the moving average method.
%   Y = MVAVERAGEC(X,N) Quickly smooths the signal X via averaging each
%   sampling with the previous and afterwards N samples.
%
%   Example:
%       t = 2*pi*linspace(-1,1);
%       xn = cos(x) + 0.25 - 0.5*rand(size(x));
%       xs = mvaveragec(xn,4);
%       plot(t,xn,t,xs), legend('noisy','smooth'), axis tight
%
%
s = size(x);
X = x(:);
X = [X(N+1:-1:2); X; X(end-1:-1:end-N)];
y0 = filter(ones(1,2*N+1)/(2*N+1),1,X);
y = reshape(y0(2*N+1:end),s(1),s(2));
```

# Script 5 (MPD.m)

```matlab
%calculates the MPD according to the standard, and also removes the slope
%using the "mvaveragec" function:
function M = MPD(P,type)

P = P-mvaveragec(P,min(50,length(P)-1));
if type == 1
    Half = floor(length(P)/2);
    M = (max(P(1:Half))+max(P(Half+1:end)))/2-mean(P);
elseif type == 2
    Third = floor(length(P)/3);
    M =
median([max(P(1:Third)),max(P(Third+1:2*Third)),max(P(2*Third+1:end))])-
mean(P);
else
    Fifth = floor(length(P)/5);
    M =
median([max(P(1:Fifth)),max(P(Fifth+1:2*Fifth)),max(P(2*Fifth+1:3*Fifth))...
        max(P(3*Fifth+1:4*Fifth)),max(P(4*Fifth+1:end))])-mean(P);
end
```

## Script 6 (gnorminv.m)

```matlab
function x = gnorminv(p,beta)

alpha = sqrt(gamma(1/beta)/gamma(3/beta));
if p<0.5
    x = -gammaincinv(1-2*p,1/beta).^(1/beta)*alpha;
else
    x = gammaincinv(2*p-1,1/beta).^(1/beta)*alpha;
end
```

## Script 7 (gnormcdf.m)

```matlab
%Generalized Normal Cumuative Distribution function
function p = gnormcdf(x,beta)

alpha = sqrt(gamma(1/beta)/gamma(3/beta));
p = 0.5*(1+sign(x).*gammainc((abs(x)/alpha).^beta,1/beta));
```

## Script 8 (ggdistfit.m)

```matlab
function [nu, s, count] = ggdistfit(x,p1lim,p2lim,nulim)

Lower = nulim(1);
Upper = nulim(end);
Mid = (Lower+Upper)/2;
Mid1 = (Lower+Mid)/2;
Mid2 = (Upper+Mid)/2;
nuVals = [Lower Mid1 Mid Mid2 Upper];
sVals = zeros(1,5);
sdev = zeros(1,5);
count = 0;
while abs(Upper-Lower)>0.002
    for i=1:5
        b = gnorminv(p1lim,nuVals(i))./quantile(x,p2lim);
        sdev(i) = sqrt(mean(b.^2));
        sVals(i) = std(b)/mean(b);
    end
    ind = find(diff(sign(diff(sVals)))~=0);
    if isempty(ind)
        [~,ind] = min(sVals);
        if ind==1
            Lower = nuVals(1);
            Upper = nuVals(2);
        else
            Lower = nuVals(4);
            Upper = nuVals(5);
        end
    else
        Lower = nuVals(ind(1));
        Upper = nuVals(ind(1)+2);
    end
    nuVals(1) = Lower;
    nuVals(5) = Upper;
    nuVals(3) = (nuVals(1)+nuVals(5))/2;
    nuVals(2) = (nuVals(1)+nuVals(3))/2;
    nuVals(4) = (nuVals(3)+nuVals(5))/2;
    count = count+1;
end
[~,ind] = min(sVals);
nu = nuVals(ind);
s = 1/sdev(ind);
```

## Script 9 (despiking.m)

```matlab
%range is chosen to fit the tail of the distribution from the 90th to the
%95th persentile (range = 0.9:0.005:0.95)
function y = despiking(x,method,FDR,range,window)

if nargin<5
    window = 100;
    if nargin<4
        range = 0.9:0.005:0.95;
        if nargin<3
            FDR = 0.1;
            if nargin<2
                method = 'universal';
            end
        end
    end
end

%below the GGD is fitted by a narrowing iterative process:
%the following functions are called: "mvaveragec", "ggdistfit","gnorminv",
%"gnormcdf"
% a number of methods are avalible (i.e FDR method is the one defined in
% the main script), FDR method fits the General Normal continuous
% distribution, by calling the "gnormcdf" fuction.
method = lower(method);
m = length(x);

meanx = mvaveragec(x,window);
y = x-meanx;
my = median(y);
y = y-my;

[nu_p,s_p] = ggdistfit(y(y>0),1-(1-range)/2,range,[0.25 30]);
[nu_n,s_n] = ggdistfit(abs(y(y<0)),1-(1-range)/2,range,[0.25 30]);

switch method
    case 'universal'
        Tp = gnorminv(normcdf(sqrt(2*log(length(y(y>0))))),nu_p)*s_p;
        Tn = gnorminv(normcdf(sqrt(2*log(length(y(y<0))))),nu_n)*s_n;
        y(y>Tp) = 0;
        y(y<-Tn) = 0;
    case 'fdr'
        pp = 2*(1-gnormcdf(abs(y)/s_p,nu_p));
        pn = 2*(1-gnormcdf(abs(y)/s_n,nu_n));
        p = pp;
        p(y<0) = pn(y<0);
        k = (1:m)/m;
        k = reshape(k,size(x,1),size(x,2));
        p_sorted = sort(p);
        ind = find(p_sorted<=k*FDR);
        if ~isempty(ind)
            Th = max(p_sorted(ind));
            y(p<=Th) = 0;
        end
```

```matlab
    case 'nonparam'
        th = nonparamoutlier(y,1.2);
        y(y<=th(1)) = 0;
        y(y>=th(2)) = 0;
    otherwise
        Tp = gnorminv(normcdf(sqrt(2*log(length(y(y>0))))),nu_p)*s_p;
        Tn = gnorminv(normcdf(sqrt(2*log(length(y(y<0))))),nu_n)*s_n;
        y(y>Tp) = 0;
        y(y<-Tn) = 0;
end

y = y+meanx+my;
```
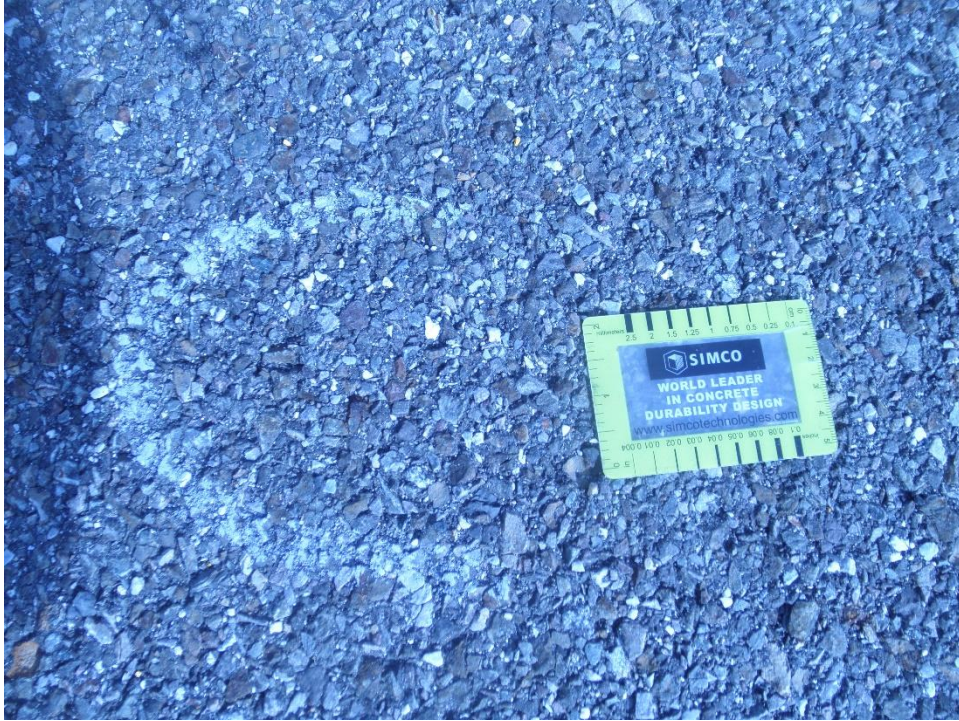
**Appendix I: Pictures of the sections**
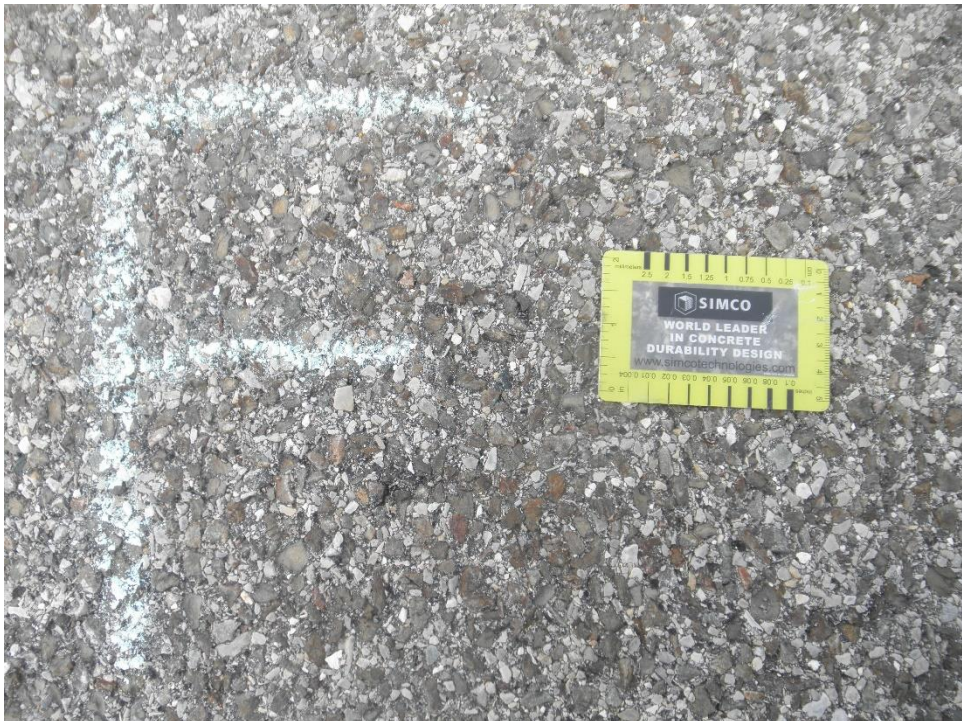


A-SM12.5D



B-SM9.5D

C-SM9.5E



D-SM9.5A

E-SM9.5D



F-SM9.5D

G-SM9.5D



H-SM9.5D

I-SM9.5A



J-SM9.5D

K-OGFC



L-SMA12.5

SR 199 SMA 9.5 - E



SR 199 AR-PFC 9.5 -E

SR 199 AR-PFC 9.5 - W



SR 199 PFC 9.5 - E

SR 199 PFC 9.5 - W



SR 199 PFC 12.5 - E

SR 199 PFC 12.5 - W



SR 288 SMA 9.5 - N

SR 288 AR-PFC 9.5 - N



SR 288 AR-PFC 9.5 - S

SR 288 PFC 9.5 - N



SR 288 PFC 9.5 - S

SR 288 PFC 12.5 - N



SR 288 PFC 12.5 – S